NREL
NATIONAL RENEWABLE ENERGY LABORATORY

Western Wind and Solar Integration Study Phase 3 – Frequency Response and Transient Stability

N.W. Miller, M. Shao, S. Pajic, and R. D'Aquila
GE Energy Management
Schenectady, New York

NREL Technical Monitor: Kara Clark

Link to Executive Summary

NREL is a national laboratory of the U.S. Department of Energy, Office of Energy Efficiency & Renewable Energy, operated by the Alliance for Sustainable Energy, LLC.

Subcontract Report
NREL/SR-5D00-62906
December 2014

Contract No. DE-AC36-08GO28308

NREL
NATIONAL RENEWABLE ENERGY LABORATORY

Western Wind and Solar Integration Study Phase 3 – Frequency Response and Transient Stability

N.W. Miller, M. Shao, S. Pajic, and R. D'Aquila
GE Energy Management
Schenectady, New York

NREL Technical Monitor: Kara Clark

Prepared under Subcontract No. KAGN-4-23474-01

National Renewable Energy Laboratory
15013 Denver West Parkway
Golden, Colorado 80401
303-275-3000 • www.nrel.gov

Subcontract Report
NREL/SR-5D00-62906
December 2014

Contract No. DE-AC36-08GO28308

NOTICE

This report is available at no cost from the National Renewable Energy Laboratory (NREL) at www.nrel.gov/publications.

Available electronically at http://www.osti.gov/scitech

Available for a processing fee to U.S. Department of Energy and its contractors, in paper, from:

U.S. Department of Energy
Office of Scientific and Technical Information
P.O. Box 62
Oak Ridge, TN 37831-0062
phone: 865.576.8401
fax: 865.576.5728
email: mailto:reports@adonis.osti.gov

Available for sale to the public, in paper, from:

U.S. Department of Commerce
National Technical Information Service
5285 Port Royal Road
Springfield, VA 22161
phone: 800.553.6847
fax: 703.605.6900
email: orders@ntis.fedworld.gov
online ordering: http://www.ntis.gov/help/ordermethods.aspx

Cover Photos: (left to right) photo by Pat Corkery, NREL 16416, photo from SunEdison, NREL 17423, photo by Pat Corkery, NREL 16560, photo by Dennis Schroeder, NREL 17613, photo by Dean Armstrong, NREL 17436, photo by Pat Corkery, NREL 17721.

Acknowledgments

The National Renewable Energy Laboratory (NREL) and GE gratefully acknowledge the support of Charlton Clark (Wind and Water Power Program) and Venkat Banunarayanan (SunShot Initiative) from the U.S. Department of Energy (DOE) Office of Energy Efficiency and Renewable Energy for funding this work.

NREL and GE also thank the members of the Technical Review Committee (TRC) for their insightful comments and assistance. Participation in the TRC does not imply agreement with the project findings. The TRC included:

- Eric Allen, North American Electric Reliability Corporation (NERC)
- Jamie Austin, PacifiCorp
- Sam Baldwin, DOE
- Venkat Banunarayanan, DOE
- Ben Brownlee, Western Electricity Coordinating Council (WECC)
- Neil Burbure, NERC
- Ray Byrne, Sandia National Laboratories
- Tom Carr, Western Governors' Association (WGA)
- Charlton Clark, DOE
- Bob Cummings, NERC
- Tom Duane, Public Service Company of New Mexico (PNM)
- Bob Easton, Western Area Power Administration (WAPA)
- Sara Eftekharnejad, Tucson Electric Power (TEP)
- Steve Ellenbecker, WGA
- Ryan Elliott, Sandia National Laboratories
- Abe Ellis, Sandia National Laboratories
- Joe Eto, Lawrence Berkeley National Laboratory (LBNL)
- Irina Green, California Independent System Operator (CAISO)
- Fred Huang, Electric Reliability Council of Texas (ERCOT)
- Dmitry Kosterev, Bonneville Power Administration (BPA)
- Doug Larson, WGA
- Debra Lew, Independent Consultant
- Yishan Li, WAPA
- Clyde Loutan, CAISO

- Jim McCalley, Iowa State University
- Jeff Mechenbier, PNM
- Mark O'Malley, University College Dublin
- Brian Parsons, Independent Consultant
- Pouyan Pourbeik, Electric Power Research Institute (EPRI)
- Jim Reilly, DOE
- Sandip Sharma, ERCOT
- Cesar Silva-Monroy, Sandia National Laboratories
- David Silver, Xcel Energy
- Charlie Smith, Utility Variable-Generation Integration Group (UVIG)
- Justin Thompson, Arizona Public Service (APS)
- John Undrill, Independent Consultant
- Vijay Vittal, Arizona State University
- Janice Zewe, Sacramento Municipal Utility District (SMUD)

NREL regrets any inadvertent omission of any project participants and contributors.

Abbreviations and Acronyms

AC	alternating current
BL	base load
COI	California-Oregon Interface
CSP	concentrating solar thermal power
DC	direct current
DG	distributed generation, embedded PV
DSW	Desert Southwest region
FIDVR	fault-induced delayed voltage recovery
FR	frequency response
FRO	frequency response obligation
GR	governor response
GW	gigawatt
Hz	Hertz
HS	heavy summer
IFRO	interconnection frequency response obligation
LSP	light spring
mHz	millihertz
MVA	megavolt ampere
MW	megawatt
MWCAP	MW capability
NERC	North American Electric Reliability Corporation
NW	Northwest region
PDCI	Pacific DC Intertie
PV	photovoltaic solar power, utility-scale photovoltaic power plant
RAS	remedial action scheme
ROCOF	rate of change of frequency
s	second
UFLS	under-frequency load shedding
WECC	Western Electricity Coordinating Council
WTG	wind turbine generator
WWSIS	Western Wind and Solar Integration Study

Table of Contents

List of Figures

List of Tables

1 Introduction

Power system operators and utilities worldwide have concerns about the impact of high-penetration wind and solar generation on electric grid reliability (EirGrid 2011b, Hydro-Quebec 2006, ERCOT 2010). The stability of North American grids under these conditions is a particular concern and possible impediment to reaching future renewable energy goals. Phase 3 of the Western Wind and Solar Integration Study (WWSIS-3) considers a 33% wind and solar annual energy penetration level that results in substantial changes to the characteristics of the bulk power system, including different power flow patterns, different commitment and dispatch of existing synchronous generation, and different dynamic behavior of wind and solar generation. WWSIS-3 evaluates two specific aspects of fundamental frequency system stability: frequency response and transient stability.

Frequency response (FR)—the ability of the power system to stabilize and restore grid frequency following large, sudden mismatches between generation and load—has always been an operational concern. With the recent approval of the revised North American Electric Reliability Corporation (NERC) *Standard BAL-003-1 Frequency Response and Frequency Bias Setting* (NERC 2012a), individual balancing authorities (BAs) now have specific frequency response obligations (FROs).

Transient stability—the ability of the power system to maintain synchronism between all elements following disturbances—is a major operational constraint in many grids, including the western U.S. and Texas systems. These constraints primarily impact large-scale bulk power system performance, as local transient stability concerns are generally addressed on a plant-by-plant basis—but grid-wide stability concerns with high wind and solar penetration have barely been addressed. (For clarity, WWSIS-3 is focused on "traditional" fundamental-frequency stability issues, such as maintaining synchronism, frequency, and voltage. This work does not explore other non-fundamental frequency issues such as sub-synchronous phenomena, harmonics, unbalances, transients, small signal analysis, etc.)

The objectives of WWSIS-3 are to:

- Illustrate the FR and transient stability of the U.S. Western Interconnection to large disturbances, including generation outages and critical tie-line disturbances, under a variety of future system conditions
- Explore the potential impact of substantially increased levels of wind and solar generation, and the accompanying displacement of thermal generation resources, on FR and transient stability
- Test various operational and control options to improve system FR and transient stability
- Examine and test metrics of system conditions intended to provide operational assistance in positioning the system for adequate frequency and transient stability performance.

1.1 Background and Related Work

1.1.1 WWSIS-1 and WWSIS-2

Phase 1 and 2 of WWSIS (GE Energy 2010, NREL 2013) established the longer-term operational and economic performance of the Western Interconnection under various high levels of wind and solar power penetration. Those studies aimed to answer the following questions:

- Can the system supply and demand be balanced across an entire year of operation with high penetrations of wind and solar?
- How do high penetrations of wind and solar impact cycling costs and emissions?
- How do wind and solar impacts compare?

Analysis included detailed examination of reserves for balancing and addressing incremental variability, as well as inter-area transmission constraints (both established and future).

These studies raised additional questions that WWSIS-3 aimed to answer:

- Can system reliability be maintained with high penetrations of wind and solar?
- How do advanced features in wind and solar technologies impact reliability and stability?

A variety of system conditions, disturbances, locations, and renewable penetration levels were evaluated to help draw broader conclusions from an analysis of two specific types of power system stability in WWSIS-3: frequency stability and transient stability. A technical definition of the different aspects of power system stability is provided in (Kundur et al. 2004). A less technical description of both frequency and transient stability is provided in the following subsections.

1.1.2 Frequency Response Discussion

Reliable operation of a large interconnected power grid such as the Western Interconnection (shown in Figure 1) requires a constant balancing of electricity generation with electricity demand. Electricity must be generated at the same instant it is used, so operating procedures have developed to forecast electricity demand, schedule electric generators to meet that demand, and ensure sufficient generating reserves are available to respond to forecast errors and system disturbances. The measure of success in this balancing act is frequency. In North America, that means maintaining system frequency at or very close to 60 Hz, as shown in Figure 2.

However, disturbances do occur, including large ones that affect overall system frequency (e.g., abrupt outage of a large generator or a major transmission line). For example, a transmission line outage may disconnect a large industrial customer. As a result, the total electricity generation exceeds the total electricity demand, and frequency rises. Because operators generally have more control over generation than demand, they can execute a generation reduction to regain the balance and return system frequency to near 60 Hz.

A potentially more significant problem is the loss of a large generating plant. As a result of this type of disturbance, the total electricity demand exceeds the total electricity generated and frequency drops, as shown in Figure 3. In general, a power grid is designed to withstand the loss of the single largest generator. However, the loss of multiple generators or plants may cause the

frequency to drop significantly such that protective devices act to disconnect customers in order to preserve the bulk of the system. It is a serious reliability failure when operators lose the ability to supply all the electricity needed to meet demand.

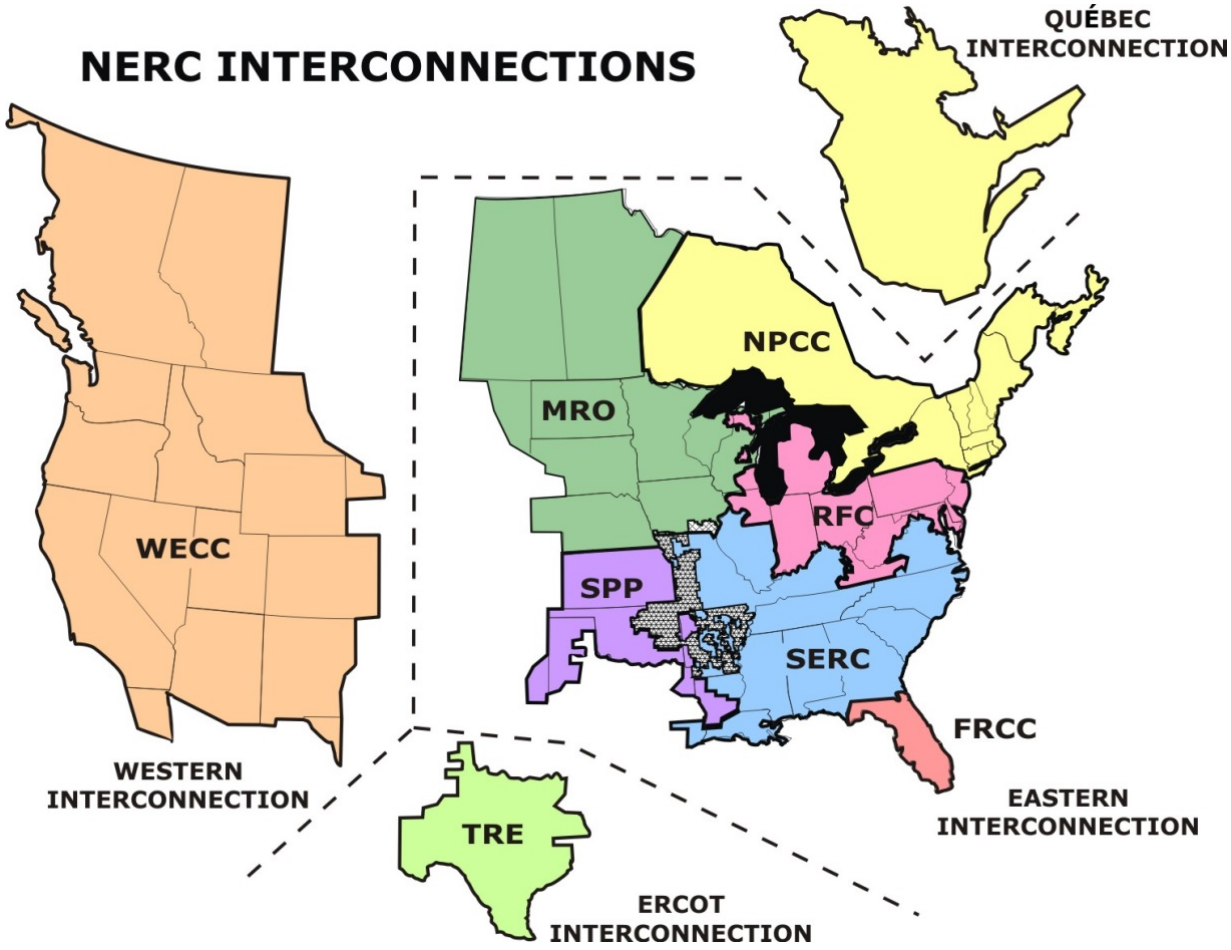

Figure 1. North American electricity grid interconnections.[1]

[1] http://www.nerc.com/AboutNERC/keyplayers/Documents/NERC_Interconnections_Color_072512.jpg

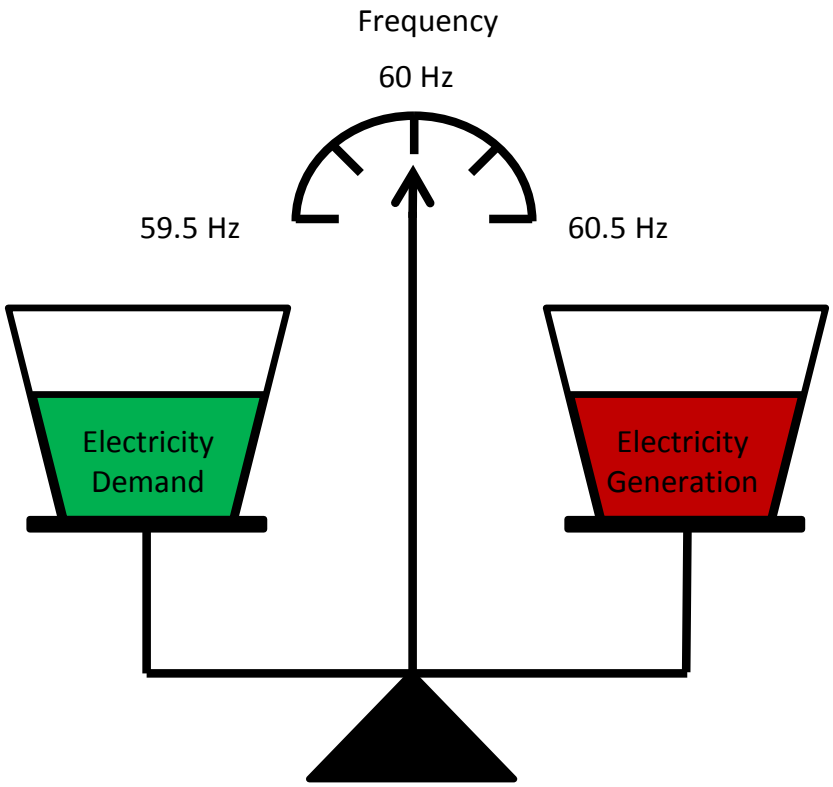

Figure 2. Balance analogy for frequency stability.

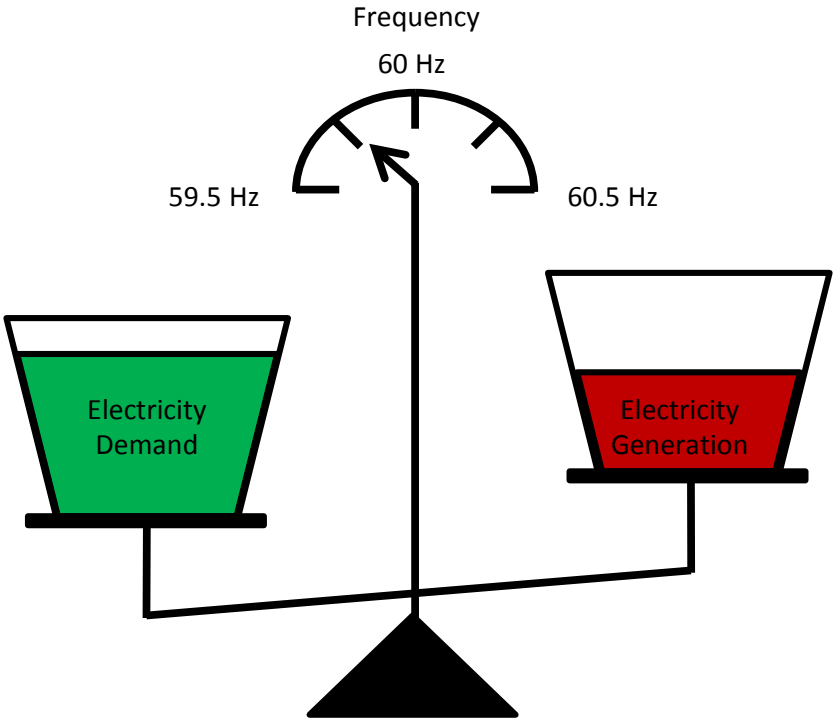

Figure 3. Electricity demand exceeds electricity generation, and frequency drops.

An example of system frequency in response to a large generation trip is shown in Figure 4. The system is operating normally, with a frequency of 60 Hz, up to 1 second. At that time, a large generating unit is abruptly lost. Load now exceeds generation, so the frequency drops. The speed of the initial decline is related to the number of conventional synchronous generators on the system. More generators mean more inertia, which retards the frequency decline. At about 10 seconds, the frequency nadir or minimum is reached. Frequency nadir is one measure of a system's frequency stability; it must be above the highest level of under-frequency load shedding (UFLS). At that point in time, the generators with governor controls have begun to act to increase power output, and thus the system frequency begins to recover. By about 60 seconds, the system frequency has settled out somewhat below the normal operating frequency of 60 Hz. A metric of frequency stability is based on the change in frequency between the nadir and this settling frequency, and the change in power within this interval. Measurements are averaged over a defined period between the nadir and the settling frequency, and the ratio of change in power to change in frequency is calculated. This is called "frequency response" (FR) and is formally defined by NERC (NERC 2012a). After 60 seconds, even more generators begin to increase their power output, and the frequency returns to normal within about 10 minutes. One part of this study focuses on system frequency behavior in the first 60 seconds after an outage.

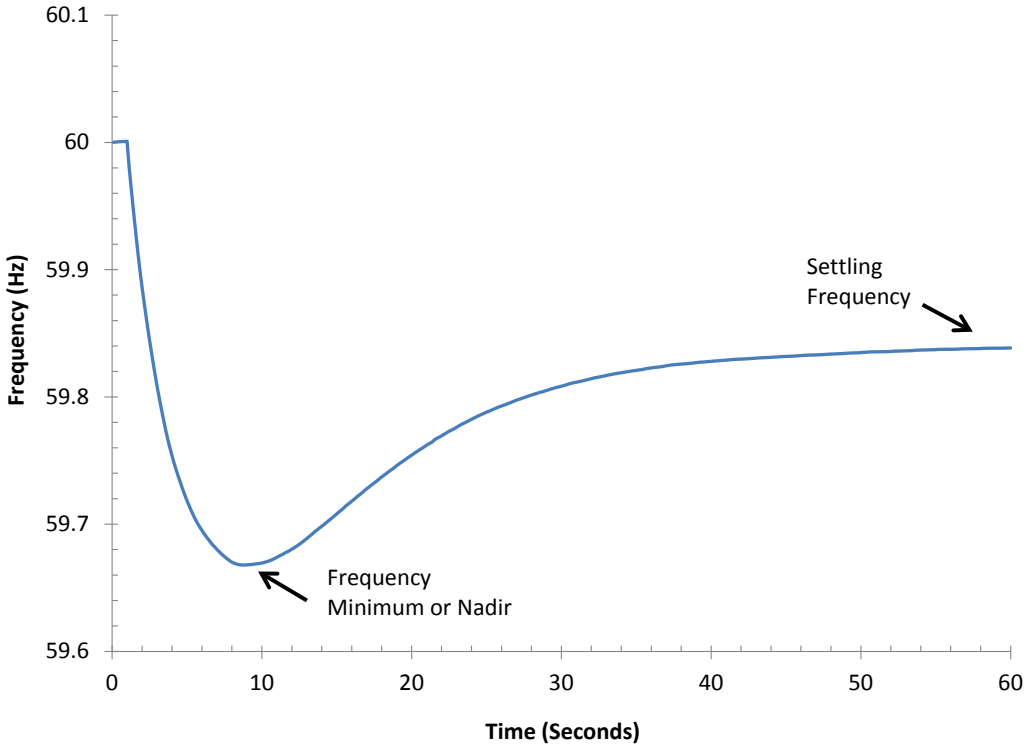

Figure 4. System frequency in response to a large generation trip.

There is general concern among power system operators and utilities regarding the degradation of FR in North America over the past two decades. The decline is due to various factors including the withdrawal of primary or governor response (GR) shortly after an event, the lack of in-service governors on conventional generation, and the unknown and changing nature of load frequency characteristics. High penetrations of inverter-based, or non-synchronous, generation technologies further complicate this issue. Without special operation or controls, wind and solar

plants do not inherently participate in the regulation of grid frequency. By contrast, synchronous machines always contribute to system inertia, and some fraction of the synchronous generation in operation at any point has governor controls enabled. When wind and solar generation displace conventional synchronous generation, the mix of the remaining synchronous generators changes and has the potential to adversely impact overall FR.

Therefore, one of the primary objectives of WWSIS-3 is to evaluate and better understand the impact of high penetrations of wind and solar power on system-wide FR to large generator outages in the first minute after the outage occurs.

1.1.3 Transient Stability Discussion

In addition to maintaining the balance between electricity generation and electricity demand, power system operators must ensure that the grid can successfully transition from normal operation (e.g., all transmission lines and generating units are in service) through a disturbance (e.g., abrupt outage of a major transmission line or large generator) and into a new stable operating condition in the 10–20 seconds immediately following the disturbance. The ability to make this successful transition is called transient stability, and is an even faster phenomenon than frequency stability.

A mechanical analogy for transient stability is illustrated in Figure 5 (Vittal 2003). Imagine a set of balls of different sizes connected to each other by a set of breakable elastic strings. The balls represent generators of different sizes and characteristics, and the strings represent the interconnecting transmission lines. The system is disturbed when one of the balls is hit with a stick. The ball begins to swing, and the string connected to the ball also swings. Other strings follow suit, and other balls start to swing. As a result of the single disturbance, the entire system of strings and balls is moving in response. If the swings die down, and the system comes back to rest, then the system is transiently stable. On the other hand, if the swings grow, one or more balls may break away from the rest, and the system is transiently unstable.

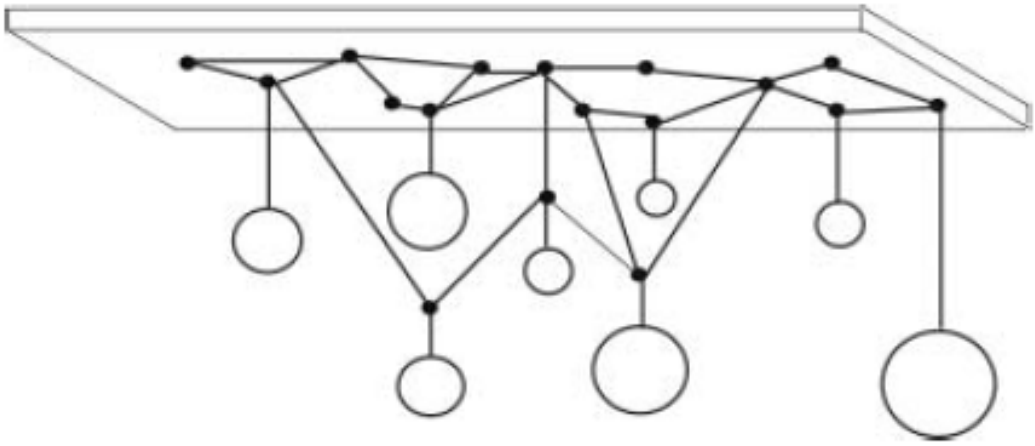

Figure 5. Mechanical analogy for transient stability (Vittal 2003).

An example of both transient stability (blue) and transient instability (red) is shown in Figure 6. The system is operating normally, with a transmission substation voltage of 100%, up to 0.5 seconds. At that time, a disturbance occurs, such as a tree falling on a transmission line. From 0.5 seconds to 0.7 seconds, the voltage is zero because the tree is connecting the transmission line to the ground. At about 0.7 seconds, an automatic protection system trips the transmission line, and the voltage returns to near normal. But as described above, the system is swinging in response to the disturbance. When the swings grow and the system separates, the substation voltage drops precipitously and the system collapses at about 1 second. When the swings die down, the substation voltage settles back to normal within 5 seconds. The second part of this study focuses on system stability in the first 5–10 seconds.

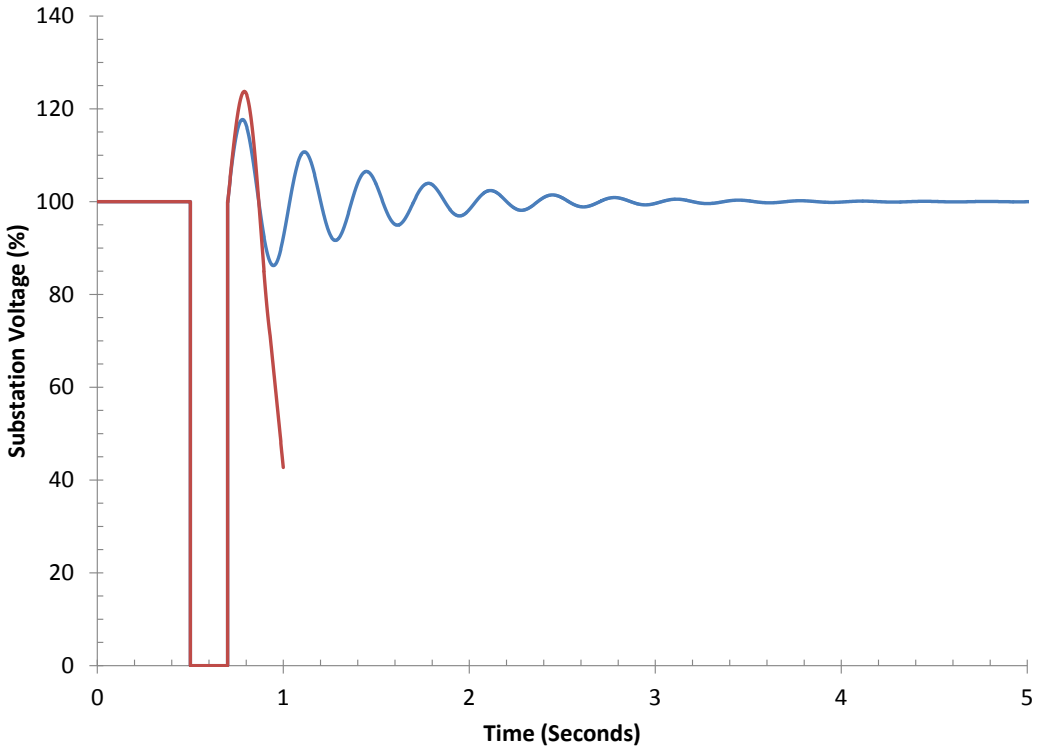

Figure 6. Substation voltage in response to transmission system disturbance.

As noted, the Western Interconnection has a long history of constraints due to transient stability limitations, which vary depending on system characteristics such as the level of electricity demand (e.g., peak summer load), the amount of power flowing on the transmission system (e.g., heavy flows on critical paths), and the location of generating plants in operation (e.g., remote from population centers). One of the primary objectives of WWSIS-3 is thus to evaluate and better understand the impact of high penetrations of wind and solar power on the large-scale transient stability of the Western Interconnection. The primary measures of transient stability are avoiding bulk system separation and individual generator loss of synchronism with the system, and meeting various voltage and frequency swing criteria, which vary with the severity of the disturbance according to NERC and Western Electricity Coordinating Council (WECC) reliability standards.

While transient stability can be both systemic and local, this study focuses on large-scale events that affect the security of the entire interconnection. Large penetrations of inverter-based, or non-synchronous, wind and solar generation may substantially alter system stability as a result of changes in angle/speed swing behavior due to reduced inertia, changes in voltage swing behavior due to different voltage control systems, different power flow patterns, and displacement of synchronous generation at key locations.

1.1.4 Other Related Work

The frequency behavior of North American grids has recently been the subject of heightened concern (Ingleson 2005, Ingleson 2010). Reports by NERC show that FR has been declining over the past two decades.

Significant research in the FR area began in 2010 (Eto 2010, Undrill 2010, Mackin 2010); additional research was performed in 2011 (Sharma 2011). Recent work by GE (Miller 2011b) examined this issue with a specific focus on the performance of California for the California Independent System Operator (CAISO). The NREL-sponsored *Eastern Frequency Response Study* (GE Energy (2013) examined the frequency performance of the Eastern Interconnection with high levels of wind. In that work, various means to improve modeling and system response were tested. Finally, NREL and the Electric Power Research Institute (EPRI) have studied the application of active power controls on wind plants to support grid reliability (Ela 2014, Gevorgian 2014).

1.2 Scope of Work and Task Structure

WWSIS-3 was divided into tasks briefly outlined here.

Task 1: Develop Study Databases and Establish Initial Conditions

In this task, NREL and GE solicited inputs from the Technical Review Committee (TRC) to jointly define the key study parameters. System conditions in the study databases, generation outages, transmission events, performance metrics, and the initial unit commitment and re-dispatch procedures were specified. This required a number of subtasks, including:

- **Transmission Model and Modifications:** Select data sets that reasonably represent the Western Interconnection in the not-too-distant future, making minimal changes to planned system transmission. The selected data sets included a number of substantial new transmission projects that are not currently in service.
- **Renewable Siting Method:** Add renewable generation at specific projects with specific interconnection substations in realistic physical locations, but avoid the detailed local transmission design that normally accompanies each individual project.
- **Stability Model and Modifications:** Add dynamic model improvements known to significantly impact the bulk system FR or inter-area transient stability, including incorporation of the latest composite dynamic load model.
- **Commitment and Dispatch Method:** De-commitment and re-dispatch thermal generation to accommodate the new wind and solar generation based on selected hourly results from the production simulation results of WWSIS-2.

- **Reference Disturbances and Performance Metrics:** Select system disturbances for evaluation of FR and transient stability. Performance targets are based on WECC stability standards and the NERC BAL-003-1 FRO.

Task 2: Evaluate Western Interconnection Frequency Response

The study evaluated the Western Interconnection FR to large generation outages under a variety of system conditions. This analysis used the existing unit commitment and dispatch procedures, as well as standard power plant controls as currently implemented. Performance was tested for the NERC BAL-003-1 reference disturbance of a two-unit outage at the Palo Verde nuclear power station (NPS) for a loss of about 2,750 MW.

Task 3: Evaluate Western Interconnection Transient Stability

Transient stability was evaluated with particular emphasis on events that challenge major western interties (e.g., California-Oregon Interface [COI] and West of the River limits). Again, this analysis used the existing unit commitment and dispatch procedures, as well as standard power plant controls as currently used. System performance, in terms of maintaining synchronism and meeting other WECC stability criteria (e.g., post-fault voltage swings, etc.), was evaluated for various faults. Particular attention was given to blocking the Pacific DC Intertie (PDCI), which is a severe transient stability event for the COI.

Task 4: Evaluate Factors Affecting Dynamic Performance

Sensitivity cases were evaluated to provide a deeper examination of factors that could affect FR and transient stability. Tests examined the following:

- Sensitivity to tripping (deliberate or unplanned) of distributed photovoltaics (PV)
- Dynamics of concentrating solar thermal power (CSP) compared to utility-scale PV
- Comparative impacts of tripping large thermal generation vs. distributed PV
- Impact of exhausting headroom of frequency-responsive generation
- Transient stability impacts of even higher wind and solar generation with extreme levels of coal generation displacement.

Task 5: Evaluate Mitigation Measures

The study evaluated the ability of a limited selection of mitigation measures to improve both FR and transient stability, including:

- Conversion of coal steam turbine generators to synchronous condensers to address "weak grid" concerns
- Inertial and governor controls on wind plants
- Frequency-responsive controls from utility-scale PV and CSP
- Energy storage for frequency control
- Transmission reinforcement for transient stability improvement.

The following sections of this report generally align with these tasks and provide additional detail.

2 Develop Study Databases and Establish Initial Conditions

This section contains definitions and context for the study. Specifically, Section 2.1 discusses the selection and improvement of the study cases. Refinement and documentation of the study cases are reported in Section 2.2. Performance and monitoring metrics are described in Section 2.3. The development of the Hi-Mix (33% annual energy penetration from wind and solar) cases is reported in Section 2.4 through Section 2.6.

2.1 Selection of Study Cases

This section covers the selection of the WECC cases from which the WWSIS-3 study cases were developed. The investigation and improvement of the selected cases are discussed in detail. The initial condition metrics for new base cases are presented.

2.1.1 Key Considerations

The study databases were selected based on the following requirements:

- The study case should be credible and meaningful.
- The study case should have a longer horizon, e.g., extend beyond the year 2020.
- The load flow in the study cases should include major system generation changes—additions and retirements—for which there is some degree of consensus in WECC.
- The study case should have a transmission build-out that is realistic and not overly optimistic.
- The study case should have high stress from a transient stability perspective.
- The study case should have high stress from a FR perspective.

2.1.2 Original Cases

In order to understand options to meet the selection criteria, extensive discussions were held with the TRC. The WECC library included nine approved cases (listed in Appendix Table 28) from which suitable starting cases were selected.

The 2022 Light Spring (LSP) case included the highest wind and solar build-out. Further, it included known plant retirements, with guidance from the WECC System Review Working Group. After extensive discussion and with the concurrence of the TRC, two WECC cases were selected for WWSIS-3:

- 2022 Light Spring Base case (LSP Original case)
- 2023 Heavy Summer Load case (HS Original case).

These two cases have different objectives, and therefore different generation, load, and transmission topologies. The 2022 Light Spring Base case represents a light spring load condition throughout the West. The renewable penetrations in this case are intended to be consistent with state renewable portfolio standard (RPS) requirements in 2022. The 2023 Heavy Summer Load case, however, is a WECC general 10-year case with typical flows throughout the

Western Interconnection. Load flow bubble diagrams for the two cases are included in the Appendix as Figure 76 and Figure 77.

For the rest of this report, "LSP" refers to cases that originated with the 2022 Light Spring Base case, and "HS" refers to cases that originated with the 2023 Heavy Summer Load case. The year of the data sets provides a useful point of reference for the study and the infrastructure included by WECC in the base cases. For the purposes of this study, however, it is the wind and solar penetration level that is important—but this is not a prediction that the Western Interconnection will reach these high levels of wind and solar by these study years.

2.1.3 Evolution of Study Cases

The flow chart in Figure 7 illustrates the evolution of the LSP cases. The study started with the WECC LSP Original case, i.e., the data as received from WECC. The dynamic data in the LSP Original case were improved to create the LSP Base case. The improvement includes fixing bad models, adding models for netted units, and adding the composite load model. In the LSP Hi-Mix case, a large number of distributed generators as well as utility-scale wind and solar plants were added, with commitment and dispatch adjusted for the same system load level as the Base case. In general, the system topology, transmission, and existing generation resources were left intact. The details of the development of the LSP Hi-Mix case are discussed below. An LSP Hi-Mix Extreme case was developed as a sensitivity and is presented in Section 5.7.

HS cases have a similar case evolution as the LSP cases, except that no HS Hi-Mix Extreme case was developed in this study. Also, because the HS Original case is a WECC 10-year planning case, both the power flow and dynamic data were in better shape from a simulation perspective and needed little refinement other than the addition of the composite load. The details of the case development and evolution are discussed in the subsequent sections.

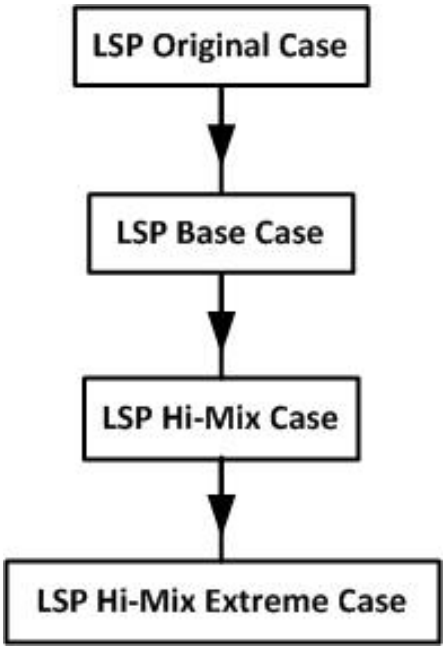

Figure 7. Evolution of LSP cases.

2.2 Investigation and Improvement of Original Cases

2.2.1 Identification of Generation Type

Detailed understanding of the type of generation in the simulations is critical to gleaning insight into the effects of increased variable renewable generation. While WECC has good processes for maintaining accurate models, the need to keep consistent track of the type (e.g., steam, CSP, combined cycle, etc.) of every generating unit is limited in power flow databases. Part of the investigation of the selected WECC cases was to try to assign generation type to every unit in the system model.

2.2.1.1 Light Spring

The LSP Original case was developed to look at a high-renewable future from the WECC planning perspective. Therefore, compared with the HS case, the LSP Original case already has high wind and solar generation built into the database. There were many units of different types added by WECC members to the cases.

Considerable efforts were made to identify the type and amount of generation mix in the LSP Original case. These efforts included:

- Reviewing associated material for two selected WECC cases
- Reviewing other related WECC documents
- Checking Positive Sequence Loadflow software (PSLF) dynamic data (dyd file) for comments
- Using the GE Multi Area Production Simulation (MAPS) software database as a reference
- Performing Google searches for information from the public domain.

In many instances, the same unit can be identified by more than one source.

One useful reference for identifying the generation mix is a reconciliation Excel spreadsheet provided by WECC as a supporting material for the LSP Original case. The purpose of this spreadsheet is to conduct a comprehensive reconciliation of the LSP Original case against the Production Cost Model (PCM). One tab named “Generators” in this spreadsheet provides the type and primary fuel information for each generation unit in the power flow data.

The generation information for each generator category from the reconciliation spreadsheet is summarized in Table 1. For each category, the number of units, total generation, total generation nameplate capacity, and flag of renewables are provided.

A few highlights from the WECC-wide summary table include:

1. Renewables in the LSP Original case total 36,436 MW, which is about 31.7% instantaneous penetration.
2. Wind is the largest resource among all renewables, followed by solar PV, geothermal, and CSP.

3. The coal units in the West were dispatched at about 86.1% of their capacity.
4. The combined-cycle (CC) and combustion turbine (CT) units were dispatched at 15% and 14% of total installed capacity, respectively. These low dispatch rates indicate these two types of units were already displaced by the high wind and solar generation.

It is important to note that Table 1 only indicates WECC's intention for generation mix for the LSP Original case, not the final reality. The dynamic model for each generator category, especially for those wind and solar units, needed close scrutiny. From a FR and transient stability perspective, the renewable generation is deemed to be renewable only if its dynamic data were correctly represented.

Table 1. Generation Mix from Reconciliation Spreadsheet

Generator Category	# of Units	Total Pgen (MW)	Total Pmax (MW)	Renewable
Wind	350	22,448	34,778	Yes
Solar PV	373	5317	7,229	Yes
Solar CSP0	22	2,275	2,171	Yes
Solar CSP6	4	585	541	Yes
Biomass RPS	124	1,148	3,047	Yes
Geothermal	113	3,807	4,820	Yes
Small Hydro RPS	122	856	1,759	Yes
Conventional Hydro	607	26,970	65,351	No
Pumped Storage	14	-2,076	3,720	No
Nuclear	8	8,077	9,681	No
Coal	122	31,387	36,470	No
Combined Cycle	418	9,257	61,600	No
Combustion Turbine	466	3,727	26,648	No
Steam	79	582	5,704	No
Negative Bus Load	23	528	528	No
All Others	101	173	1,341	No
Total	**2,947**	**115,061**	**265,388**	

Table 2 shows the on-line generation production by type and by area after all the information had been considered. This is referred to as the LSP Base case. The areas have been grouped into five regions: California, Desert Southwest (DSW), Northeast, Northwest (NW), and Outside. Generation is summed by type, by area, and by region. Note that the NW region contains only the Northwest area. Also, the areas defined in the WECC power flow databases may cover more than is implied by their names. For instance, PSCOLORADO includes Platte River Power Authority, Tri-State Generation and Transmission Association, Black Hills Corporation, and independent power producers, as well as Public Service of Colorado (now Xcel Energy). Only 977 MW of generation in the West was not identified by any type and was given the label

"Other." These are all modeled as synchronous generation in the stability database. Generation type categories were aligned with those in WWSIS-2. Table 2 is repeated as a bar chart in Figure 8.

The minimum power levels (Pmin) from the original WECC power flow cases were used in WWSIS-3. If no Pmin was in the power flow database, a default value equal to 20% of the maximum power level (Pmax) was used.

Table 2. Generation Type for the LSP Base Case by Area

Area	Biomass	Combined Cycle	Coal	CSP	DG	Gas CT	Geothermal	Hydro	Nuclear	Other	PSH	PV	Steam	Wind	Total
California	**66**	**2,702**	**2,060**	**858**	**64**	**2,113**	**1,958**	**4,918**	**4,390**	**258**	**-1,277**	**3,630**	**1,319**	**4,405**	**27,464**
IMPERIALCA	49	0	0	0	0	348	533	49	0	224	0	0	0	0	1,202
LADWP	0	180	1,900	0	0	0	0	177	0	0	-149	0	227	190	2,525
PG AND E	0	1,609	66	0	0	1,009	823	3,826	2,240	8	-1,128	1865	1,052	764	12,133
SANDIEGO	0	107	0	0	64	150	0	4	0	1	0	464	0	272	1061
SOCALIF	17	806	94	858	0	607	603	863	2,150	25	0	1301	40	3,179	10,543
DSW	**0**	**3,518**	**13,849**	**0**	**0**	**1,714**	**18**	**2,674**	**2,756**	**47**	**17**	**162**	**334**	**4,003**	**2,9093**
ARIZONA	0	1,841	7,231	0	0	346	0	2,462	2,756	47	17	50	0	350	15,100
EL PASO	0	252	0	0	0	286	0	0	0	0	0	0	92	0	630
NEVADA	0	1,254	0	0	0	0	0	0	0	0	0	60	242	0	1,556
NEW MEXICO	0	0	1,122	0	0	0	18	7	0	0	0	28	0	1,091	2,266
PSCOLORADO	0	171	1,959	0	0	1,004	0	0	0	0	0	24	0	1,822	4,980
WAPA R.M.	0	0	3,538	0	0	78	0	206	0	0	0	0	0	739	4,561
Northeast	**0**	**997**	**7,607**	**0**	**0**	**310**	**239**	**2,138**	**0**	**369**	**0**	**0**	**532**	**2,468**	**14,659**
IDAHO	0	275	2,156	0	0	0	56	1,534	0	0	0	0	53	390	4,464
MONTANA	0	0	2,491	0	0	0	0	299	0	0	0	0	0	390	3,180
PACE	0	613	2,470	0	0	142	36	304	0	0	0	0	106	1,408	5,079
SIERRA	0	109	490	0	0	168	147	0	0	369	0	0	373	280	1,936
NW	**0**	**536**	**0**	**0**	**0**	**33**	**49**	**12,644**	**1,139**	**7**	**-25**	**17**	**165**	**8,357**	**22,923**
NORTHWEST	0	536	0	0	0	33	49	12,644	1,139	7	-25	17	165	8,357	22,923
Outside	**0**	**5,753**	**4,578**	**0**	**0**	**1,987**	**155**	**10,037**	**0**	**297**	**-21**	**0**	**263**	**1,671**	**24,720**
ALBERTA	0	5,039	4,578	0	0	1,987	0	304	0	63	-21	0	131	1,665	13,746
B.C.HYDRO	0	382	0	0	0	0	0	8,634	0	0	0	0	132	6	9,153
FORTISBC	0	0	0	0	0	0	0	1,029	0	0	0	0	0	0	1,029
MEXICO-CFE	0	333	0	0	0	0	155	0	0	234	0	0	0	0	722
WAPA U.M.	0	0	0	0	0	0	0	70	0	0	0	0	0	0	70
Total	**66**	**13,506**	**28,094**	**858**	**64**	**6,157**	**2,420**	**32,411**	**8,285**	**977**	**-1,305**	**3,810**	**2,612**	**20,904**	**118,860**

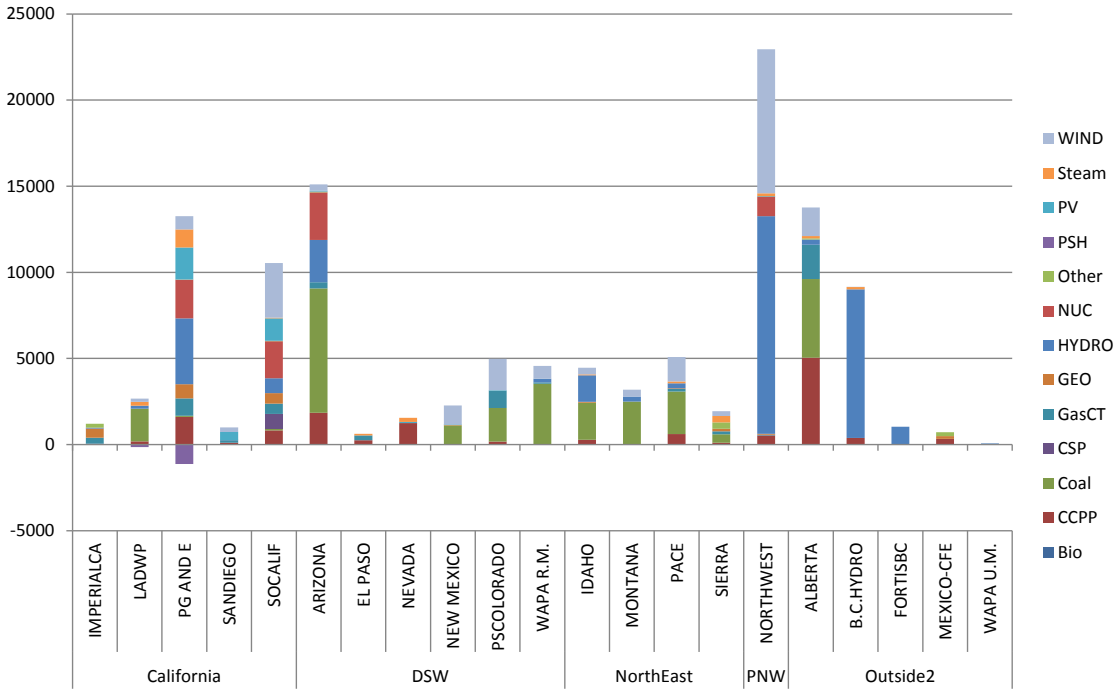

Figure 8. Generation type in the LSP Base case.

2.2.1.2 Heavy Summer

The generation type information identified in the LSP Base case can be used for the HS Base case. Table 3 and Figure 9 show the generation type information for the HS Base case.

Table 3. Generation Type for HS Base Case by Area

Area	Biomass	Combined Cycle	Coal	CSP	Gas CT	Geothermal	Hydro	Nuclear	Other	PSH	PV	Steam	Wind	Total
California	**158**	**18,439**	**2,104**	**355**	**7,545**	**1,630**	**6,646**	**4,550**	**11,687**	**825**	**1,134**	**4,608**	**2,121**	**61,801**
IMPERIALCA	49	0	0	0	346	544	40	0	440	0	0	115	0	1,534
LADWP	0	1,263	1,900	0	297	0	160	0	570	1,079	0	845	1,90	6,303
PG AND E	0	10,074	84	0	4,953	821	5,747	2,399	3,361	-294	701	1,398	787	30,032
SANDIEGO	0	2,233	0	0	449	0	4	0	920	40	388	0	325	4,359
SOCALIF	109	4,869	120	355	1,499	265	695	2,150	6,396	0	45	2,250	819	19,573
DSW	**0**	**17,986**	**16,447**	**0**	**4,961**	**0**	**3,947**	**4,134**	**3,747**	**394**	**113**	**1,395**	**769**	**53,893**
ARIZONA	0	8,940	8,117	0	1,198	0	2,822	4,134	1,189	114	0	737	227	27,478
EL PASO	0	704	0	0	454	0	0	0	288	0	0	176	47	1,669
NEVADA	0	4,580	0	0	884	0	0	0	281	0	61	310	0	6,116
NEW MEXICO	0	769	2,044	0	479	0	13	0	0	0	0	153	20	3,478
PSCOLORADO	0	2,554	1,864	0	1,936	0	0	0	1,304	100	52	19	444	8,273
WAPA R.M.	0	439	4,422	0	10	0	1,112	0	686	180	0	0	31	6,879
Northeast	**0**	**2,254**	**10,446**	**0**	**1,061**	**215**	**1,887**	**0**	**827**	**0**	**0**	**1,281**	**1,724**	**19,695**
IDAHO	0	261	2,210	0	371	0	1,337	0	0	0	0	25	142	4,346
MONTANA	0	40	2,583	0	0	0	502	0	0	0	0	58	108	3,290
PACE	0	1,750	4,894	0	519	36	49	0	552	0	0	482	1,155	9,435
SIERRA	0	203	760	0	172	179	0	0	275	0	0	716	320	2,625
NW	**0**	**6,025**	**0**	**0**	**520**	**0**	**24,096**	**1,151**	**1,100**	**-25**	**0**	**402**	**0**	**33,269**
NORTHWEST	0	6,025	0	0	520	0	24,096	1,151	1,100	-25	0	402	0	33,269
Other	**0**	**5,859**	**4,659**	**0**	**865**	**322**	**12,266**	**0**	**2,207**	**-21**	**0**	**868**	**1,000**	**28,025**
ALBERTA	0	4,931	4,659	0	865	0	552	0	750	-21	0	192	899	12,829
B.C.HYDRO	0	112	0	0	0	0	10,573	0	187	0	0	319	101	11,291
FORTISBC	0	0	0	0	0	0	1053	0	0	0	0	87	0	1,140
MEXICO-CFE	0	816	0	0	0	322	0	0	1,270	0	0	270	0	2,678
WAPA U.M.	0	0	0	0	0	0	87	0	0	0	0	0	0	87
Total	**158**	**50,562**	**33,657**	**355**	**14,952**	**2,167**	**48,842**	**9,835**	**19,568**	**1,174**	**1,247**	**8,554**	**5,614**	**196,683**

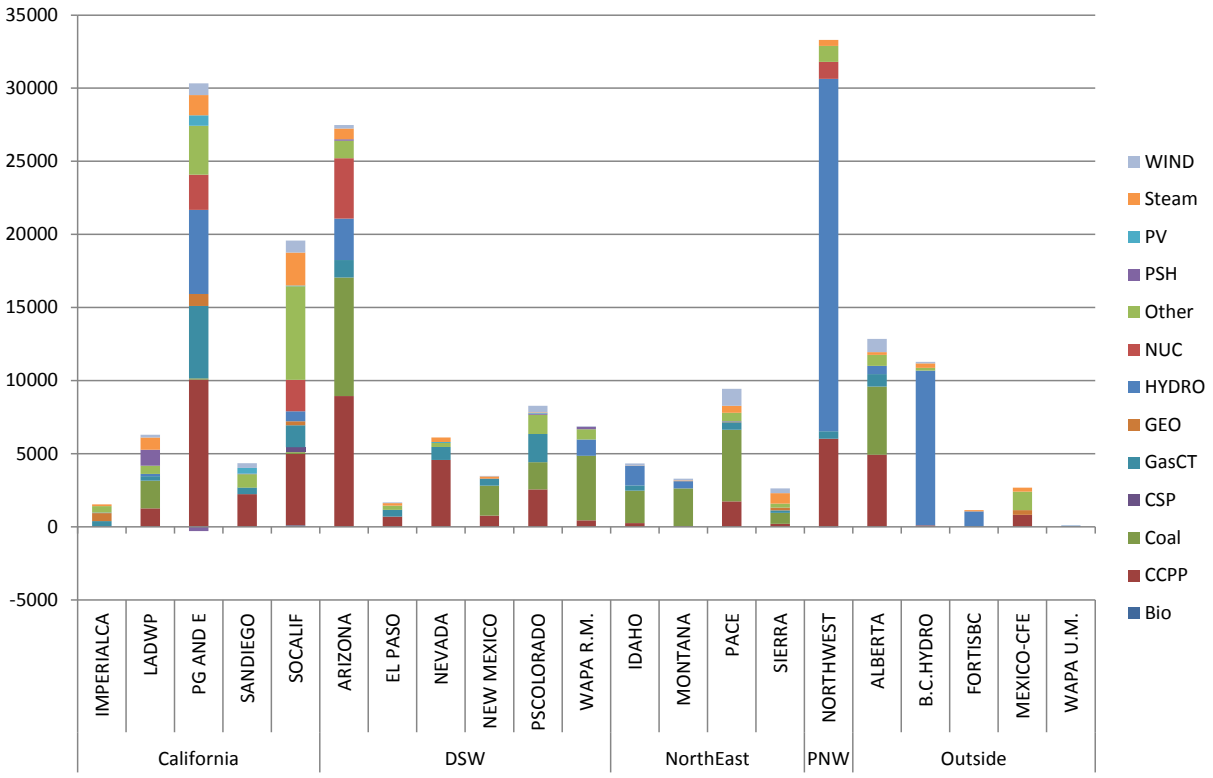

Figure 9. Generation type for HS Base case.

2.2.2 Dynamic Model Reconciliation

It is well understood in the Western Interconnection that accurate dynamic modeling is important to power system dynamic simulation. In the course of long-term planning, sometimes approximate models are used—particularly when the specifics of future plants are not firmly established. Because the dynamic behavior of wind and solar plants is substantially different from that of thermal and hydro plants, it is important that estimated models have the right basic dynamic characteristics.

Comparing the identified generation type against the model in the dynamic database enabled identification of incorrectly applied models. 182 wind and PV plants with a total generation of 4,505 MW were modeled as synchronous machines. As an example, Appendix Table 29 shows some wind plants that were represented by a synchronous generator model. Dynamic data for those 182 wind and PV plants were replaced with appropriate models.

In the LSP Original case, 54 wind, PV, and CSP units with total generation of 2,722 MW were netted. Appendix Table 31 lists those netted units. Netting was disabled and appropriate dynamic models were added for these units.

2.2.3 Composite Load Model

The original data sets used the standard WECC load model. This consists of roughly 20% induction motor and 80% static with voltage dependence, located at the transmission or sub-transmission level. At the request of the TRC, the new WECC composite load model

(CMPLDWG) was used (WECC 2012, WECC 2014), which represents the load at the distribution level and includes a significantly higher level of induction motor. The parameters for the composite load model were based on the WECC Modeling and Validation Working Group (MVWG) Load Model Data Tool, which takes into account regional differences in the characteristics of the load. The new CMPLDWG model was used to allow for addition of distributed PV (as discussed later in this section). This model was applied to most of the loads throughout the database. Loads less than 5 MW and loads whose characteristics were not identified in the load modeling data tool were modeled as static with voltage dependence. The load modeling for the LSP and HS cases is summarized below.

For LSP:

- 4,420 composite load models, 95.1 GW total load + distribution losses
- 22.3 GW of load not modified (modeled as static).

For HS:

- 4,408 composite load models, 143.9 GW total load + distribution losses
- 48.2 GW of load not modified (modeled as static).

Approximately 1.8 GW of large synchronous motor load was explicitly modeled in the dynamic data set.

The topology of the composite load, as shown in Figure 10, is intended to give a more realistic representation of dynamic load behavior than present practice. The parameters of the four equivalent motors are particularly important for dynamics, as the tendency for motor groups to stall (or not) during major voltage depressions has a substantial impact on system stability. One of the key features of the composite load model is the ability to control whether stalled motors trip (by contactors opening) or continue to run and draw starting current. For WWSIS-3, all motor tripping in the composite model is disabled because the motor stalling behavior has such a major and acutely non-linear effect on stability results. This is conservative, and allows for a simpler and more illuminating comparison between dynamic simulation cases.

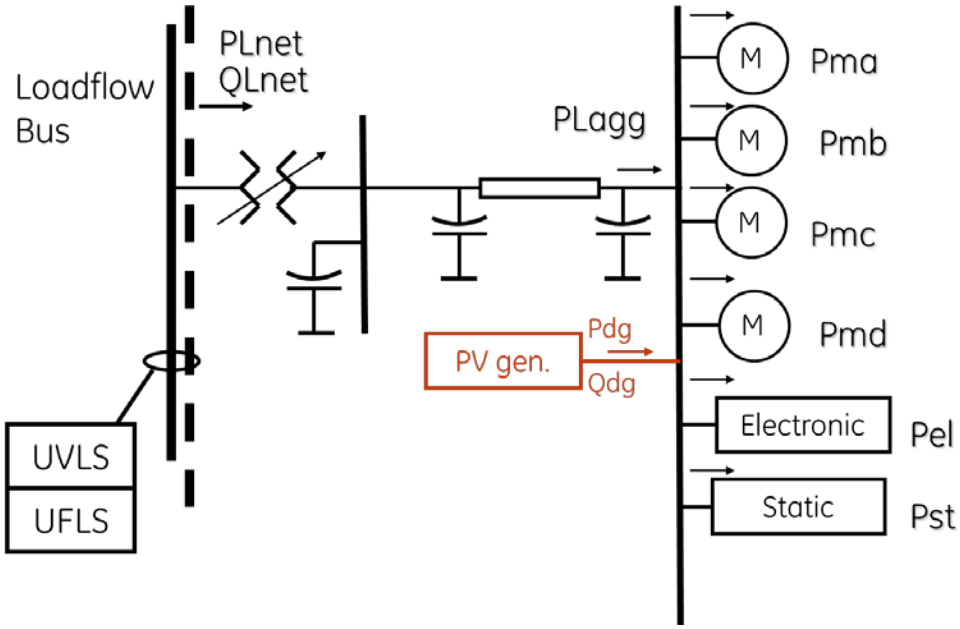

Figure 10. Composite load model topology.

The ability of the PV distributed generation (DG) to ride through voltage and frequency excursions is handled by a separate logic. The block diagram for this rather complex function is shown in Appendix Figure 78. The model allows selection of different levels of voltage and frequency excursion that will result in the DG blocking. A further part of the logic allows specification of how much DG will recover if the excursion returns within the user input bounds. The result is a high level of flexibility for modeling fault ride-through. However, the current model does not support user input time delays on the blocking functions, and so is limited in its ability to reflect deliberate time thresholds for tripping (e.g., of the type in NERC low-voltage ride-through [LVRT] and IEEE 1547 standards).

The topology of the composite load requires that the load flow initial condition be changed when DG is added. Specifically, the load flow active and reactive power load are labeled as PLnet and QLnet in the figure, respectively. The actual power consumed by the six constituents (four motor equivalents, electronic equivalent, and static equivalent) is less than PLnet by the losses in the equivalent feeder. Further, when DG is added, the generated power is consumed by the load, reducing the power from the grid. Thus, the addition of DG shows up in the load flow as reduced system load. The reduced flow on the equivalent feeder reduces the distribution system losses.

2.2.4 Dispatch and Commitment Characterization

The FR and transient stability of the system are dominated by the amount and type of generation committed and how it is dispatched. Throughout this report, care is exercised to distinguish classes of generation in accordance with their FR behavior. According to the power flow and dynamic data, each of the generators in the study system can be characterized as one of the following types:

Governor-responsive units have governor models and positive headroom. These will provide FR. *Base load units* have governors blocked from increasing mechanical power, but can respond to over-frequencies. Units with *no governor* models will be unresponsive regardless of the sign of

the frequency deviation. Base load and no governor units will not provide FR. All synchronous machines will provide inertial response. The default modeling assumption in this study is that wind and solar will not provide FR. CSP plants are modeled as base load, and are included in the total of unresponsive synchronous generation.

2.2.4.1 Metrics for Characterization

Throughout this report, tables summarize important aspects of the initial conditions used for various cases. These tables are intended to capture the critical characteristics of the generation and load as they relate to frequency performance. Table 4 lists the reported metrics, with a brief explanation of each. New monitoring was introduced for this study, which allows dynamic monitoring of the metrics during the course of dynamic simulation. Monitoring by WECC, by region, and by area was included, and selected traces are provided in the report below, as results are presented.

Table 4. Key to Case Summary Metrics

ID	Description
fr	Frequency (Hz) calculated from MVA weighted speed of synch machines
pg	Pgen of units with GR (GW)
mc	Capacity of units with GR (GW)
hr	Headroom of units with GR (GW)
nu	Number of units with GR
pm	Mechanical power of units with GR (GW)
mv	MVA rating of units with GR (GVA)
px	Pgen of units without GR (GW)
mx	Mechanical power of units without GR (GW)
nx	Number of units without GR
ps	Pgen of all synchronous generators (GW)
qs	Pgen of all synchronous generators (GVAr)
pl	P load (GW)
ql	Q load (GVAr)
pw	Pgen – Wind (GW)
qw	Qgen – Wind (GVAR)
pv	Pgen – Solar PV (GW)
qv	Qgen – Solar PV (GVAr)
ps	Pgen – CSP (GW)
dg	Pgen – Distributed solar PV generation (GW)
nh	Number of units with GR
Kt	The ratio of governor-responsive generation to total

The ratio of generation that provides GR to all generation running on the system is used to quantify overall system readiness to provide FR. A Lawrence Berkeley National Laboratory (LBNL) report (Undrill et al. 2010) introduces this ratio as the metric Kt; the lower the Kt, the smaller the fraction of generation that will respond. The exact definition of Kt is not standardized. For this report, it is defined as "mc / (mc+px+pw+pv)" or "GR MWCAP / GW Capability." This is the ratio of power generation capability of units with GR to the MW capability of all generation units. Power capability is defined as equal to the MW dispatch rather than the nameplate rating of nonresponsive generation because these units will not contribute beyond their initial dispatch. This is a reasonable definition, but industry discussion of a standard definition of Kt is warranted. Non-synchronous resources, including wind, solar, energy storage, and responsive loads, complicate the question. In all tables, only synchronous generation is included in the calculation of the capacity of units with GR (mc). Therefore, only synchronous generation is included in the calculation of Kt.

Tables documenting the initial conditions of all the study cases are included in the Appendix. At the end of this section, after other aspects of the case developments have been explained, a WECC-level comparison of the initial state of the most important metrics is presented.

2.2.5 Initial Condition Summary of Base Cases

A high-level view of the initial conditions for the LSP Base case is shown in the pie charts and table of Figure 5. Notice that there is no DG (i.e., distribution-connected PV) in this case. Explicit equivalents that were added by WECC in southern California are included with the (utility-scale) PV.

The generation information for the LSP Base case is summarized in Appendix Table 31, using the definition presented in Table 4. Appendix Table 32 shows details for all the areas.

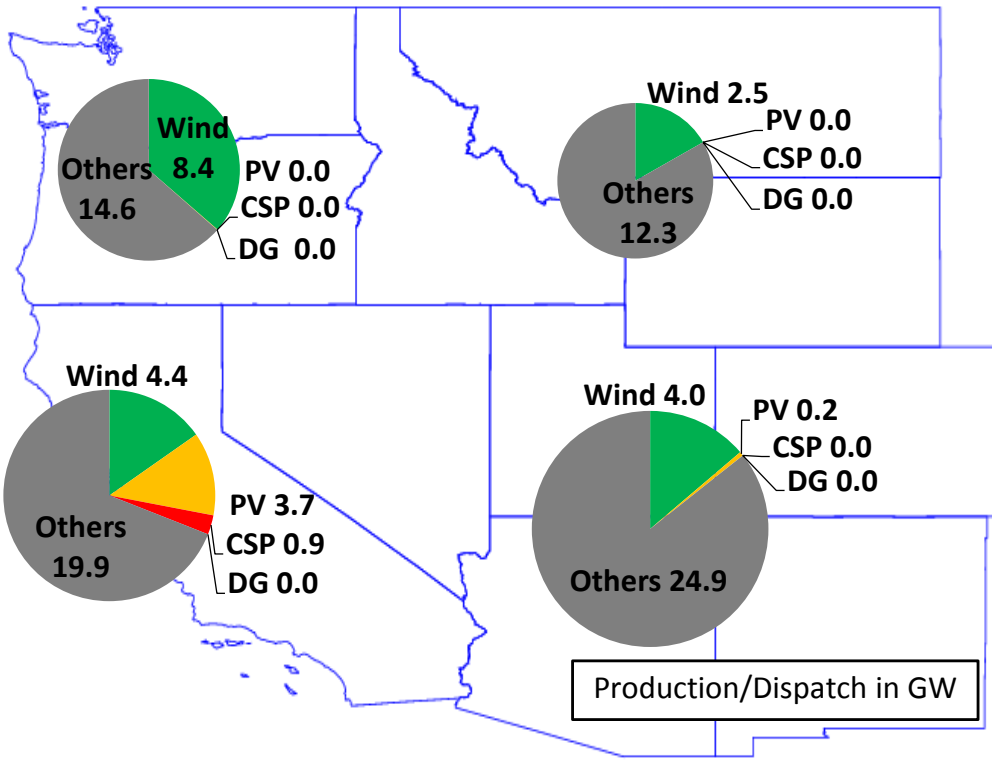

	WECC	California	DSW	Northeast	Northwest
Wind (GW)	20.9	4.4	4.0	2.5	8.4
PV (GW)	3.9	3.7	0.2	0.0	0.0
CSP (GW)	0.9	0.9	0.0	0.0	0.0
Distributed PV (GW)	0.0	0.0	0.0	0.0	0.0
Others (GW)	94.7	19.9	24.9	12.3	14.6
Total (GW)	120.3	28.9	29.1	14.7	22.9
Penetration (%)	21%	31%	14%	17%	36%

Figure 11. Wind and solar generation in the LSP Base case.

A high-level view of the initial conditions for the HS Base case is shown in Figure 6. This figure, when compared to the previous one, emphasizes that the HS Base case assumes a dramatically lower level of wind and solar than the LSP case, as intended by WECC. The initial condition details by region are shown in Appendix Table 33 and by area in Appendix Table 34.

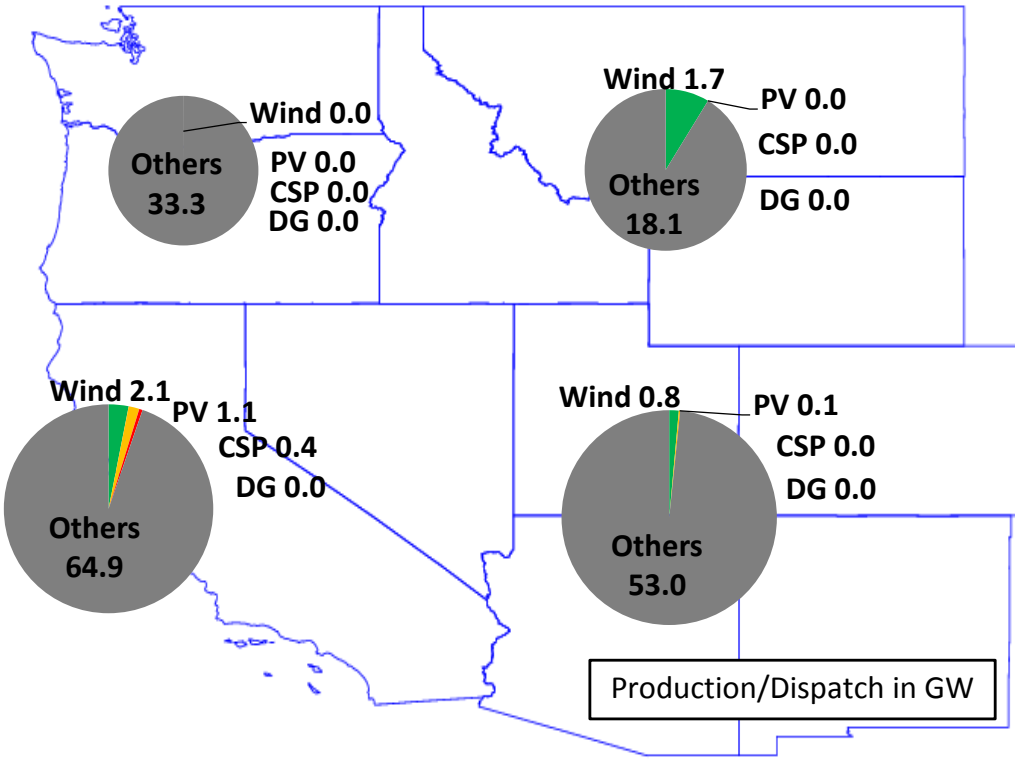

	WECC	California	DSW	Northeast	NW
Wind (GW)	5.6	2.1	0.8	1.7	0.0
PV (GW)	1.2	1.1	0.1	0.0	0.0
CSP (GW)	0.4	0.4	0.0	0.0	0.0
Distributed PV (GW)	0.0	0.0	0.0	0.0	0.0
Others (GW)	196.2	64.9	53.0	18.1	33.3
Total (GW)	203.4	68.5	53.9	19.8	33.3
Penetration (%)	4%	5%	2%	9%	0%

Figure 12. Wind and solar generation in the HS Base case.

2.3 Performance and Monitoring Metrics

2.3.1 Performance Metrics

2.3.1.1 Frequency Response

FR metrics are established by the new NERC BAL-003-1 (NERC 2012a). The primary requirement is that the minimum frequency during design-basis disturbances should not cause UFLS. In the West, the first stage of UFLS is normally at 59.50 Hz. Some margin above that level to account for normal pre-disturbance variation in frequency (24 mHz) is needed for simulations.

2.3.1.2 Transient Stability

The transient stability performance requirements are well defined by WECC. Appendix Table 35 specifies the system performance requirements for various categories of events. As an example, the WECC rules dictate that a category B disturbance in the system shall not cause a transient voltage dip that is greater than 20% for more than 20 cycles at load buses at any time other than during the fault.

2.3.2 Area and Regional Monitoring

To make the comparisons of the study results less confusing, all protective relays explicitly modeled in the database were switched off. New dynamic models (epcmod) had been developed to record metrics in Table 4 for all of WECC, each of the 21 areas defined in the databases, and four regions (California, NW, DSW, and Northeast). These metrics were monitored dynamically and output to the channel file for each simulation.

Voltage, frequency, and angle were monitored at key high-voltage buses in the Western Interconnection. Appendix Figure 80 and Appendix Table 36 show the detailed information for these key buses. Voltage and frequency were also monitored for all buses that are 230 kV and above. Flows on all major interfaces were monitored.

2.3.3 Reference Disturbances

Five disturbances (shown below in Table 5) were selected to evaluate the impacts of high penetrations of wind and solar generation on the FR and transient stability. Some of these contingencies (e.g., loss of PDCI) normally involve a remedial action scheme (RAS) to improve post-contingency system performance. However, the TRC agreed that such non-linear actions obscure rather than illuminate the differences caused by added wind and solar. The added complexity only makes the results more difficult to interpret. In general, therefore, RAS were not simulated. For similar reasons, the relay models, including UFLS, were also de-activated.

There is an exception: the analysis of the loss of PDCI examined system performance both with and without a simple generation-tripping RAS.

Table 5. Study Disturbances

Name	Description
Loss of Two PV	Loss of the two Palo Verde nuclear power station units
Loss of PDCI	Bi-polar loss of the PDCI 500 kV line
Vincent Fault	Three-phase Vincent 500 kV fault and loss of one Midway-Vincent 500 kV line
Laramie Fault	Three-phase Laramie 345 kV fault and loss of the Laramie-Story 345 kV line
Aeolus Fault	Three-phase Aeolus 500 kV fault and loss of the Aeolus-Anticlin 500 kV line

2.4 Renewables Siting

The wind and solar data used in this study are based on the WWSIS-2 High Mix scenario. This scenario defined an equal mix of wind and solar resources totaling approximately 33% energy penetration for the year 2020 load for the Western Interconnection. Specifically, 16.5% of load was supplied by wind resources and 16.5% by various solar technologies including distributed PV, utility-scale PV, and CSP.

Most of the 16.5% wind plants are between 100 MW and 200 MW. There are 276 wind plants representing approximately 44,000 MW assigned to the Hi-Mix scenario. Of the 16.5% solar resources, 60% were PV and 40% were CSP. The 60% PV was further divided as 40% distributed PV, 20% utility-scale PV near population centers, and 40% utility-scale PV located at best resources. In the WWSIS-2 data, there are a total of 326 utility-scale PV plants (best-resource and population-centered combined) with an average plant size of 72 MW, median of 52 MW, and maximum of 200 MW. There are 108 CSP plants with an average size of 130 MW, median of 105 MW, and maximum of 200 MW.

Note that most of the wind, PV, and CSP sites from the WWSIS-2 data have a corresponding substation (bus) in the LSP Base case and HS Base case, and were therefore candidates to be added. Only a few sites are excluded due to a missing bus or isolated bus. Figure 13 shows the wind and solar sites that were identified in the WECC case.

The addition of distributed PV was handled differently. As discussed in Section 2.2.3, the distributed PV was embedded with the complex load model. The dispatch of these renewables varies with the different cases, depending on the instantaneous renewable power penetrations.

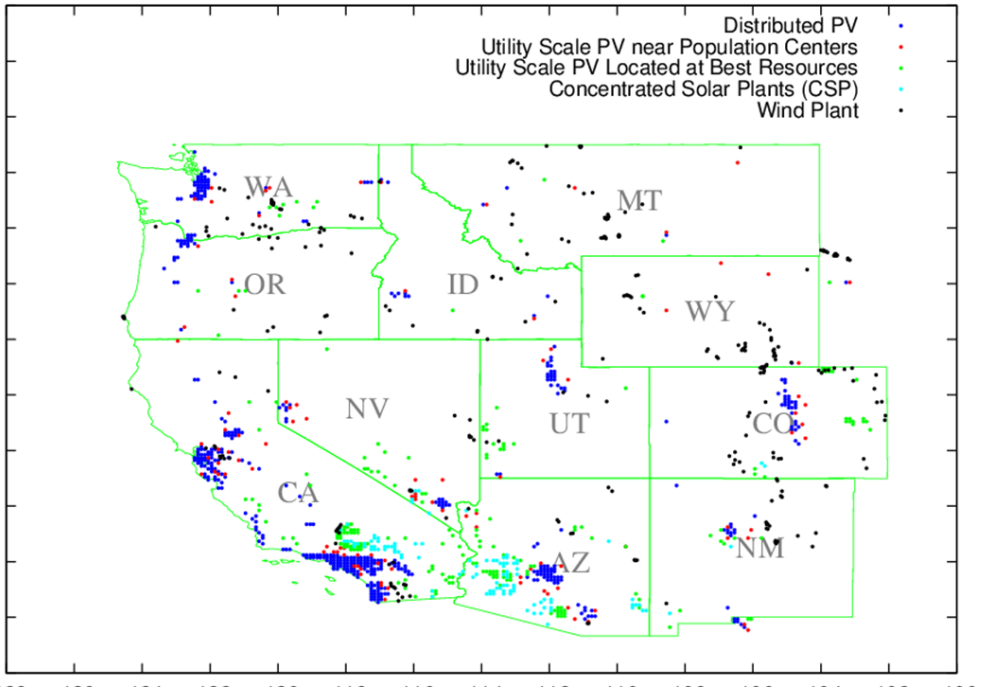

Figure 13. All potential renewable sites.

Table 6 shows the actual breakdown by state for the various wind and solar technologies from the WWSIS-2 Hi-Mix scenario. This breakdown guided the incremental changes made to the WECC LSP and HS Base cases in the creation of the Hi-Mix cases for this study, with the intent of matching the capacity by area in the Hi-Mix cases for this study to the Hi-Mix capacity in the WWSIS-2 cases. As noted above, the mapping between the WWSIS-2 system topology and the WECC cases is good, but not perfect, so the capacity numbers do not perfectly align with the Hi-Mix cases of this study.

Table 6. Wind and Solar Generation in WWSIS-2 Hi-Mix Scenarios

	Rooftop PV			Utility-Scale PV			CSP			Wind			Total		
State	**Capacity (MW)**	**Capacity Factor**	**Energy (GWh)**	**Capacity (MW)**	**Capacity Factor**	**Energy (GWh)**	**Capacity (MW)**	**Capacity Factor**	**Energy (GWh)**	**Capacity (MW)**	**Capacity Factor**	**Energy (GWh)**	**Capacity (MW)**	**Capacity Factor**	**Energy (GWh)**
Arizona	3,655	19%	6,160	5,394	25%	12,029	9,374	42%	34,385	1,440	30%	4,009	19,863	33%	56,582
California	8,412	18%	12,984	9,592	24%	19,715	3,594	45%	13,884	6,157	27%	16,690	27,754	26%	63,272
Colorado	1,127	18%	1,794	1,653	21%	3,143	169	37%	541	4,396	36%	12,869	7,344	29%	18,346
Idaho	3	17%	5	2	18%	2				1,093	29%	2,787	1,098	29%	2,794
Montana	25	15%	33	34	18%	51				4,288	37%	13,659	4,347	36%	13,742
Nevada	772	19%	1,275	3,282	26%	7,593	562	40%	1,963	1,560	31%	4,373	6,177	28%	15,204
New Mexico	943	20%	1,638	1,280	27%	3,031	298	40%	1,032	3,134	39%	10,520	5,654	33%	16,221
Oregon	101	14%	120	126	20%	231				5,413	25%	12,283	5,640	26%	12,634
South Dakota	4	17%	6	6	20%	10				1,950	36%	6,231	1,960	36%	6,248
Texas	208	20%	361	193	25%	428							401	22%	789
Utah	1,204	17%	1,801	1,216	21%	2,305				683	30%	1,950	3,102	22%	6,056
Washington	405	13%	460	709	18%	1,186				5,762	28%	13,781	6,876	26%	15,427
Wyoming	10	18%	16	18	21%	32				7,244	43%	27,711	7,272	44%	27,759
Total	**16,870**	**18%**	**26,651**	**23,504**	**24%**	**49,756**	**13,997**	**42%**	**51,805**	**43,118**	**34%**	**126,861**	**97489**	**30%**	**255,073**

2.5 Incremental Commitment and Dispatch

A credible method to change commitment and dispatch is critical to the creation of meaningful and comparable cases for this study. A one-to-one de-commitment of conventional generation to accommodate wind and solar is overly simplistic. Transient stability and FR are dominated by the generation initial conditions. Thus, realistic and economically rational initial conditions are needed. The load flow that provides the starting point for dynamic simulations is a single snapshot in time and not, in itself, an economic tool. Therefore, it is necessary to use economic tools to guide the commitment and dispatch process.

The process outlined in this section is based on the WWSIS-2 PLEXOS results. In that study, a base level of wind plus solar was compared to the Hi-Mix system with much more wind and solar. The result was annual simulations at 5-minute intervals—about 100,000 system-wide data points per year per case.

As discussed above, LSP and HS load cases were selected for this study. The previous section documented the addition of new wind and solar generation capacity. The overall intent of this step is to re-commit and re-dispatch the conventional generation to allow meaningful investigation of the impact of adding wind and solar to the system. As wind and solar generation pick up, other generation will be displaced in a fashion that results in the lowest operating cost that satisfies the system physical and security constraints. The process is more complex than might be expected, as the two starting cases do not have the same infrastructure. In other words, there are differences in the generation portfolio, the load level, and the resultant commitment and dispatch, as well as some minor topological differences. More important, there are significant differences between the two power flow base cases and the WWSIS-2 PLEXOS Base case. The objective was to get clearer insight into the effective dispatch and commitment rules that apply during LSP periods.

The overall process is as follows:

1. Mine the WWSIS-2 PLEXOS Base case to select sample periods similar to the power flow conditions (e.g., LSP morning with high wind and solar production).
2. Compare the incremental changes between the WWSIS-2 Base and the Hi-Mix scenarios for the selected periods.
3. Determine how the commitment and dispatch of other generation in the West tends to change during these time periods by examining the differences between the two WWSIS-2 scenarios.
4. Increase the wind and solar dispatch in the WWSIS-3 LSP and HS Base cases consistent with the new capacity added.
5. Use the trends extracted from the WWSIS-2 incremental changes to guide changes to the LSP and HS Base cases in order to create new LSP Hi-Mix and HS Hi-Mix cases. Start with unit de-commitments, and then re-dispatch non-wind and non-solar generation.

The rest of this section examines the details of these five steps. Additional supporting material is included in the Appendix.

2.5.1 Mining PLEXOS Results from WWSIS-2

The WWSIS-2 PLEXOS Base case results were filtered to capture periods of operation that are close to that of the WECC LSP case. The 105,120 PLEXOS results (8,760 hour/year x 12 5-minute periods/hour) were searched for periods that met the following criteria:

- Daytime (PV ≠ 0.0)
- First month of spring (March 21–April 21)
- Load within 10 GW of WECC LSP case: 115 GW
- Total wind plus solar production > 18 GW in PLEXOS Base (WECC LSP case has 24.4 GW of wind and solar in the United States).

A total of 487 5-minute samples (about 0.5% of the full year) met these criteria. The samples were spread across nine contiguous windows on nine different days (as listed in Appendix Table 37). Of those sample periods, the average wind plus solar production was 20.6 GW in the PLEXOS Base case and 48.3 GW in the PLEXOS Hi-Mix case. The single highest condition was 26.5 GW in the Base case and 62.9 GW in the Hi-Mix case.

2.5.1.1 Mining PLEXOS Spring Samples

In order to understand the general impact of wind and solar generation on dispatch and commitment, the dispatch of all of the committed generation is collected and summarized by type. As the only change between the PLEXOS Base and Hi-Mix cases is the addition of wind and solar, the dispatch reflects both the instantaneous penetration and sequential history of load, weather, outages, and, most important, commitment constraints such as minimum downtime, startup costs, and marginal heat rates.

Thus, pairing of the two cases effectively filters out only the impact of wind and solar generation for operations under LSP load with high wind and solar availability.

Previous work in WWSIS-1 and WWSIS-2 showed that displacement of marginal thermal generation is a strong function of net load and renewable penetration levels. Figure 14, which includes data from all three spring months, reveals important trends and differences between the behaviors of CC generation for the two cases. This figure contains four colored clusters of data points. The idea is to illuminate how CC dispatch changes as a function of wind and solar production, and as a function of system load. Each point is an XY pair of total CC dispatch (MW) vs. wind plus solar power, or of total CC dispatch (MW) vs. system load. The key to the clusters is as follows:

- Blue: PLEXOS Base case CC Power vs. Wind + Solar Production (MW)
- Red: PLEXOS Base case CC Power vs. System Load (MW)
- Green: Hi-Mix CC Power vs. Wind + Solar Production (MW)
- Purple: Hi-Mix CC Power vs. System Load (MW).

Each cluster includes (in black) a linear regression with the equation printed on the figure. Further, the mean value of each cluster is noted with a balloon. So, for example, examining the cluster of blue points shows that the mean value of the grouping is 20,633 MW of CC dispatch

for 9,028 MW of wind plus solar production. The regression shows that the slope of the line is -0.5061, which means that for every 1 MW increase in wind plus solar production, about 0.5 MW of CC generation will be backed down. In other words, CC plants are balancing much of the changes in wind and solar production in the Base case. Having CC generation on the margin and responsible for a substantial part of balancing is not surprising at these moderate levels of wind and solar. The CC plants are also important in balancing system load in the Base case. The red cluster shows that during a LSP day with good wind and solar production, about two-thirds of the load following (0.6512) is done by CC plants.

The contrast with the Hi-Mix case is dramatic. The mean CC plant production drops by 83% to 1,562 MW. The 27,653 MW increase in wind and solar production pushes the majority of the CC out of the stack. The remaining CC plants contribute about 5% of the wind and solar balancing, and are largely inactive for load following. They are mostly at or near minimum, so the wind and solar following is apparently driven by drops in the renewable production. These data do not explicitly show the fraction of units that change commitment rather than only changing dispatch. The difference between backing down and de-committing has big implications for both FR and transient stability. This is addressed below.

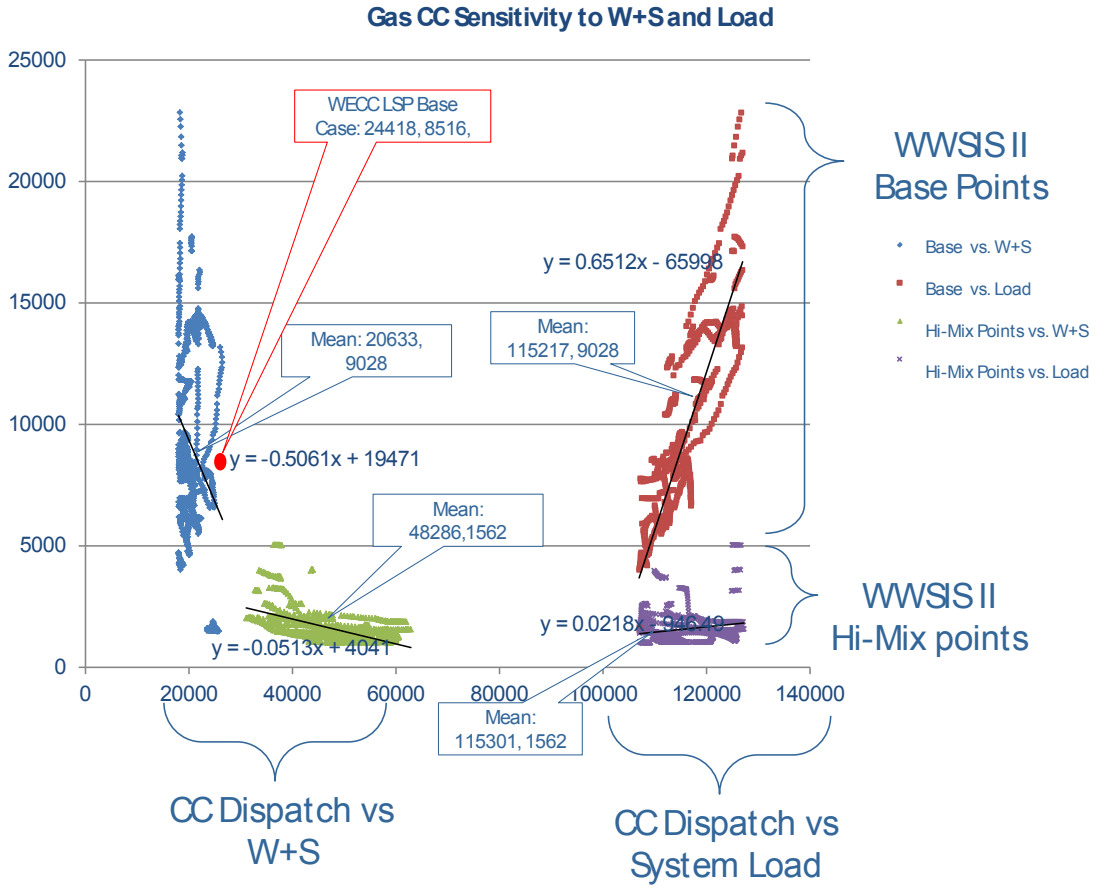

Figure 14. Dispatch sensitivity of CC plants in LSP window.

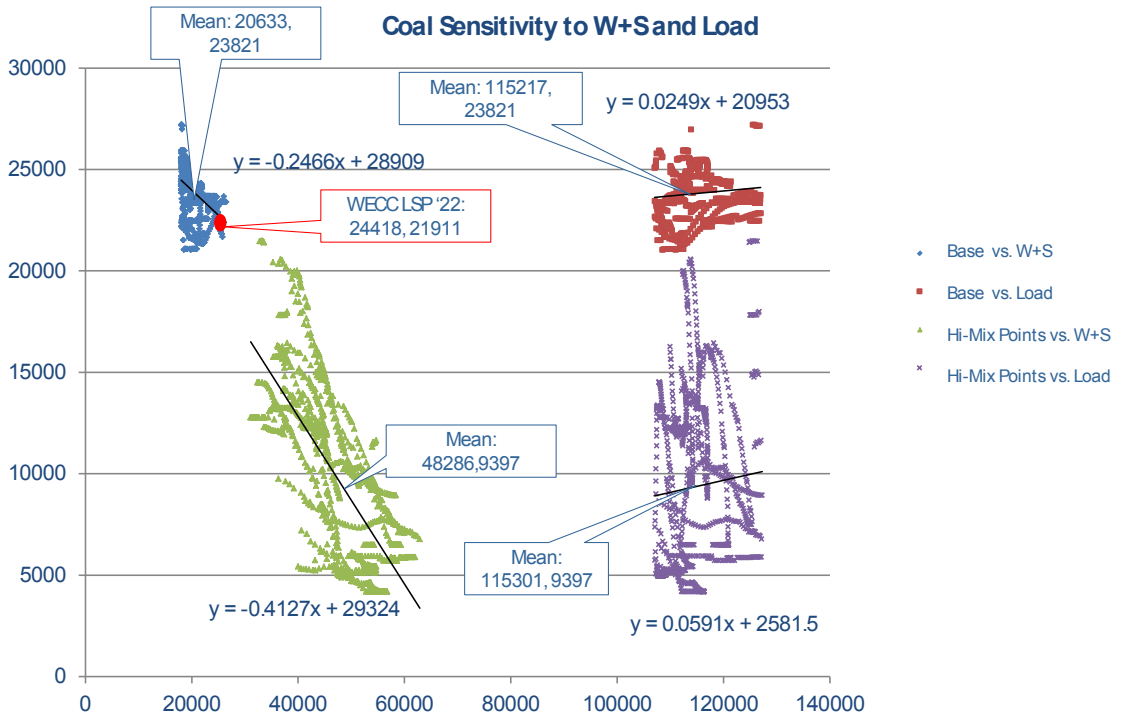

Figure 15. Dispatch sensitivity of coal plants in LSP window.

A similar investigation of the coal plants (see Figure 15) shows another fundamental change in operations. In the PLEXOS Base case, the coal plants do essentially no load following—they are baseload, but they do about one-quarter of the wind plus solar following. There is a substantial reduction of coal in the Hi-Mix case, but coal continues to do essentially no load following. The coal plant participation in following the variation in wind and solar increases to about 40%. As noted, this plot alone does not provide direct data about de-commitments, but subsequent mining shows that about 10 GW tends to be de-committed, and on average another 5 GW is dispatched down.

Participation in load following or wind plus solar following varies in other types of generation. The simple-cycle combustion turbines (see Appendix Figure 86) are on average insensitive to load or wind plus solar. For this analysis, the use of combustion turbines (CTs) is assumed to be primarily driven by forecast errors and reserve constraints. Consequently, CTs have been left untouched in the de-commitment and re-dispatch work. Hydro (see Appendix Figure 87) is also relatively insensitive to wind and solar, but tends to be more sensitive to load. The hydro in the Northwest is rather more sensitive, and provides a resource for adjustment to changes in wind and solar. Pumped-storage hydro (see Appendix Figure 88) is sensitive to both wind and solar, and to load. For this work, it is not addressed except in one of the sensitivities reported later.

This macro investigation gives broad guidance on how to modify the dispatch and commitment of the non-variable renewable resources in the Hi-Mix stability load flow. The next step was to develop rules for de-committing and re-dispatching generation within each area for periods of operation that look like the LSP condition. Because the mapping of individual generation from PLEXOS to WECC LSP 2022 is imperfect, the approach focuses on the delta, leaving the LSP base case dispatch and commitment unchanged from that provided by WECC.

Investigation of individual CC and coal plants shows that during this type of operation, the plants tend to be either at maximum or minimum. Some plants tend to be rarely de-committed; others come on- and off-line more often.

There is a broader question of whether the generation portfolio will meet load under other system conditions or at other times of year. However, that question was already addressed by WWSIS-1 and WWSIS-2. WWSIS-3 focuses solely on specific snapshots in time.

2.5.1.2 Create Light Spring Hi-Mix Case

The LSP Hi-Mix case was created from the LSP Base case using the results of the trend investigation. Because the intent was to create a meaningful counterpoint to the LSP Base case, a single sample wind and solar data point was required. The mean value of the wind and solar production for all the 487 samples would unrealistically smooth the plant outputs, which will in reality vary substantially over the geography of the Western Interconnection at any instant of time. The sample that closely represents the mean of the sample space is sample #31775 (April 4, 2012 at 7:50). That sample was selected as the target for the Hi-Mix case. The new LSP Hi-Mix dispatch was developed to approximately replicate the PLEXOS sample without changing the dispatch (or commitment) of any of the wind or solar generation in the LSP Base case.

The process of mapping the PLEXOS Base and Hi-Mix cases to the LSP Base power flow case included the following steps:

- Map bus numbers, area, and zone information for existing plants
- Map bus numbers, area, and zone information for added renewables
- Disregard PLEXOS Hi-Mix plants without corresponding bus number in the LSP Base case
- Extract wind, CSP, and PV dispatches by area (for all 17 U.S. areas) for sample #31775
- Establish the split of PV between utility-scale PV and distributed PV (DG)
- Add new wind, CSP, and utility-scale PV plants to load flow and stability databases
- Add distribution-connected PV, as DG, to the load flow by modifying Pload and Qload, and then adjusting the composite load model to include the correct amount of DG
- Dispatch utility-scale wind and solar toward the target for sample #31755
- De-commit CC and coal plants that were likely to be displaced by wind and solar under this condition
- Re-dispatch remaining CC, coal and, where necessary, hydro, to solve the load flow satisfactorily.

2.5.1.3 Renewables in Light Spring Base and Hi-Mix Cases

The final variable renewable capacity for the LSP cases is shown in Table 7. These are nameplate values and dictate the ratings of the connecting load flow elements [e.g., generator step up (GSU) transformers] and the dynamic models.

Table 7. Renewable Capacity for LSP Cases

	LSP Base Case			LSP Hi-Mix Case			
Area	**CSP**	**Utility-Scale PV**	**Wind**	**CSP**	**Utility-Scale PV**	**Distributed PV**	**Wind**
ALBERTA	0	0	2,707	0	0	0	2,707
ARIZONA	0	971	347	6,879	4,923	3,655	1,435
B.C.HYDRO	0	0	108	0	0	0	108
EL PASO	0	0	0	142	343	368	50
IDAHO	0	0	643	0	0	0	643
IMPERIALCA	0	0	0	188	611	71	917
LADWP	0	0	576	1,043	913	1,961	576
MEXICO-CFE	0	0	0	0	0	15	0
MONTANA	0	0	707	0	11	21	3,975
NEVADA	0	64	0	229	556	285	0
NEW MEXICO	0	100	1,726	156	1,260	758	3,108
NORTHWEST	0	59	8,680	0	869	500	11,655
PACE	0	0	2,384	0	390	1,126	4,111
PG AND E	0	3,232	2,399	0	3,232	1,474	2,399
PSCOLORADO	0	79	2,134	169	1,016	547	2,134
SANDIEGO	0	528	712	0	528	421	712
SIERRA	0	0	432	0	1,504	432	777
SOCALIF	1,436	2,139	4,497	2,814	5,913	4,741	4,497
FORTISBC	0	0	0	0	0	0	0
WAPA R.M.	0	4	739	0	690	594	8,136
WAPA U.M.	0	0	0	0	0	0	60
Total	**1,436**	**7,164**	**28,616**	**11,618**	**22,747**	**16,969**	**47,999**

The LSP Base case, which reflects a commitment and dispatch for the LSP case, does not align perfectly with the starting point of the WWSIS-2 PLEXOS runs. Consequently, the *increment* between the WWSIS-2 PLEXOS Base and High Mix cases is used to give the *increment* targeted when changing from the LSP Base case to the LSP Hi-Mix case. The word "target" is important. Unit ratings, as well as a degree of topological mismatch, influence the ability to reach the target. From the perspective of this investigation, the results are desirable. The net capacity, commitment, and dispatch of wind and solar generation are greater than those of the WWSIS -2 High Mix case.

The target capacity factor of the added wind and solar provides an additional constraint to that of maintaining the renewable dispatch in the Base case. In a few areas, the new plants couldn’t be

dispatched high enough to meet the target (>100%), and so dispatch was limited to rated power. In Appendix Table 40, the differences between the WWSIS-2 PLEXOS Base dispatch and the High Mix (data point #31775) are listed by area. A comparison of final renewable dispatches for the LSP cases is shown in Table 8.

The WWSIS-2 PLEXOS simulation results, and in particular the difference between the Base and High Mix cases, were credibly mapped to the power flow and dynamic model databases.

Table 8. Renewable Dispatch for LSP Cases

	LSP Base Case			LSP Hi-Mix Case			
Area	**CSP**	**Utility-Scale PV**	**Wind**	**CSP**	**Utility-Scale PV**	**Distributed PV**	**Wind**
ALBERTA	0	0	1,665	0	0	0	1,665
ARIZONA	0	50	347	6,395	1,407	1,400	775
B.C.HYDRO	0	0	6	0	0	0	6
EL PASO	0	0	0	142	226	193	2
IDAHO	0	0	390	0	0	0	390
IMPERIALCA	0	0	0	124	275	30	339
LADWP	0	0	190	490	402	823	190
MEXICO-CFE	0	0	0	0	0	0	0
MONTANA	0	0	390	0	3	2	1,599
NEVADA	0	60	0	112	374	158	0
NEW MEXICO	0	28	1,091	156	295	207	999
NORTHWEST	0	17	8,354	0	317	196	8,361
PACE	0	0	1,408	0	86	228	2,662
PG AND E	0	1,861	764	0	1,860	561	764
PSCOLORADO	0	24	1,822	169	605	339	1,822
SANDIEGO	0	528	272	0	528	111	272
SIERRA	0	0	280	0	722	203	625
SOCALIF	858	1,300	3,177	857	2,696	2,182	3,177
FORTISBC	0	0	0	0	0	0	0
WAPA R.M.	0	0	739	0	425	347	3,328
WAPA U.M.	0	0	0	0	0	0	27
Total	**858**	**3,868**	**20,895**	**8,445**	**10,221**	**6,980**	**27,003**

2.5.1.4 De-Commitment/Re-Dispatch from WWSIS-2 PLEXOS Base to Hi-Mix

The overall dispatch trends for periods similar to the LSP condition were used to develop rules for de-committing and re-dispatching conventional generation. A total of 583 coal and CC units

were examined in the 487 sample space for patterns of operational change due to increased wind and solar.

For each unit, the tendency to be re-dispatched or de-committed for similar conditions was examined. Units that were de-committed for more than 30% of the samples were shut down. The net results are summarized in Table 9, which gives the plant count and average MW of generation dropped. So, for example, 20 individual plants in Arizona are de-committed for an expected drop of 1,265 MW in generation.

These are based on the PLEXOS results; not all the individual units expected to shut down would necessarily be on-line in the WECC LSP case, nor would they necessarily be at the dispatch suggested by the mean numbers listed.

Table 9. Coal and Combined-Cycle De-Commitment

Area Name	Area #	# of Units	Average Change in P [MW]
ALBERTA	54	6	223
ARIZONA	14	20	1,265
BC HYDRO	50		
EL PASO	11		
IDAHO	60	5	203
IMPERIALICA	21	1	37
LADWP	26	1	35
MEXICO-CFE	20	2	36
MONTANA	62	3	139
NEVADA	18		
NEW MEXICO	10	3	86
NORTHWEST	40	3	229
PACE	65	14	661
PG&E	30	6	497
PSCOLORADO	70	10	555
SAN DIEGO	22	1	35
SIERRA	64	3	156
SOCALIF	24	2	72
FORTISBC	52		
WAPA R.M.	73	21	1,226
WAPA U.M.	63		
Total		**101**	**5,455**

Re-dispatch follows de-committing the available plants. The units that were often re-dispatched in the sample space (i.e., more than 50 times in the sample space) were backed down. For the

majority of plants, this meant that they were dispatched down to their minimum power. Displacing thermal plants (other than CTs, per the discussion above), is insufficient to meet the wind and solar displacement, so hydro in the Northwest and British Columbia are also dispatched back. Hydro units that had $\Delta P > 0$ more than 10 times in the sample space were used.

The key point of all this detail is that location matters. Displacement by wind and solar is not one-for-one in each area. Further, in this sample space, the economic tendency is for more downward dispatch than de-commitment. This has stability and FR implications and is explored later in this report.

Table 10. Re-Dispatch for Coal, Combined-Cycle, and Hydro

Area Name	Area #	# of Units	Average Change in P [MW]
ALBERTA	54	3	102
ARIZONA	14	15	3,645
BC HYDRO	50	1	90
EL PASO	11		
IDAHO	60	4	719
IMPERIALICA	21		
LADWP	26	3	1,234
MEXICO-CFE	20	3	149
MONTANA	62	5	1,113
NEVADA	18	2	164
NEW MEXICO	10	5	1,071
NORTHWEST	40		
PACE	65	21	2,254
PG&E	30	16	334
PSCOLORADO	70	6	715
SAN DIEGO	22	3	41
SIERRA	64	3	378
SOCALIF	24	7	253
FORTISBC	52		
WAPA R.M.	73	15	1,847
WAPA U.M.	63		
Total Coal+CC		**112**	**14,109**
BC HYDRO	50	7	1,072
NORTHWEST	40	126	1,797
Total Hydro		**133**	**2,869**

2.5.1.5 Mining PLEXOS Summer Samples

A similar process was used to develop the HS Hi-Mix case. Screening PLEXOS base and Hi-Mix data for summer (July 16–August 26, 2020) with high wind and solar conditions resulted in 95 5-minute samples, spread across 10 contiguous windows on 10 different days (listed in Appendix Table 38). Sample #68417, August 25 at 13:20, is closest to the mean of the samples.

Overall, the same approach used for LSP was pursued here. However, the differences between the WWSIS-2 systems and the HS Base power flow were more significant given that the PLEXOS data represented a 2020 load condition and the HS power flow data represented a 2023 load condition. Most notably, the HS Base case has a load of ~192 GW, whereas the highest load ever in the PLEXOS study was 169 GW. This causes the mapping to be of lower fidelity.

The PLEXOS results were filtered to capture periods of operation that are close to that of the WECC HS 2023 case, with characteristics as shown in Table 11.

Table 11. Renewable Averages from HS PLEXOS Screening

Resource	Screening Criteria	Base Average	Hi-Mix Average
CSP	>4,000 MW	4,568 MW	9,745 MW
PV	>4,000 MW	4,201 MW	24,887 MW
Wind	>3,000 MW	4,513 MW	9,362 MW
Load	>150 GW	152.8 GW	152.8 GW

The average wind plus solar production in the PLEXOS samples is 13.3 GW, which is substantially higher than the 6.4 GW in the WECC HS data (U.S. only). This makes sense, as the HS case was not developed by WECC for specific consideration of a higher-renewable future. The Hi-Mix samples have an average renewable generation of 44.0 GW.

As with the LSP cases, the commitment and dispatch under HS conditions shows that most of the load following is done by CC plants (Appendix Figure 89), and to a lesser degree, hydro. There is essentially no change in the coal plants, as shown in Appendix Figure 90.

The process of adding renewable capacity was similar to that used for the LSP Base to Hi-Mix development. More wind and solar plants needed to be added, as the HS Base case starts with fewer plants than the LSP Base case. A comparison of the total capacity of the two HS cases is shown in Table 12. Appendix Table 42 gives the total capacity, including the WWSIS-2 case for reference.

Table 12. Renewable Capacity for HS Cases

	HS Base Case			HS Hi-Mix Case			
Area	**CSP**	**Utility-Scale PV**	**Wind**	**CSP**	**Utility-Scale PV**	**Distributed PV**	**Wind**
ALBERTA	0	0	1,061	0	0	0	1,061
ARIZONA	0	700	227	7,654	5,202	3,655	1,457
B.C.HYDRO	0	0	237	0	0	0	237
EL PASO	0	0	47	142	350	305	68
IDAHO	0	0	407	0	0	0	564
IMPERIALCA	0	0	0	188	611	71	917
LADWP	270	0	574	837	913	1,961	574
MEXICO-CFE	0	0	0	0	0	15	294
MONTANA	0	0	364	0	27	21	3,989
NEVADA	0	64	0	229	656	324	0
NEW MEXICO	0	27	396	156	1,157	758	3,120
NORTHWEST	0	0	0	0	1,607	500	11,642
PACE	0	0	2,309	0	409	1,126	4,032
PG AND E	0	2,570	1,033	0	2,570	1,474	1,758
PSCOLORADO	0	79	2,134	169	960	547	2,134
SANDIEGO	0	516	1,562	0	516	357	1,562
SIERRA	0	0	352	0	1,511	432	802
SOCALIF	822	49	887	2,825	6,100	4,741	3,147
FORTISBC	0	0	0	0	0	0	0
WAPA R.M.	0	0	139	0	696	594	8,137
WAPA U.M.	0	0	0	0	0	0	60
Total	**1,092**	**4,052**	**11,680**	**12,199**	**23,286**	**16,882**	**45,535**

The final renewable dispatches for the HS cases are shown in Table 13. The data show that even under high wind and solar conditions, the capacity factor in the summer is lower, especially for wind. Again, the HS Hi-Mix dispatch is slightly different than the PLEXOS sample, as differences in topologies between the cases and maximum powers are respected on the individual renewable plants.

Table 13. Renewable Dispatch for HS Cases

	HS Base Case			HS Hi-Mix Case			
Area	**CSP**	**Utility-Scale PV**	**Wind**	**CSP**	**Utility-Scale PV**	**Distributed PV**	**Wind**
ALBERTA	0	0	899	0	0	0	899
ARIZONA	0	0	227	3,162	2,144	1,858	227
B.C.HYDRO	0	0	101	0	0	0	101
EL PASO	0	0	47	0	142	0	68
IDAHO	0	0	142	0	0	0	167
IMPERIALCA	0	0	0	187	385	43	28
LADWP	0	0	190	568	566	1,167	190
MEXICO-CFE	0	0	0	0	0	0	0
MONTANA	0	0	107	0	14	11	652
NEVADA	0	61	0	197	255	138	0
NEW MEXICO	0	0	20	0	361	240	102
NORTHWEST	0	0	0	0	245	283	6,869
PACE	0	0	1,154	0	221	596	1,447
PG AND E	0	701	787	0	701	966	787
PSCOLORADO	0	52	444	169	519	295	444
SANDIEGO	0	388	325	0	388	239	325
SIERRA	0	0	320	0	1,073	294	320
SOCALIF	355	45	814	2,359	3,790	2,943	803
FORTISBC	0	0	0	0	0	0	0
WAPA R.M.	0	0	30	0	390	321	910
WAPA U.M.	0	0	0	0	0	0	0
Total	**355**	**1,247**	**5,607**	**6,642**	**11,194**	**9,394**	**14,339**

2.5.2 Initial Condition Summary of Hi-Mix Cases

The system load flow diagram for the LSP Hi-Mix case is included in Appendix Figure 91. With the massive increase in solar generation in California and the DSW, both the PDCI and Intermountain high-voltage direct current (HVDC) line are off. Notice that the "total system load" as reported in the load flow and the bubbles is reduced due to the composite load model with distributed PV.

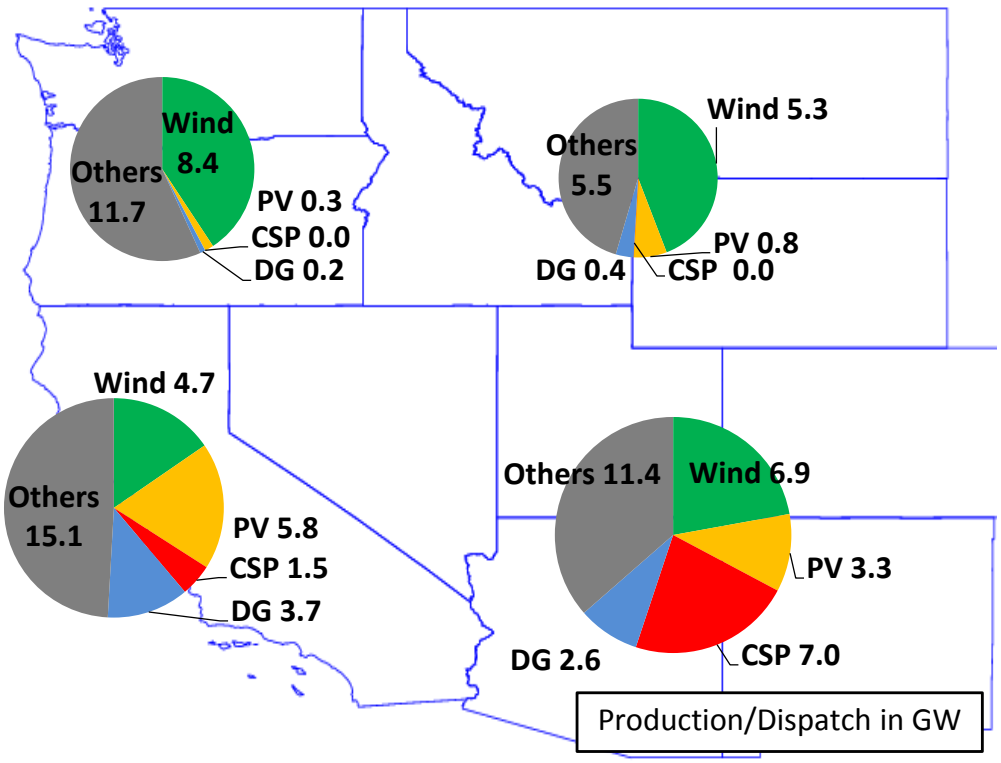

	WECC	California	DSW	Northeast	NW
Wind (GW)	27.0	4.7	6.9	5.3	8.4
PV (GW)	10.2	5.8	3.3	0.8	0.3
CSP (GW)	8.4	1.5	7.0	0.0	0.0
Distributed PV (GW)	7.0	3.7	2.6	0.4	0.2
Others (GW)	65.7	15.1	11.4	5.5	11.7
Total (GW)	118.4	30.8	31.3	12.0	20.5
Penetration (%)	44%	51%	64%	55%	43%

Figure 16. Wind and solar generation in LSP Hi-Mix case.

The renewable production in the LSP Hi-Mix case is shown in Figure 16 in both pie chart and tabular format. With about 52.8 GW of wind and solar total, the case has more than double the approximately 25 GW of wind and solar total in the LSP Base case. The totals for the four regions listed are for the U.S. WECC only and do not include Canada or Mexico. The wind and solar in Canada and Mexico for the Hi-Mix case are the same as in the Base case. Details, by region and area, of all the dynamic initial conditions are included in Appendix Table 43 and Table 44, respectively. The load flow bubble for the HS Hi-Mix case is shown in Appendix Figure 92.

This HS Hi-Mix case, as shown in Figure 17, has about 41.5 GW of wind and solar—substantially more than the approximately 7.2 GW of wind and solar (U.S. only) in the Base case. This table gives the initial renewable production for the dynamic simulations.

Details of the HS Hi-Mix dynamic initial conditions are included by region in Appendix Table 45 and by area in Appendix Table 46.

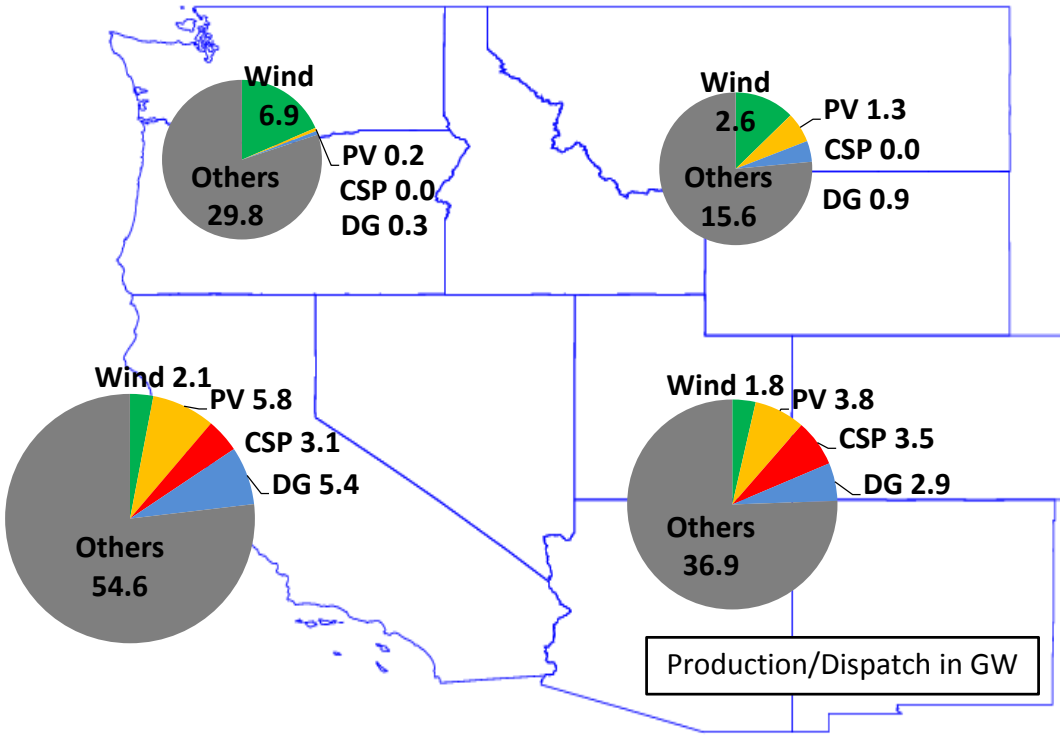

	WECC	California	DSW	Northeast	NW
Wind (GW)	14.3	2.1	1.8	2.6	6.9
PV (GW)	11.2	5.8	3.8	1.3	0.2
CSP (GW)	6.6	3.1	3.5	0.0	0.0
Distributed PV (GW)	9.4	5.4	2.9	0.9	0.3
Others (GW)	162.7	54.6	36.9	15.6	29.8
Total (GW)	204.2	71.0	48.9	20.4	37.2
Penetration (%)	20%	24%	22%	24%	22%

Figure 17. Wind and solar generation in HS Hi-Mix case.

A comparison of several key metrics from the four cases is shown in Table 14. Complete details for all four cases, for all areas and regions, are included in the Appendix.

A few points are of particular note. The entire WECC system Kt was 0.46 in the LSP Base case, and it declined to 0.42 in the LSP Hi-Mix case. Both levels are well above the nominal 0.30 level

considered to be a warning (Undrill 2010). However, the regional distribution of Kt is important. The NW region, with a large amount of responsive hydro generation committed, has Kt above 60% for both cases. California remains at around a Kt of 1/3, a substantial portion of which is hydro in both cases (as explored later in this report). The DSW region sees Kt drop rather dramatically, from 0.44 to 0.27, as responsive thermal units, especially gas CC plants, are de-committed. The Northeast sees Kt increase slightly, as responsive units are left committed, but dispatched back from maximum power, and some non-responsive units are de-committed.

In addition, the headroom is a measure of the generation reserves in each study scenario. In the LSP Base case, WECC has a total of 20.7 GW of reserves. In the HS Base case, WECC has a total of 24.1 GW of reserves. With the addition of significant wind and solar, the WECC-wide reserves are 21.9 GW for the LSP Hi-Mix case, and 27.2 GW for the HS Hi-Mix case.

As discussed above, the displacement of conventional generation to accommodate wind and solar is accomplished by a combination of re-dispatching down and de-committing units. In comparison to the PLEXOS case, the initial dispatch and commitment of thermal generation in the LSP Base case left relatively little room to dispatch down thermal plants. Therefore, most of the displacement is accomplished by de-committing units. From a stability perspective, this is conservative, as de-commitment is more stressful than re-dispatch down. The mix of frequency-responsive units and non-responsive units that were de-committed was about 1:2; i.e., about 2 MW of non-responsive generation were de-committed for each MW of responsive generation de-committed. The 1.2 GW increase in reserves is because much of the conventional generation that was re-dispatched down was frequency responsive.

Table 14. Key Initial Conditions for Synchronous Units with Governor Response

LSP Base	WECC	California	DSW	Northeast	NW
Pgen (GW)	43.5	6.4	10.4	2.9	12.4
Capacity (GW)	64.2	11.7	15.0	4.2	17.3
Headroom (GW)	20.7	5.3	4.6	1.3	4.9
Number (GW)	800	169	128	91	202
Kt	0.46	0.34	0.44	0.26	0.62
Penetration (%)	21.3%	31.0%	14.3%	16.8%	36.5%

LSP Hi-Mix	WECC	California	DSW	Northeast	NW
Pgen (GW)	34.4	5.4	5.4	2.7	9.5
Capacity (GW)	56.3	10.7	8.7	3.9	17.2
Headroom (GW)	21.9	5.3	3.3	1.2	7.7
Number (GW)	768	167	103	89	200
Kt	0.42	0.33	0.27	0.31	0.61
Penetration (%)	44.5%	50.9%	63.6%	54.5%	43.2%

HS Base	WECC	California	DSW	Northeast	NW
Pgen (GW)	84.8	26.5	17.0	3.3	24.4
Capacity (GW)	109.1	32.3	21.4	4.3	32.6
Headroom (GW)	24.1	5.7	4.4	1.0	8.1
Number (GW)	1,135	295	242	91	301
Kt	0.48	0.43	0.37	0.21	0.78
Penetration (%)	3.5%	5.3%	1.6%	8.7%	0.0%

HS Hi-Mix	WECC	California	DSW	Northeast	NW
Pgen (GW)	83.6	26.4	18.1	3.1	23.4
Capacity (GW)	111.2	31.8	26.4	4.0	31.9
Headroom (GW)	27.2	5.1	8.2	0.9	8.4
Number (GW)	1,152	298	267	89	298
Kt	0.50	0.45	0.49	0.19	0.70
Penetration (%)	20.4%	24.0%	22.2%	24.2%	22.2%

2.6 Transmission and Dynamic Model Changes

2.6.1 Method for Adding Incremental Transmission

Following recommitment and re-dispatch of the Hi-Mix study cases, they were tested for static thermal and voltage violations. In practice, the recommitment and re-dispatch was done in steps of several thousand MW until the final Hi-Mix condition was achieved. This step-by-step process was needed to obtain satisfactory load flow solutions with the massive generation shift from Base to Hi-Mix.

The overall approach approved by the TRC was to add minimal transmission. As noted above, the topology of the Western system, as provided by WECC in the selected data sets, includes a number of substantial transmission additions that are not currently in service. Improvements to allow satisfactory load flow solutions for the Hi-Mix cases did not include the addition of any further major transmission.

Adjustments to phase angle regulator or phase-shifting transformer schedules, HVDC schedules, and other minor adjustments were used to avoid overloading major transmission lines and exceeding path ratings. The path ratings observed were according to the 2013 rating catalog. Whether these path ratings will still apply for the future system is outside the scope of this study. Equally important, it is possible that path ratings would be affected by the addition of wind and solar. By observing the present limits, the study has made it possible to observe problems that might arise with the current limits. However, WWSIS-3 is not a system planning study, and it does not include the necessary but enormous effort required to validate and update all the path ratings.

In order to achieve satisfactory static initial conditions, about 4.5 GVAr of shunt capacitors were added to the LSP Hi-Mix case. No shunt capacitors were added to the HS Hi-Mix case. The large amount of solar added in central Nevada stressed the system there. In addition to localized shunt support and transformer upgrades, a synchronous condenser was added at Frontier.

Overall, the minimally enhanced transmission used for the Hi-Mix case gives a valuable reference, as both FR and transient stability concerns will tend to improve with added transmission. If the system has acceptable dynamic performance, new transmission might still make economic sense, but will not be needed to maintain stability and adequate FR even with high levels of wind and solar.

2.6.2 Dynamic Models for Renewables

The load flow topology is modified to accommodate the new utility-scale plants. Wind plants and utility-scale PV plants have two transformations, one for the substation transformer and an equivalent for the unit transformer (from collector voltage to inverter voltage) with an intervening equivalent of the collector system. CSP plants have the same electrical topology as other steam plants, and only need a single GSU transformer. The two arrangements are shown in Figure 18. The hundreds of new renewable plants add many buses to the load flow.

For dynamic modeling, the CSP plants are modeled as synchronous machines, with a standard WECC model without GR. The utility-scale PV plants are modeled with full four-quadrant dynamic models (based on the Type 4 wind turbine generator [WTG] model) with voltage

regulation and LVRT (gewtg and wtgfc). All new wind plants use the Type 3 GE WTG model with voltage regulation and LVRT (gewtg, wtg, wndtge). The distributed PV embedded with the load is modeled separately in the composite load model as discussed above.

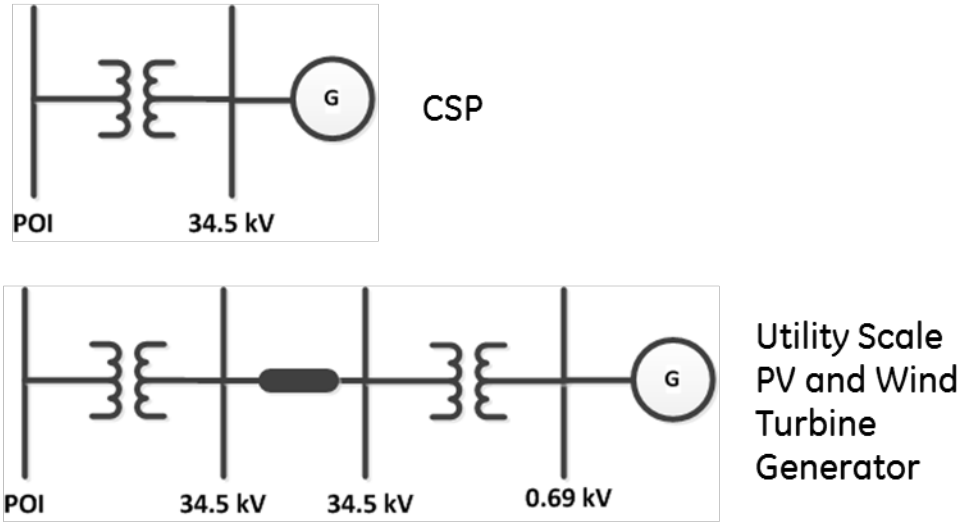

Figure 18. Renewable generation topology in load flow model.

2.6.3 Other Stability Data Refinements

During the data checking, 60-second no-disturbance simulations were run. This time period is relatively long for typical stability studies, and it uncovered two problems. Unstable power oscillations were observed after 30 seconds. Root cause analysis revealed these oscillations were caused by three units with a total MVA rating of about 100 MVA. Several attempts to fix the data, including using default dynamic data and removing the exciter and turbine model, did not correct the issue. The final solution for this oscillation was to net these three units. In addition, low-level power oscillations were observed in the Northeast after ~35 seconds. These were found to be due to initial conditions exceeding part of the dynamic model rating on a small plant. The plant dispatch was slightly reduced.

3 Frequency Response Analysis

The investigation of FR presented in this section focuses on the impact of higher levels of wind and solar generation on the system.

3.1 Frequency Response Obligation

The WECC interconnection frequency response obligation (IFRO) is given in Table 15 and throughout the report as 840 MW/0.1 Hz. Part of the NERC BAL-003-1 standard that sets the obligation includes periodic update of the IFRO. Consequently, this is only a reference point, rather than a static and absolute statement of obligation. The other FROs in that table are estimates based on the HS Base case initial conditions, using the generation and load from that condition as an approximation for the peak generation and load levels dictated by the standard. All of these figures are for reference only. FRO is assigned by BA and is in proportion to the relative size of the individual BA compared to the entire interconnection. This calculation is only an approximation and should not be used to determine whether any BA is in compliance. The Appendix includes a more complete discussion of FR (NERC 2012c).

Later, when the FR is calculated and compared to the FRO, the WECC totals always include the contribution of resources in WECC Canada and Mexico. Only U.S. resources are included in the regional and area levels.

There is also a locational aspect of FRO. There is no rule that says that the BAs have to meet their FRO with their own resources. However, it is not clear that practice has evolved yet to allow individual BAs to procure FR from other entities. A formal contractual arrangement is required. This is new ground for the industry. Throughout this report and investigation, the results are reported based on how regions and areas meet the estimated FROs. This is not a statement that BAs need to meet their FRO with their own resources; rather, these are metrics on how much the regions and entities contribute.

Table 15. WECC IFRO and Approximate Regional and Area FROs

ID	Name	Generation (GW)	Load (GW)	FRO (MW/0.1 Hz)
1	WECC	204	185	840
By Region				
2	CALIFORNIA	68.8	67.9	296
3	DSW	53.9	47.8	220
4	NORTHEAST	19.7	18.0	82
40	NORTHWEST	33.3	27.2	131
By Area				
14	ARIZONA	27.5	20.8	104
11	EL PASO	1.7	2.3	9
60	IDAHO	4.3	3.9	18
21	IMPERIALCA	1.5	0.3	4
26	LADWP	6.3	7.2	29
62	MONTANA	3.3	1.9	11
18	NEVADA	6.1	6.8	28
10	NEW MEXICO	3.5	3.1	14
65	PACE	9.4	9.9	42
30	PG AND E	32.4	29.0	133
70	PSCOLORADO	8.3	8.1	36
22	SANDIEGO	4.4	5.5	21
64	SIERRA	2.6	2.3	11
24	SOCALIF	24.2	25.9	108
73	WAPA R.M.	6.9	5.8	27
63	WAPA U.M.	0.1	0.0	0

The FR performance of the interconnection and the individual entities is given by the ratio of the change in power resulting from a disturbance-induced change in frequency. For this metric, the frequency change is assumed to be uniform across the interconnection. In the work presented here, the only power change measured and included in the calculations is that of the turbine power of the responsive generation. Load response is not considered in the calculation of FR. Load modeling and losses are included as discussed in Sections 3.1 and 3.3.3. This study focuses on system-wide FR, as measuring the frequency at a single node in the grid following a disturbance can be confusing and misleading. In this study, an MVA-weighted sum of synchronous machine speeds is calculated and used as a composite frequency. Details of the calculation are included in the Appendix.

3.1.1 Focus on Light Load Conditions

The system-wide concerns for FR tend to be greatest under light load conditions, as has been observed in several investigations (NERC 2012b, Eto 2010). In basic terms, under light load conditions, much less generation is operating, but the size of the design-basis disturbance remains the same. Thus, the upset is proportionally larger and has more significant consequences.

For WECC, the design-basis event, per NERC (NERC 2012b), is the largest category C (N-2) event, i.e., the simultaneous trip of two of the Palo Verde NPS units for a total instantaneous loss of 2,756 MW of generation. The IFRO (see discussion in Appendix) is based on this event. UFLS action or violation of other stability criteria (e.g., separation or extreme voltage swing) for this event is not acceptable.

In the WECC Base cases (both LSP and HS), two Palo Verde NPS units are on-line and dispatched near their maximum net power. In all the cases presented in this report, these two units are tripped, resulting in the loss of 2,756 MW of generation. Figure 19 presents the WECC frequency in response to the Palo Verde trip for the LSP (red trace) and HS (blue trace) Base cases. The calculation of system frequency is discussed in the Appendix. Appendix Figure 96 and Figure 97 show selected bus voltage and interface flow swings for the event; these voltages and power swings are relatively benign.

As expected, the LSP FR is much worse than that of the HS case. The depth of the frequency nadir for the LSP case is below 59.7, at 59.668, compared to a nadir of 59.839 for the HS case. Note that the event (as measured by frequency nadir) is twice as severe for the LSP case, even though the load is more than 50% of the heavy load (~111 GW vs. ~185 GW). The relationship between load level and FR is a strong function of generation responsiveness and headroom.

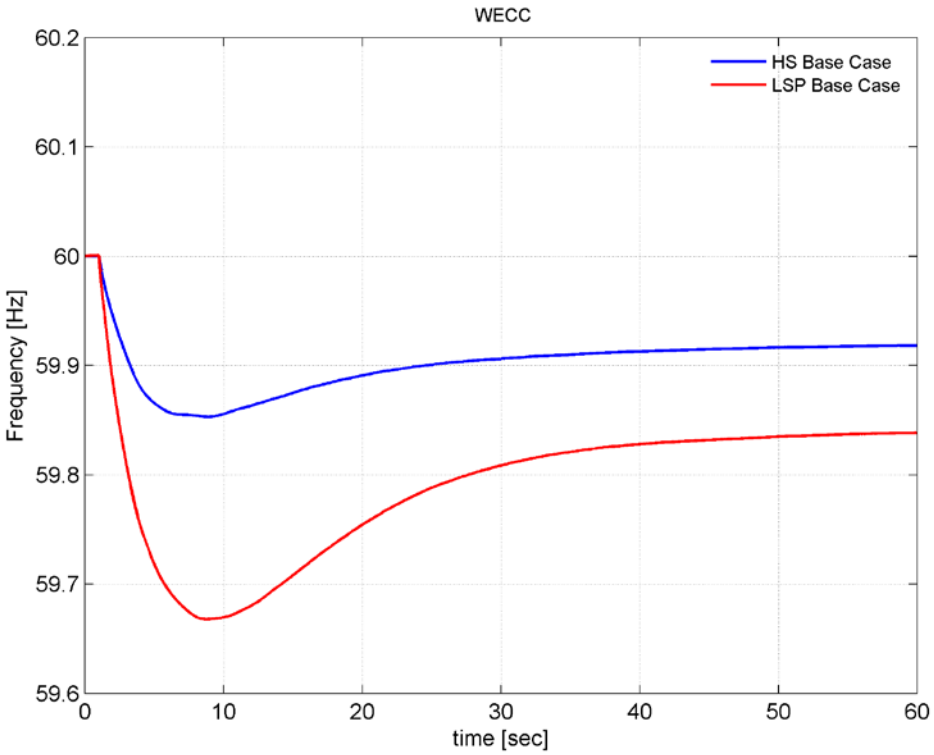

Figure 19. Frequency response to loss of two Palo Verde units – LSP vs. HS Base.

3.2 Light Spring Base and Hi-Mix Comparisons

In this section, the FR of the Base and Hi-Mix systems is discussed.

A few of the key system-wide metrics compare as follows (LSP Base vs. Hi-Mix, respectively):

- Kt: 0.46 vs. 0.42
- Headroom: 20.7 GW vs. 21.9 GW
- Number of responsive units on-line: 800 vs. 740.

Two of the three metrics are such that the expected FR for the Base case should be somewhat better than that of the Hi-Mix case.

3.2.1 Trip of Two Palo Verde Units

The design-basis generation trips for the two cases result in quite similar performance. As suggested by the initial condition metrics, the performance of the Base case is slightly better than the Hi-Mix case. The WECC frequency swings are shown in Figure 20, with the exact details of the system FR performance being summarized in Table 16 and Table 17. The frequency nadir drops from 59.668 Hz to 59.646 Hz, a 22 mHz (7%) degradation, and the FR drops from 1,352 MW/0.1 Hz to 1,311 MW/0.1 Hz, a 3% degradation. The performance in both cases meets WECC and NERC criteria at the system level. Note that the initial rate of change of frequency (ROCOF), i.e., the slope of the frequency trace at the instant following the generation trip, is

greater in the Hi-Mix case. This is the effect of reduced system inertia. As the Western Interconnection generally does not rely on ROCOF-based protection, the increased ROCOF is of limited system-wide consequence. However, the combination of the rate of frequency drop and the opposing action of primary FR does dictate the frequency nadir—and therefore the margin above UFLS. Note also that the PSCOLORADO area, which covers more than just Public Service of Colorado (now Xcel Energy), has a negative FR. This occurs because several generators in this area have supervisory load controls modeled that override the GR.

Comparative details of the system performance are shown in the subsequent figures. Figure 21 shows the electrical (solid traces) and mechanical (dotted traces) power excursions of the responsive generation. The characteristics of the two cases are similar, with the reduced initial generation from responsive units causing the roughly 8 GW difference between the cases. Appendix Figure 98 shows load swings that have slightly different starting points, due to different methods of accounting for losses in the complex load model and the treatment of the distributed PV. This is not significant to the results, but the amplitude of the load power deviation has some impact on the frequency swing and ROCOF. The depression of system load voltages during the initial stages of the disturbance affects the Base case more than the Hi-Mix case, resulting in slightly more load relief. This helps reduce the severity of the frequency swing. Load effects, while not dominant, do play an observable role in system FR. Specifically, load voltage sensitivity will be shown later to have a significant impact on FR.

Figure 22 shows how the GR is geographically distributed across the West. Notice that the predominantly thermal generation in the regions outside of the NW is faster and leads the system response. However, as the event continues, the predominantly hydro resources in the NW become the dominant contributor to FR. Thus, the thermal generation has a somewhat more significant impact on the frequency nadir than the FR metric (as reported in Table 16 and Table 17) suggests. The relative time separation of the regional GR impacts the interregional power swings, as is reflected in the flows of Figure 23. The slow drift of the flows over the course of the 60-second simulation are due to the hydro generation slewing into steady-state response. System voltages, a sampling of which is plotted in Appendix Figure 99, are similar and well behaved for the two cases. In this case, the timing difference has limited impact on system performance. The headroom of the responsive generation, shown in Appendix Figure 100, mirrors the mechanical power swing. The headroom drops and returns everywhere but the hydro-rich NW, which supports the observation about the difference in speed of response between the different types of resources. Figure 24 shows the dynamic count of generation supplying GR. The figure shows some units saturating during the swing; these are units that have insufficient headroom to sustain the requested power increase for this event. For example, in California, about 15 units or about 10% of the total responsive units saturate. Other units had more headroom than was useful for this event. This saturation has implications for other frequency-responsive resources that could be used to maintain stability and to meet FRO. This is discussed further in Section 1.

Details for two areas, PG&E and Arizona, are shown in Figure 25, which illustrates the diversity of the response. The effects of apparent governor withdrawal in the Arizona traces can also be seen. As noted in other work [NERC (2012c), Eto (2010)], this is a source of concern.

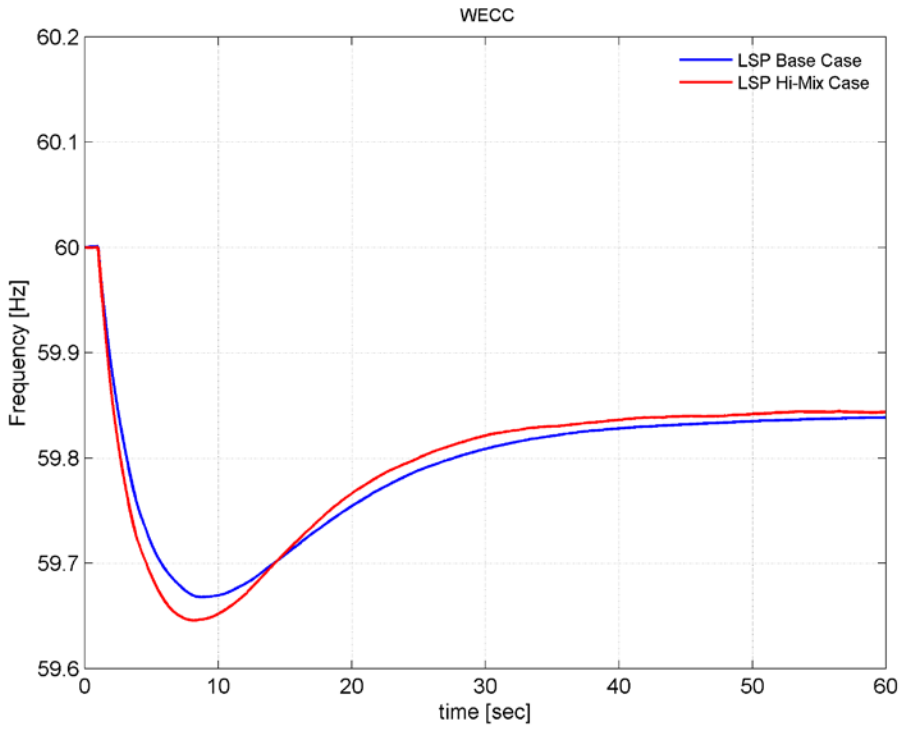

Figure 20. Frequency response to loss of two Palo Verde units – LSP Base vs. Hi-Mix.

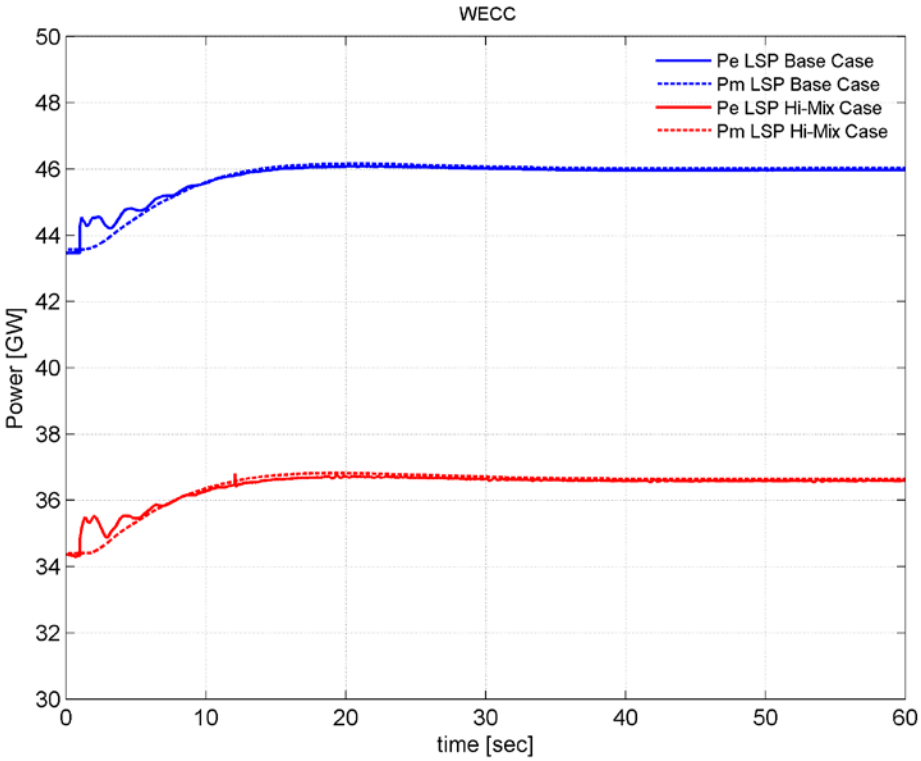

Figure 21. Generation response to loss of two Palo Verde units – LSP Base vs. Hi-Mix.

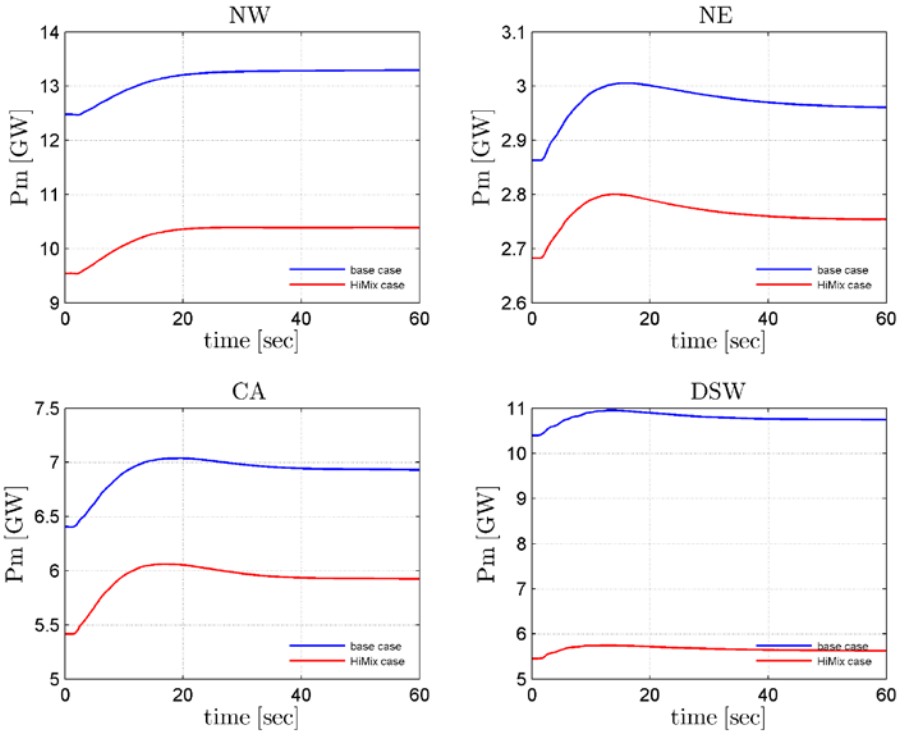

Figure 22. Governor response to loss of two Palo Verde units – LSP Base vs. Hi-Mix.

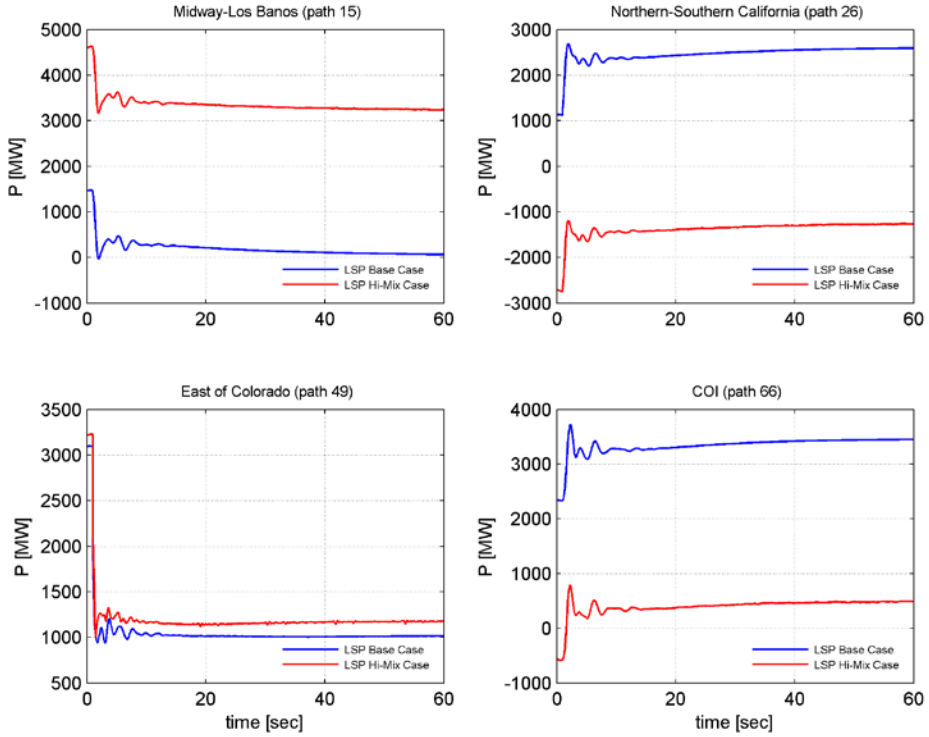

Figure 23. Interface response to loss of two Palo Verde units – LSP Base vs. Hi-Mix.

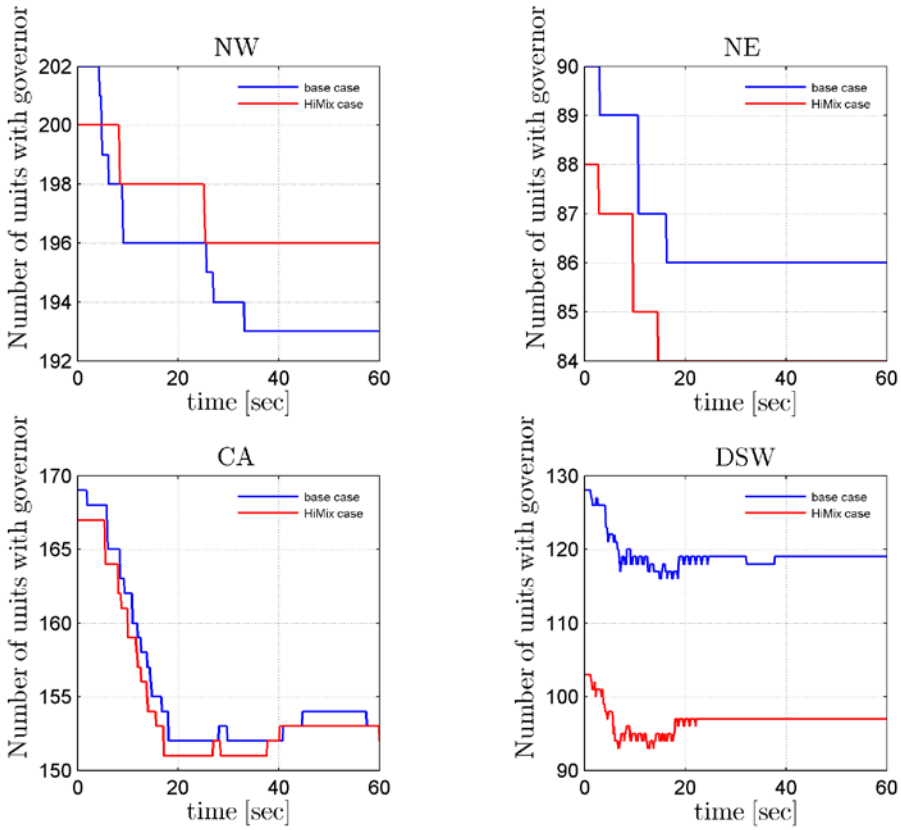

Figure 24. Responsive plant count for loss of two Palo Verde units – LSP Base vs. Hi-Mix.

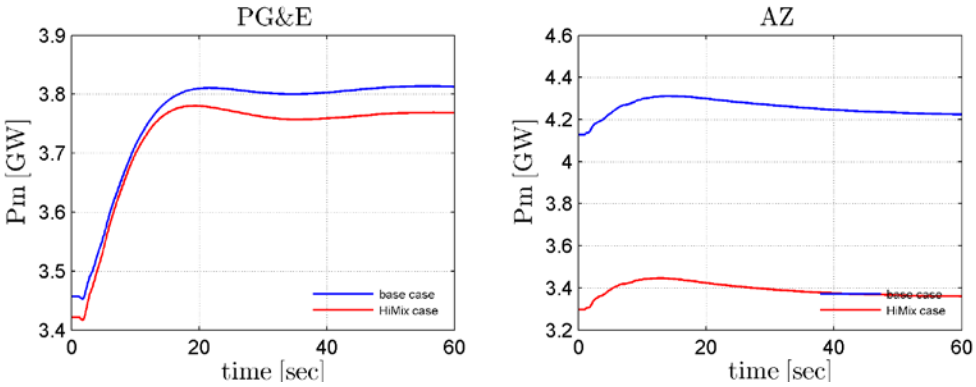

Figure 25. Response of generation in two areas to loss of two Palo Verde units – LSP Base vs. Hi-Mix.

Table 16. WECC Frequency Response Metrics for LSP Base and Hi-Mix Cases

	LSP	
	Base	**Hi-Mix**
Generation (GW)	204	204
Load (GW)	185	185
FRO (MW/0.1 Hz)	840	840
FR (MW/0.1 Hz)	1,352	1,311
FR Margin (MW/0.1 Hz)	512	471
Frequency Nadir (Hz)	59.668	59.646
Nadir Time (s)	7.77	7.19
Settling Frequency (Hz)	59.839	59.844
Kt	0.46	0.42

Table 17. Area Frequency Response Metrics for LSP Base and Hi-Mix cases

	LSP Base Case					LSP Hi-Mix			
Name	**FRO (MW/ 0.1 Hz)**	**FR (MW/ 0.1 Hz)**	**FR Margin (MW/ 0.1 Hz)**	**FR % of WECC**	**Kt**	**FR (MW/ 0.1 Hz)**	**FR Margin (MW/ 0.1 Hz)**	**FR % of WECC**	**Kt**
WECC	840	1,352	512	100.0	0.46	1,311	471	100.0	0.42
By Region									
CALIFORNIA	296	305	9	22.6	0.34	312	16	23.8	0.33
DSW	220	215	-5	15.9	0.44	119	-101	9.1	0.27
NORTHEAST	82	61	-20	4.5	0.26	47	-34	3.6	0.30
NORTHWEST	131	434	303	32.1	0.62	483	353	36.9	0.62
By Area									
ARIZONA	104	69	-35	5.1	0.37	50	-55	3.8	0.29
EL PASO	9	4	-5	0.3	0.42	4	-5	0.3	0.30
IDAHO	18	21	3	1.6	0.38	22	4	1.7	0.68
IMPERIALCA	4	14	10	1.0	0.24	14	10	1.1	0.16
LADWP	29	31	1	2.3	0.60	30	1	2.3	0.42
MONTANA	11	10	-1	0.7	0.17	10	-1	0.8	0.23
NEVADA	28	44	16	3.2	0.72	34	6	2.6	0.52
NEW MEXICO	14	50	35	3.7	0.49	2	-13	0.1	0.03
PACE	42	23	-19	1.7	0.22	8	-34	0.6	0.19
PG AND E	133	190	57	14.1	0.40	197	64	15.0	0.46
PSCOLORADO	36	-14	-50	-1.1	0.34	6	-30	0.4	0.25
SANDIEGO	21	7	-14	0.5	0.15	7	-14	0.6	0.16
SIERRA	11	7	-3	0.6	0.23	7	-4	0.5	0.18
SOCALIF	108	63	-45	4.7	0.23	63	-45	4.8	0.21
WAPA R.M.	27	63	35	4.6	0.67	24	-3	1.8	0.19
WAPA U.M.	0	3	3	0.2	0.94	3	3	0.2	0.76

3.3 Frequency Response Summary

There are no obvious FR-related stability problems that become apparent as the system moves to the Hi-Mix condition for the NERC design-basis event in the West. Doubling the wind and solar production to more than 50 GW leaves the *characteristics* of the system response to this large generation trip event essentially unchanged. There is a 7% degradation in the frequency nadir (i.e., the difference between nadir and nominal is 332 mHz in the LSP Base case and 354 mHz in the LSP Hi-Mix) and a 3% degradation in the FR for these conditions (i.e., from 1,352 MW/0.1 Hz to 1,311 MW/0.1 Hz). There are significant locational impacts on FR, with some regions and areas providing substantially less response from resources within their own areas than are indicated by the NERC standard.

4 Transient Stability Analysis

4.1 COI Stability Under Heavy Summer Conditions

As discussed in Section 2.3.3, a block or shutdown of both poles of the PDCI was identified by the TRC as one of the most severe transient stability events in the Western Interconnection. The loss of PDCI should not result in UFLS or any cascading outages.

To simulate this event, all power transfer on both poles of the PDCI is stepped to zero. The resultant loss of power transfer from the NW to California causes a substantial incremental power flow on the Pacific AC intertie across the COI, as well as increased loading on an aggregate of transmission paths farther east. This event has long been subject to scrutiny, and under some conditions requires a relatively complex RAS that can include trip of generation and switching of reactive devices. In this investigation, the focus is primarily comparative. For simplicity and clarity, only the PDCI power is blocked, and in this sequence of comparisons there is no further RAS of any type in this simulation.

The change in system dispatch with the added wind and solar results in the COI and PDCI loading being initially much higher in the Hi-Mix compared to the Base case. The Base case loading is 3,589 MW and 2,527 MW, respectively, considerably lower than the path rating. Conversely, the Hi-Mix COI loading is slightly greater than 4,800 MW, which is the path rating. This rating is further subject to constraints due to northern California hydro, which is discussed below in Section 4.1.2. The PDCI is loaded to about 3,000 MW in the Hi-Mix case. As system stability for this event is a function of the loading on the AC and DC interties, a third case was added. The Base case was modified by de-committing the two San Onofre units in southern California, and increasing hydro generation in the NW by both committing additional units and dispatching up other units. The San Onofre units were in service in the original WECC cases. The resulting initial condition, named Base-COI in the plots, has the COI AC flow and PDCI flow within 10 MW of the Hi-Mix case. The wind and solar generation remains the same as for the Base case.

The active power flow on the COI is shown for the three cases in Figure 26. The Base case (blue trace) is stable. Both the Hi-Mix case (red trace) and the Base-COI case are unstable. The Base-COI case is somewhat worse, as the separation occurs faster. Flows on other interfaces are included in Appendix Figure 101.

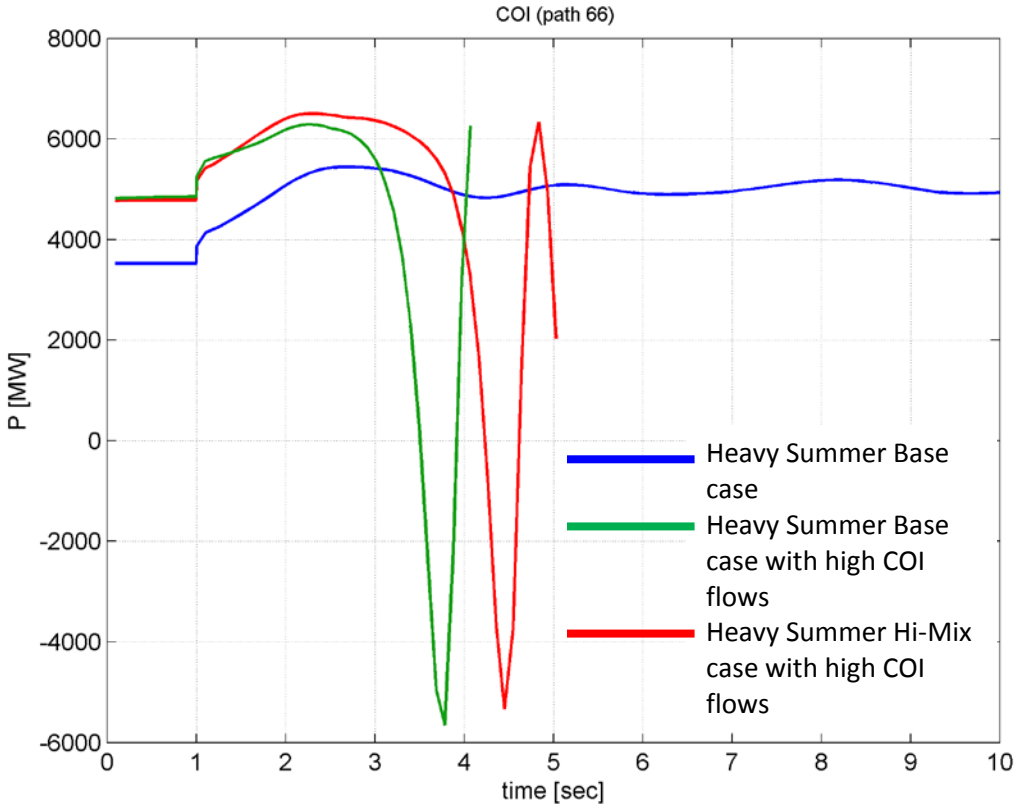

Figure 26. COI flows for PDCI event for HS cases.

Selected bus voltages from throughout the Western Interconnection are plotted in Figure 27. The precipitous drop in voltage at Malin is characteristic of a system separation in that vicinity. The system separation is also evident in Figure 28, which shows the four regional frequencies. In the Hi-Mix case, the frequencies in the generation-rich northern areas become unstable due to high frequency, and those to the south experience a frequency drop. In the Base-COI case, all areas become unstable due to high frequency.

As noted earlier, these simulations are deliberately kept simple, with no RAS and with no protective relaying action. The intent here is to observe the difference in performance, not to determine whether or how the system might tolerate a separation. The rate at which separation occurs is an indication of the degree of instability, but separation is not allowed for this event. With the COI and PDCI at the same loading, the system is less stable with lower wind and solar generation for this particular study condition.

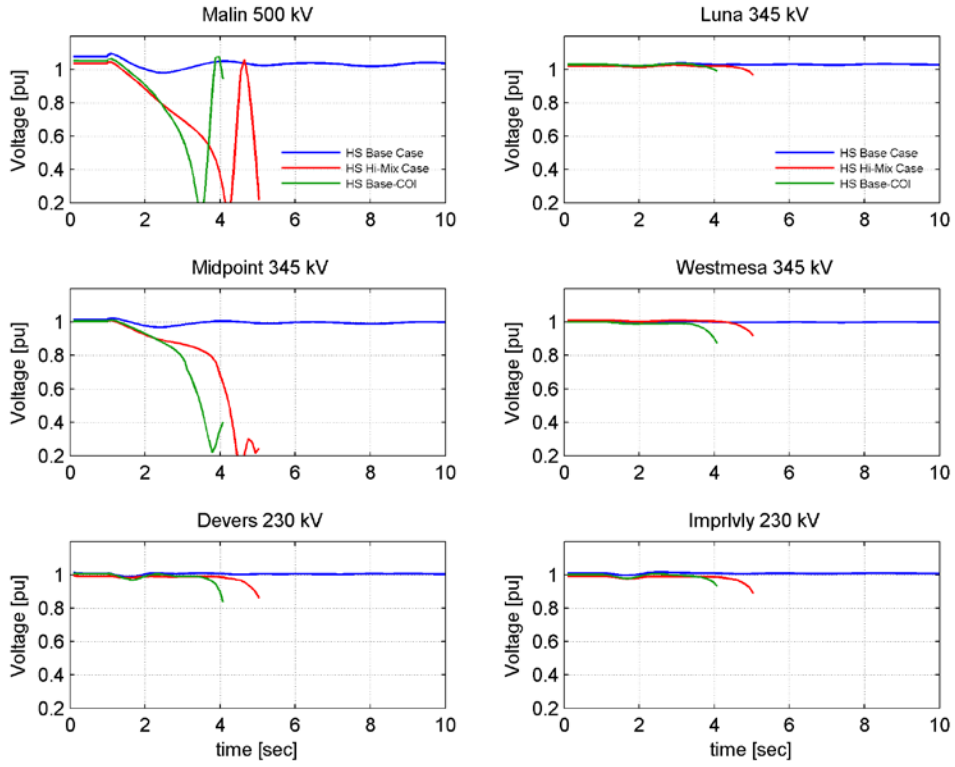

Figure 27. Bus voltages for PDCI event for HS cases.

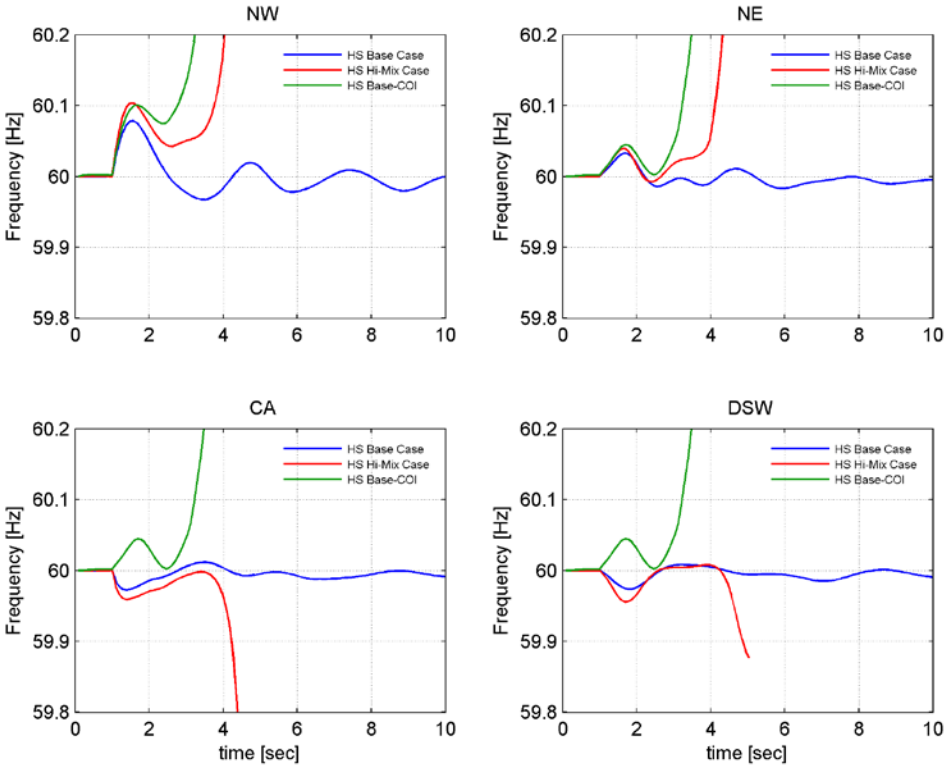

Figure 28. Regional frequencies for PDCI event for HS cases.

4.1.1 COI Stabilization with Generation Trip Remedial Action Scheme

As noted earlier, system separation for the PDCI event is not allowed. As the Base-COI case showed, system separation is a risk today under conditions that include high flow levels on the COI. Present practice is to trip generation in the NW for the PDCI event, depending on the initial COI and other conditions. A complex set of rules is used to enable specific generation tripping for specific operating conditions. This exercise does not attempt to replicate the details of the current practice; rather, this is an investigation to understand if the currently accepted practice of generation tripping will be effective at mitigating the separation observed in the Hi-Mix case.

A sequence of three tests, tripping about 1,000 MW, 2,000 MW, and 2,800 MW of generation, results in a stable system with relatively small voltage swings. The introduction of deliberate generation tripping raises concern about the impact on system frequency. The system frequency for this sequence of cases is shown in Figure 29. A case with no generation-tripping RAS is shown in blue, along with the three cases with increasing levels of unit tripping.

The result is not surprising: the more generation tripped, the deeper the nadir and the lower the settling frequency. Also, the FR for tripping about 2,800 MW is similar to that for the Palo Verde event on the HS Hi-Mix case described earlier. While tripping this level of generation is overkill for this event, the frequency is still within limits. This suggests that use of a standard generation-tripping RAS with the Hi-Mix level of wind and solar does not carry appreciable frequency risk for this condition. There is no obvious need to be overly timid with tripping.

The plots of Appendix Figure 102 and Figure 103 show interface flows and voltages for this sequence of cases. The differences when the system is stabilized are relatively small.

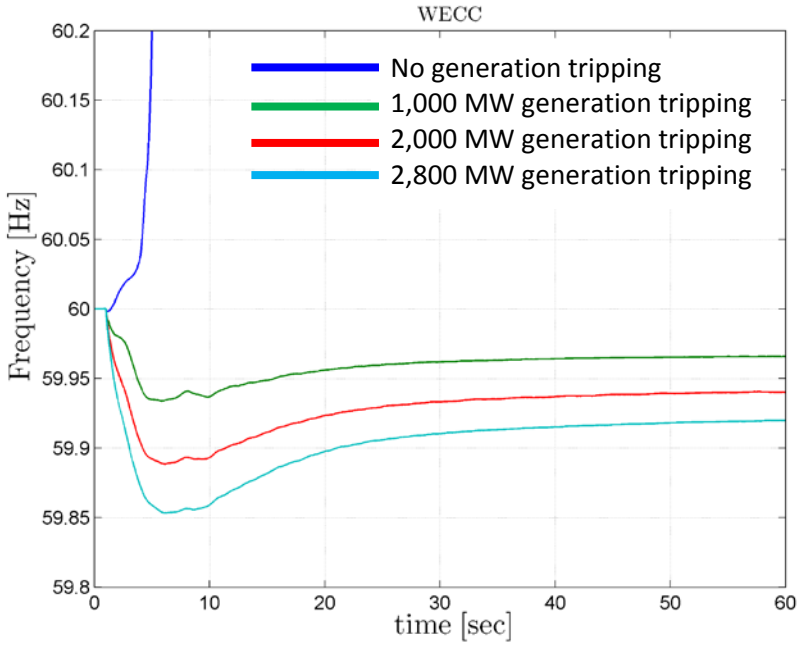

Figure 29. Frequency response of Hi-Mix for PDCI event with various generation-tripping RAS.

The sequence presented above shows that tripping about 1,000 MW of generation is effective at stabilizing COI. This raises the question of how much generation is enough. In this exercise, a

further search for the minimum generation trip that will stabilize the system was pursued. As the amount of generation tripping is reduced, the difference in voltage swings becomes more apparent.

Figure 30 shows the voltages along the AC intertie. Shown on the left is the unstable Hi-Mix case with no RAS. The separation occurs at about 4 seconds, with Malin and Captain Jack shown at the bottom. On the right, a case is shown in which two 138 MW generators (John Day units) are tripped. Notice that separation is avoided. The voltage swing at Malin and Captain Jack meets WECC criteria. Tripping one unit of this size is stable, but it does not bring the voltage swing into compliance with WECC voltage criteria.

This exercise shows that heavy loading on the AC intertie is more stressful than a high wind and solar condition. High flows on the COI currently require a generation-tripping RAS. This exercise suggests that this practice can continue, and that the transient stability of the system for one of the well-known and critical events, while somewhat improved, is not fundamentally changed by high wind and solar generation. This conclusion is not a statement that the system behaves identically. It is possible, and perhaps likely, that the system dynamics are sufficiently different to require somewhat different levels of generator tripping or different arming criteria. A complete evaluation of the current practice would be prudent. There is, however, nothing in this exercise that indicates that the system dynamics have fundamentally changed and that radically different means to ensure stability for this event are required.

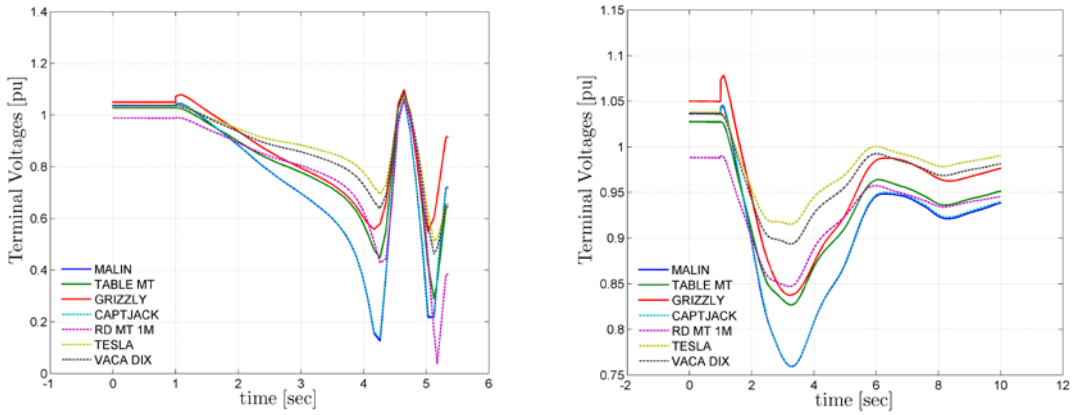

Figure 30. Dynamic voltage collapse avoided by RAS.

4.1.2 Northern California Hydro and COI Stress

The loading on the COI has a further constraint that is dictated by the northern California hydro (NCH) generation. An operating nomogram that applies during the summer is shown in Figure 31. Under conditions of high (i.e., >70%) NCH generation, the COI transfer limit is reduced.

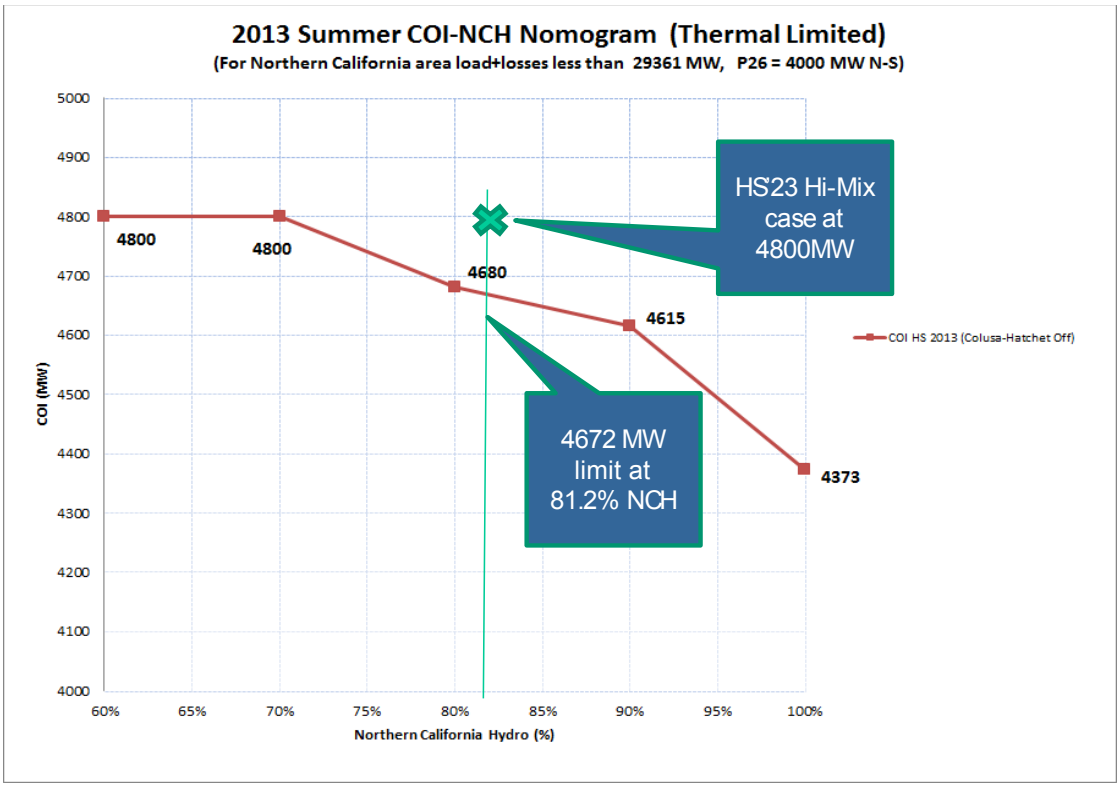

Figure 31. 2013 Summer COI – northern California hydro nomogram.

The NCH is divided into five groups. The dispatch of this hydro has been left essentially untouched as renewables were added moving from the Base cases to the Hi-Mix cases. A review of the four cases shows NCH generation as follows:

- HS Base and Hi-Mix: 81%
- LSP Base and Hi-Mix: 47%.

Consequently, the actual limit on the COI because of the thermal limit to the south is 128 MW lower than was enforced in HS. This is noted on the nomogram. Therefore, the HS Hi-Mix cases are at slightly higher stress than thermal limits would allow. Stability performance would be expected to improve if system stress was relieved by re-dispatching to lower the COI loading. It is interesting to note that the COI is overloaded 128 MW, which is on the order of half the amount of generation needed to be tripped by a RAS to stabilize the case and meet voltage swing criteria. It is entirely possible that no generation-tripping RAS would be necessary at this lower transfer level.

4.2 Local Stability Examples

There are many localized stability limits in the West. The addition of substantial wind and solar generation has the potential to alter the system dynamics of the events that dictate these limits. The two examples included here are intended to illustrate possible impacts on more localized limits. While interesting, they are not a substitute for thorough system engineering.

4.2.1 Colstrip Area Fault

One well-known stability concern in the West is maintaining the synchronism of the Colstrip thermal plants. Over the years, the 500 kV backbone running east from Colstrip and the surrounding 230 kV systems were designed and tuned to give satisfactory stability results for Colstrip. With the addition of substantial amounts of wind, and some solar, in the region, the stability of that part of the system could be compromised.

For this investigation, a three-phase fault at the Broadview 500 kV bus is applied. It is cleared after three cycles by tripping one 500 kV line: Broadview – Town – Garrison. This fault was chosen because it is just downstream of a connection to the underlying 230 kV system with many new wind power plants in the vicinity. The angle swings of the four Colstrip units are shown in Figure 26. There are three interesting aspects of these results. First, one of the Colstrip units is de-committed in the Hi-Mix case. This makes economic sense, as the wind and solar will displace at least some of the coal generation in the West, even under heavy load conditions. Second, the initial angle of the three remaining Colstrip units is greater in the Hi-Mix case. This is evidence that this part of the system—and probably the entire northeastern part of the Western Interconnection—is exporting heavily. The implication is that the exporting transmission is loaded with wind and solar, as well as the usual thermal power exports from the region. Third, the net angle swing of the Colstrip units is smaller in the Hi-Mix case. This suggests a higher level of stability. The angle change shows that the acceleration of the units is lower in the Hi-Mix case, a significant consideration because of the specialized type of stability protection used there.

The results raise the question of the causality of the lower acceleration: is it because one of the units at the plant is off-line, or because of some other dynamic characteristic associated with the higher wind and solar? In Figure 33, an additional case is reported in which the de-committed Colstrip unit is returned to service at the same dispatch as in the Base case. The plot is for the speed of the four Colstrip units. The blue trace is for the Base case, and the green trace is for this new sensitivity: Hi-Mix with all four Colstrip units committed. Interestingly, the speed increase appears to be the same, with the maximum speed—a good proxy for the maximum acceleration—still lower in the Hi-Mix case. This result suggests that stability is not degraded in the Hi-Mix case, and arguably is slightly improved for this particular system condition. It is an interesting data point, but it does not show conclusively that the stability will inevitably improve.

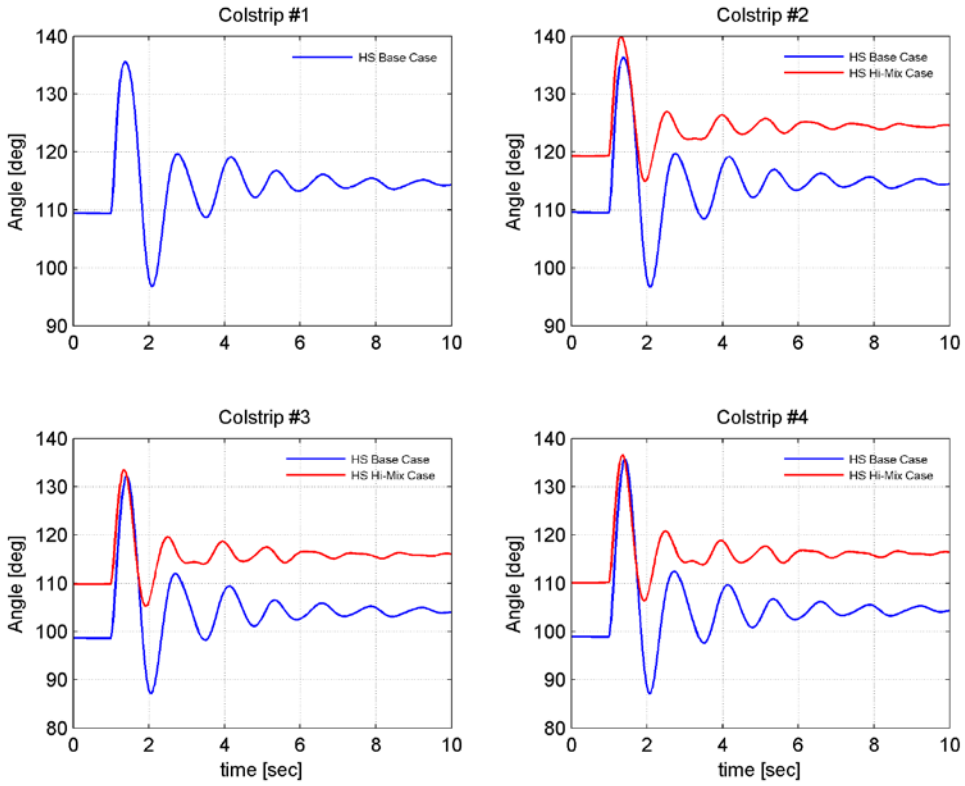

Figure 32. Colstrip machine angles for Broadview fault – HS Base vs. Hi-Mix.

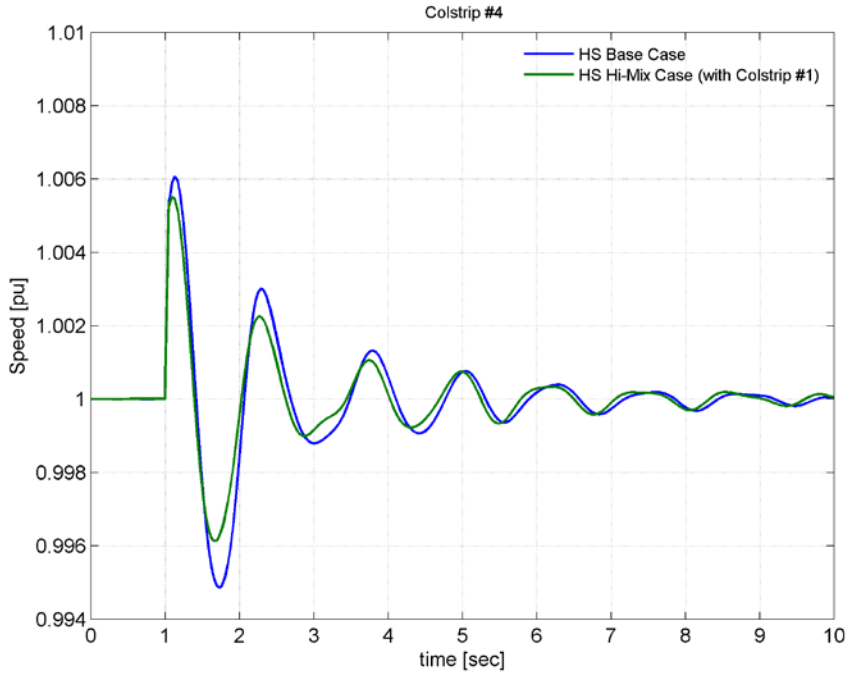

Figure 33. Colstrip #4 speed – HS Base vs. HS Hi-Mix with Colstrip #1 committed.

4.2.2 Laramie River Station Fault

Figure 34 shows a comparison between a pair of HS transient stability cases with a three-phase, four-cycle fault applied at the Laramie River 345 kV substation. After the fault is cleared by trip of the Laramie River – Archer TS – Story line, the system recovers in both cases. The recovery is faster in the Hi-Mix case, apparently because of the newly added renewables nearby.

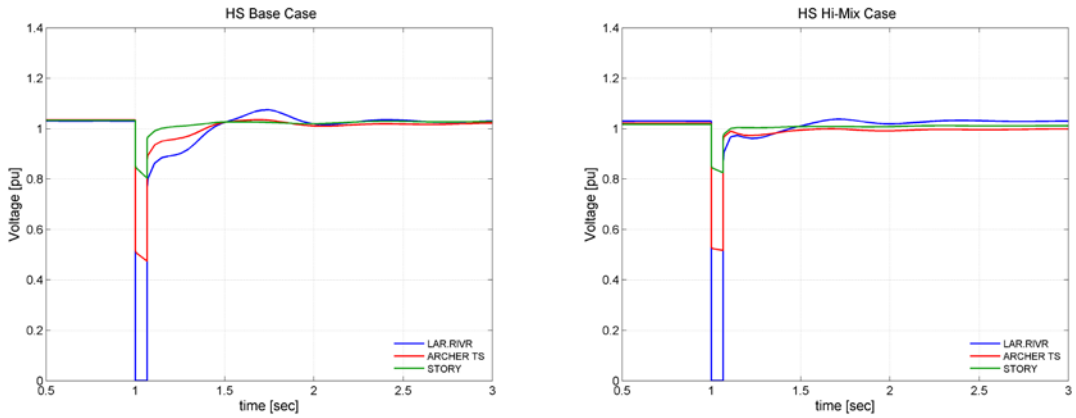

Figure 34. Bus voltages for Laramie River Station fault – HS Base vs. Hi-Mix.

5 Sensitivity Analysis

The objective of the WWSIS-3 sensitivity analysis was to define a band of potential responses, indicate general impact (e.g., better or worse), and provide insight into specific dynamic performance questions raised by the TRC.

This section reports on a number of investigations developed to provide specific insights into the impact of key elements related to FR and transient stability under conditions of high wind and solar generation.

5.1 Load Model Impact on Fault-Induced Delayed Voltage Recovery

The impact of load behavior is explored in the set of sensitivity investigations reported here. The impacts of load modeling assumptions and the fault tolerance or ride-through capability of distributed PV are also tested. The phenomena of fault-induced delayed voltage recovery (FIDVR) (NERC 2009) is of particular concern.

5.1.1 Composite Load Model in Base Cases

In both original WECC cases, load is modeled with induction motor (motorw) and static components. Specifically, for the HS original case, 5,848 loads are modeled as 20% induction motor (~36 GW) and static (~156 GW). The static or ZIP (constant impedance [Z], current [I], power [P]) components vary by area, but the majority use constant impedance for reactive load and constant current for real load. The total load is about 185 GW.

The composite load model, as discussed in Section 2.2.3, has a complex topology and flexible load characteristics. It accommodates DG and a variety of tripping characteristics. In all results presented in this report, stalled motor tripping is not allowed, giving a conservative view of stability impacts. About three-quarters of the total load is converted to the composite load in the base cases.

5.1.2 Midway-Vincent Fault with Composite Load Model

The results of a three-phase fault at Vincent 500 kV in California for the HS Original and Base cases are shown in Figure 35. The fault is cleared by tripping two Midway-Vincent lines in six cycles. In the figure, the original case (blue trace) with WECC standard load modeling (20% induction motor, 80% static) exhibits fast voltage recovery and a stable response. The Base case (red trace), with 143.9 GW composite load, fails to recover. There is a dynamic voltage collapse about 3 seconds after the fault clears. The simulation after that point is meaningless, and the plot is truncated. This is an extreme case of FIDVR. The difference shows that load behavior dominates system response for this event. No protection was modeled.

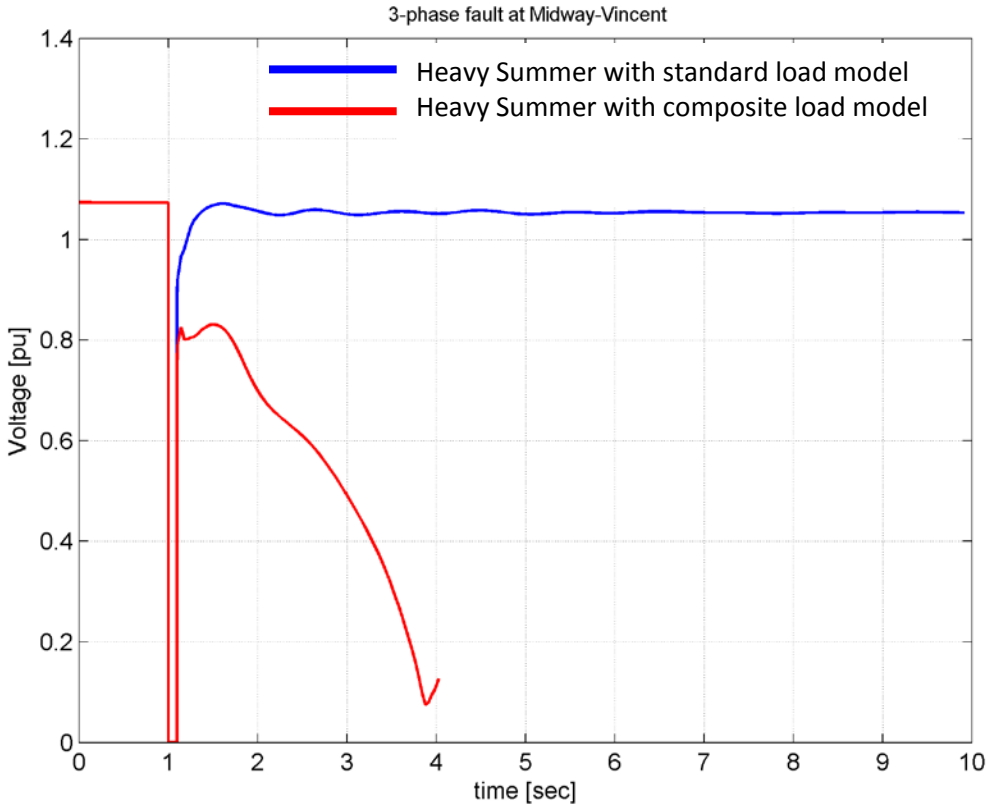

Figure 35. Load-induced voltage collapse in HS Base case.

To examine the relative impact of renewables, and particularly the DG, a comparison of the HS Base case (blue trace) and the HS Hi-Mix case (red trace) is shown in Figure 36. Both cases show dynamic voltage collapse, but the Hi-Mix case collapses about twice as fast.

Two contributing factors to the faster collapse in the Hi-Mix case were considered. One contribution is the low-voltage blocking of the distributed PV inverters during the voltage depression. The inverters are modeled to maintain full output down to 80% voltage; between 80% and 70% they begin to block. Below 70%, they fully block, recovering only when the voltage recovers. Modeling this behavior is a proxy for the fact that smaller inverters generally cannot continue firing during deep voltage depressions. In this context, blocking is distinct from tripping. Tripping removes the inverter from operation so that it will not return when the voltage recovers. Tripping could be due to inverter limitations, or it could be deliberate, such as in response to default requirements of IEEE 1547. In this case, about half of the PV (4.4 GW of 9.3 GW) blocks during the fault. The vast majority of that generation is near the fault, in the Los Angeles Department of Water and Power and Southern California Edison areas. Blocking the local current injection of the PV exacerbates the stalling behavior of the motors, making the event somewhat more severe.

A second factor is that the displacement of synchronous generation by renewables was expected to reduce the system strength in the vicinity of the fault. Reduced system strength is known to aggravate FIDVR. A good proxy for system strength is short-circuit current level. However,

when examined, the fault current level was found to be nearly identical for the two cases. This suggests that the PV blocking, which causes additional current to be drawn from the bulk power system, is the dominant factor in the difference between the cases.

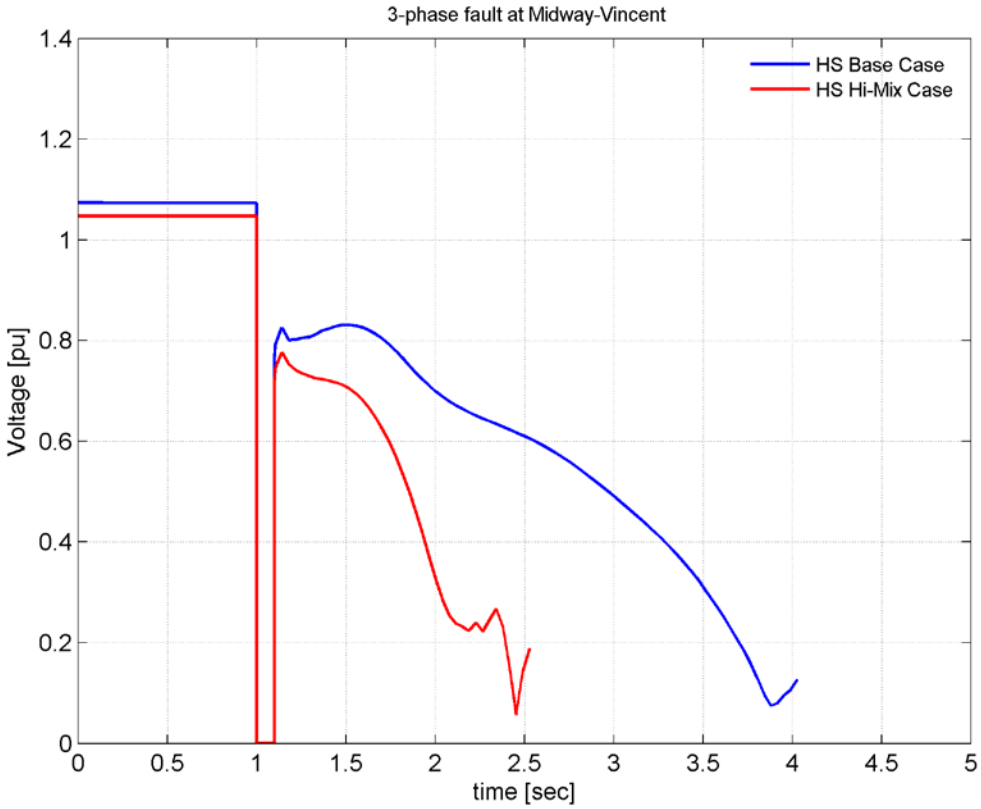

Figure 36. Voltage collapse for Midway-Vincent fault – HS Base vs. Hi-Mix.

The depth of the voltage depression that causes the motors in the composite load model to decelerate is a function of the location and severity of the fault. A sequence of tests was run to determine sensitivity to fault severity. A case in which the Midway fault impedance is set to .00005 + j.005 to approximate a single-phase fault results in no FIDVR. The voltage (as shown in Appendix Figure 104) and the load recovered within 50 ms of fault clearing. The DG blocking was reduced to about 900 MW. With this single-phase fault equivalent, the difference in the characteristic of the successful recovery between the Base case and Hi-Mix case was small. The Hi-Mix recovery is slightly faster. In a further test of sensitivity to fault severity, the fault impedance for the successful single-phase event was progressively reduced, until FIDVR occurred. This sequence, which includes a case where the system exhibits classic FIDVR for about 30 seconds before recovering, is shown in Appendix Figure 105.

5.1.2.1 Details of Composite Load Model Behavior

The dynamics of the composite load model are considerably more complex than those of the standard WECC load model, and as shown, dominate the system behavior for some faults. The details of the behavior of two of the composite loads for the unstable Midway-Vincent fault are

shown in Figure 37. Two buses are shown: one in southern California that is close to the faulted bus, and another in Arizona, remote from the fault. The voltage never recovers for the bus near the fault. The remote bus finally collapses as the entire system becomes unstable at around 2 seconds. The simulation after that point is meaningless, and the plot is truncated. In Figure 38, the details of these two loads are shown, with the red trace being the load near the fault. The dynamic part of the load, as represented by one of the four motor equivalents, is ill-mannered, with an aggressive but failed attempt to recover on fault clearing driving up the reactive power consumption. Some load reduction is observed in the static and electronic components, but it is insufficient to save the system. The drop-out of the PV, shown in the bottom left plot, exacerbates the problem. When the fault clears, the voltage does not recover enough for the distributed PV to restart. Had some of the motor load been allowed to trip (as discussed above), the system would likely recover. That behavior would, however, make the impact of the incremental wind and solar extremely difficult to discern.

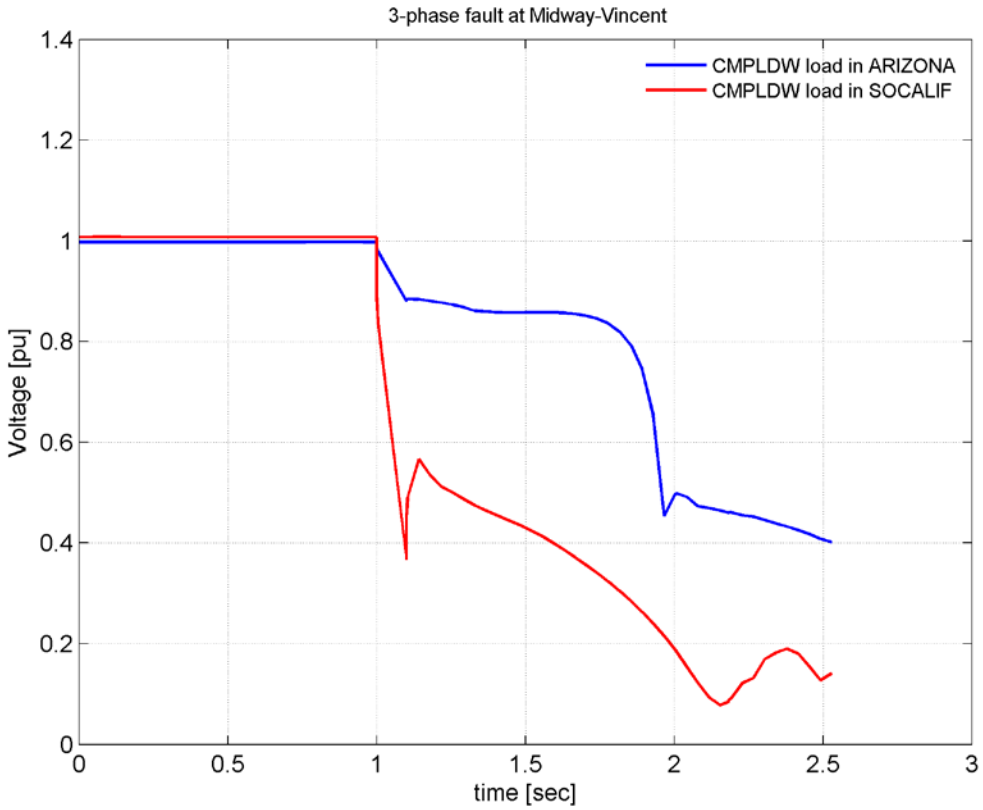

Figure 37. Load bus voltages at different distances from fault location.

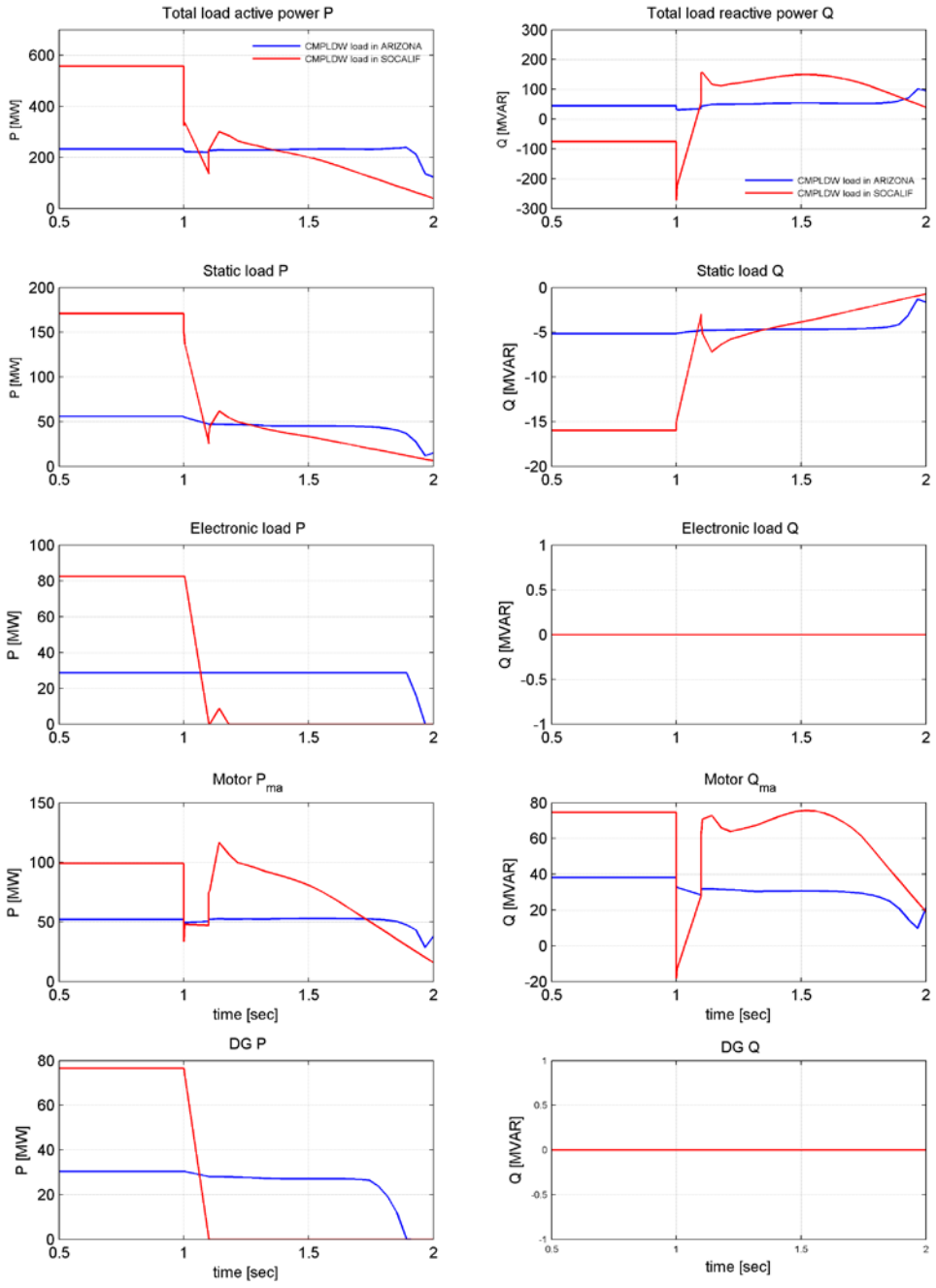

Figure 38. Details of load behavior relative to fault proximity.

The conclusion to be drawn from this sequence of tests is that with this load modeling, the system is on the edge, regardless of renewable generation. The behavior of the system for deep faults is completely dominated by the load model, and more specifically by the trip vs. stall behavior assumed for the motor models. Drop-out of the distributed PV during the voltage depression exacerbates the problem, as does the fact that voltage stays low enough to prevent the DG from restarting after the fault clears. This is an extraordinarily complex issue for planning

and for research. However, this stability risk is not primarily one of renewable integration on the bulk power system. Overall, the utility-scale renewables have relatively little impact on voltage recovery here, especially compared to the sensitivity and uncertainty of the load modeling. The ride-through and recovery characteristics of the embedded PV contribute to the motor stall as modeled, which suggests that PV controls designed to address this behavior could be beneficial. Further investigation of the load behavior, the motor tripping, and the behavior of the PV DG is warranted. In the next section, some aspects of DG tripping are investigated.

5.1.3 Distributed Generation Voltage Ride-Through Sensitivity

The operation of inverter-based DG, including PV, during and following system disturbances is governed by two factors: equipment physical capability and deliberate and/or mandated reactions.

The physical constraints on inverter-based generation are substantially different from those on synchronous machines. During system disturbances, fast, high-bandwidth controls must measure and react to depressed, occasionally distorted, and unbalanced voltage waveforms while respecting the sensitive current-carrying capability of the power electronics. Therefore, it is a non-trivial challenge for PV to continue operation through disturbances. As was shown in the preceding example, inverters may block (i.e., stop carrying current) briefly or for extended periods.

For utility-scale generation, fault ride-through capability has been mandated by FERC and NERC rules (FERC 2005, NERC 2013), and wind and utility-scale PV suppliers have designed equipment that will continue operation through disturbances. However, for distribution-connected generation, such requirements have not been imposed, so the ride-through behavior of the embedded PV currently in operation is not well known. Further, IEEE Standard 1547 addresses the obligation of DG to trip in order to avoid inadvertent islanding. That standard provides ranges of voltage and frequency depression depth and duration for which DG must trip (see Appendix Figure 106 and Figure 107). The standard has been recently modified, with the intent to provide a mechanism by which the must-trip behavior can be modified. The issues and details of the tension between the desire to avoid inadvertent islanding and the desire to maintain bulk power system reliability are complex.

5.1.4 Impact of Distributed PV Recovery

5.1.4.1 Midway-Vincent Fault

For the single-phase fault at Midway presented above, about 825 MW (out of 9.4 GW) of distributed PV blocked during the fault and then recovered following the fault. A sensitivity case in which the blocked PV does not recover was run. This simulates DG tripping due to physical limitations (i.e., a sympathetic trip) or deliberately (i.e., to comply with IEEE 1547 or other objectives).

Even with the loss of this DG, the system is stable and voltages recover. The aggregate behavior of the DG active power is shown in Appendix Figure 108. The majority of the lost active power is picked up by responsive generation. Voltage recovers slightly slower to a level 1.2% lower with tripped DG. More dramatically, the tripping of the DG has a large impact on the reactive power balance. The total reactive power generation from all generation is plotted in Figure 39.

The blue trace is for full recovery (temporary blocking), and the red trace is for no recovery (trip). In the post-fault-clearing condition, the 825 MW of tripped DG "costs" the system about 3,100 MVAr – almost 4 MVAr/MW. This is indicative of a significant level of system stress. This result suggests that inadvertent or deliberate tripping of DG during system disturbances may have significant voltage stability effects. These effects could be more problematic than frequency impacts.

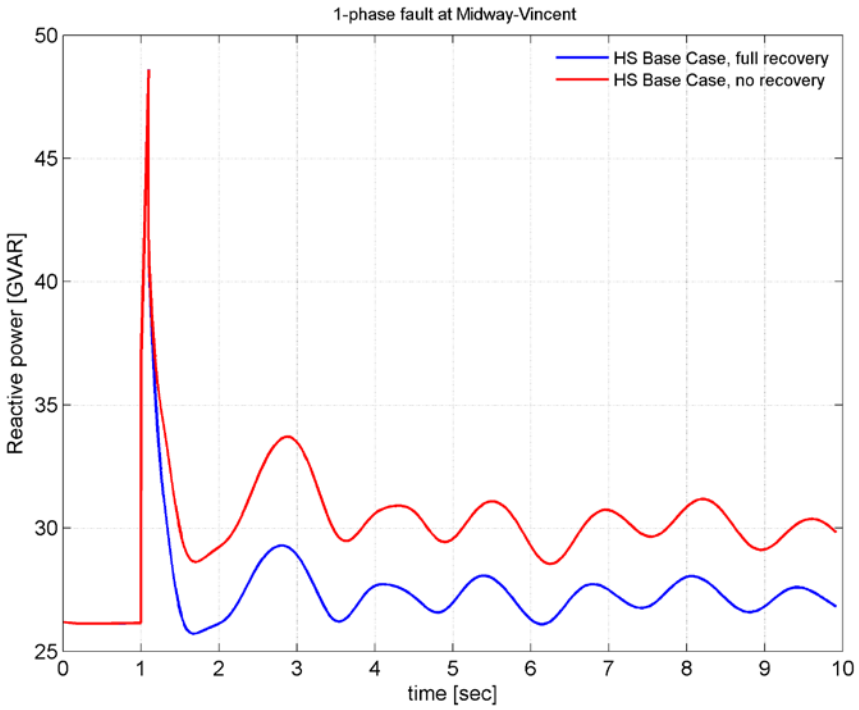

Figure 39. Reactive power depletion due to DG tripping on voltage dip.

5.1.4.2 PDCI Event

The results of the PDCI block event were presented above. For the HS Hi-Mix case, RAS tripping of a single NW hydro plant was shown to stabilize the power swing across the COI, but it does not quite meet the WECC voltage swing criteria.

That event behaves quite differently if there is a significant tripping of DG due to the post-disturbance voltage swing. In this exercise, the DG is modeled with a pessimistic under-voltage tripping characteristic. The DG only maintains full current output down to 88% voltage. Below 83%, all the current is stopped and is not allowed to recover. This is allowed under IEEE 1547, but normally a time delay of up to 2 seconds would be imposed before the DG is deliberately tripped.

The result of DG tripping during the power swing is to exacerbate the voltage stress and cause the system to lose synchronism, as shown in Figure 40. Other voltages are shown in Appendix Figure 109.

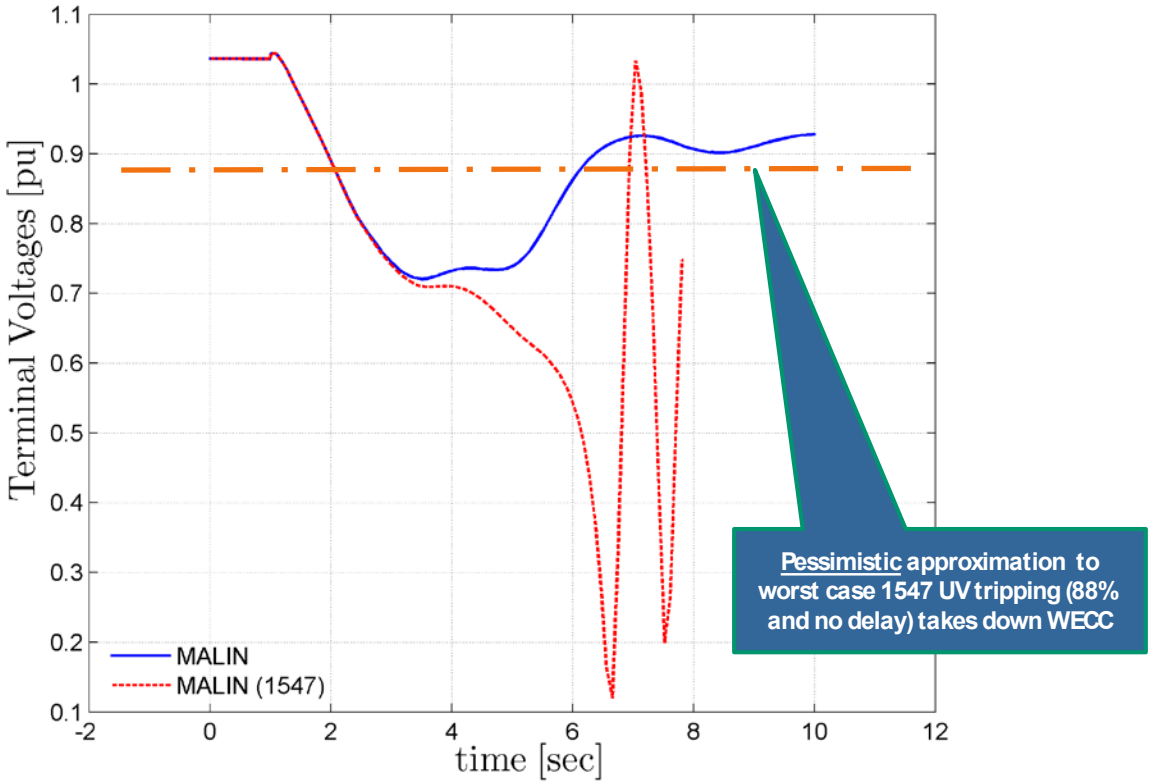

Figure 40. COI destabilization due to DG tripping on voltage dip.

5.2 Impact of Widespread Distributed Generation Tripping

The results presented above give rise to the question: what is the impact of tripping a large amount of small, widely distributed DG? How does that compare to the impact of a single large event such as the Palo Verde outage? A test was run in which a fraction of all the DG in the system was tripped, for a total amount approximately equal to the generation of the two units tripped in the Palo Verde event.

In Figure 41, the system frequency plots show that the DG event results in a less severe frequency nadir and a better settling frequency. The difference is relatively small and is primarily due to two factors. First, the loss of DG partially starves the loads for locally generated power. Additional MW must be drawn from the grid, not only through the bulk power system but down through the distribution system to the load (see the composite load topology in Figure 10). The result is depressed voltages at the load buses, as can be seen in Figure 42. This causes the net load to drop in the DG case, as shown in Figure 43. The effect is especially pronounced in the California and DSW regions, where most of the DG resides. This load relief helps the system frequency. A second relatively minor effect is that the DG that trips is ultimately a few hundred MW smaller than the 2,756 MW of the Palo Verde event. This is partly due to voltage effects on the tripping logic in the composite load model, as can be observed in Appendix Figure 110.

Broadly, the location of the generation tripping is not terribly significant compared to the amount of generation that is tripped. The impact on loads due to voltage change is a different face of the effect observed in other cases: namely, post-disturbance flows tend to be different and can have

substantial impacts on load voltages. Dropping load voltage results in some beneficial load relief due to load voltage sensitivity. Conversely, improved voltages can aggravate the frequency drop. This result tends to reinforce the conclusion that load voltage sensitivity is a more important consideration for FR than for load frequency sensitivity.

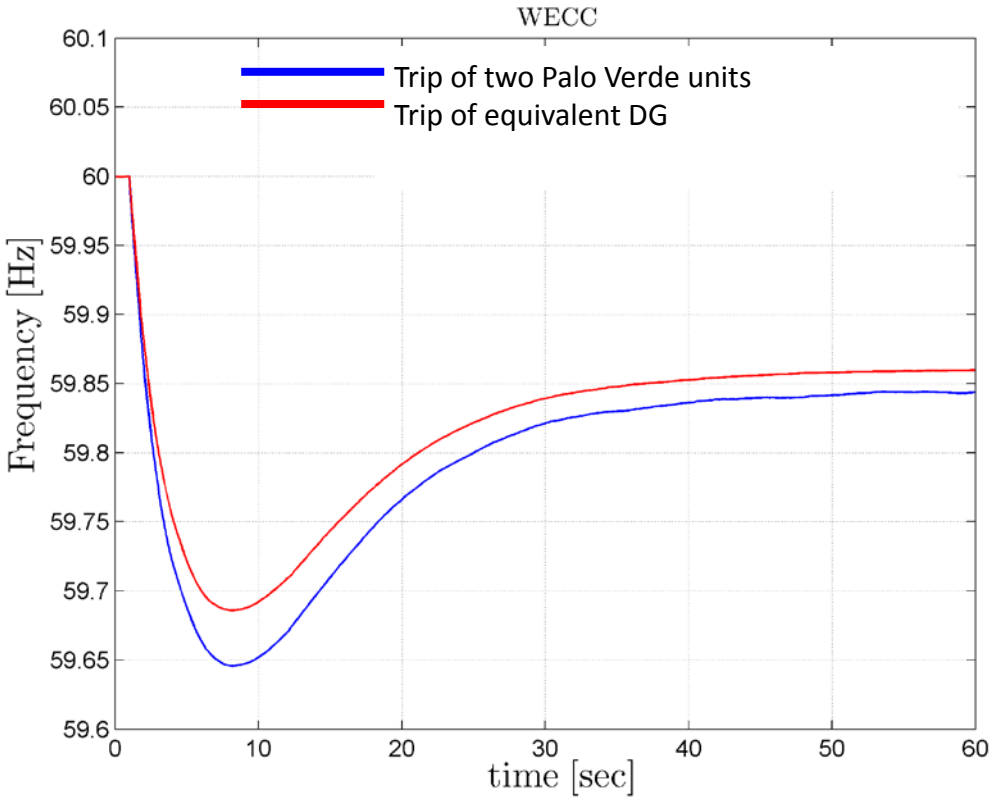

Figure 41. Frequency response of LSP Hi-Mix case – DG trip vs. two Palo Verde unit trip.

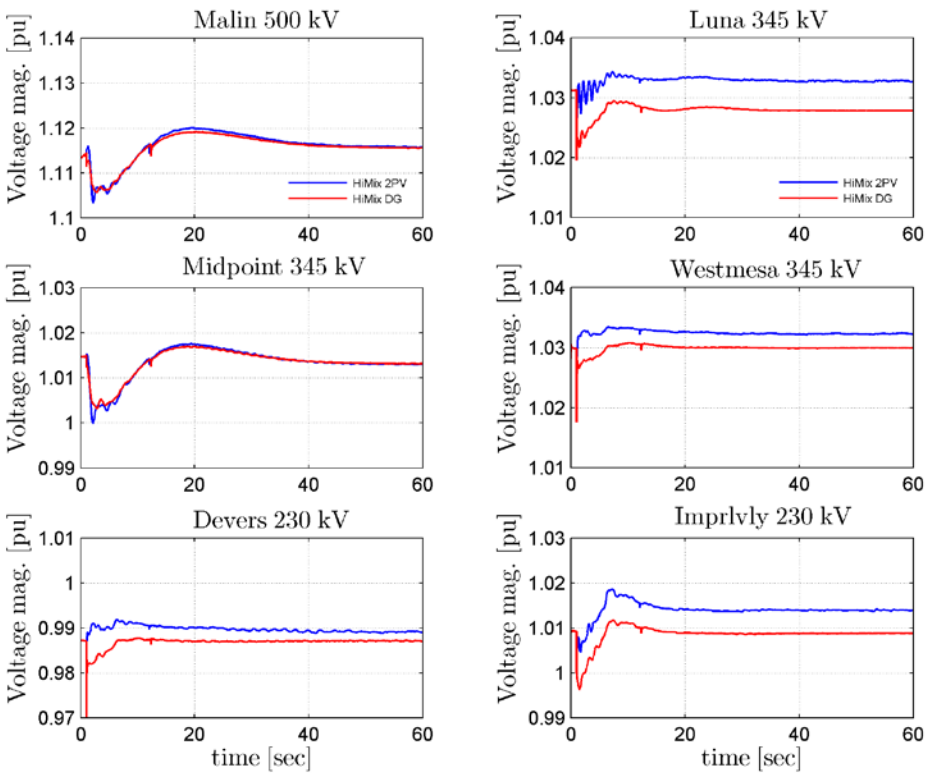

Figure 42. Voltage response of LSP Hi-Mix case – DG trip vs. two Palo Verde unit trip.

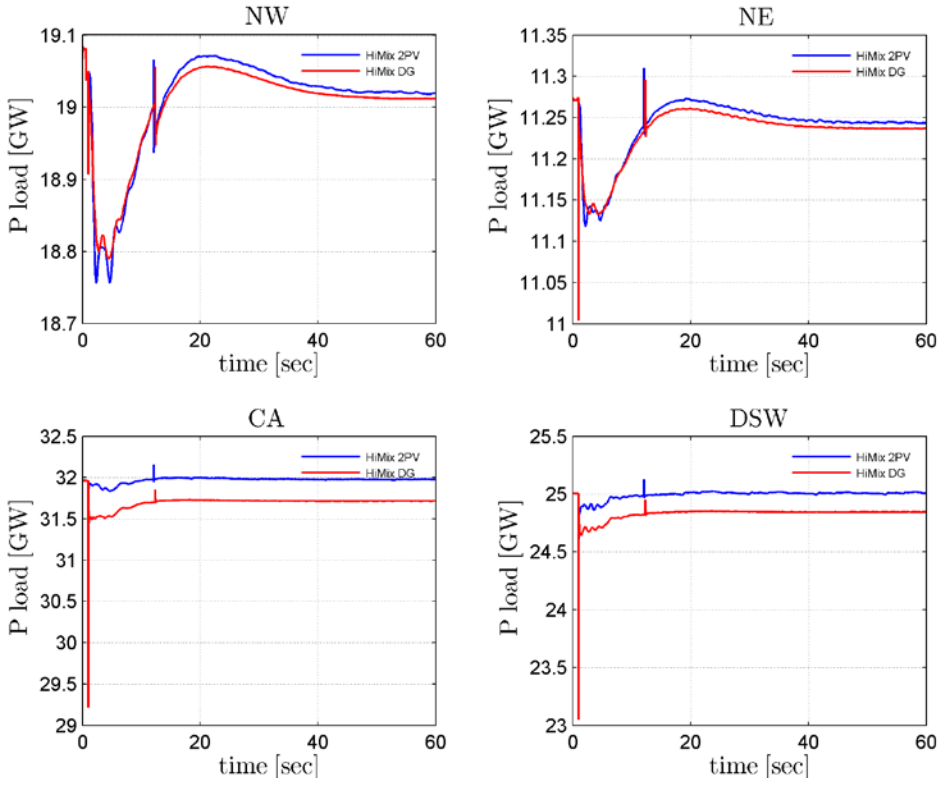

Figure 43. Load response of LSP Hi-Mix case – DG trip vs. two Palo Verde unit trip.

5.3 Extreme Generation Tripping

The FR results presented thus far have focused primarily on the loss of two Palo Verde NPS units, as this is the design-basis event for FR in WECC. Here, simulations on the LSP Hi-Mix case are presented showing the design-basis event (trip of two Palo Verde units) and a more severe event (trip of all three Palo Verde units).

The WECC frequency for these two events is shown in Figure 44. Notice that the frequency nadir drops below 59.5 for the three-unit outage—which is the frequency at which UFLS would occur. The UFLS is deliberately not modeled here, so the relative performances can be compared. Some selected voltages are shown in Appendix Figure 115. Note that the decrease in frequency nadir is nearly proportional to the size of the event. The WECC FR response metrics, 1,311 MW/0.1 Hz vs. 1,265 MW/0.1 Hz, are similar. This extends to the individual regions and areas, as shown in Appendix Table 47. The FR behavior for this substantially larger event is close to linear, showing only a slight degradation due to the larger-sized event and more governor controls saturating. This is reassuring from a robustness perspective, though obviously an event this severe will still cause UFLS-triggered interruptions, just as it does today.

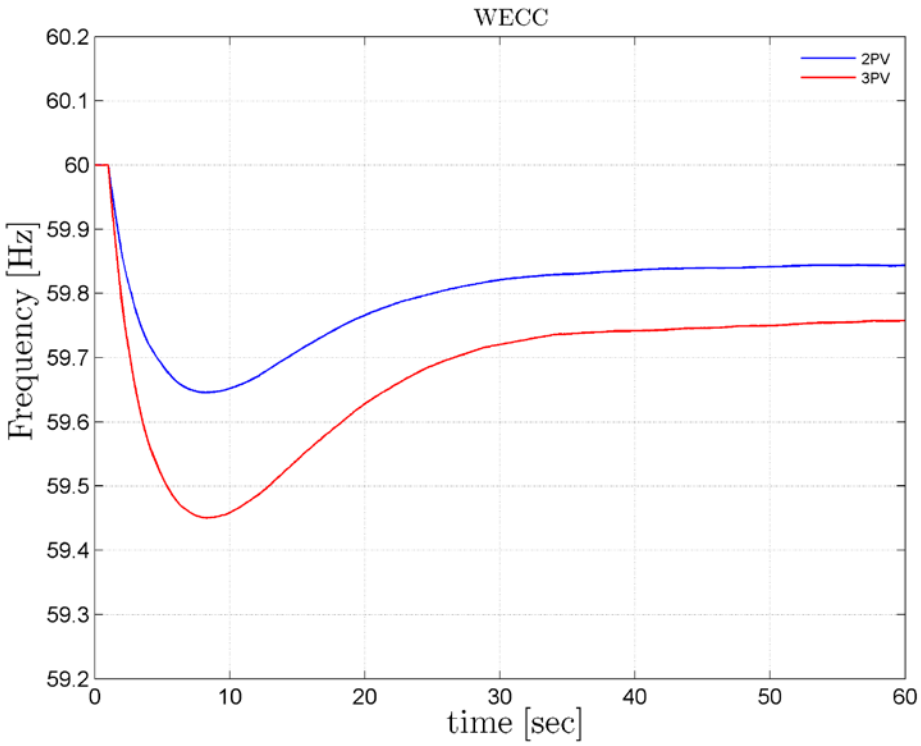

Figure 44. Frequency response of LSP Hi-Mix to Palo Verde trip – two units vs. three units.

5.3.1 Under-Frequency Tripping of Distributed Generation

The rather extreme frequency excursion shown for the trip of three Palo Verde units raises an interesting question about the deliberate or inadvertent under-frequency tripping of DG.

In this sensitivity, all of the PV DG is modeled with high sensitivity to under-frequency. The settings for under-frequency trip modeling (as described in Section 2.2.3) are such that some DG

starts to drop out at 59.5 Hz and all of it is tripped by 59.4 Hz. This frequency tripping is instantaneous and latching.

This representation is deliberately pessimistic. Inverter systems are relatively tolerant of smooth frequency deviations of this type. If this sensitivity is viewed in the context of tripping to meet compliance with IEEE 1547, the representation is also pessimistic in that there is no delay between hitting the tripping threshold and actual tripping.

The results are rather dramatic. A comparison of system frequency between the three-unit Palo Verde trip case (blue traces) and this sensitivity with DG tripping on under-frequency is shown in Figure 45. Appendix Figure 116 and Figure 119 show voltages and interface flows, respectively. When the grid frequency drops below 59.5 Hz, the resultant tripping of DG causes a further drop in frequency. While the system does stabilize below 59.2 Hz, there is no reason to think that the Western system would actually tolerate such a violent swing. As the reference case (blue trace) drops below 59.5 Hz for a number of seconds, under-frequency tripping would be likely even with the minimum 2-second time delay allowed by IEEE 1547. A much longer delay (e.g., >100 seconds) would have largely decoupled the anti-islanding tripping from the frequency excursion. This is uncertain territory. While UFLS action is allowed for a severe event like this, cascading failure is not. Consequently, widespread DG tripping for moderately severe frequency excursions is unwise.

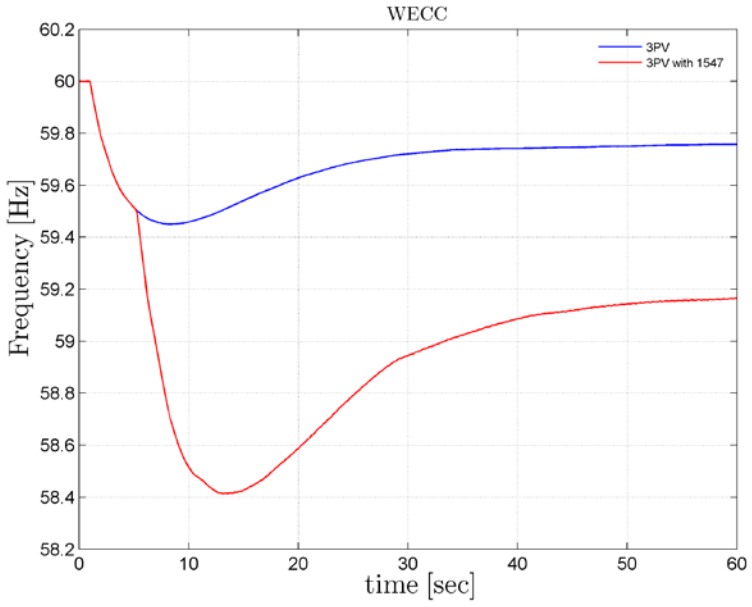

Figure 45. Frequency of LSP Hi-Mix to trip of three Palo Verde units – DG trip vs. no DG trip.

5.4 Headroom Depletion Analysis

This investigation examines growing concern over emerging net load profiles with strong midday solar generation. These so-called “duck curves” first appeared in Europe, with net load profiles in Germany and Italy being particularly affected. The midday depression of net load presents some particular challenges to the system. Based on discussions with CAISO, there is

concern that commitment and dispatch to accept high solar can leave the system short of responsive resources in the evening when solar drops off and before wind picks up.

A particular concern is that that FRO will not be met, especially for some individual BAs. The investigation presented in this section aims to develop a better understanding of the FR (and transient stability) consequences of possibly extreme measures for following the rapid net load rise.

5.4.1 Evening Net Load Rise and Duck Curves

In order to illustrate this concern, a single-day dispatch chart is shown in Figure 46 from April 20 of the WWSIS-2 Hi-Mix PLEXOS runs. The contribution of the solar (both PV and CSP) is outlined in green to show the "duck" curve.

The LSP Hi-Mix case was developed to investigate a high instantaneous penetration in the morning. The case has a total load of 111 GW, with wind and solar at 52.8 GW for 48% penetration. The total headroom is 21.9 GW. The wind and solar production was from a high wind and solar spring morning and is highlighted with the vertical blue line (7:50 on April 4, 2020).

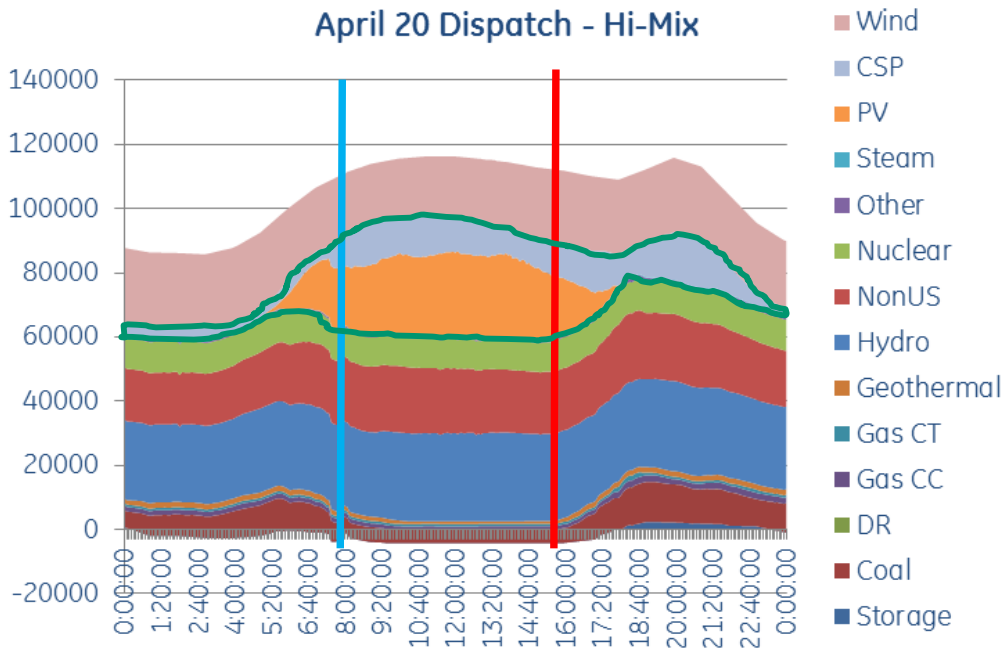

Figure 46. LSP Hi-Mix representative dispatch showing "duck" curve.

A key point here is that the wind and solar output, load, generation commitment, and dispatch in the morning are similar to those in late afternoon (shown with the vertical red line). That means that the LSP Hi-Mix condition is a good starting point to examine the impact of the relatively rapid drop in PV production that occurs in the afternoon. The same-day dispatch with no wind or solar is shown in Appendix Figure 118. For comparison, the HS and Extreme LSP cases are shown in Appendix Figure 119 and Figure 120.

5.4.2 Case Development

A primary concern about the evening drop-off of solar production is that the committed units need to be dispatched up to compensate for the combinations of lost solar production and evening load rise. The timing makes it a challenge for system operators to commit more units. As a result, generation headroom tends to be used up rather than saved to meet FRO. This investigation aims to examine the consequences of that headroom depletion. The investigation followed this sequence:

1. Hold commitment constant
2. Decrease solar PV production
3. Dispatch up committed units
4. Recalculate headroom, Kt, and other metrics
5. Run Palo Verde two-unit event
6. Observe frequency and calculate FR performance
7. Return to step 2 and repeat until solar PV is off.

Freezing the commitment is a conservative approach. The objectives were to see how far the system can go without committing more generation, determine how much quick-start capability needs to be kept ready, and determine whether additional commitment and dispatch constraints are needed to hold headroom. This also provides some insight into the consequences of making mistakes (e.g., due to poor forecasts). In the longer term, this type of investigation could drive changes in the generation portfolio in the future.

A sequence of cases is summarized in Table 18, with a shorthand name provided in the left column and notes on the re-dispatch and other changes needed to accommodate the drop in PV in the second column. As the table notes, re-dispatch to cover the drop in distributed PV was accomplished using units identified by the PLEXOS dispatch sensitivity. As the utility-scale PV dropped, other committed units were dispatched upwards. The only hydro that was changed was in the NW.

More than 30 intermediate steps were required to develop the first three cases (Hi-Mix, DGoff, PVoff) shown in the table. Changing more than 13 GW of solar generation required trimming voltages, monitoring flows, and many minor adjustments to create satisfactory initial conditions for meaningful stability simulations. The final steps of the re-dispatch squeezed remaining on-line resources.

In addition to the need to trim the system load flows, many steps were made in reducing the PV because it was the expectation that the system would indeed fail. As will be shown below, the system did not fail in the sense of losing stability or hitting UFLS. The FR relative to FRO dropped further, and in California the contribution of hydro, mostly in the PG&E area, was critical. This last point is important, and was the motivation for the additional five cases shown in the table. In the Hi-Mix, DGoff, and PVoff cases, there is 3.2 GW of headroom on the California hydro. The contribution of that hydro to FR in these cases is critical, especially for California's FRO. In the additional cases in this sequence (e.g., case "1.2BL"), the California hydro headroom is removed by turning the governors to base load (BL), thereby removing their

under-frequency responsiveness. This is a modeling proxy for the possibility that these plants might not be able to provide extra power (e.g., because of lower water levels and gates wide open).

The impact of the re-dispatch on regional headroom is summarized in Figure 41. The three bars on the left in each chart are for the Hi-Mix, DGoff, and PVoff cases. The five bars to the right only affect California headroom. Note that the headroom in the eastern regions is relatively unaffected. This is because the generation available for re-dispatch under this condition is not responsive, so dispatching closer to maximum has no impact on FR. However, the headroom in the NW is reduced by about half, and the California headroom drops about 1 GW. Figure 121 in the Appendix shows Kt.

Table 18. Headroom Depletion Cases

Case	Description
Hi-Mix	2022 LSP Hi-Mix case
DGoff	Starting from Hi-Mix case, DG is turned completely off (≈7.2 GW); based on PLEXOS results, units were dispatched up; hydro in NW (responsive), and coal and CC (mostly unresponsive).
PVoff	Starting from DGoff case, utility-scale PV is switched off (≈6.4 GW); pumped storage units switched to generating mode; hydro units in CA dispatched up; the rest of PLEXOS list units dispatched up. Phase shifters (BLGS PHA, RMRK PHA, and CROS PHA) adjusted and limit increased. Valmont capacitor bank added and BLACKWTR DC increased from 50 MW to 200 MW.
1.2BL	1.2 GW of California hydro units with governor switched to base load units
1.8BL	1.8 GW of California hydro units with governor switched to base load units
2.1BL	2.1 GW of California hydro units with governor switched to base load units
2.8BL	2.8 GW of California hydro units with governor switched to base load units
3.2BL	3.2 GW (all) of California hydro units with governor switched to base load units

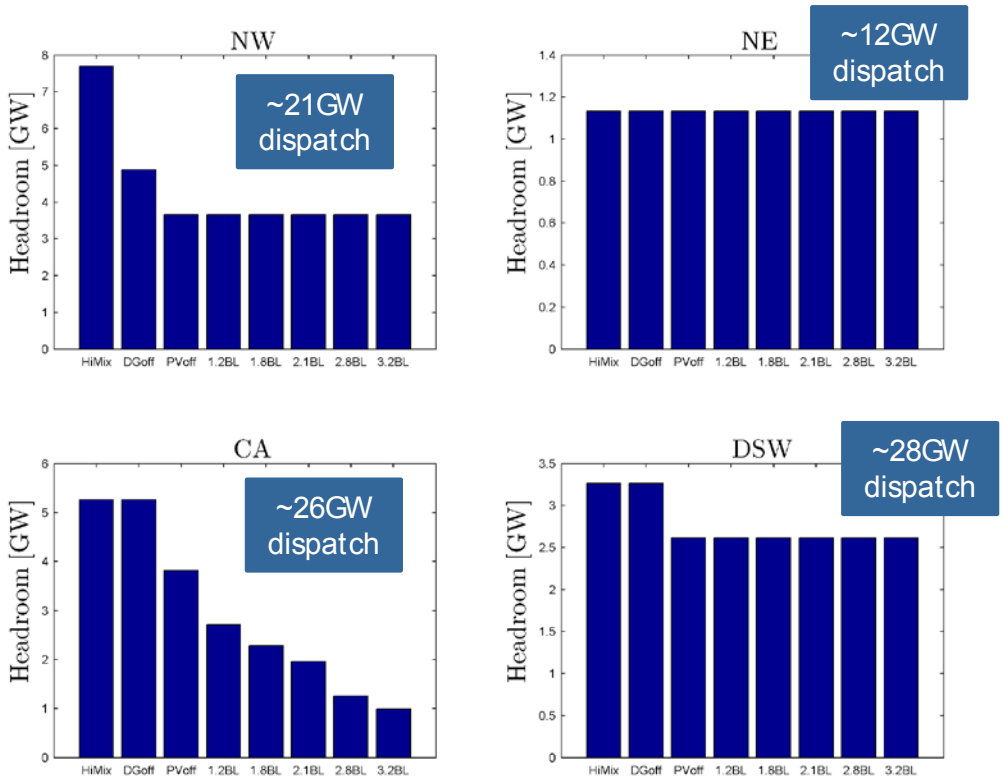

Figure 47. Headroom by region for all headroom depletion cases.

5.4.3 Impact on Frequency Response

The impact of declining headroom on overall frequency is shown in Figure 48. The intermediate cases between PVoff and all CA hydro unresponsive (3.2BL) are not plotted to make the figure more legible.

The impact of reduced headroom on the frequency nadir and settling frequency is substantial. However, the frequency does not drop below 59.5 Hz, where UFLS would act, even for the most extreme case with all CA hydro unresponsive. The nadir of 59.58 Hz gives some margin. The regional frequencies, dynamics of the GR, and various network voltages and flows are shown in the Appendix starting with Figure 124. The dynamics of the loads are interesting: in the last case (3.2BL), there is several hundred MW of load response due to voltage changes that did not occur in the reference case.

The overall WECC FR is shown in Figure 49. Note that WECC meets the IFRO, even with all PV off and no new generation committed (PVoff case). As the California hydro drops out, the WECC FR declines below the IFRO. At the regional level, the FR shown in Figure 50 illustrates the decline associated with re-dispatch, with the major impact being in the NW as hydro dispatches up. It is interesting to note that the FR there decreases roughly in proportion to the drop in headroom. Figure 51 shows, as expected, that most of the decline in FR from disabling hydro in California occurs in the PG&E area.

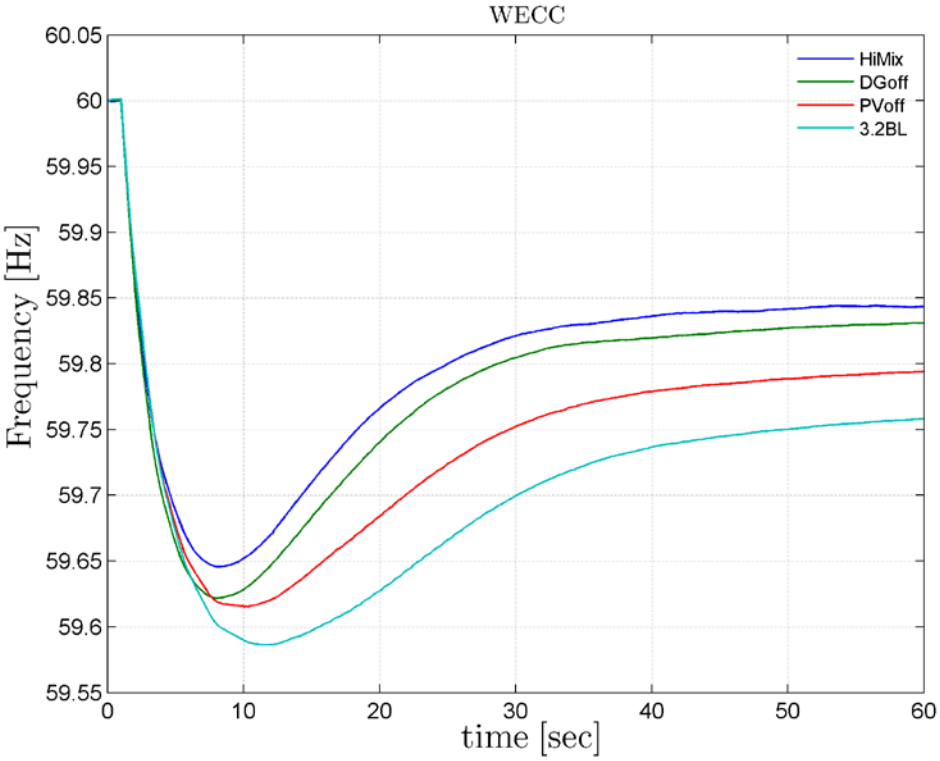

Figure 48. WECC frequency in response to two Palo Verde unit trip for all headroom depletion cases.

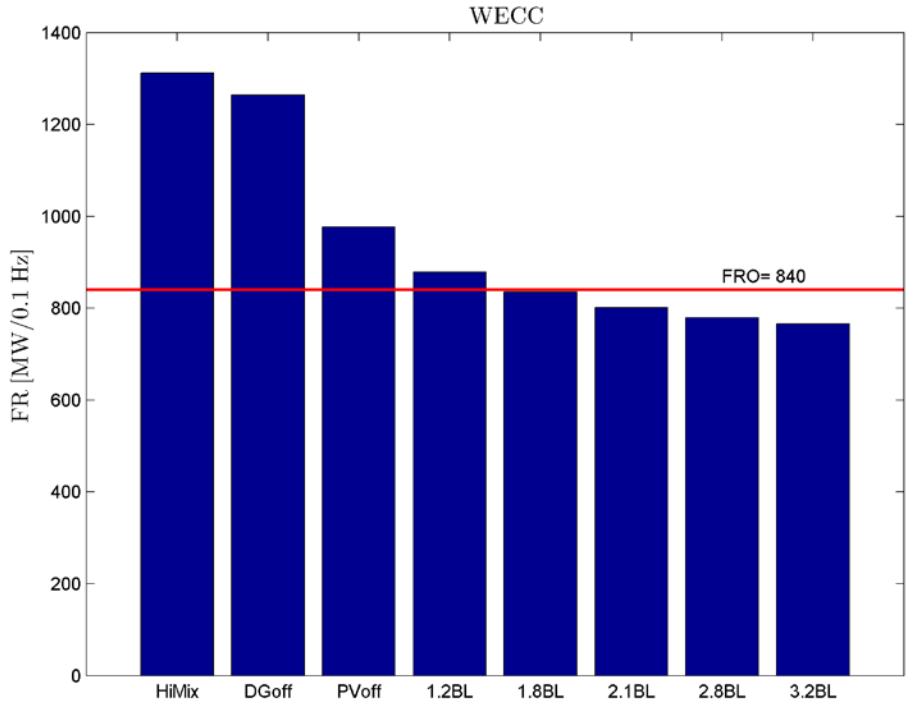

Figure 49. WECC FR metric for two Palo Verde unit trip – all headroom depletion cases.

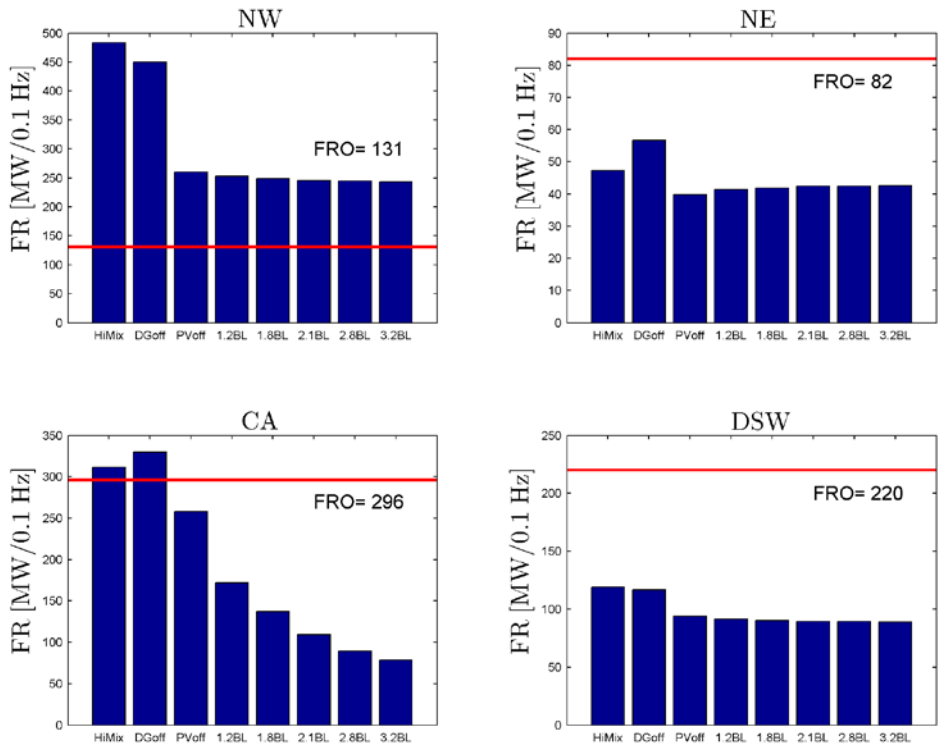

Figure 50. Regional FR metric for two Palo Verde unit trip – all headroom depletion cases.

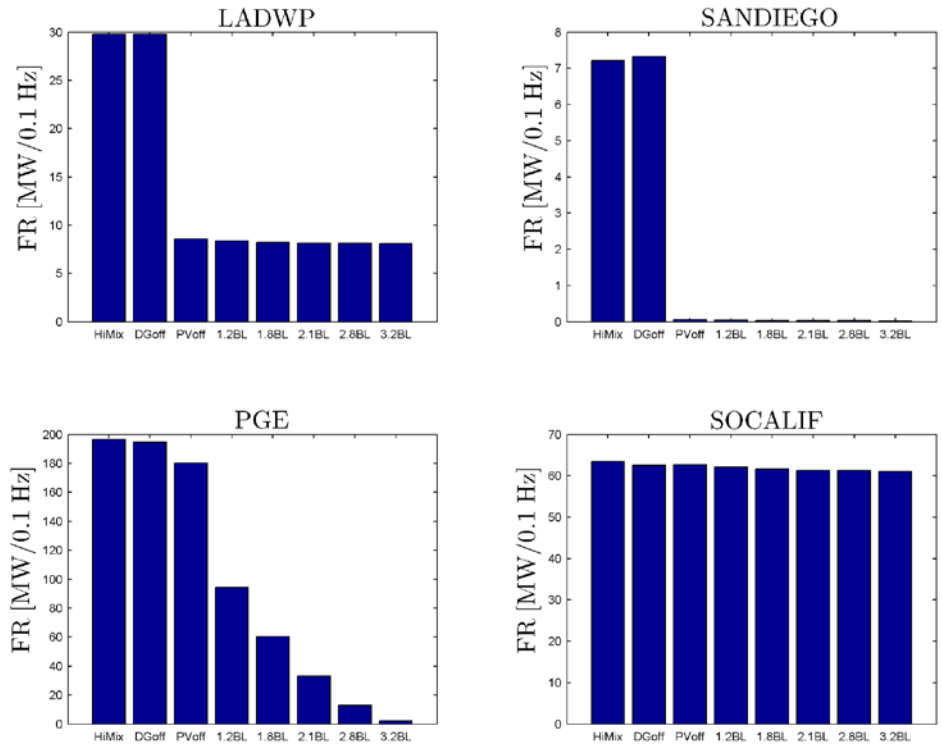

Figure 51. California FR metrics for two Palo Verde unit trip – all headroom depletion cases.

5.4.4 Headroom Depletion Summary

The rather extreme case of shutting down all PV generation in the West, while allowing no additional generation to be committed, does not create a catastrophic failure in the system performance. No dramatic non-linearities in performance trends were observed as the PV dropped out (i.e., there was no cliff). Rather, the degradation of FR is steady and monotonic.

However, once the PV output has reached zero, the overall WECC FR is marginal, even with significant contribution from CA hydro. The FR for CA is below the approximate FRO. As the CA hydro becomes unresponsive, the overall WECC FR drops. WECC fails to meet the IFRO, with about half of the CA hydro unresponsive.

As the system re-dispatches, there are many local stress points (e.g., poor voltage) as PV output drops. This suggests that the need to commit/recommit units could be driven as much by local constraints as by overall stability. The details will be important as the system stress builds. Further, there are minor local stress-related stability issues. For example, individual units were observed to have low dynamic voltage capability, and some units dispatched at their maximum lost synchronism. This further suggests that locational issues may drive some constraints on FR.

5.5 Effect of Unit De-Commitment on Base Case

In creating the LSP Hi-Mix case, there was an intermediate step in which only the distributed PV was added. This is a substantially different case, which embeds about 7 GW of distribution-connected PV with the load.

To balance the added DG, thermal units were de-committed. Only de-commitment was used in this step; no units were dispatched down. The net result is a case in which Kt drops and headroom does not increase. The renewable profile and initial condition metrics are shown in Appendix Table 48.

This is unrealistic in the sense that the economics are unlikely to cause only de-commitments. However, the stability results are of some interest. Therefore, a simulation of the two Palo Verde unit outage was run. Figure 52 shows the WECC frequency of this case (green trace) compared to that of the Base case (blue trace) and Hi-Mix case (red trace). De-commitment of governor-responsive units causes a slight degradation of frequency nadir. This case has poorer frequency performance than when the rest of the utility-scale renewables are added to create the Hi-Mix case. However, while the trends of this case are consistent with the preceding headroom depletion exercise, the correlation with headroom does not prove causality. Changes in flow patterns and other factors could also contribute. The result illustrates that specific details of commitment and dispatch impact overall system performance, as well as increasing renewable generation.

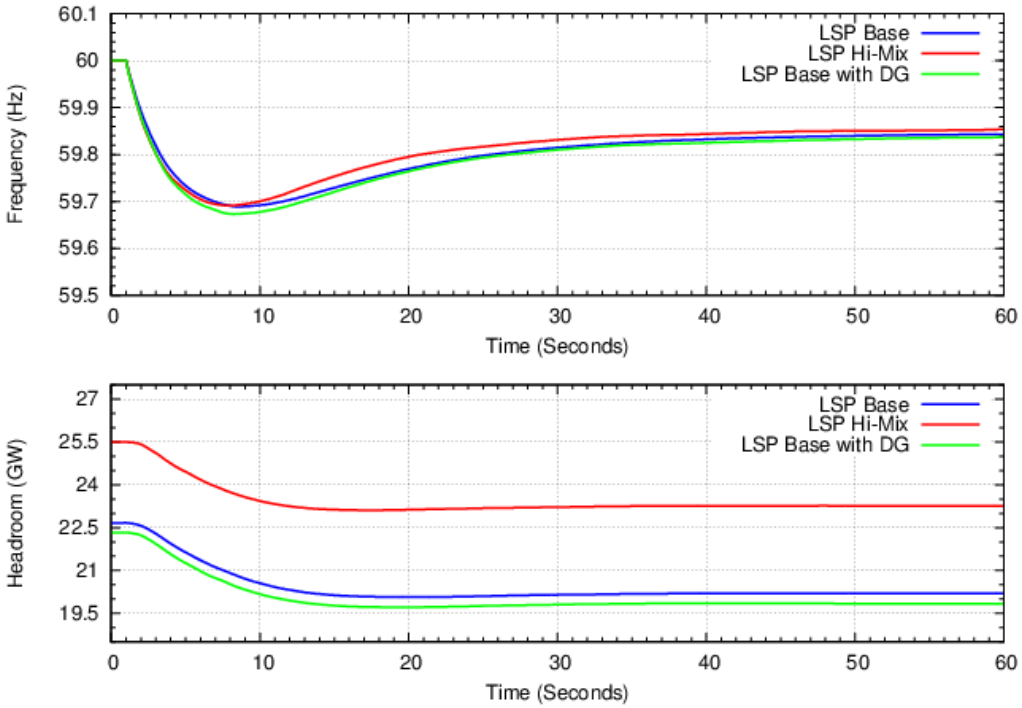

Figure 52. Effect of thermal plant displacement on frequency and headroom for LSP cases.

5.6 CSP Sensitivity

About 10 GW of CSP capacity is added to the Hi-Mix cases. Recent development trends in the West appear to be shifting to utility-scale PV instead of CSP. The Hi-Mix cases therefore benefit from having this well-mannered CSP synchronous generation in Arizona and California, and the stability results for the Hi-Mix cases may be optimistic. This investigation explores the possible impact of replacing CSP synchronous generation with utility-scale PV.

5.6.1 Converting CSP to Utility-Scale PV

The LSP Base case includes about 900 MW of CSP plants. The Hi-Mix case increases that by 7.5 GW to about 8.4 GW. For this sensitivity, only 3.3 GW of CSP was retained in the Hi-Mix case. All other CSP plants were converted to PV.

All the CSP in the LSP Base case was retained and matched to NREL's CSP database where possible.[2] Then, the NREL and other data were used to identify high-probability CSP plants that were under construction or fully financed. Five CSP plants (Ivanpah, Mojave, Tonopah, Genesis, and Solana) were identified. New CSP plants in the Hi-Mix case that roughly aligned with these projects were retained. All other new CSP plants were converted to utility-scale PV. Several figures in the Appendix, starting with Figure 129, show this mapping. The net result was that 70 of 81 plants totaling about 5,100 MW were converted from CSP to utility-scale PV.

[2] Thanks for support from Mark Mehos at NREL for source material/CSP database.

5.6.2 Impacts of CSP and System Inertia on Frequency Response

The new CSP sensitivity case (green trace) is shown with the Base (blue trace) and Hi-Mix (red trace) cases in Figure 53. The impact on FR of conversion of the CSP to PV is directionally as expected, with the biggest impact on ROCOF: the PV has no inertia, and so loss of the inertia from the CSP would be expected to cause a more rapid initial frequency decline. The initial ROCOF, shown in detail in Figure 54, was 0.096 Hz/s in the LSP Base case, and 0.113 Hz/s with the Hi-Mix case. This is an 18% increase in ROCOF. For the CSP sensitivity case, the initial ROCOF rises further to 0.118 Hz/s; this is 4% lower than the Hi-Mix case and 23% lower than the Base case.

The impact of this increased ROCOF on the system stability is nearly invisible in terms of FR. Both the nadir and the settling frequency are essentially unchanged. These levels of ROCOF, on the order of 0.1 Hz/s, are quite small. Some smaller systems around the world have ROCOF concerns primarily driven by the use of ROCOF relays. In the United States, ROCOF relays are not in significant use. Similar, but less severe, results were observed for the HS case, as shown in Appendix Figure 131 and Figure 132.

This exercise further reinforces the observation that for large U.S. interconnections, the loss of system inertia associated with increased wind and PV is of little consequence for up to 50% instantaneous levels of penetration.

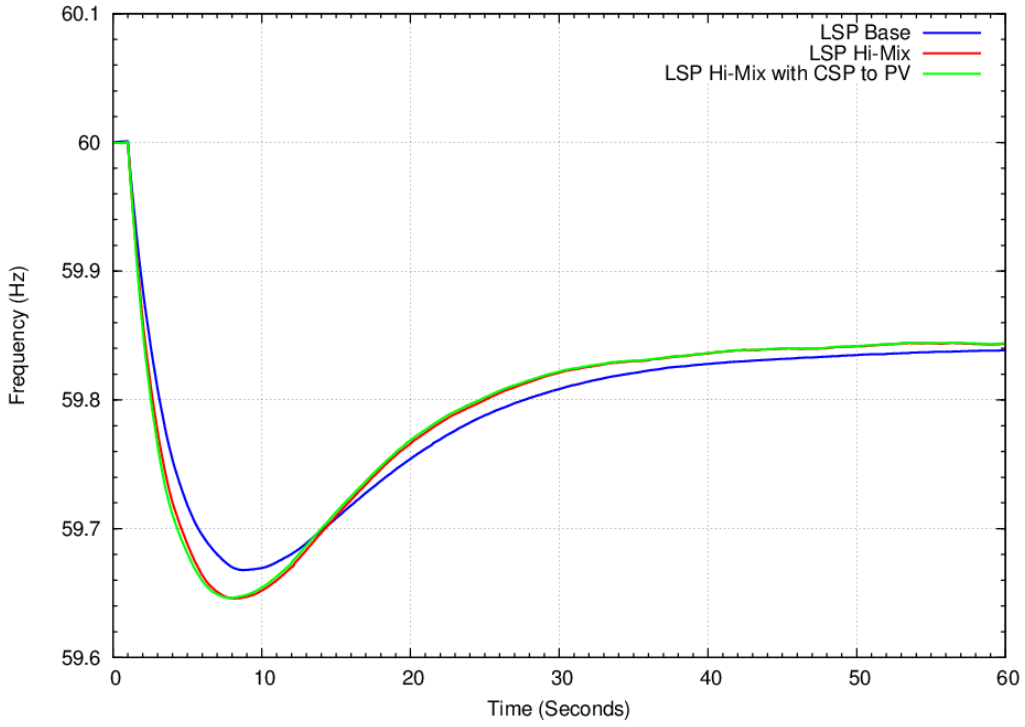

Figure 53. Frequency response to trip of two Palo Verde units – LSP Base vs. Hi-Mix vs. CSP sensitivity.

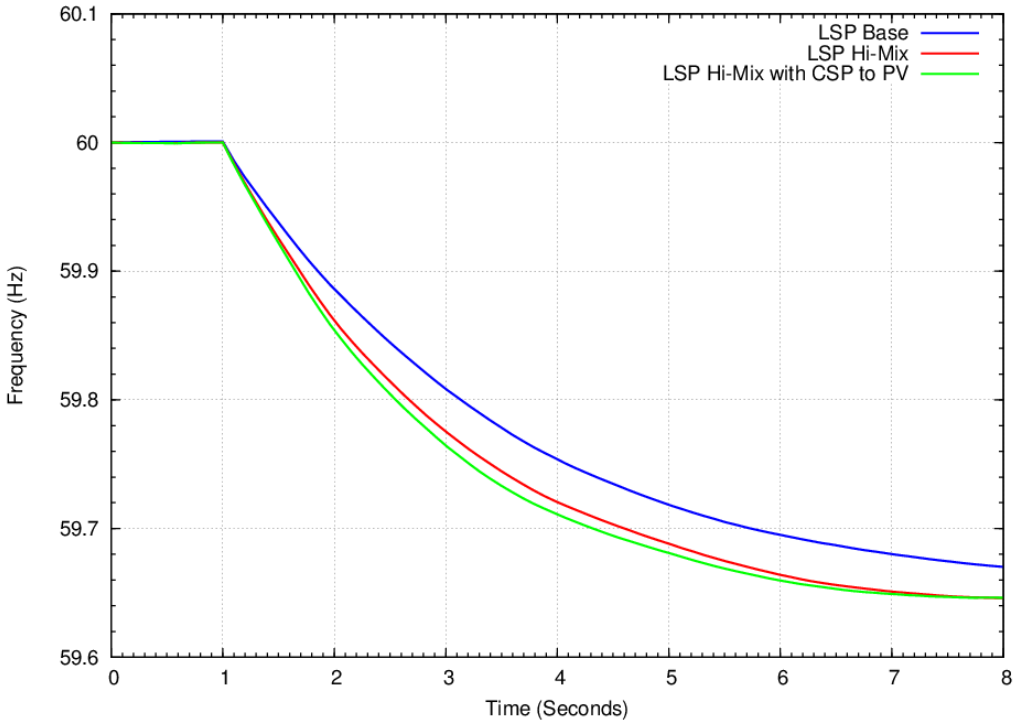

Figure 54. ROCOF response to trip of two Palo Verde units – LSP Base vs. Hi-Mix vs. CSP sensitivity.

5.7 Light Spring Extreme Instantaneous Renewable Penetration

The LSP Hi-Mix case represents a system condition with high instantaneous wind and solar penetration likely to present operational challenges—especially for FR. The evolution of the commitment and dispatch of the generating resources from the Base case to the Hi-Mix case is described in detail in Section 2.5. The Hi-Mix condition was deliberately selected to be both challenging and representative, rather than an extreme outlier or the absolute worst possible condition. In this section and in Section 6, such an extreme condition is developed and analyzed.

5.7.1 Dispatch and Commitment

The coal dispatch figure used to describe the process of changing commitment and dispatch on the coal plants is shown again in Figure 55 (this figure was first shown as Figure 9 and is described in detail in the accompanying text in that section). In the Hi-Mix case, a specific sample of wind and solar generation near the middle of the cloud of green points was used to dispatch the wind and solar. That sample (# 31775 on April 4, 2020, at 7:50) had about 48 GW of wind and solar production, representing a point close to the mean of the sample space. In this version of the figure, the point with the absolute highest wind and solar generation of that sampling of 5-minute points is highlighted with a vertical green line. That point, with about 62 GW of wind and solar production (sample # 30692 on April 16, 2020, at 13:35), is used for this Extreme case.

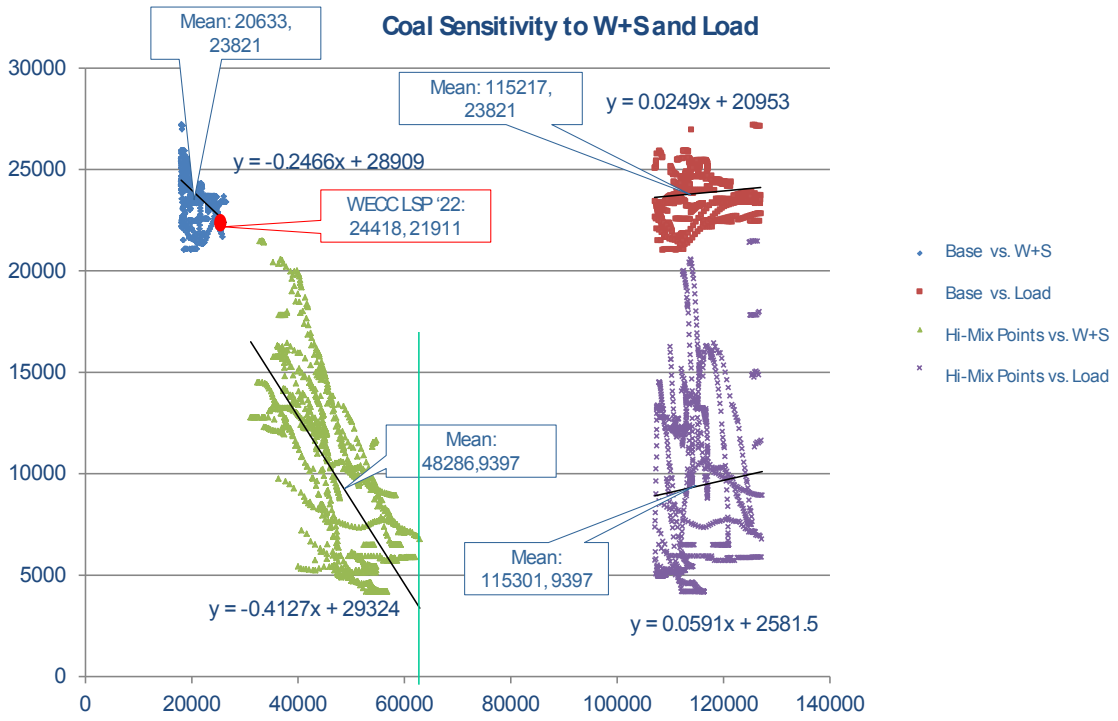

Figure 55. Extreme renewable case within LSP coal dispatch samples.

To develop this extreme case, the production of the wind and solar plants in the Hi-Mix case was changed (usually—but not always—increased) to the levels of the Extreme sample. The same relatively minor differences between the WWSIS-2 Hi-Mix renewable capacity and that in the final Hi-Mix case for this study were taken into account.

During the commitment and dispatch to accommodate the added wind and solar production, it became apparent that the difference in the system load level between this LSP case and the WWSIS-2 PLEXOS model was important. Specifically, the load level for this case (about 111 GW) is about 10 GW lower than the smallest load in any sample of the WWSIS-2 PLEXOS cases. This difference in load level was easily handled in the development of the Hi-Mix case and resulted in a rather conservative initial condition, in the sense that the system dynamics would be more challenging than the WWSIS-2 system would suggest. However, for this extreme condition, it proved challenging to reduce generation by another 12 GW to accommodate more wind and solar. The net result is truly extreme for the 33% wind and solar energy scenario: extremely high wind and solar generation combined with extremely low system load.

The details of the difference between the Hi-Mix and Extreme PLEXOS samples are shown in Appendix Table 49. The totals for DG, PV, and wind each increase more than 3 GW. The CSP is essentially unchanged because CSP production is substantially less volatile, especially with the thermal energy storage assumed for these plants from WWSIS-2. The topological differences between the WWSIS-2 wind and solar capacity and the capacity in this case results in another 1 GW difference. Thus, the total additional wind and solar production is 12 GW.

The de-commitment and re-dispatch approach applied to the coal and CC plants was similar to that described in Section 2.5, but there were some differences. For the Hi-Mix case, changes in commitment and dispatch were made to units that the production simulation showed as likely to change with the added wind and solar. Because this case is extreme, a reasonable assumption was that any unit that PLEXOS showed as de-committed between the Base and Hi-Mix cases for any sample pair would be de-committed. Obviously, many units were de-committed to evolve from the Base case to the Hi-Mix case, so the remaining candidates had a total of 3,580 MW available. This is only the first step in the process of displacing 12 GW of other generation to make room for the incremental wind and solar. Other CC plants that are in the WECC case but not in the WWSIS-2 PLEXOS data set (and were therefore invisible to the difference-based selection process) were de-committed. This provided about 5 GW of reduction. A further 2 GW of hydro plants in the NW and in Canada were de-committed. Any peaking CTs that had been committed were retained, in order to reflect their likely participation in secondary FR or regulation.

The net result is a dispatch and commitment that is credible for this condition but does not have the degree of economic rigor applied to the Hi-Mix cases. It is likely that the overall profile includes some deviations from normal practice.

A summary of the regional dispatch is shown in Figure 56. For quick comparison, the three LSP cases have wind and solar totals of:

- ~25.6 GW in the Base case
- ~52.7 GW in the Hi-Mix case
- ~64.6 GW in the Extreme case.

The WECC-wide and regional summary of the FR initial condition is given in Appendix Table 50, with details given in Appendix Table 51. A key point is that the overall WECC Kt is 0.38. Kt was 0.42 in the Hi-Mix case. The regions to the east have Kt less than 0.30, and there is only 1.0 GW of headroom in the Northeast. This is evidence of stress on the system.

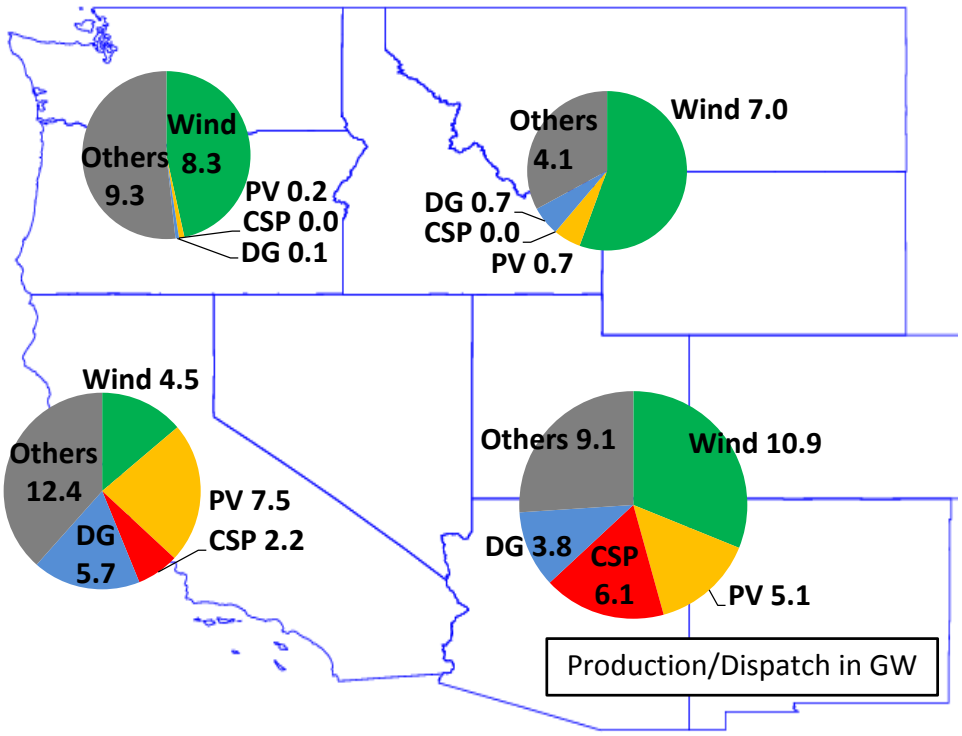

	WECC	California	DSW	Northeast	NW
Wind (GW)	32.4	4.5	10.9	7.0	8.3
PV (GW)	13.5	7.5	5.1	0.7	0.2
CSP (GW)	8.3	2.2	6.1	0.0	0.0
Distributed PV (GW)	10.4	5.7	3.8	0.7	0.1
Others (GW)	56.6	12.4	9.1	4.1	9.3
Total (GW)	121.2	32.3	35.1	12.6	17.9
Penetration (%)	53%	62%	74%	67%	48%

Figure 56. Wind and solar generation in the LSP Extreme case.

The difference in commitment and dispatch from the Hi-Mix to the Extreme case results in some substantial changes in flow patterns—and equally important, the removal (by de-commitment) of important sources of voltage support. In order to obtain successful load flow solutions and achieve reasonable voltage profiles, the process of increasing the wind and solar production and reducing the other generation was carried out in many relatively small steps. In the intermediate steps, the displaced generation was typically dispatched down to zero, but left in service to regulate voltage to get an interim load flow solution. Then, the displaced generation was de-committed, thereby eliminating voltage support. At each step of the way, various locations experienced poor voltages. This was especially true in the East and in more geographically distributed parts of the system. In a few locations, transformers (e.g., between 138 kV and 230 kV) experienced overloads. These local voltage problems were generally addressed by the addition of shunt capacitors, and in a few cases by adding a parallel transformer. Appendix

Figure 133 gives a sense of the areas and sequence of these additions. It should be emphasized that these reinforcements are not the result of the rigorous process that would be needed to identify robust and economic mitigation of local voltage and thermal problems. Rather, they are reinforcements to allow reasonable initial conditions for the transient stability and FR investigations. In order to correct these types of problems—which are inevitable under these extreme conditions—much more detail of individual wind and solar projects, and of local transmission, is needed. The basic system engineering required to accommodate a high wind and solar build-out is well established and is not in the scope of this work. Appendix Figure 134 shows the bubble diagram for the Extreme case.

5.7.2 Path Loading

As noted above, the re-dispatch to achieve the wind and solar penetration of the Extreme case was challenging. Table 19 shows a comparison of the loadings on some key paths in the Western Interconnection. In the Extreme case, a few of the paths are over their catalog ratings; these are highlighted in red. These paths are inside California and in the vicinity of particularly high-density wind in eastern Wyoming and Colorado. Even though the results presented to this point in the study have not identified radical changes in system dynamics, the acute changes in system flow patterns suggest that rigorous analytical checks of the events that dictate the path ratings (and any new events) are warranted. Certainly, all the regional paths in the high wind parts of the eastern part of the Western Interconnection will change as transmission is added to accommodate the new plants.

Table 19. Path Loadings in LSP Cases

Path Number	Path Name	Path Loading (MW)			Path Rating (MW)
		LSP Base	LSP Hi-Mix	LSP Extreme	
10	West of Colstrip	2,025	297	-193	2,598
15	Midway-Los Banos	1,467	4,545	5,997	4,800–5,400
22	Southwest of Four Corners	1,829	-339	485	2,325
26	Northern-Southern California	1,140	-2,654	-4,181	4,000
30	TOT 1A	414	154	875	650
37	TOT 4A	357	259	1,088	810
43	North of San Onofre	664	1,018	-682	2,440
46	West of Colorado River (WOR)	4,204	7,126	7,365	10,623
48	Northern New Mexico (NM2)	-18	-357	-1,790	-1,970
49	East of Colorado River (EOR)	3,100	3,588	4,062	9,300
66	California-Oregon Interface (COI)	2,346	-267	-1,593	4,800/-3,675

5.7.3 Frequency Response

A comparison of the WECC frequency for the new Extreme case (red trace) to the Base (blue trace) and Hi-Mix (green trace) results for the Palo Verde event are shown in Figure 57. The frequency nadir decreases to 59.613 Hz, and the FR decreases to 1,055 MW.

Note that even for this extreme condition, the frequency nadir is above UFLS and the WECC-wide FR meets NERC criteria. The summary of individual area FR in Table 21 shows that about half of the areas are deficient in terms of meeting their estimated FRO with reserves within their areas. The DSW region has less than half of the approximate FRO. Appendix Figure 135 shows the regional headroom being dynamically depleted. Appendix Figure 136 shows the governor-responsive units saturating. The impact is incremental, and in many regards it looks similar to the headroom depletion cases presented in Section 5.4.

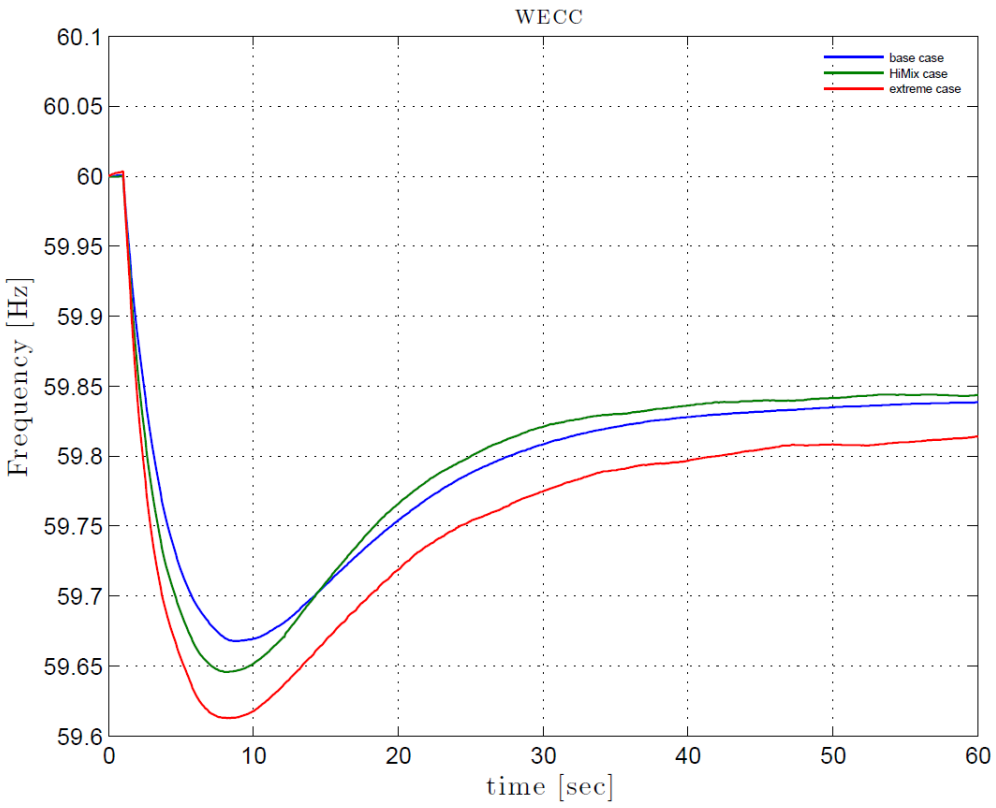

Figure 57. Frequency response to two Palo Verde unit trip – LSP Base vs. Hi-Mix vs. Extreme.

Table 20. LSP FR Metrics Including Extreme Case

	LSP		
	Base	**Hi-Mix**	**Extreme**
Generation (GW)	204	204	204
Load (GW)	185	185	185
FRO (MW/0.1 Hz)	840	840	840
FR (MW/0.1 Hz)	1352	1311	1055
FR Margin (MW/0.1 Hz)	512	471	215
Frequency Nadir (Hz)	59.668	59.646	59.613
Nadir Time (s)	7.77	7.19	7.38
Settling Frequency (Hz)	59.839	59.844	59.814
Kt	0.46	0.42	0.38

Table 21. WECC, Region, and Area FR Metrics for LSP Extreme Case

		LSP Base Case				LSP Extreme Case			
Name	**FRO (MW/ 0.1 Hz)**	**FR (MW/ 0.1 Hz)**	**FR Margin (MW/ 0.1 Hz)**	**FR % of WECC**	**Kt**	**FR (MW/ 0.1 Hz)**	**FR Margin (MW/ 0.1 Hz)**	**FR % of WECC**	**Kt**
WECC	840	1,352	512	100.0	0.46	1,055	214.7	100	0.38
By Region									
CALIFORNIA	296	305	9	22.6	0.34	295	-0.6	28	0.32
DSW	220	215	-5	15.9	0.44	97	-123.4	9	0.22
NORTHEAST	82	61	-20	4.5	0.26	51	-30.8	5	0.27
NORTHWEST	131	434	303	32.1	0.62	280	149.5	27	0.53
By Area									
ARIZONA	104	69	-35	5.1	0.37	45	-59.7	4	0.27
EL PASO	9	4	-5	0.3	0.42	3	-5.6	0	0.32
IDAHO	18	21	3	1.6	0.38	21	3.2	2	0.68
IMPERIALCA	4	14	10	1.0	0.24	14	10.2	1	0.18
LADWP	29	31	1	2.3	0.60	29	-0.1	3	0.33
MONTANA	11	10	-1	0.7	0.17	11	-0.3	1	0.16
NEVADA	28	44	16	3.2	0.72	19	-9.3	2	0.45
NEW MEXICO	14	50	35	3.7	0.49	2	-12.7	0	0.01
PACE	42	23	-19	1.7	0.22	11	-30.5	1	0.13
PG AND E	133	190	57	14.1	0.40	189	55.8	18	0.47
PSCOLORADO	36	-14	-50	-1.1	0.34	6	-29.8	1	0.25
SANDIEGO	21	7	-14	0.5	0.15	7	-14.4	1	0.16
SIERRA	11	7	-3	0.6	0.23	7	-3.2	1	0.21
SOCALIF	108	63	-45	4.7	0.23	56	-52.3	5	0.19
WAPA R.M.	27	63	35	4.6	0.67	23	-4.5	2	0.12
WAPA U.M.	0	3	3	0.2	0.94	3	2.5	0	0.61

6 Coal Displacement/Retirement and Weak Grid Concerns

The growth of renewable generation in the West, coupled with other economic and societal factors, raises the possibility of retirement of coal generation. Consideration of all the factors involved is outside of the scope of WWSIS-3. However, the displacement of coal, as discussed in the previous section and illustrated in Figure 55, provides an opportunity to investigate the transient stability implications of not only temporary de-commitment of coal generation but also the impact of possible coal plant retirements. The specific point is that evaluation of transient stability is always based on snapshots of operation. It matters little whether a specific resource, including a coal plant, is off-line because it was de-committed for this particular operating condition or because it was retired. Aside from the possibility of changes in overall system commitment and dispatch associated with a retirement, the system dynamics will be the same. In short, any coal plants de-committed in a snapshot power flow could be considered retired.

This section explores the impact of this on system performance, with particular attention to changes to transient stability.

6.1 Coal Displacement by Wind and Solar Generation

As described above, the evolution from the LSP Base case to the LSP Hi-Mix case and then to the LSP Hi-Mix Extreme case displaces thermal generation, especially in the Northeast and DSW regions.

The following sequence of figures illustrates the changes in dispatch with increasing wind and solar production. Figure 58 shows the regional dispatches by generation type for all five cases. Because the distributed PV appears as a load modifier, it is not included in these tables. This reflects the reality facing the grid operators, as the embedded DG will likely remain largely outside of operator controls, and absent monitoring and estimation systems may be nearly invisible to operators as well. The differences between the HS cases, while substantial, are much less dramatic than for the LSP cases. The next plot, Figure 59, shows the same information, but only for the LSP cases in the DSW and Northeast regions. This figure shows the dramatic reduction in coal dispatch (dark red bar) as the wind and solar generation increase from the Base case to the Hi-Mix case, and then a further drop in the Extreme case. Figure 60 and Figure 61 show a further breakdown for those two regions, with the individual area dispatch plotted. The differences are substantial. For example, essentially 100% of the coal generation in Idaho, Montana, and Arizona is off-line in the Extreme case. By comparison, coal is a relatively minor component of the change in dispatch in California (shown in Figure 62).

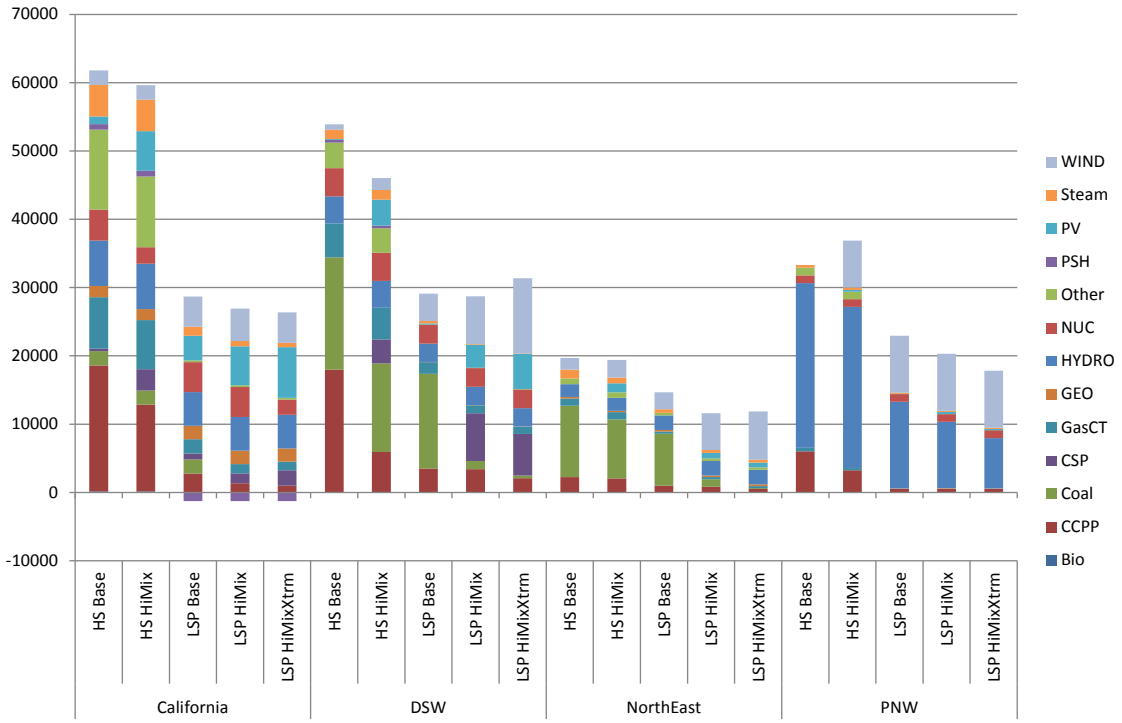

Figure 58. Regional generation dispatch for LSP and HS cases (no DG shown).

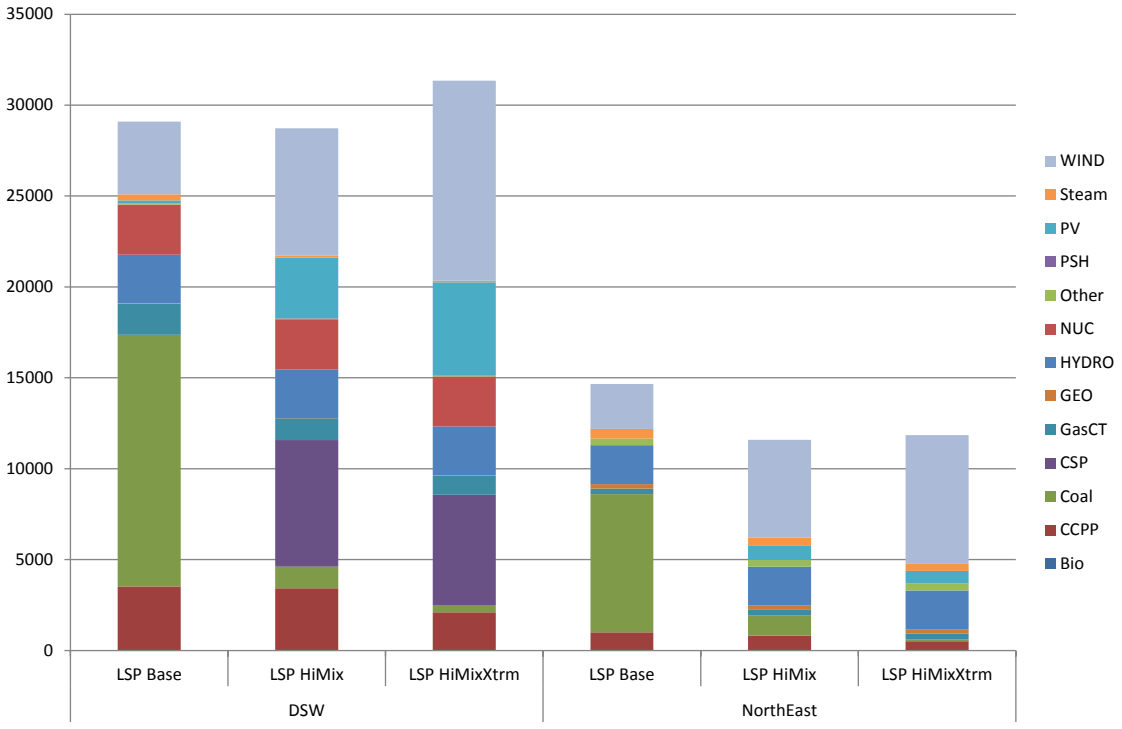

Figure 59. Coal displacement in Desert Southwest and Northeast regions for LSP cases.

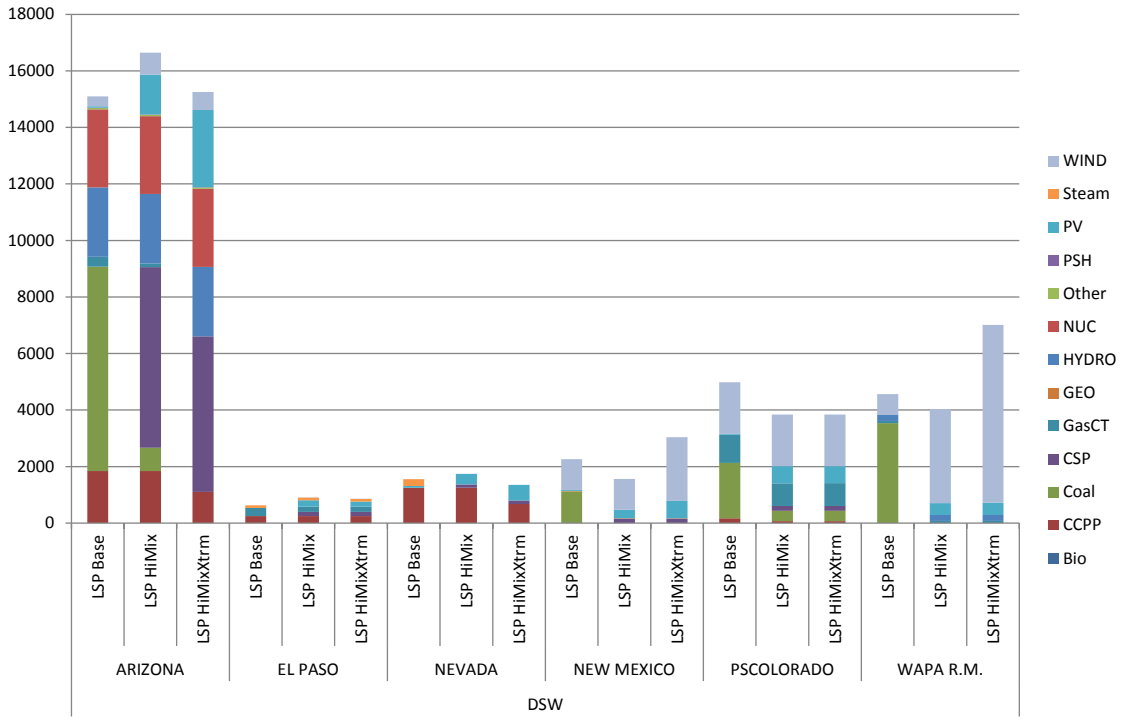

Figure 60. Coal displacement in Desert Southwest areas for LSP cases.

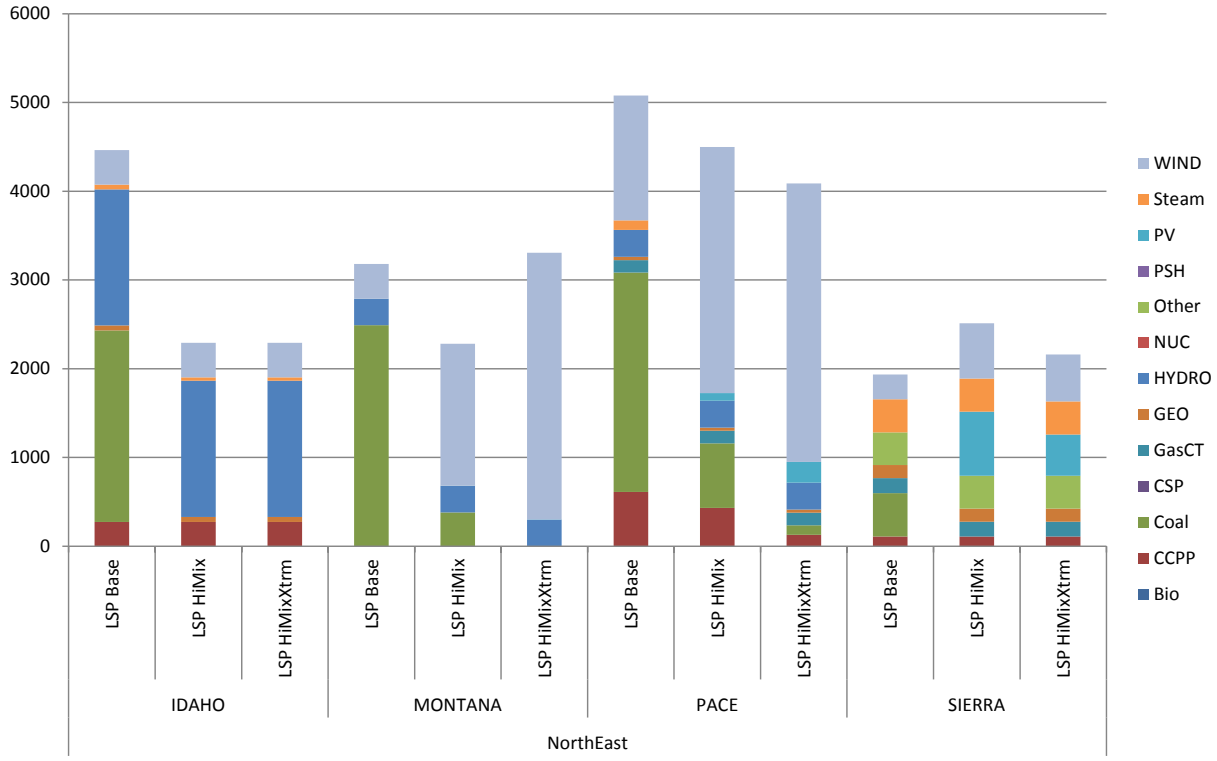

Figure 61. Coal displacement in the Northeast areas for LSP cases.

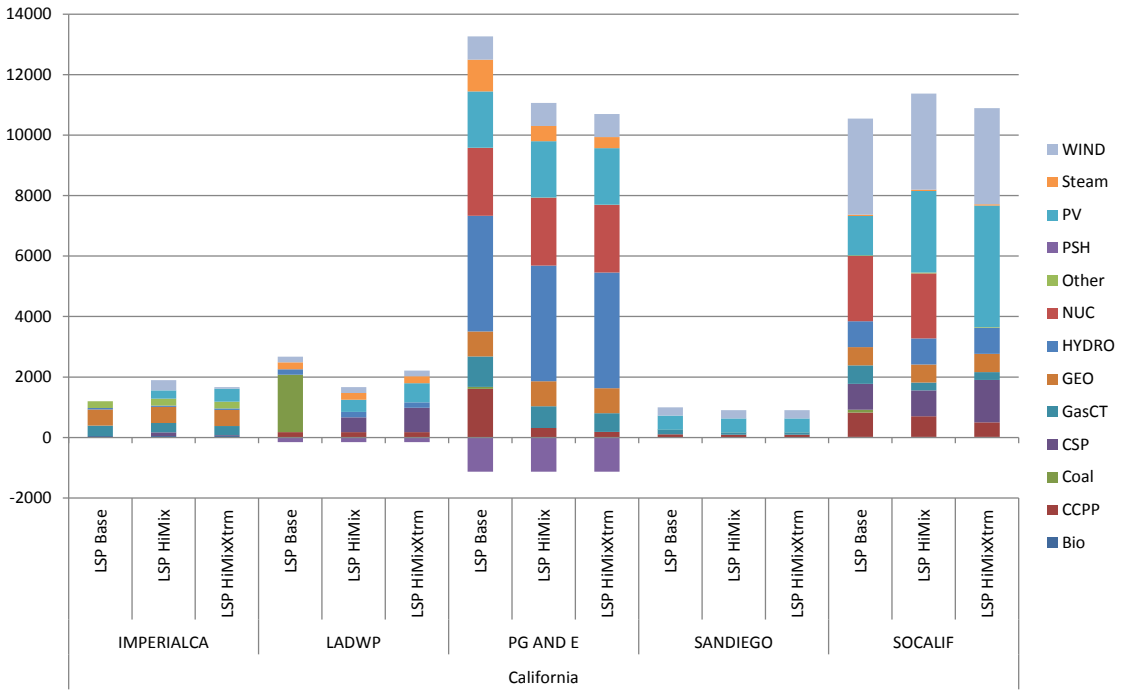

Figure 62. Change in dispatch in the California areas for LSP cases.

6.2 Northeast Region Stability Analysis

A major new 500 kV transmission project across the Northeast portion of the Western Interconnection is included in the WECC planning databases. It terminates in Eastern Wyoming at a new 500/230 kV substation named Aeolus. This project is currently under construction, and what is ultimately built may not match what was included in the data set.

The new project provides a significant path for power from both thermal and variable renewable generation in Eastern Wyoming to be exported toward the western part of the system. The flow on the two 500 kV lines out of Aeolus is 1,159 MW, 1,051.7 MW, and 1,787 MW for the LSP, LSP Hi-Mix and LSP Hi-Mix Extreme cases, respectively. A disturbance on the new 500 kV system thus presents a new and potentially significant stress to the grid. This section examines a four-cycle, three-phase to ground fault at the Aeolus 500 kV bus, cleared by tripping one of the 500 kV circuits to Anticline. A segment of the WECC planned transmission additions map[3] is shown in Figure 63 below, with a few added notations. The new Aeolus bus is called out, and the approximate location of the fault is indicated. Other elements discussed below are also highlighted.

[3] http://www.wecc.biz/committees/StandingCommittees/PCC/Shared%20Documents/2014-10yrmap%20Model%20(1).pdf

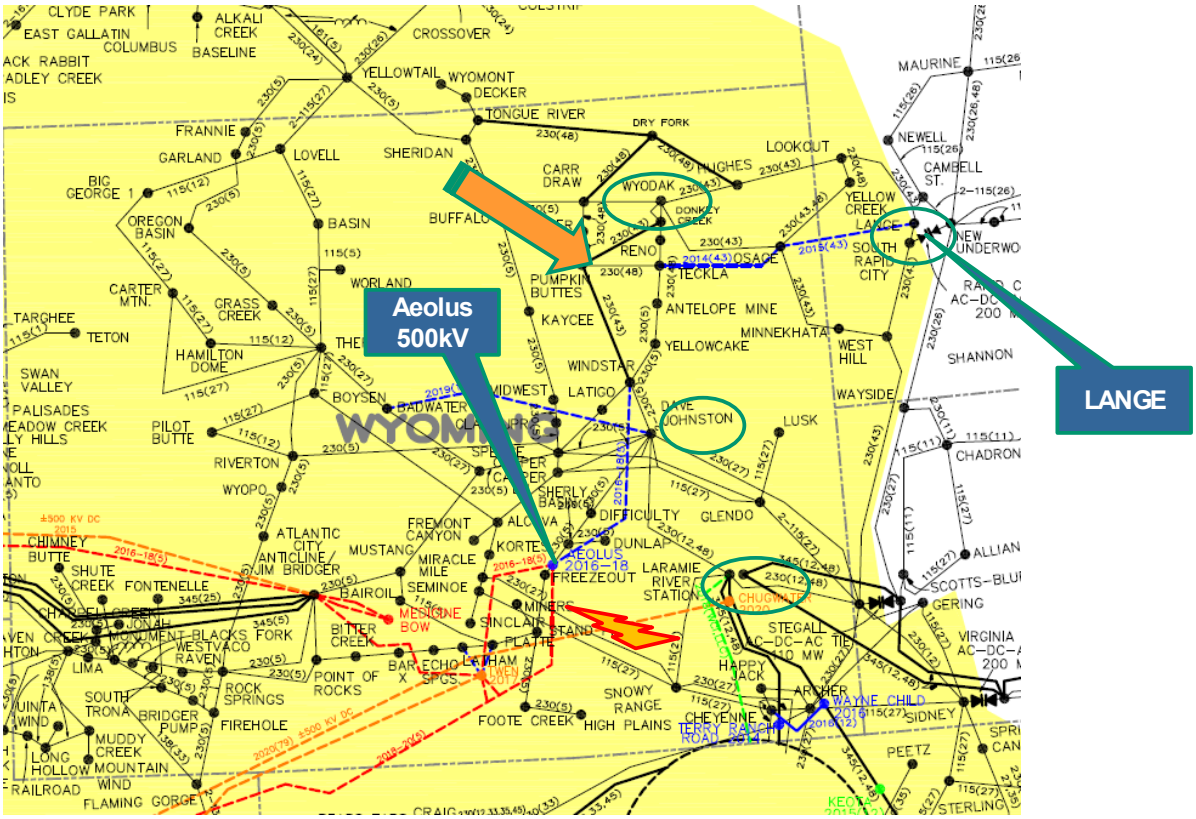

Figure 63. Planned transmission map of Aeolus 500 kV vicinity.

The dispatch summaries presented in the previous section show that the majority of coal generation in the eastern regions in the LSP Hi-Mix and Hi-Mix Extreme cases is off-line. This represents a radically different operating condition than the historic norm in which many of the coal plants in the region are base-loaded even under light load conditions. The difference in dynamic response to large disturbances in the vicinity has the potential to be substantial.

Figure 64 shows the voltage at Aeolus for the three system conditions in response to the Aeolus fault. The Base case (blue trace) and Hi-Mix case (red trace) show an acceptable recovery from the fault. The traces for these two cases included some numerical noise, which has been filtered out here and in some of the following plots. The Hi-Mix Extreme case (green trace) fails to recover. The simulation is meaningless after that point, so the plot was truncated.

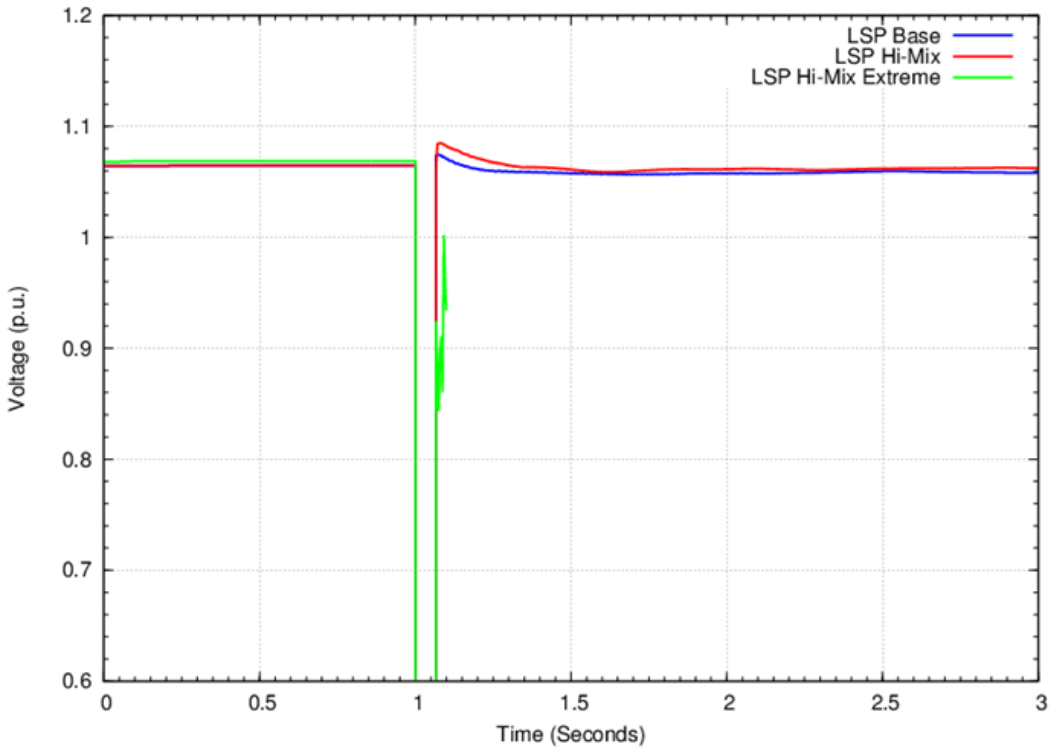

Figure 64. Aeolus bus voltage in response to Aeolus fault – LSP Base vs. Hi-Mix vs. Extreme.

The voltage behavior during the fault is of considerable interest in this case. In Figure 65, the voltages during the fault are shown at several 230 kV buses near and to the north of the Aeolus bus. These buses, except Windstar, are visible in Figure 63. At every node, the voltage drops as the fault is applied, then continues to decay. This decay is rapid, but not uniform. Notice that the voltages of the more northerly buses at Wyodak and Lookout decay faster and reach zero before the fault is cleared. This suggests that the system around Rapid City, South Dakota, cannot export all the wind power, resulting in a localized system separation. The fact that the voltages are better at Dave Johnson and Windstar, which are electrically closer to the fault, is significant. This is evidence that the collapse is driven by resources between the point of voltage collapse and the actual fault. The system dynamics in this part of the system are dominated by the wind plants. The system voltage behavior is also quite ill-mannered because of the composite load model dynamics and the fact that they do not allow motor tripping. In that sense, these simulations are similar to those presented in Section 5.1 and are almost certainly pessimistic. However, from a comparative performance perspective, the poor voltages at Wyodak and Dave Johnson are undoubtedly exacerbated by the fact that all the units at those two plants are off-line in this case. The question of whether system separation might be avoided by tripping motor load, rather than letting it stall, is examined below.

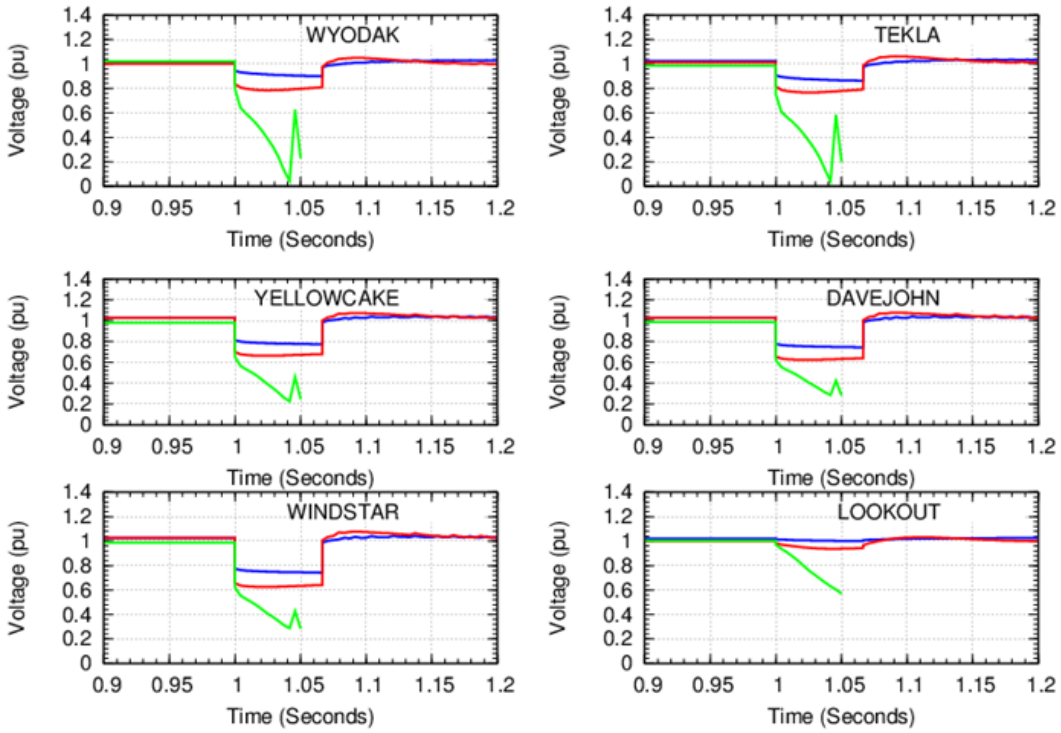

Figure 65. Bus voltages in response to Aeolus fault – LSP Base vs. Hi-Mix vs. Extreme.

The impact on the remaining relatively small synchronous machines in the area can be observed in Figure 66, which shows the machine speed of the Lange CT (highlighted in Figure 63). The acceleration of Lange during the fault is dramatically higher for the Hi-Mix case (which it survives) and even more so for the Extreme case (which is a failure).

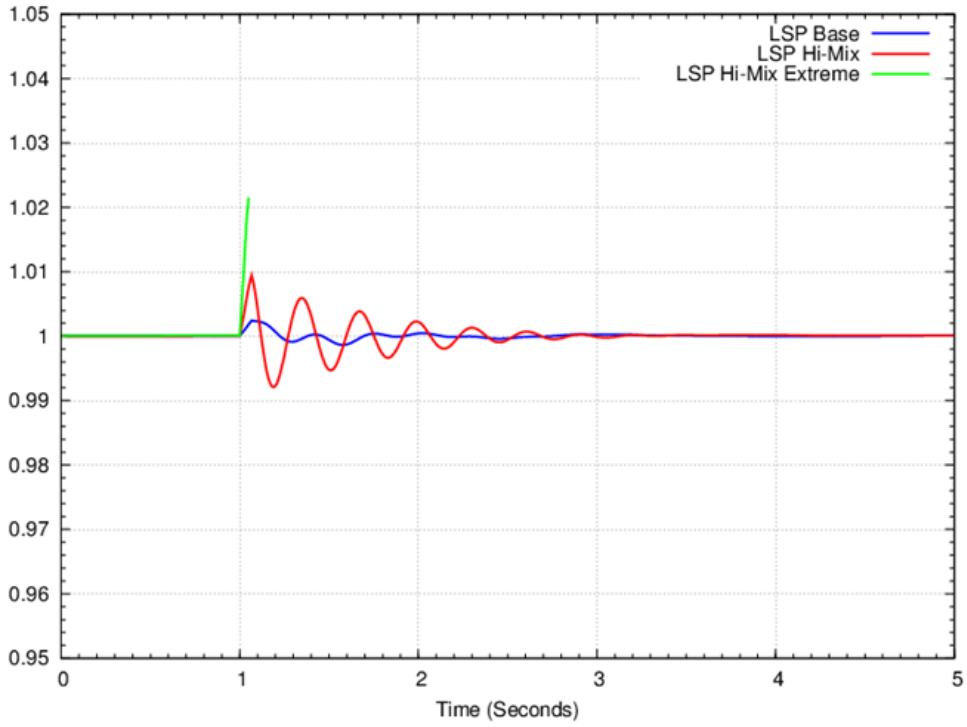

Figure 66. Lange CT speed in response to Aeolus fault – LSP Base vs. Hi-Mix vs. Extreme.

The observation that the stability problem is primarily due to acceleration during the fault is reinforced by the simulation captured in Figure 67. The red trace shows the 500 kV line opened without an initiating fault. The line-open case is well behaved, indicating that the stability problem is substantially due to the voltage depression during the fault. The voltage depression has multiple effects, including reducing synchronizing strength, driving the complex load towards motor stall, and aggravating swings of the Type 1 wind turbines in the vicinity. This was explored further by experimenting with different fault impedances. The results confirm that as the fault becomes progressively more severe, with decreasing fault impedance as a proxy for severity, the stability degrades. The stability limit without any mitigation is for a fault impedance between 0.05 pu and 0.06 pu.

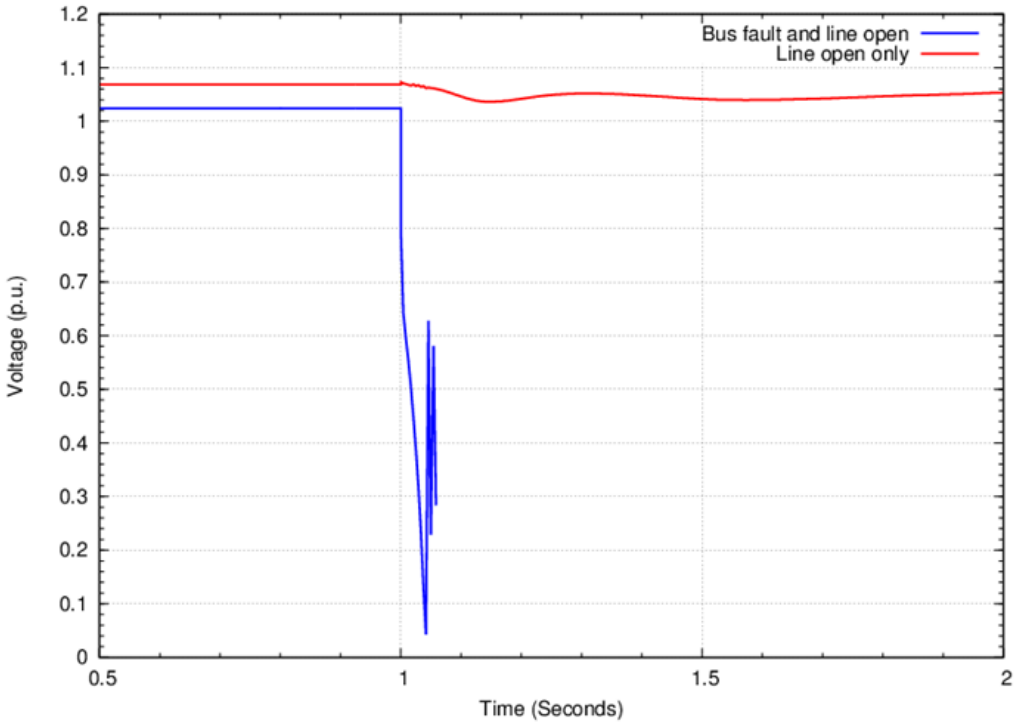

Figure 67. Aeolus bus voltage response – Aeolus line trip with and without bus fault.

6.3 Coal Plant Conversion to Synchronous Condensers

The Northeast portion of the Western Interconnection evolved with the expectation that the large coal plants would be base-loaded, providing an anchoring effect on system voltage. The poor voltage behavior for the Extreme case suggests a need for additional system strength. For this experiment, three of the de-committed coal plants were converted to synchronous condensers as follows:

- Dave Johnson, unit 4 – 400 MVA (65445 DAVEJON4)
- Wyodak, unit 1 – 402.3 MVA (66730 WYODAK 1)
- Laramie River, unit 1 – 690 MVA (73129 MBPP-1).

In order to convert these machines to synchronous condensers in the model, the load flow is changed so that the unit status is on and dispatch is set to 0 MW. This causes the unit to regulate voltage and initialize to a non-zero reactive power. In the dynamic model, the governor is removed, and the inertia constant is changed to 1.0 pu. This is an estimate based on the need to remove the turbine. For steam plants, conversion to synchronous condenser operation is a significant and irreversible step. Thus, this conversion only makes sense for a unit that is to be permanently retired. There are several such conversions recently completed or underway in the United States, including units at the Cherokee plant in Colorado, the Eastlake plant in Ohio, and the Turkey Point plant in Florida.

The voltage depression further suggests that additional dynamic response from the generation that is synchronized in the case could be beneficial. Thus, in addition to the three synchronous

condensers, shunt capacitors (beyond those discussed in Section 5.7.1) were added to free up dynamic range on generation as follows:

65420 DAVEJOHN	230 kV	100 MVAr
65425 DAVEJOHN	115 kV	100 MVAr
70122 COMANCHE	230 kV	60 MVAr
70821 CEDARCRK	230 kV	150 MVAr
76400 PUMPKIN BTS	230 kV	100 MVAr

In Figure 68, the Dave Johnson 230 kV bus voltage is shown for the three LSP cases plus the new sensitivity case with synchronous condensers (pink trace). With the condensers added, the Extreme system is now stable.

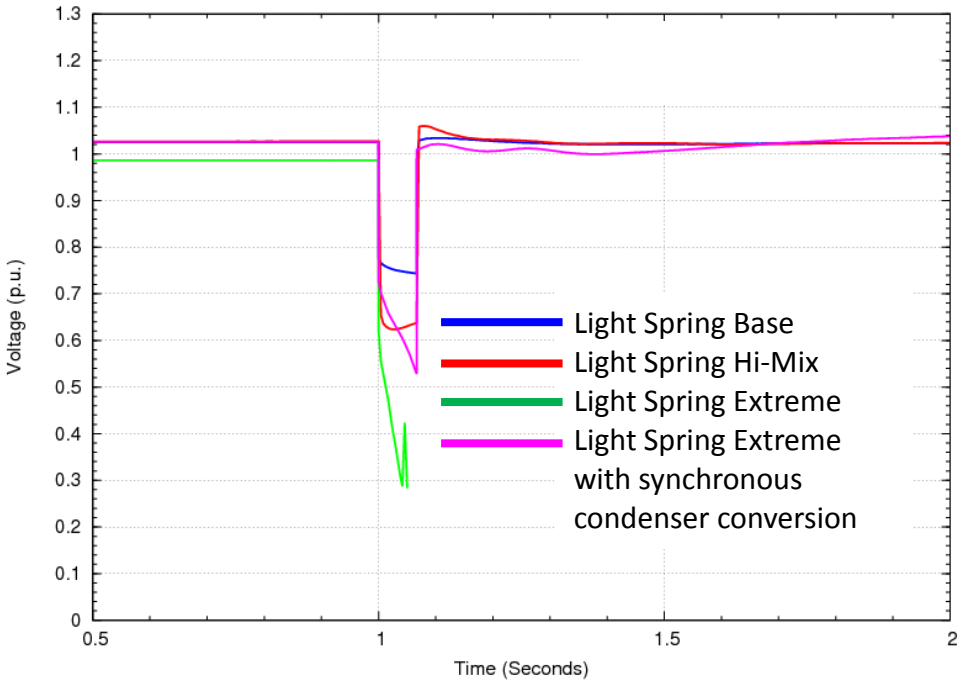

Figure 68. Dave Johnson bus voltage for Aeolus fault – LSP Base vs. Hi-Mix vs. Extreme vs. Extreme with synchronous condenser conversion.

In Figure 69, the same bus voltages that were displayed in Figure 65 are shown for the Extreme case, with and without the synchronous condensers added. Notice that the rapid decay of voltage during the fault is greatly improved by the addition of the condensers. The system recovers in an orderly fashion when the fault is cleared.

The behavior of the Dave Johnson generator unit 4 is shown in Figure 70. Two cases are plotted: the LSP Base case, in which the unit is committed and running as a generator, and the new Extreme case with the synchronous condenser conversions. Recall that for the other two cases (Hi-Mix and Extreme), the unit is off-line. The initial and average active power of the synchronous condenser are, of course, zero. The active power swings as the machine inertia interacts with the rest of the system dynamics. The reactive power output swings following the

fault clearing. The frequency of the reactive power swings in the first half-second after fault clearing is relatively high. This is partly due to the reduced inertia of the synchronous condenser, but closer inspection of the simulation results suggests that this rather fast swing in post-fault voltage is primarily due to the dynamics of nearly 1 GW of Type 1 induction generator wind turbines in the vicinity. A few spot checks suggest that this oscillation is quite sensitive to the model for these wind plants. Further, the tripping behavior of these machines could be an important stability consideration for this and similar events. With most of the large thermal units de-committed, the dynamic characteristics of the wind plants become important. This is a significant observation; extra care will likely be needed in the future to ensure that dynamic models of previously relatively unimportant plants are up to WECC standards for accuracy.

Another important observation is that the system dynamics and the support provided by the synchronous condensers during the fault are the critical element in maintaining system stability. The support from electromagnetic synchronous devices (i.e., generators and synchronous condensers) is instantaneous and inherent to the equipment. This is evident in the difference in the amplitude of the voltage drop immediately following the application of the fault. This inherent response applies for real-world complexities that accompany violent grid faults: unbalance, distortion, saturation, etc. Creating functionally similar performance with power-electronics-enabled devices is challenging. The voltage collapse of these simulations occurs within about two cycles of fundamental frequency (i.e., about 32 msec)—an extraordinarily short timeframe from the perspective of closed-loop controls. The design and verification of power electronics devices in this timeframe and for this type of disturbance requires analytical tools other than standard fundamental frequency, positive sequence, and dynamic stability programs like PSLF or Power System Simulator for Engineering (PSS/e). This is an important aspect of the "weak grid" concerns discussed next.

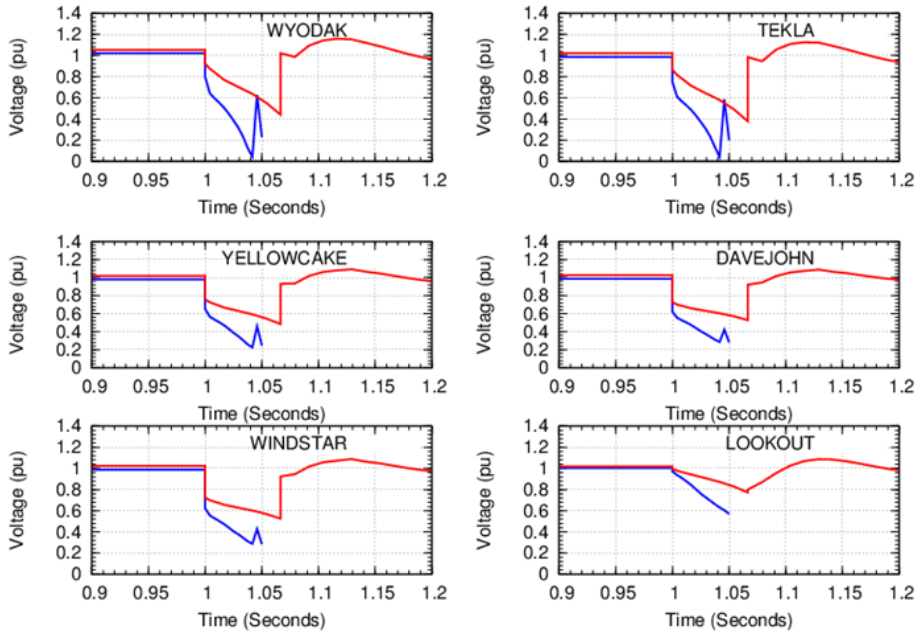

Figure 69. Bus voltages in response to Aeolus fault for LSP Extreme case – with and without synchronous condenser conversion.

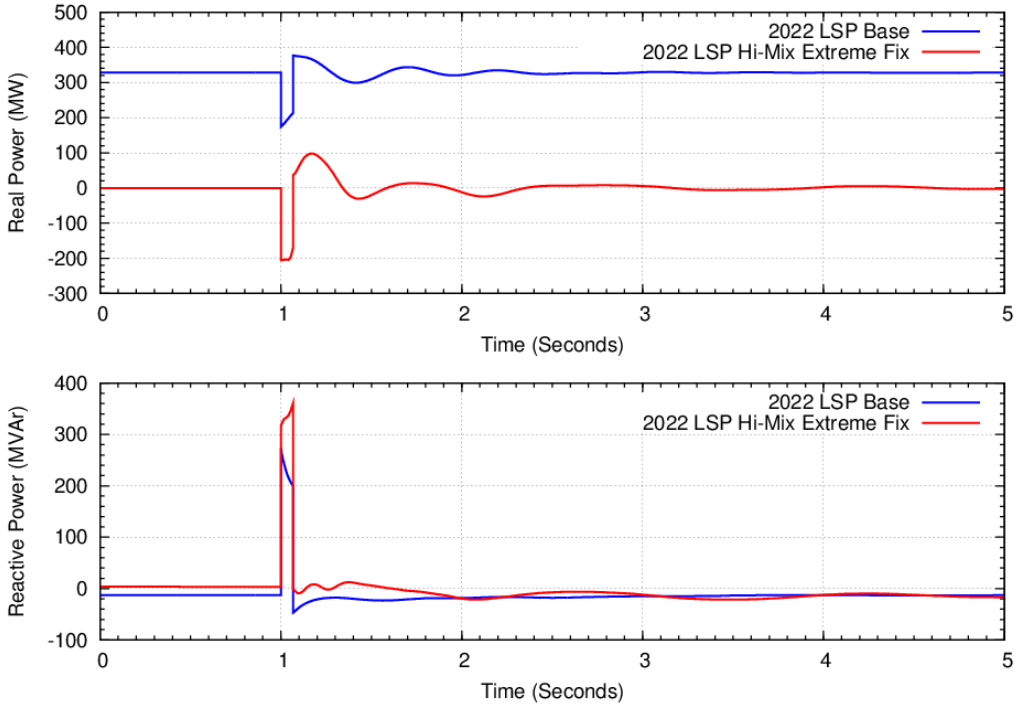

Figure 70. Real and reactive power output from Dave Johnson unit 4 in response to Aeolus fault – LSP Base vs. Extreme with synchronous condenser conversion.

6.4 Weak Grid Discussion

The rapid voltage collapse and system separation observed during the fault described above is representative of so-called “weak grid” issues. Systems at or approaching very high levels of wind penetration, such as those in west Texas, Australia, and Brazil, are challenged to provide fast, confident control during faults as wind and solar generation becomes the dominant generation resource in a particular portion of the grid.

Modern wind turbines and all PV systems depend on power electronics that must behave well during grid disturbances. Until recently, this concern has primarily focused on fault ride-through capability. The wind industry has largely addressed the ride-through questions, and the solar industry is following suit. (Questions of PV ride-through in distribution applications are discussed in Section 5.1.) However, no commercially available wind or utility-scale solar PV generation is capable of operation in a system without the stabilizing benefit of synchronous machines. There is a point at which the amount of short-circuit strength provided by synchronous machines becomes insufficient and operation becomes impossible with known, current technology. "Weak grid" is a generic term that describes operating near that point. The factors that dictate that point are complex, evolving, and not fully understood. The rest of this discussion addresses some aspects revealed by this study work.

6.4.1 Sensitivity to WTG Models and Controls

The behavior observed in these study cases is representative of these "weak grid" concerns. The failure of the Extreme case is largely due to the forced injection of active power current into a part of the system that cannot accept the power. There are two factors at play in this

phenomenon: modeling and equipment controls. Both models and actual controls of WTGs have been advancing and evolving for the past decade. The model used in these cases is the result of this evolution and is a compromise between model simplicity, numerical behavior, accuracy, and functionality. In general, development of the model tended to be conservative, with the model structured to underestimate desirable performance. The intent is to help ensure that planning decisions based on simulations are conservative with respect to system reliability. Further, the models evolved for the applications most commonly under investigation by planners that can be meaningfully evaluated with fundamental frequency stability simulation tools.

Stable and reliable operation of WTGs in weak grids requires dedicated designs of various controls. Some of these controls have bandwidths of more than a few cycles and can be reflected accurately in stability simulation tools (e.g., PSLF, PSS/e). There are also control loops in WTGs with sub-cycle bandwidth that could cause instabilities and trips if not properly designed or adjusted. Detailed representation of these very fast control loops is outside the realm of stability simulation tools. Hence, the simulation work described here addresses important interaction aspects of WTGs and the system within the bandwidth allowed by a stability tool. In specific wind plant applications, confirmation from the relevant vendors that designs are compatible for weak grid conditions may be required to complement the simulation work.

This philosophy applies to the next sensitivity case, in which all of the new WTGs have been changed from the part-Thevenin model used for Type 3 machines to the pure current injection model used for Type 4 machines. In this sensitivity case, the system is unstable at initialization, with no grid disturbance applied. Roughly 5 Hz oscillations start spontaneously shortly after the simulation begins. Appendix Figure 138 shows a comparison of the Extreme case with the synchronous condenser fix for the two different WTG models.

Note the choice of words here: the pure current source model is initially unstable. This is almost certainly a modeling issue, and not evidence that Type 4 WTGs are necessarily less stable than Type 3 machines. However, this behavior is indicative that the system is weak.

To further investigate sensitivity to wind plant controls, another variation of the wind turbine model was tested. This model was updated to be more realistic, i.e., less pessimistic, and to reflect recent improvements in turbine controls for weak grids. Figure 65 shows system response to the Aeolus fault with the synchronous condenser fixes for two cases. The blue trace is for the Extreme case with the standard model. The red trace is for the new model and controls. Notice that the severity of the dynamic voltage decline during the fault is dramatically reduced. This rather encouraging result is further evidence that the controls and models of the WTGs are critical in this high-stress condition.

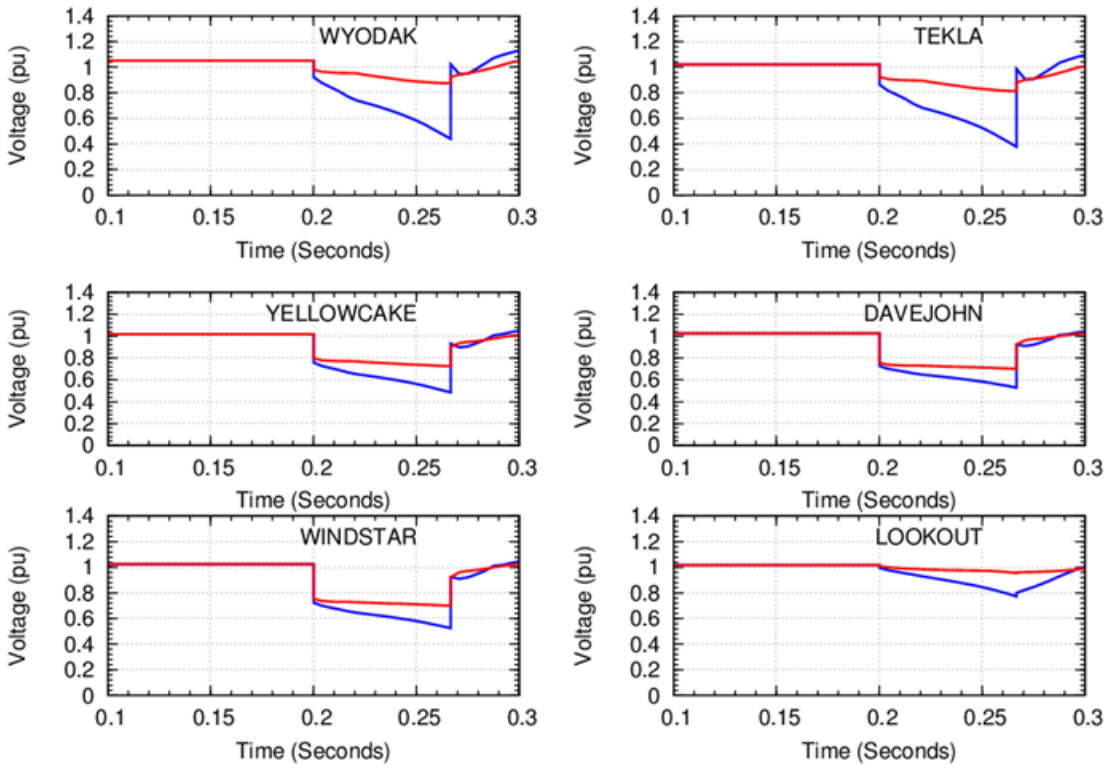

Figure 71. Impact of weak grid WTG controls for Aeolus fault.

6.4.2 Sensitivity to Load Models

Additional investigations were made on the impact of load modeling on the Extreme case failure. A case with the standard WECC load model was stable and did not exhibit the dynamic voltage collapse and separation. However, a case in which the default composite load motor tripping settings were restored, allowing the motors to trip as voltage collapses, still fails. Had the Type 1 WTGs tripped, it is possible that the system would survive the event.

6.4.3 Sensitivity to Non-Synchronous Generation

The weak grid investigation is representative of growing industry concern about operating with a low fraction of total generation coming from synchronous generation. One leader in this area is Ireland. The Irish grid operator EirGrid monitors SNSP, or "system non-synchronous penetration" (EirGrid 2011a). For EirGrid, non-synchronous resources consist primarily of wind generation and their large HVDC interconnections with Great Britain. Ireland is on a trajectory to have the highest annual energy penetration of wind power of any major power system in the world. At 40% (EirGrid 2014), Ireland's target exceeds the 33% energy penetration for this study. In order to reach these annual energy targets, the instantaneous penetration of wind generation will occasionally need to be very high. However, concerns about FR and a weak grid resulted in SNSP being limited to less than 50%. In the near-term future, EirGrid expects to raise that limit to 75%. In other systems, including those in west Texas, Brazil, and Australia, weak grid concerns have also emerged.

The bar charts of Figure 72 show the mix of synchronous and non-synchronous generation for each of the four regions and for the five main cases. The y-axis is not dispatch (MW), but the

capacity, in MVA, of the committed resources. A primary weak grid concern is the relative size of the electronic devices that depend on the stabilizing influence of the synchronous resources. Note that added condensers have been shown in green. These would increase the blue bar.

Figure 73 shows exactly the same information, but displayed as the relative fraction of synchronous and non-synchronous (inverter) resources. The red bars (inverters) are analogous to the EirGrid SNSP metric.

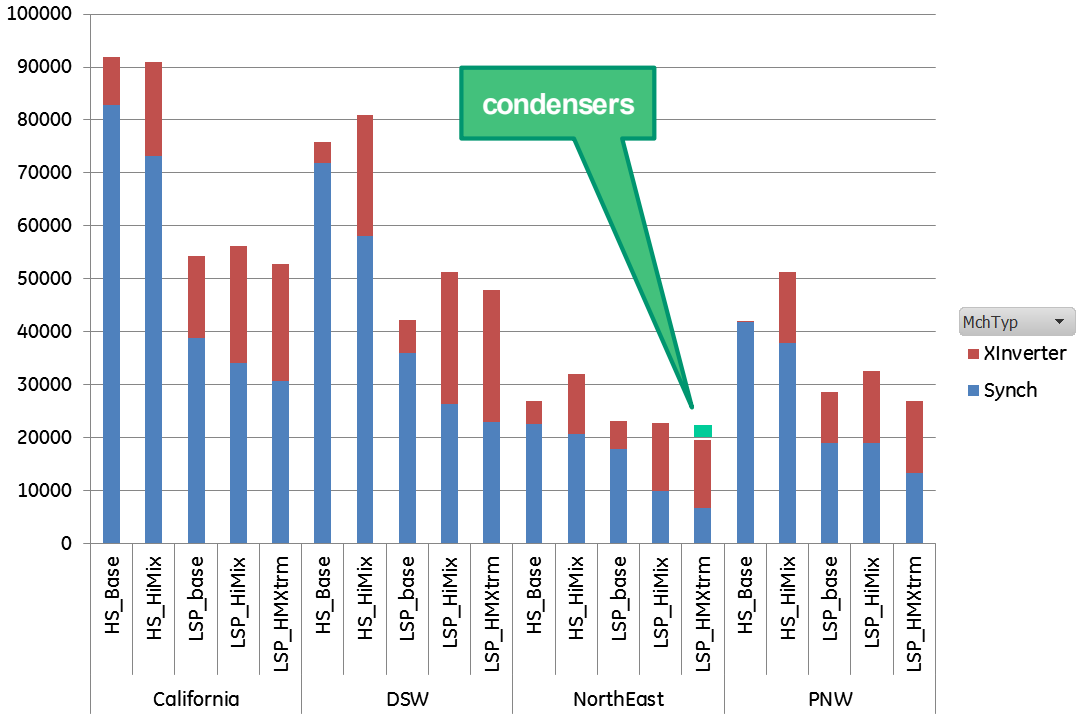

Figure 72. Synchronous vs. non-synchronous generation commitment in MVA.

It is interesting to note that in the Northeast, where the Aeolus disturbance is investigated, the system is well behaved at SNSP (red bar) of about 56% in the LSP Hi-Mix case, but shows poor behavior at ~66% SNSP for the LSP Extreme case. Further, the SNSP improves to about 61% with 1,600 MVA (green bar) of condensers added, and the system behavior greatly improves.

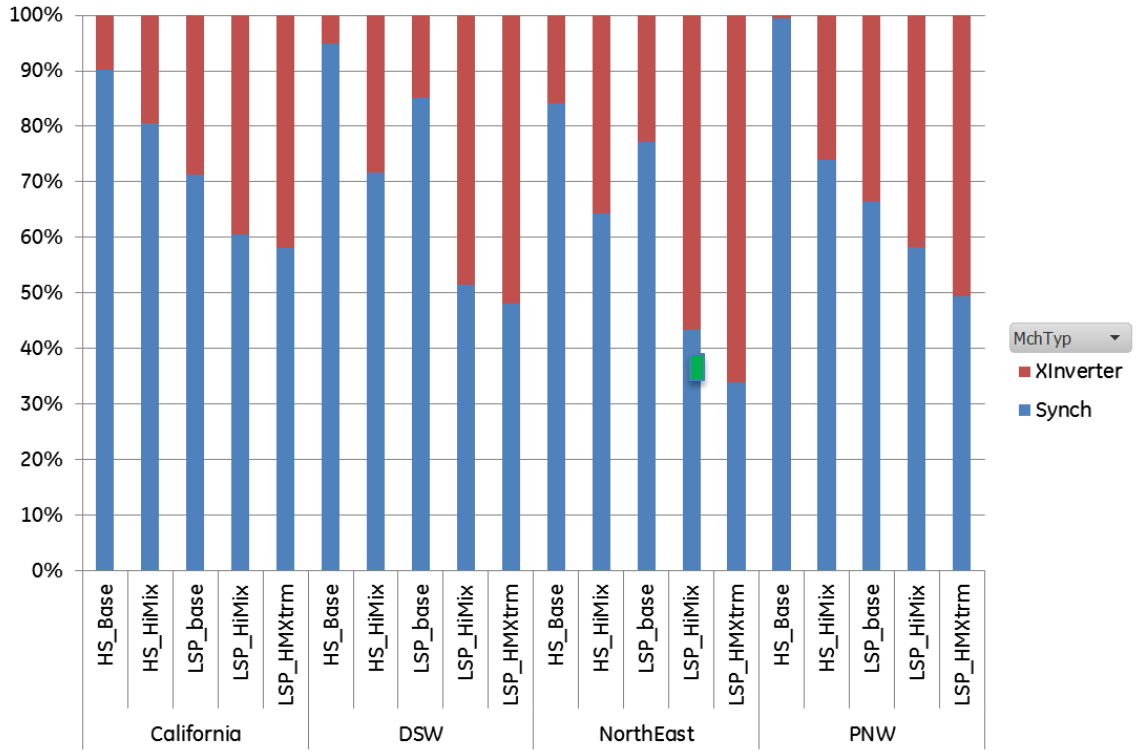

Figure 73. Synchronous vs. non-synchronous generation commitment in percent.

6.4.4 Fault Current Levels

Short-circuit levels decline significantly in the 230 kV system when the majority of coal generation is de-committed, as shown in Table 22. The lower fault levels are related to the increased electrical distance between the wind generator and synchronous generator discussed in previous sub-sections. The industry often uses indicators based on the ratio of fault levels to rating of power electronic generation to quantify how weak the grid is for an application or for a region with several wind plants. There are variations on where to calculate the short-circuit power and how to aggregate multiple wind plants. As a reference, the short-circuit levels at Dave Johnson and Populus for the base and the extreme scenarios are shown in the table below. These values are calculated without considering the contributions from the wind plants, as a measure of the system strength seen by the wind plants. The difference between scenarios is significant. Review of system protection is recommended.to ensure proper behavior at reduced short-circuit levels

Table 22. Fault Current Levels

Location	LSP Base	LSP Hi-Mix Extreme
Dave Johnson 230 kV	19.7 kA/7,730 MVA	10.7 kA/4,260 MVA
Populus 345	25.1 kA/15,000 MVA	20.1 kA/12,000 MVA

6.5 Coal Displacement and Weak Grid Summary

A high de-commitment of coal does not obviously over-stress the system. A greater than 80% reduction of coal commitment from the LSP Base case in the Northeast region exhibited acceptable dynamic behavior for the limited tests performed.

The regional transmission system evolved with the coal plant at "anchor" nodes. Displacement by wind and solar that is more dispersed results in those nodes being less supported. Consequently, increasing wind and solar dispatch, and de-committing and re-dispatching thermal generation, resulted in localized voltage and thermal problems. These problems were particularly acute in the evolution from the Hi-Mix case to the Extreme case. These problems were "fixed" mainly with added shunt capacitors and a few 230 kV line upgrades or transformer additions (i.e., fixed in the sense that the results were satisfactory for the conditions investigated, but questions of voltage stability and "brittleness" need closer investigation). These improvements are not in any sense optimized, which would require much more precise information on the specifics of individual projects. The solutions used are relatively straightforward reinforcements. Ohm's Law still applies, and good planning practices need to be followed.

System dynamics for the extra-high-voltage Aeolus fault were stable for the Hi-Mix case with about an 80% reduction in coal commitment from the LSP Base case. The extreme de-commitment further stresses the system, with a greater than 90% reduction of coal commitment. Additional shunt compensation and some rotating dynamic reactive compensation stabilized the Aeolus fault. Conversion of some coal plants to synchronous condensers (assuming retirement) works well to stabilize the system. Improved wind and solar plant controls may be sufficient to mitigate problems with extreme coal de-commitment.

Results suggest that substantial displacement of coal can likely be tolerated, with the application of good utility practice for local transmission mitigation. The last few steps (i.e., de-committing the final 1–2 GW in the eastern half of the Western Interconnection), while possible, will need to be carefully examined.

Results suggest that when wind and solar are the predominant source of generation throughout the region, care to use good-fidelity dynamic models is critical. WECC has a longstanding best practice to keep dynamic models up to date. Wind and solar plant modeling need to be held to the same level of accountability in a very-high-penetration future. The fidelity of the load model assumes increased importance with the increase in power-electronics-based generating resources.

This single sequence of sensitivities is illuminating, but in no way complete or conclusive. More analysis is needed, but in summary, these results suggest:

- Displacement of 80% of the coal generation is possible.
- Displacement of 90% of the coal generation is possible with some mitigation.
- Good-fidelity dynamic models are critical.

7 Mitigation Analysis

WWSIS-3 investigated mitigation strategies for any adverse impact on transient stability and FR due to high levels of wind and solar. With the exception of the Extreme case, the results showed no loss of stability or other fundamental changes in system behavior due to high wind and solar penetration. Therefore, this investigation focuses on the potential performance improvement achievable with various means of mitigation, rather than mitigation per se. While individual areas do not meet their NERC FRO, the current NERC rules do not mandate that each entity meet their obligation with their own resources. Depending on how practice and rules evolve, and as long as the overall system meets the IFRO and other performance criteria, the results so far do not require mitigation of individual BA FR shortfalls with physical (as opposed to contractual) means.

However, system performance does change with high wind and solar penetration. This section presents a variety of investigations that could broadly be characterized as mitigation, in that they tend to improve system performance. These investigations are focused on changes to the renewables or to the system that might affect the findings reported above. In general, the investigations reported here look at the same initial conditions and events, with changes in the assumptions about the renewables or other infrastructure.

7.1 Frequency Controls on Wind Plants

The use of frequency-sensitive controls on wind plants is the subject of considerable interest in the United States and has been analyzed in WECC and California. Requirements for this functionality started in Ireland, but are rapidly gaining traction in North America. The Electric Reliability Council of Texas (ERCOT 2010) and the Alberta Electric System Operator (AESO 2010), at least, require wind plants to have primary response (governor) functionality. Hydro-Quebec continues to be the only North American system that requires inertial controls, but again, considerable interest is growing.

In this section, the two Hi-Mix cases (LSP Hi-Mix and HS Hi-Mix) are tested with the primary frequency control or governor function (active power control [APC] is the GE PSLF implementation of this function), inertial control (WindINERTIA [WI] is the GE PSLF implementation of this function), and a combination of both (Miller 2011a, Miller 2009).

The load flow and initial dispatch are identical in all cases. For the case with the governor function, 5% of each new wind plant's output is held for primary FR. This assumes a higher wind speed than in the original cases for plants operating at less than 95% of rated output. The net result is that about 300 MW is held in reserve on about 19 GW nameplate of new wind plants. About 350 MW of new plants are running at rated power, so they do not participate. The curtailed power is headroom that is used to increase power output when the frequency drops below the dead band. This ~300 MW is 5% of the 6.3 GW of production on the new plants, or about 1% of the total wind production of all plants.

A comparison of the system frequency for four cases is shown in Figure 74. The corresponding power response of the new wind plants is shown in Figure 75. The power traces have some numerical noise filtered out. This causes the initial increase in power to be slightly larger than expected, but there is no practical impact on the results. The Hi-Mix case with no wind plant

frequency controls is shown in blue. With only GR, as shown by the green trace, the frequency nadir is slightly improved and the settling frequency—which is critical to the calculation of FR—is noticeably improved. The active power of the wind plants, again in green, shows that the GR of the wind plants is relatively slow, rising to steady state about 20–30 seconds into the event. The total change in wind power output is about 310 MW by this time. Both the speed and time of response are important. The control modeling assumptions drive this behavior, not the fundamental physics of the wind turbines. First, the gain between power and frequency deviation (i.e., the frequency droop) is set at 5%, the NERC standard. Qualitatively, this means that change in MW output is proportional to frequency error once the frequency deviation exceeds the dead band, regardless of the loading of the wind plant.[4] This means that a 0.25% frequency error (150 mHz + 36 mHz dead band) is needed to create a 0.05 pu increase in power. In this case, 5% of the available power is kept in reserve. When the plant is running at a fraction of its rating, then the frequency error necessary to "use up" the reserved power is lower. The average loading of the new wind plants in this case is about 33%, so a relatively small sustained frequency error (about 86 mHz) is enough to saturate the controls. Because the settling frequency in the APC cases is about 59.86 Hz (i.e., 140 mHz error), the response is saturated. Thus, essentially all of the power kept in reserve is contributing to the FR in this case. Second, the speed of response roughly matches the speed of response of typical hydro machines. In general, wind turbines can respond faster if so required, though there are physical limits on increasing the mechanical torque on the turbine. One significant limit is that the turbine blades, while relatively quick, do take time to move (pitch in). This leads to the introduction of inertial controls.

Unlike the governor function, which relies on capturing more wind power through pitching the turbine blades, inertial control relies primarily on fast control of the electrical torque to temporarily extract inertial energy from the turbine drive train and deliver it to the grid. This energy loss slows down the turbine, thus the control is only a short-term measure, and the energy must be returned to the drivetrain. The control objective of the inertial control shown here (GE's WI function) is to help reduce the severity of the frequency nadir, and it is not intended to improve FR as defined by NERC. The impact of just the inertial control is shown in the red traces of the figures. The control makes a significant—45 mHz or 13%—improvement in the frequency nadir. The power trace shows that the control has exhausted its contribution by about 10 seconds and can then be seen to be recovering energy back from the grid. This tends to stretch out the frequency depression, but in this case, a substantial improvement in the margin above UFLS is realized. Unlike the governor function, the inertial control has no opportunity or lost energy cost. The two controls work well together, as can be observed in the pink traces. The frequency nadir is improved, but the excursion is not as stretched out in time, and the settling frequency improves.

The detailed FR metrics for the four cases are reported in Table 23. Overall, this particular GR improves the WECC FR by about 300 MW/0.1 Hz, from 1,311 MW/0.1 Hz to 1,610 MW/0.1 Hz, as shown in both the APC cases. The FR of the combined governor and inertial control case (APC+WI) is not quite as good as APC alone: the inertial term greatly

[4] This is in distinct contrast to the Irish grid code, which makes power change proportional to available wind power, not the nameplate. There is substantial potential for confusion in using the models and interpreting results between the two approaches.

improves the frequency nadir, but at a slight penalty in the early part of the 20–52 second window during which FR is calculated.

The governor control raises the FR above the 1,352 MW/0.1 Hz for the Base case. The regional improvement in DSW and the Northeast are rather more striking, with both regions going from a substantial deficit to a positive margin with the governor control.

As one measure of efficacy, the contribution of the governor function to FR is 299 MW/0.1 Hz per 310 MW of function, or 0.96 MW per MW per 0.1 Hz (an admittedly odd unit). Similarly, with both controls, the 47 mHz improvement in nadir works out to about 0.15 mHz/MW of control.

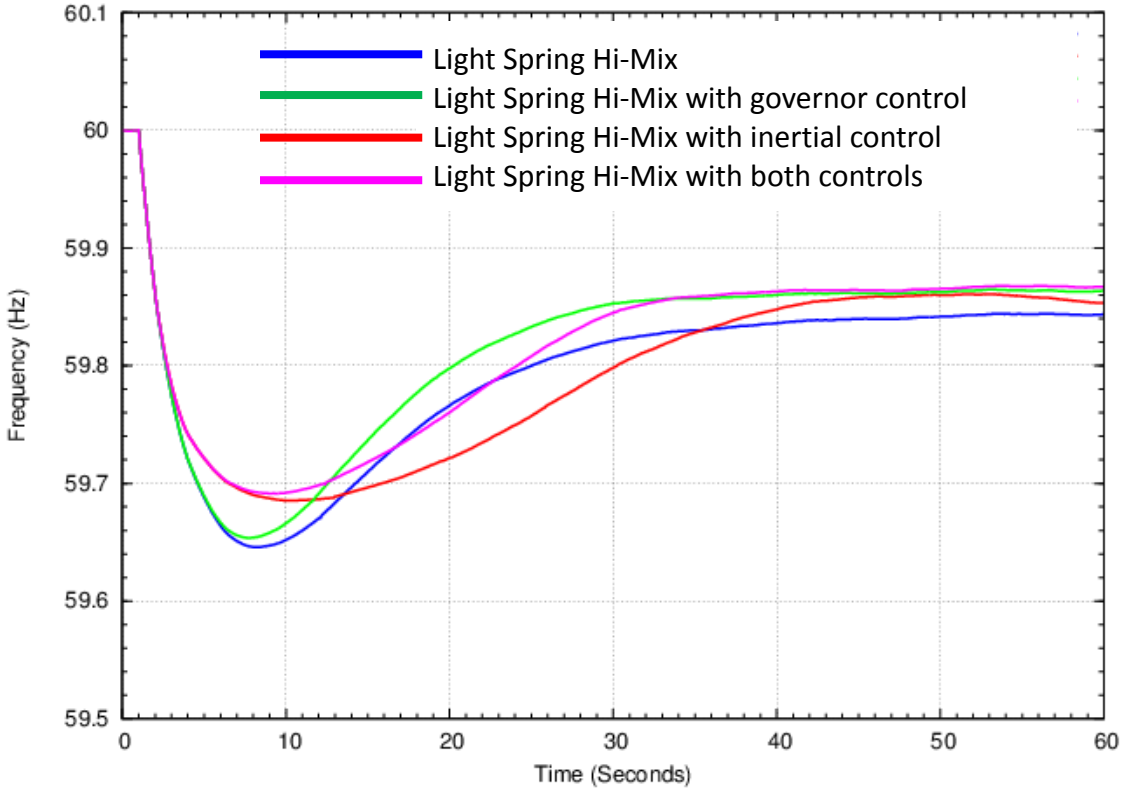

Figure 74. Frequency response to two Palo Verde unit trip for LSP Hi-Mix case with three combinations of frequency controls on wind plants.

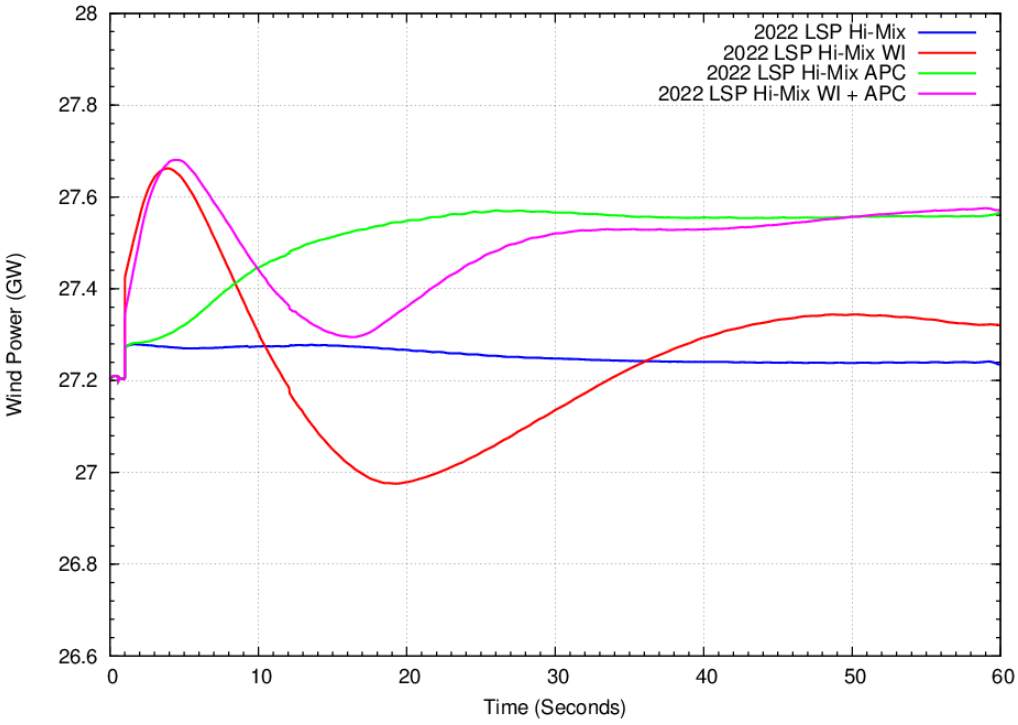

Figure 75. Wind plant active power response to two Palo Verde unit trip for LSP Hi-Mix case with three combinations of frequency controls on wind plants.

Table 23. Frequency Response Metrics for LSP Hi-Mix Cases with Three Combinations of Frequency Controls on Wind Plants

		LSP Hi-Mix (MW/0.1 Hz)		Governor Control (MW/0.1 Hz)		Inertial Control (MW/0.1 Hz)		Governor and Inertial Controls (MW/0.1 Hz)	
	FRO (MW/0.1 Hz)	FR	FR Margin	FR	FR Margin	FR	FR Margin	FR	FR Margin
WECC	840	1,311	471	1,610	770	1,323	483	1,571	731
By Region									
CALIFORNIA	296	312	16	335	39	315	19	334	38
DSW	220	119	-101	240	20	111	-109	215	-5
NORTHEAST	82	47	-34	140	59	40	-41	129	47
NORTHWEST	131	483	353	528	397	507	376	528	397
By Area									
ARIZONA	104	50	-55	67	-38	48	-56	63	-41
EL PASO	9	4	-5	5	-4	3	-5	4	-4
IDAHO	18	22	4	23	5	22	4	23	5
IMPERIALCA	4	14	10	27	23	13	9	24	21
LADWP	29	30	1	31	1	30	1	31	2
MONTANA	11	10	-1	53	42	5	-7	44	33
NEVADA	28	34	6	34	7	34	7	35	7
NEW MEXICO	14	2	-13	9	-5	8	-6	9	-5
PACE	42	8	-34	58	16	6	-36	55	14
PG AND E	133	197	64	205	72	198	66	205	72
PSCOLORADO	36	6	-30	6	-29	6	-29	6	-29
SANDIEGO	21	7	-14	7	-14	7	-14	7	-14
SIERRA	11	7	-4	7	-4	7	-3	7	-4
SOCALIF	108	63	-45	64	-44	65	-43	66	-43
WAPA R.M.	27	24	-3	118	91	11	-17	98	70
WAPA U.M.	0	3	3	4	4	3	3	4	3

The results of a similar investigation for the HS Hi-Mix case are shown in Appendix Table 52 and Figure 139. The new controls have some beneficial impact on the system, but it already had a substantial FR margin. The controls on the wind plants have largely displaced the response of other plants.

7.2 Frequency Controls on Solar Plants

7.2.1 Utility-Scale Solar PV Plants

Compared to wind plants, there is even less industry experience with providing under-frequency regulation services with solar PV plants. Conceptually, the process is similar to that for wind: an amount of power can be kept in reserve for regulation by curtailing the power output of the installation. And like wind, there is substantial opportunity cost associated with the lost energy production. However, unlike wind power, there are no rotating components, and consequently there is no inherent mechanism to provide inertial response. However, fast FR controls could operate in the inertial time frame of 5–10 seconds post-disturbance.

For this investigation, all new utility-scale PV plants are assumed to be equipped with frequency-responsive controls, and every plant is assumed to be curtailed by 5% of rating. This causes about ~820 MW curtailment on ~16 GW nameplate, leaving ~10.2 GW production for all solar (of which about 6.4 GW is from the new PV plants).

Unlike the governor controls for wind plants presented in the previous section, the control used here for PV is aggressive: the response is fast, with gains and time constants selected to saturate relatively quickly once the system frequency is outside of the 36 mHz dead band. From an equipment perspective, there is essentially no mechanical risk or penalty for fast response, as there are significant mechanical stresses associated with rapidly changing power output. Further, from the perspective of this specific investigation, it is illuminating to show the potential impact of aggressive governor control compared to the relatively slower response modeled for the wind plants.

Figure 76 and Figure 77 show the impact of this level of governor control on the LSP Hi-Mix system for the trip of two Palo Verde NPS units. The impact on both the frequency nadir and the settling frequency is substantial. The frequency nadir is improved by 110 mHz, from 59.646 Hz to 59.752 Hz. The improvement in FR is about 765 MW/0.1 Hz, to 2,065 MW/0.1 Hz. The per-unitized improvement in FR is 0.93 MW per MW per 0.1 Hz, and 0.13 mHz/MW on the frequency nadir. By this measure, the efficacy of the PV plant controls is essentially the same as for the wind plants. The FR metrics are detailed in Table 24.

Figure 77 shows the aggressive response of the PV to the frequency drop. This non-linear response raises some interesting questions. The control is deliberately set to provide as much support to the grid as possible for this design-basis event. Philosophically, the idea is to take maximum advantage of this highly responsive resource—there is essentially no penalty on the PV resource for aggressive response, and it reduces the duty on synchronous generating resources. Had the event been somewhat less severe, the control would still have saturated, providing proportionally greater response—so the FR metric would show a greater benefit. Conversely, had the event been even larger, the FR metric would not be as good. Other resources for FR, such as triggered demand response and energy storage, will likely exhibit such non-linearities. With the inevitable addition of non-linear frequency-responsive resources, practice

will need to evolve to adapt to the reality that overall system FR will itself be a function of the size of the disturbing event. This is not necessarily a problem, but it certainly adds complexity to the overall FR issue. The deliberately aggressive control in this case is almost certain to have other undesirable side effects not evident in this particular case. The objective of this investigation is to place an upper bound on the benefit of potentially fast frequency controls.

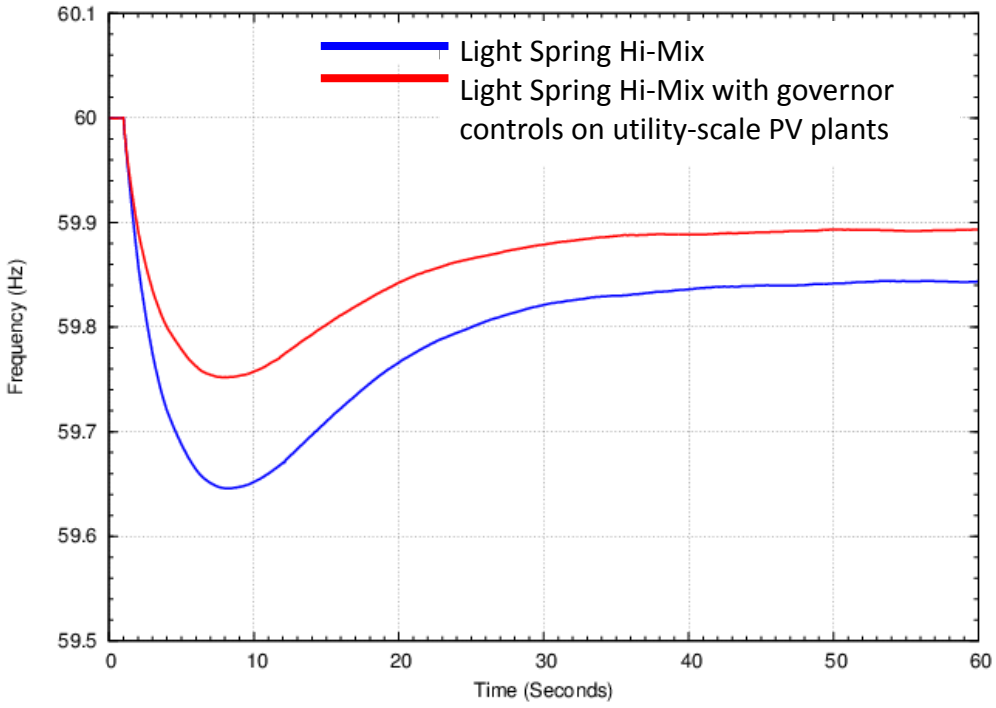

Figure 76. Frequency response to two Palo Verde unit trip for LSP Hi-Mix – with and without governor control on utility-scale PV plants.

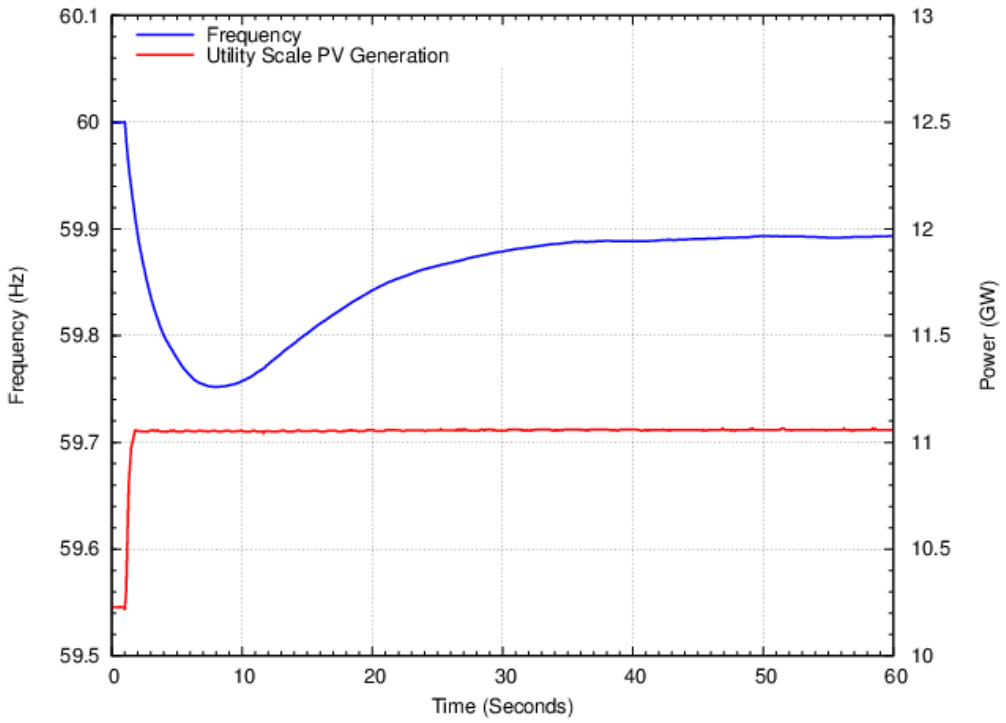

Figure 77. Frequency and power output in response to two Palo Verde unit trip for LSP Hi-Mix with governor controls on utility-scale PV plants.

Table 24. FR Metrics for LSP Hi-Mix Case With and Without Governor Control on Utility-Scale PV Plants

		LSP Hi-Mix			LSP Hi-Mix with 5% Frequency Control on Utility-Scale PV		
Name	FRO (MW/ 0.1 Hz)	FR (MW/ 0.1 Hz)	FR Margin (MW/ 0.1 Hz)	FR % of WECC	FR (MW/ 0.1 Hz)	FR Margin (MW/ 0.1 Hz)	FR % of WECC
WECC	840	1,311	471	100.0	2,065	1,225	100.0
By Region							
CALIFORNIA	296	312	16	23.8	562	266	27.2
DSW	220	119	-101	9.1	475	255	23.0
NORTHEAST	82	47	-34	3.6	135	54	6.6
NORTHWEST	131	483	353	36.9	537	407	26.0
By Area							
ARIZONA	104	50	-55	3.8	237	133	11.5
EL PASO	9	4	-5	0.3	21	13	1.0
IDAHO	18	22	4	1.7	23	5	1.1
IMPERIALCA	4	14	10	1.1	42	38	2.0
LADWP	29	30	1	2.3	71	42	3.5
MONTANA	11	10	-1	0.8	9	-3	0.4
NEVADA	28	34	6	2.6	56	28	2.7
NEW MEXICO	14	2	-13	0.1	55	41	2.7
PACE	42	8	-34	0.6	26	-16	1.3
PG AND E	133	197	64	15.0	202	70	9.8
PSCOLORADO	36	6	-30	0.4	49	13	2.4
SANDIEGO	21	7	-14	0.6	7	-14	0.4
SIERRA	11	7	-4	0.5	76	65	3.7
SOCALIF	108	63	-45	4.8	240	131	11.6
WAPA R.M.	27	24	-3	1.8	56	29	2.7
WAPA U.M.	0	3	3	0.2	3	3	0.1

7.2.2 CSP Plants

In all of the cases presented up to this point, the CSP plants are modeled as base load steam plants. This assumption is based on the expectation that, like other steam generation, there is an efficiency penalty associated with throttling steam to provide fast GR. In this section, the potential contribution of CSP steam turbines to FR is examined by enabling GR on all the new CSP plants. This is accomplished by turning off the base load flag in the turbine governor model.

It is important to note that the CSP dynamic models are based on plants currently in operation. In the WWSIS-2 work, it was assumed that all CSP had significant amounts of thermal storage. It is possible that such plants could be designed to have the ability to relatively rapidly increase power output. Details of such a design are outside the scope of this study.

The frequency nadir is improved by 13 mHz, and the settling frequency is also improved for the HS Hi-Mix case. The frequency traces are shown in Appendix Figure 141.

As discussed in Section 4.1, the PDCI event can cause system separation at the COI in the HS Hi-Mix condition, unless some generation-tripping RAS is enabled. Figure 78 shows a different potential benefit of enabling CSP GR. In this case, the PDCI event is imposed with the CSP GR enabled (blue trace). The figure shows that the system is stabilized without resorting to a RAS.

This is because the beneficial contribution of CSP is geographically advantageous for this event. Most of the CSP is to the south of COI, so the transient increase in power output from these plants is such that power swing from north to south on the COI is slightly reduced and eliminates the voltage collapse along the corridor. Thus, the beneficial CSP contribution to FR also has a positive locational aspect.

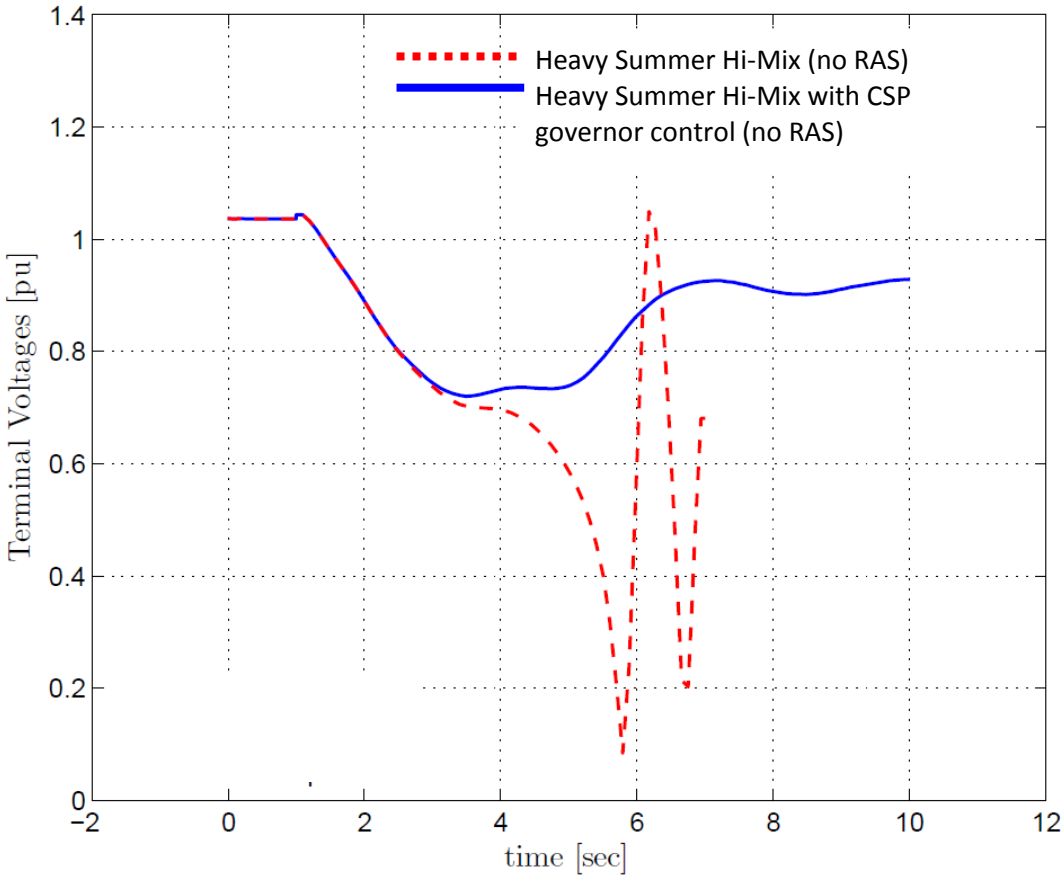

Figure 78. Malin bus voltage in response to PDCI event – with and without CSP governor control.

7.3 Energy Storage for Frequency Response

The FR results presented thus far have shown that the WECC-wide system FR meets NERC criteria, and the system avoids UFLS for all cases examined.

However, many individual areas are short of FR. As previously noted, all of the FROs assigned to individual areas are estimates for illustration. The NERC rules apply specifically and exclusively to individual BAs. There is no requirement that BAs meet their FRO with resources within their Bas; however, a formal contractual arrangement is required to use resources outside their own area.

Energy storage has the potential to help individual BAs meet their FRO with resources that could be deployed within their territories. In this investigation, inverter-based energy storage systems are added to areas short of FR. The model used for this investigation is deliberately independent

of the storage medium (e.g., batteries, flywheels, super conducting magnetic energy storage [SMES], etc.). It is assumed that the medium has sufficient energy to supply the nominal power rating for 60 seconds, and that it has the dynamic capability necessary to follow the change in power required for the control. Again, this is focused solely on FR, and only concerned with the first minute following a disturbance. There is neither a requirement nor a prohibition that the energy storage provide other services, such as balancing, secondary control, arbitrage, etc.

In this investigation, two cases are considered: the LSP Hi-Mix and Extreme response to the loss of two Palo Verde units.

7.3.1 Estimate Energy Storage Rating

An estimate of the amount of energy storage required to bring up the FR in those areas that are short of their FRO is summarized in Table 25. The FR from the LSP Hi-Mix case is shown in the middle. Those areas with negative FR margin are short. The last column shows an estimate of the energy storage power rating sufficient to make up the deficit for this settling frequency.

The math is as follows, using the Arizona area as an example:

- The actual FR = 49.7 MW/0.1 Hz.
- The estimated FRO = 104.4 MW/0.1 Hz.
- The shortfall in FR is therefore = 54.7 MW/0.1 Hz.
- The settling frequency deviation from 60 Hz for this case = -0.156 Hz.
- Therefore, the extra response needed = 54.7 MW x 0.156/0.1, which is 85.3 MW.

An estimated total of 316 MW of energy storage deployed in 10 areas should bring these areas to approximately 100% FRO. As noted earlier, the system response is non-linear, so this method is necessarily approximate.

Table 25. Estimate of Energy Storage Rating Required to Meet FRO

		LSP Hi-Mix		
	FRO	FR	FR Margin	Estimated BESS Rating
Name	(MW/0.1 Hz)	(MW/0.1 Hz)	(MW/0.1 Hz)	(MW)
WECC	840	1,311	471	0.0
By Region				
CALIFORNIA	296	312	16	0.0
DSW	220	119	-101	157.3
NORTHEAST	82	47	-34	53.6
NORTHWEST	131	483	353	0.0
By Area				
ARIZONA	104	50	-55	85.3
EL PASO	9	4	-5	7.6
IDAHO	18	22	4	0.0
IMPERIALCA	4	14	10	0.0
LADWP	29	30	1	0.0
MONTANA	11	10	-1	1.6
NEVADA	28	34	6	0.0
NEW MEXICO	14	2	-13	19.6
PACE	42	8	-34	52.6
PG AND E	133	197	64	0.0
PSCOLORADO	36	6	-30	46.7
SANDIEGO	21	7	-14	22.0
SIERRA	11	7	-4	5.6
SOCALIF	108	63	-45	69.9
WAPA R.M.	27	24	-3	5.1
WAPA U.M.	0	3	3	0.0

A similar exercise for the Extreme case is summarized in Appendix Table 53. For this more challenging condition, a total of 412 MW of energy storage is estimated to be required.

7.3.2 Frequency Performance with Energy Storage

The system frequency for the LSP Hi-Mix case tripping the two Palo Verde NPS units is shown in Figure 79. The energy storage results in improved frequency nadir and settling frequency. The nadir improves by 45 mHz to 59.690 Hz. FR metrics, as reported in Table 26, improve by 201 MW/0.1 Hz at the WECC level. Per-unitized, the benefit on the nadir is 0.14 mHz/MW of energy storage, and the benefit on FR is 0.63 MW per MW per 0.1 Hz.

More important for this investigation, the individual areas that were short of FR are brought up approximately to compliance. The reader's attention is directed to the FR margin columns: the reference in blue and with energy storage in pink. The areas with added energy storage are highlighted in yellow. Notice that FR margins are close to zero, having changed from significantly negative. As noted above, the rating method is approximate, so having the FR exactly equal to the FRO is not expected.

It is of interest to examine the performance of one of the energy storage devices in more detail. In Figure 80, the power output of the Arizona energy storage system is plotted with the Arizona frequency. The case with no energy storage is shown for reference (blue trace). In this case, the

frequency gain and control time constant are selected to have a less aggressive rise than was used in the PV case (above), but more aggressive than the wind plant controls, and to just saturate for this frequency nadir. The output of the Arizona energy storage reaches maximum after 2–3 seconds, well before the frequency nadir, and slightly declines after about 28 seconds, when the frequency is recovering. This decline, coupled with the dynamic impact of the fast-responding resource on the other conventional governors, makes the efficacy in terms of impact on FR per MW of energy storage look worse than that for the wind and solar controls. However, this combination of fast initial response, to benefit the nadir, and less aggressive sustained response, to facilitate coordination with other responsive resources, is arguably better.

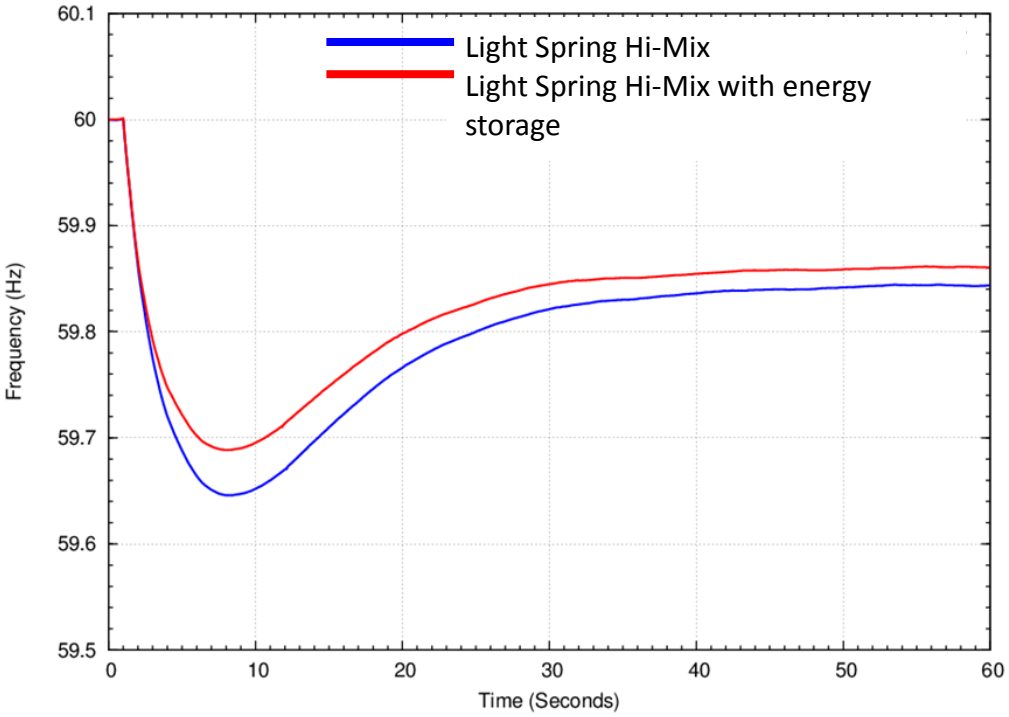

Figure 79. Frequency response to two Palo Verde unit trip for LSP Hi-Mix – with and without energy storage.

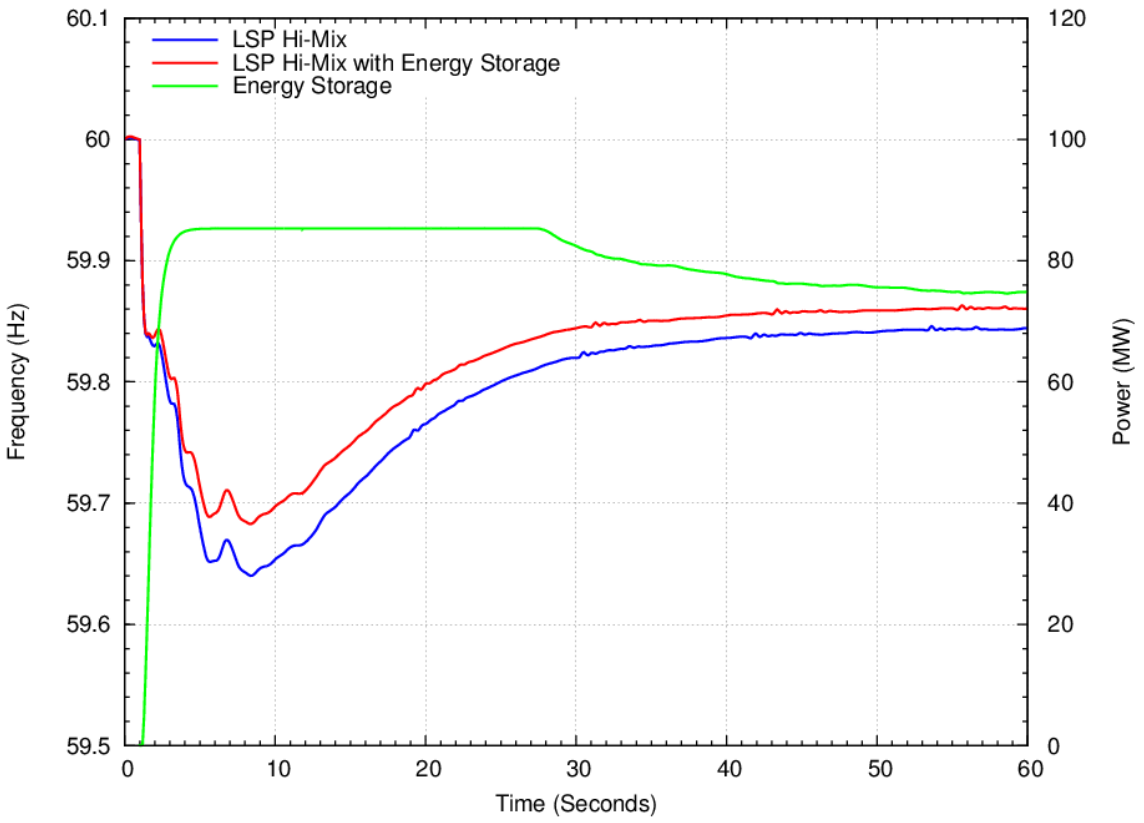

Figure 80. Frequency and power output of an Arizona energy storage plant for LSP Hi-Mix case.

Table 26. FR Metrics for LSP Hi-Mix With and Without Energy Storage

	LSP Hi-Mix				LSP Hi-Mix with Energy Storage	
	FRO	FR	FR Margin	Estimated BESS Rating	FR	FR Margin
Name	(MW/0.1 Hz)	(MW/0.1 Hz)	(MW/0.1 Hz)	(MW)	(MW/0.1 Hz)	(MW/0.1 Hz)
WECC	840	1,311	471	0.0	1,513	672.6
By Region						
CALIFORNIA	296	312	16	0.0	369	73.5
DSW	220	119	-101	157.3	224	4.0
NORTHEAST	82	47	-34	53.6	85	3.8
NORTHWEST	131	483	353	0.0	487	356.4
By Area						
ARIZONA	104	50	-55	85.3	105	1.0
EL PASO	9	4	-5	7.6	9	0.3
IDAHO	18	22	4	0.0	22	4.0
IMPERIALCA	4	14	10	0.0	14	10.4
LADWP	29	30	1	0.0	30	0.4
MONTANA	11	10	-1	1.6	10	-1.0
NEVADA	28	34	6	0.0	34	6.0
NEW MEXICO	14	2	-13	19.6	14	-0.6
PACE	42	8	-34	52.6	40	-1.7
PG AND E	133	197	64	0.0	197	64.2
PSCOLORADO	36	6	-30	46.7	33	-2.1
SANDIEGO	21	7	-14	22.0	21	-0.7
SIERRA	11	7	-4	5.6	10	-0.3
SOCALIF	108	63	-45	69.9	103	-5.1
WAPA R.M.	27	24	-3	5.1	26	-1.6
WAPA U.M.	0	3	3	0.0	3	2.5

Similar results for the system response in the Extreme case with 412 MW of energy storage are shown in Appendix Figure 142 and Figure 143, and in Appendix Table 54. Qualitatively, the results are similar to the Hi-Mix case. The FR improves by 252 MW/0.1 Hz from 1,055 MW/0.1 Hz to 1,307 MW/0.1 Hz. The per-unitized benefit is 0.61 MW per MW per 0.1 Hz, essentially the same as that for the Hi-Mix case. The frequency nadir improves 56 mHz, from 59.614 Hz to 59.670 Hz, or 0.14 mHz/MW. This linearity reflects the fact that the energy storage is sized and controlled with the same objectives and constraints.

7.4 Relative Performance of Frequency Controls

Primary response from fast energy storage (e.g., batteries, flywheels, etc.) is effective at improving both nadir and settling frequency. Relatively small amounts (total ~400 MW for all WECC) "fixed" all area FRO deficiencies in these cases. The benefits are similar to those observed from aggressive control of solar PV. In comparison, the impact of controls on wind plants varied depending on the speed of response. The fast response of the inertial control improved the frequency nadir; the sustained governor output improved the FR metric. The CSP response example highlighted a locational aspect that, in this case, was beneficial to transient stability.

The combined findings suggest that the best use of rapidly responding power-electronics-enabled resources for FR is non-linear. The medium (i.e., wind or solar or energy storage or a combination) is less important than the control philosophy employed. Other technologies, such as fast control of loads that deliver similar dynamic response, would likely produce similar improvements. The results illustrate that improvement in frequency nadir and beneficial impact on system security are not necessarily perfectly aligned with the FR metric. In the past, the primary available control variable was gain, in the form of governor droop, and speed of response was not readily adjusted. Practice to coordinate droops and to ensure adequate response were more straightforward. With the added flexibility of new resources that have the ability to easily adjust speed of response, there is the potential for FR that equals or exceeds that of the present system. However, the frequency control problem gains dimensionality and complexity, as both control flexibility and the necessity to consider energy as well as power constraints, are introduced. As in the past, locational aspects may prove important in some cases.

7.5 COI Stabilization with Transmission Additions

In this study, a minimalist approach has been used, adding only the reinforcements necessary to relieve performance problems for the specific cases under consideration.

In this mitigation exercise, a portion of the WWSIS-2 transmission additions are made to the HS Hi-Mix case to examine their impact on stability.

Table 27 is adopted from transmission build-out work from WWSIS-2, which used 500 MW increments on PLEXOS inter-area paths. Path capability for that type of model does not necessarily provide simple mapping to actual new physical lines. Rather than postulate new corridors or attempt to replicate specific project proposals, this exercise was limited to duplicating, and thereby doubling, existing circuits in the dataset. The work explicitly did not consider other potential transmission projects.

The original WECC case included significant new transmission. One project is a major new 500 kV line from central Oregon at Grassland to outside Las Vegas at Harry Allen, via a route well east of the Sierras through the Hemingway, Midpoint, and Robinson substations. The three highlighted improvements in the table provide an approximate proxy for the build-out of this test, which is to make this new line a double circuit. The addition of this path provides an additional north-to-south transfer path that decreases flow across the COI and increases the synchronizing strength of the system. COI flow drops about 400 MW. Appendix Figure 144 shows the bubble chart, with some of the major flow changes noted.

Table 27. Selected WWSIS-2 Transmission Additions

		Transmission Path Upgrades (MW)	
WWSIS-2 Interface	**Initial Rating**	**TEPPC ($10 Hurdle Rate)**	**Hi Mix ($10 Hurdle Rate)**
AZ to CA so	1,600	1,000	1,000
AZ to CO	200	0	500
AZ to IID	195	500	500
AZ to DWP	468		500
AZ to UT	250		500
CA no to NV no	100	500	1,500
CA no to SF	1,272	500	1,500
ID to NV no	350	500	500
MO to NW	2,000		1,000
NV no to NW	300	1,000	1,000
UT to WY	2,100		500
Total		**4,000**	**9,000**

The added transmission stabilizes the system without a generation-tripping RAS for the PDCI event. Figure 81 shows the interface flow power swings for the unstable LSP Hi-Mix case and the stabilized Hi-Mix case with added transmission. Appendix Figure 145 and Figure 146 show voltages for the event, which comfortably meet WECC voltage criteria.

The improvement in system stability due to transmission additions is not surprising. The key observation from this test is that transmission additions that are *economically* justified for their reduction in overall variable operating cost (from WWSIS-2) will tend to improve system transient stability as well.

Again, this raises the question of whether the interface limits should change. It is possible that this improved parallel path increases the COI limit, but it is also possible that there are other consequences. A complete system evaluation is needed to assess the impact of a major transmission change like this on path limits.

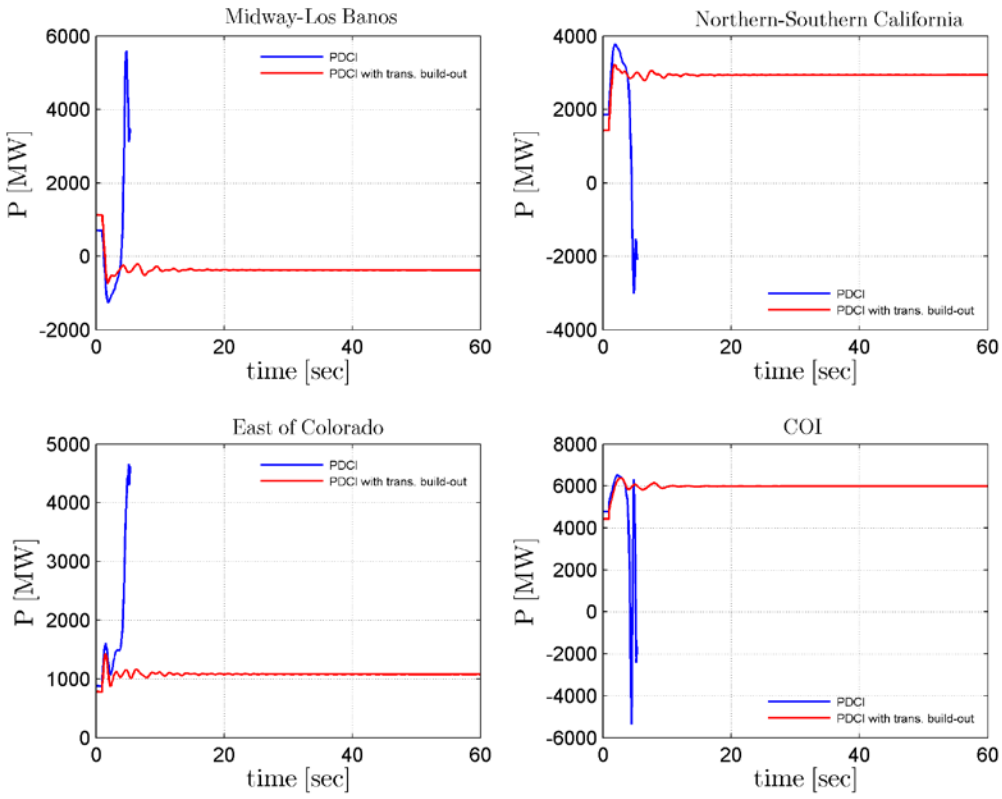

Figure 81. Path flows in response to PDCI event for LSP Hi-Mix case with and without transmission build-out.

8 Summary and Conclusions

8.1 Frequency Response

Frequency response (FR) is the overall response of the power system to large, sudden mismatches between generation and load, and it is measured according to NERC BAL-003 (NERC 2012a). The primary concern is that the minimum frequency, or nadir, during design-basis disturbances should not cause under-frequency load shedding (UFLS). In the West, the first stage of UFLS is normally at 59.5 Hz. The NERC standard also provides a specific definition of the quantitative metric "frequency response." It is this metric that is compared to the frequency response obligation (FRO) to determine compliance.

WWSIS-3 focused on light spring conditions, as the relatively low level of generation may present a challenge for FR. Similarly, the analysis focused on the single largest design-basis generation outage in the Western Interconnection. According to BAL-003-1, this design-basis event is the trip of two fully loaded Palo Verde nuclear power station units for a loss of about 2,750 MW. The subsequent frequency excursion is severe; however, all cases avoid UFLS relay action and meet the interconnection frequency response obligation (IFRO), which is 840 MW/0.1 Hz for this study. To help understand the system frequency performance, estimates of regional FROs were made. Actual FROs are assigned to individual balancing authorities (BAs) and are updated annually, so these estimated obligations are for reference only and should not be used to determine individual BA compliance with the NERC standard. As noted above, the WECC-wide FR meets its obligation in all cases, with some margin. Portions of the system that rely primarily on thermal generation, however, tend to be short of meeting their approximate FRO with their own generation resources, especially in the Hi-Mix case (e.g., the DSW and Northeast regions). This occurs because that thermal generation was displaced by wind and solar, which do not provide FR unless equipped with specific controls. Other regions, particularly the NW, far exceed their approximate FRO due to high levels of responsive hydro.

As expected, the WECC-wide response is substantially improved for the HS condition compared to the LSP condition.

Extreme Generation Loss

The FR to an extreme event (i.e., loss of three Palo Verde units) compared to that of the design-basis event (i.e., loss of two Palo Verde units) is close to linear and showed a slight degradation due to the larger-sized event and more governor controls saturating. This is reassuring from a robustness perspective, though obviously a severe event will still cause UFLS-triggered interruptions, just as it does today.

While UFLS action is allowed for a severe event like this extreme generation tripping, cascading failure is not. One sensitivity case in which the embedded PV DG was pessimistically assumed to have aggressive under-frequency tripping resulted in an acute frequency depression and would have likely caused widespread outages.

Distributed vs. Central Station Generation Tripping

System performance in response to a large distributed generation outage was compared to a large central station outage. The DG event results in a less severe frequency nadir and a better settling frequency. The difference is relatively small and is primarily due to two factors. First, the loss of

locally generated power depresses the load voltage and causes the net load to drop. This load relief helps the system frequency. A second factor is that the tripped DG is less than the 2,750 MW of the Palo Verde event, due to voltage effects on the tripping logic in the composite load model. The post-disturbance voltages tend to be different, however, which can have substantial impact on load active power. This result tends to reinforce the conclusion that load voltage sensitivity is a more important consideration for FR than load frequency sensitivity. Broadly, the location of the generation tripping is not as important as the amount of generation that is tripped. The mechanisms for widespread DG tripping are complex, so it may be possible for more DG to trip than was used in this sensitivity case.

System Inertia

Much has been said about the possible impact of loss of system inertia due to the displacement of synchronous generation by inverter-based resources. Between the LSP Base case and the Hi-Mix case, the initial rate of change of frequency (ROCOF) increases about 18%. The impact of this increased ROCOF on the system stability is nearly invisible in terms of FR: both the nadir and the settling frequency are essentially unchanged. It should be noted that these levels of ROCOF, on the order of 0.1 Hz/s, are quite small compared to some of the smaller systems around the world that have ROCOF concerns primarily driven by the use of ROCOF relays. This reinforces other results that suggest that the loss of system inertia associated with increased wind and solar generation is of little consequence for up to at least 50% levels of instantaneous penetration for the Western Interconnection as long as adequately fast primary frequency-responsive resources are maintained.

Headroom Depletion

The effects of headroom depletion due to a relatively rapid afternoon decline in solar PV generation—the so-called “duck curve”—is a growing concern. In an effort to bound the problem, an extreme case was simulated where all PV generation in the Western Interconnection was shut down, mimicking sunset, while no other generation was committed. This does not create a catastrophic failure in the system performance for the given commitment and dispatch. No dramatic changes in performance were observed (i.e., there was no cliff) as the PV dropped out. Rather, the degradation of FR is steady and monotonic, while transient stability was maintained.

However, once the PV output is reduced to zero, the overall WECC FR is marginal, even with significant contribution from California hydro. The FR for California is below the approximate statewide FRO. To test the impact of having less responsive hydro, governors were removed as a proxy for low water levels or other constraints on the hydro generators' ability to provide more power. As the California hydro becomes less responsive, the overall WECC FR drops, and eventually WECC fails to meet the IFRO.

As PV output drops, the system re-dispatches, creating many local stress points (e.g., poor voltage). This suggests that the need to commit/recommit units could be driven as much by local constraints as overall stability. The details will be important as the system stress builds. This further suggests that locational issues may drive some constraints on how system operators strive to maintain adequate FR.

8.2 Means to Improve Frequency Response

Current operating practice uses traditional approaches (e.g., commit conventional plants with governors) to meet all FR needs. Selected non-traditional frequency-responsive controls on wind, solar PV, CSP plants, and energy storage were examined in this study.

Frequency-Responsive Controls on Wind Plants

This study examined two types of frequency-responsive controls for wind plants. The inertial control helps improve the nadir, but the energy recovery tends to stretch out the frequency depression. A substantial improvement in the margin above UFLS is realized. Unlike the governor function, the inertial control has no opportunity or lost energy cost. There is, however, a capital cost associated with the controls.

The governor or active power control (APC) alone greatly improved the settling frequency and the FR, but had little impact on the nadir. The combination of the governor and inertial control improved the frequency nadir, settling frequency, and FR. Note that the wind governor controls were set to emulate those on conventional generation. Both the wind governor and inertial controls could be made more aggressive, as is examined with the utility-scale PV and energy storage controls below.

Frequency-Responsive Controls on Solar PV Plants

Primary FR from utility-scale solar PV generation is effective at improving both nadir and settling frequency. Unlike the governor controls for wind plants, the control used here is aggressive: the response is fast, with gains and time constants selected to saturate relatively quickly once the system frequency is outside of the dead band. The PV plant response to the design-basis event (i.e., loss of two Palo Verde units) is so fast that it is essentially a step response. Had the event been somewhat less severe, the control still would have saturated and provided proportionally greater response. Thus, the FR metric would show a greater benefit. Conversely, had the event been even larger, the FR metric would be worse.

Frequency Response from Energy Storage

This study shows that the WECC-wide FR meets NERC criteria, and the system avoids UFLS for all cases examined. However, many of the individual areas are short of FR. Note that the FROs assigned to individual areas in this study are estimates. The NERC rules apply specifically and exclusively to individual BAs; there is no requirement that BAs meet their FRO with resources within their BAs.

In this investigation, inverter-based energy storage systems are added to areas short of FR. The model used for this investigation is deliberately independent of the storage medium (e.g., batteries, flywheels, super conducting magnetic energy storage [SMES], etc.). It is assumed that the medium has sufficient energy to supply the nominal power rating for 60 seconds, and that it has the dynamic capability necessary to follow the change in power required for the control. The storage systems for each area were sized specifically to meet that area's estimated FRO, and an aggressive governor control was applied to each system. Primary FR from fast energy storage is effective at improving both nadir and settling frequency. A total of about 400 MW of energy storage for all of the Western Interconnection allowed the individual areas that were short of FR to meet their approximate FROs with resources in their areas. The NERC requirements allow

individual areas to contract with others for sufficient frequency-responsive resources to meet their obligation.

8.3 Transient Stability

During heavy load conditions, the addition of high levels of wind and solar generation increases the heavy loading on the Pacific AC and DC Interties to about their present path ratings. High flows on the COI are well known to be stressful and to require a generation-tripping remedial action scheme (RAS). This investigation suggests that this practice can continue, and that the transient stability of the system for one of the well-known and critical events for the Western Interconnection is not fundamentally changed by the high wind and solar generation. One sensitivity case in which the Base case had the same PDCI and COI loading had slightly worse performance than the Hi-Mix case. This conclusion is not a statement that the system behaves identically. It is possible, and perhaps likely, that the system dynamics are sufficiently different to require somewhat different levels of generator tripping or different arming criteria. A complete evaluation of the current practice to check for refinements would be prudent. There is, however, nothing in this analysis to indicate that the system dynamics have fundamentally changed and that radically different means to ensure stability for this event are required.

Local Stability

There are many localized stability limits in the West. The addition of substantial wind and solar generation has the potential to alter the system dynamics of the events that dictate these limits.

For the limited examples, the local system stability is slightly better in the Hi-Mix case.

Distributed Generation Fault Ride-Through

The deliberate or sympathetic trip of distributed PV during disturbances results in a slower recovery and lower sustained voltages. Local reactive power balance can be disrupted, with reactive power demand increasing many times the amount of active power tripped. In one test, with a pessimistic approximation to a worst-case under-voltage tripping, the loss of the DG causes a system collapse.

A number of cases showed adverse consequences, up to and including system collapse, from widespread tripping of embedded PV distributed generation. Consequently, both prudence and existing reliability rules would argue against widespread, common-mode DG tripping for moderately severe voltage dips or frequency excursions.

IEEE Standard 1547a, published in May 2014, revises three existing requirements for interconnection of DG with electric power systems. It now has significantly wider mandated ranges for DG allowable trip settings in response to utility abnormal voltages and frequency with different specified settings allowed via mandatory mutual agreement between the power system and DG operators. However, when the grid experiences a large disturbance, if the 1547 default trip settings are used for all DG sites, that may result in widespread DG tripping at the same time. The draft IEEE Standard 1547.8 further permits additional DG functions to support the grid, again via mutual agreement. Although this draft has initially been approved by IEEE balloters, it is undergoing final revisions before publication.

The system-wide impact of common mode tripping of significant amounts of DG, regardless of the mechanism, requires more study.

Coal Displacement and Weak Grid in the Northeast Region

A high de-commitment of coal did not overstress the system. A greater than 80% reduction of coal commitment in the Northeast region, compared to the LSP Base case, resulted in acceptable dynamic behavior for the limited tests performed. System dynamics were stable for an extra-high-voltage fault at Aeolus, in the heart of the high wind area of the Northeast. The system non-synchronous penetration (SNSP) was driven to 56% in the Hi-Mix case.

The regional transmission system was designed based on the size and location of the large coal power plants, which thus became critical nodes in the network. As a result, the transmission system operators have historically counted on those plants to provide the voltage and reactive power support needed for reliable operation. Displacement of those central plants by more dispersed wind and solar generation results in those nodes being poorly supported. Not surprisingly, local voltage and thermal problems occur, and good planning practices need to be followed.

The de-commitment in the Extreme case further stresses the system, with a greater than 90% reduction of coal commitment from the LSP Base case. This gives an SNSP of about 66%. There was a rapid voltage collapse and system separation during the fault representative of so-called "weak grid" issues. Systems with very high levels of inverter-based generation are challenged to provide fast, confident control during faults and other disturbances. No commercially available wind or utility-scale solar PV generation is capable of operation in a system without the stabilizing benefit of synchronous machines. Therefore, the conversion of some coal plants to synchronous condensers and the addition of mechanically switched shunt compensation were needed to stabilize the Aeolus fault with the pessimistic load and wind plant modeling used. The synchronous condenser conversion (assuming retirement) works well to stabilize the system. The system recovers in an orderly fashion when the fault is cleared.

8.4 Means to Improve Transient Stability

Transmission Additions

The mitigation investigation in WWSIS-3 included a portion of the WWSIS-2 transmission additions to examine their impact on the transient stability of the COI. The added transmission stabilizes the system without a generation-tripping RAS. This reinforces the need to analyze whether the interface limits should change.

Frequency-Responsive Controls on CSP Plants

The CSP plants are modeled as base load steam plants under most conditions. However, the potential contribution of CSP steam turbines to FR was examined by enabling GR on all the new CSP plants.

The PDCI event can cause system separation at the COI unless some generation-tripping RAS is enabled. However, there is a potential benefit of having CSP GR when the PDCI event is imposed: the system is stabilized without resorting to a RAS. This is because the beneficial contribution of CSP is geographically advantageous for this event. Most of the CSP is to the

south of COI, so the transient increase in power output from these plants is such that power swing from north to south on the COI is slightly reduced and eliminates the voltage collapse along the corridor. Thus, the beneficial CSP contribution to FR also has a positive locational aspect that benefits transient stability.

8.5 Model Improvement and Further Analysis

Load Model

Changing the load model had a greater impact on system performance than did changing the level of renewable generation. The behavior of the system for deep faults is completely dominated by the load model, and more specifically by the tripping vs. stalling behavior assumed for the motor constituents of the composite load. The motor stalling behavior is exacerbated by blocking or tripping of embedded PV. This is an extraordinarily complex issue for planning and for research. This stability risk is not primarily one of utility-scale renewable integration. Further investigation of the load behavior, the motor tripping, and the behavior of the embedded PV DG is warranted.

Wind and Solar Models

When wind and solar are the predominant source of generation throughout the region, it will be important to have appropriate dynamic models. WECC has a longstanding best practice to keep dynamic models up to date. Wind and solar plant models needs to be held to the same level of accuracy in a high-penetration future. Adoption of wind plant controls designed for weak grids greatly improved system stability. Further, the results were extremely sensitive to the assumptions about load modeling, as described above.

Frequency-Responsive Control Philosophy

The combined findings of the wind, solar, and energy storage investigations suggest that the best use of rapidly responding power-electronics-enabled resources for FR is non-linear. The medium—wind or solar or energy storage or a combination —is less important than the control philosophy employed. Other technologies that deliver similar dynamic response, such as fast control of loads, would likely produce similar improvements.

In the past, the primary control variable was gain, in the form of governor droop, and speed of response was not readily adjusted. Coordinating droops and ensuring adequate response were more straightforward. With the added flexibility of easily adjustable speed of response, and the necessity to consider energy as well as power constraints, the frequency control problem also gains complexity. With the addition of non-linear frequency-responsive resources, practice will need to evolve and incorporate FR that is a function of the size of the disturbing event. As in the past, locational aspects may prove important in some cases.

Path Rating Analyses

The majority of the results presented in this study used the transmission topology directly from the WECC planning databases. These WECC cases included significant new transmission that is not currently in service. With the exception of some local patches, no further major reinforcements were added. In general, the study did not identify dramatic changes in system dynamics. However, the large changes in system flow patterns suggest that a rigorous analysis of individual paths is needed to ensure reliability. Certainly, all the regional paths in the high wind

parts of the Northeast region will change as transmission is added to accommodate the new plants. A complete system evaluation is needed to assess the impact of such a major transmission change on path limits.

Coal Displacement Analysis

The sequence of coal displacement sensitivities in this study is illuminating, but in no way complete or conclusive. It provides an opportunity to investigate the transient stability implications of not only temporary de-commitment of coal generation, but also the impact of possible coal plant retirements. The key point is that transient stability analysis is always based on snapshots of operation. From a system dynamics perspective, whether a specific generating resource is off-line because it was de-committed for a particular operating condition is indistinguishable from a permanent retirement. The displacement by wind and solar was based on the economic analysis of WWSIS-2, rather than an arbitrary, plant-by-plant choice.

The system appears to behave well for the Hi-Mix case when almost all of the large coal plants in the eastern regions are off-line. However, displacing even more coal units and pushing SNSP above 60% appears to cause problems. This small sample suggests that care must be exercised in driving the system from a high level of coal displacement to an extreme level of coal displacement. More analysis is needed.

8.6 Conclusions

This work did not identify any fundamental reasons why the Western Interconnection cannot meet transient stability and FR objectives with high levels of wind and solar generation. However, good system planning and power system engineering practices must be followed. At a minimum, local voltage and thermal problems will inevitably require some transmission system improvements. The dynamic behavior of distributed PV generation was shown to have the potential to substantially impact the bulk power system. Distribution is not decoupled from transmission and will impact bulk power system operation. Mechanisms are needed to allow BAs to both share frequency-responsive resources and to ensure that they have adequate frequency-responsive resources within their control. From a transient stability perspective, the system appears to tolerate substantial displacement of thermal generation. However, care will be needed in the event that the system, especially the DSW and Northeastern regions, is driven to near zero commitment of coal plants. Note that this investigation is not a substitute for thorough system planning studies. The conclusions of WWSIS-3 are provided in bullet format below.

Transient Stability Conclusions

For the conditions studied:

- System-wide transient stability can be maintained with high levels of wind and solar generation if local stability, voltage, and thermal problems are addressed with traditional transmission system reinforcements (e.g., transformers, shunt capacitors, local lines). With these reinforcements, an 80% reduction in coal plant commitment, which drove SNSP to 56%, resulted in acceptable transient stability performance.
- With further reinforcements, including non-standard items such as synchronous condenser conversions, a 90% reduction in coal plant commitment, which drove SNSP to 61%, resulted in acceptable transient stability performance.

- Additional transmission and CSP generation with frequency-responsive controls are effective at improving transient stability.

Frequency Response Conclusions

For the conditions studied:

- System-wide FR can be maintained with high levels of wind and solar generation if local stability, voltage and thermal problems are addressed with traditional transmission system reinforcements (e.g., transformers, shunt capacitors, local lines).
- Limited application of non-traditional frequency-responsive controls on wind, solar PV, CSP plants, and energy storage are effective at improving both frequency nadir and settling frequency, and thus FR. Refinements to these controls would further improve performance.
- Individual BA FR may not meet its obligation without additional FR from resources both inside and outside the particular area. As noted above, non-traditional approaches are effective at improving FR. Current operating practice uses more traditional approaches (e.g., commit conventional plants with governors) to meet all FR needs.
- Using new, fast-responding resource technologies (e.g., inverter-based controls) to ensure adequate FR adds complexity, but also flexibility, with high levels of wind and solar generation. Control philosophy will need to evolve to take full advantage of easily adjustable speed of response, with additional consideration of location and size of the generation trip.
- For California, adequate FR was maintained during acute depletion of headroom from afternoon drop in solar, assuming the ability of California hydro to provide FR.

Other Conclusions

- Accurate modeling of solar PV, CSP, wind, and load behavior is extremely important when analyzing high stress conditions; all of these models had an impact on system performance.
- Attention to detail is important. Local and locational issues may drive constraints on both FR and transient stability.
- The location of generation tripping, e.g., DG vs. central station, is not as important as the amount of generation that is tripped. However, widespread deliberate or common-mode DG tripping after a large disturbance has an adverse impact on system performance. It is recommended that practice adapt to take advantage of new provisions in IEEE 1547 that allow for voltage and frequency ride-through of DG to improve system stability.
- Further analysis is needed to determine operational limits with low levels of synchronous generation, to identify changes to path ratings and associated remedial action schemes, and to quantify DG impact on transmission system performance.
- Because a broad range of both conventional and non-standard operation and control options improved system performance, further investigation of the most economic and effective alternatives is warranted. This should include consideration of the costs and

benefits of constraining commitment and dispatch to reserve FR, as well as the capital and operating costs of new controls and equipment.

9 References

AESO (2010). *Proposed New Level 1 ISO Rules, Part 500, Facilities, Division 502, Technical Requirements, Section 502.1, Wind Aggregated Generating Facilities, Technical Requirements, External Draft 2.0.* Calgary: Alberta Electric System Operator. May 6, 2010.

EirGrid (2011a). *EirGrid Grid Code, Version 3.5.* Dublin: EirGrid. Effective March 15, 2011. Accessed February 23, 2013: http://www.eirgrid.com/media/2011%20Mar%2008%20EirGrid%20Grid%20Code%20Clean%20Version%203.5.pdf.

EirGrid (2011b). *EirGrid 2011 Curtailment Report.* http://www.eirgrid.com/media/2011_Curtailment_Report.pdf

EirGrid (2014). *EirGrid Renewables.* www.eirgrid.com/renewables.

Ela, E., et al. (2014). *"Active Power Controls from Wind Power: Bridging the Gaps*. NREL/ Technical Report TP-5DD05D00-60574, January, 2014.

ERCOT (2010). "Primary Frequency Response Requirement From Existing WGRs." Electric Reliability Council of Texas PRR833. Approved May 18, 2010.

ERCOT (2010). "Primary Frequency Response Requirement from Existing WGR." March 2010.

Eto, J., et al. (2010). "Use of Frequency Response Metrics to Assess the Planning and Operating Requirements for Reliable Integration of Variable Renewable Generation." LBNL-4142E, December 2010.

FERC (2005). "Interconnection for Wind Energy." Federal Energy Regulatory Commission Order No. 661-A. December 12, 2005.

GE Energy (2010). *Western Wind and Solar Integration Study.* NREL/SR-550-47434. Golden, CO: National Renewable Energy Laboratory. Accessed February 22, 2013: http://www.nrel.gov/docs/fy10osti/47434.pdf.

GE Energy (2013). *Eastern Frequency Response Study.* NREL/SR-5500-58077. Golden, CO: National Renewable Energy Laboratory. May 2013.

Gevorgian, V.; Zhang, Y.; Ela, E. (2014). "Investigating the Impacts of Wind Generation Participation in Interconnection Frequency Response." *IEEE Transactions on Sustainable Energy*, Vol. PP, no. 99; pp. 1-9, 2014.

Hydro-Quebec (2006). "Transmission Provider Technical Requirements for the Connection of Power Plants to the Hydro-Quebec Transmission System." Item 14.4 Frequency Control. March 2006.

Ingleson, J.W.; Allen, E. (2010). "Tracking the Eastern Interconnection Frequency Governing Characteristic." IEEE Power and Energy Society General Meeting, 25-29 July 25–29, 2010.

Ingleson, J.W.; Ellis, D.M. (2005). "Tracking the Eastern interconnection Frequency Governing Characteristic." IEEE Power Engineering Society General Meeting, June 12–16, 2005.

Kundur, P., et al. (2004). "Definition and Classification of Power System Stability." *IEEE Transactions on Power Systems*, Vol. 19, No. 2; pp. 1387-1401.

Mackin, P., et al. (2010). "Dynamic Simulation Studies for the Frequency Response of the Three U.S. Interconnections with Increased Wind Generation." LBNL-4146E, December 2010.

Miller, N.; Clark, K.; Walling, R. (2009). "WindINERTIA: Controlled Inertial Response from GE Wind Turbine Generators." Presented at the 45th Annual Minnesota Power Systems Conference, Minneapolis, MN, November 2009.

Miller, N.W.; Clark, K.; Shao, M., (2011a). "*Frequency Responsive Wind Plant Controls: Impacts on Grid Performance*." IEEE Power and Energy Society General Meeting, Detroit, MI, July 2011.2011.

Miller, N.W.; Shao, M.; Venkataraman, S., (2011b). *California ISO (CAISO) Frequency Response Study, Final Draft.* Schenectady, NY: GE Energy. Accessed February 22, 2013: http://www.caiso.com/Documents/Report-FrequencyResponseStudy.pdf.

NERC (2009). *A Technical Reference Paper: Fault-Induced Delayed Voltage Recovery.* Version 1.2. June 2009.

NERC (2012a). *Standard BAL-003-1, Frequency Response and Frequency Bias Setting.* November 30, 2012.

NERC (2012b). *Standard BAL-003-1, Attachment A - Frequency Response and Frequency Bias Setting –Supporting Document.* November 30, 2012. http://www.nerc.com/docs/standards/sar/Attach_A-Frequency_Response_Standard_Support_Document-Clean.pdf.

NERC (2012c). *Frequency Response Initiative Report.* Draft. September 30, 2012. http://www.nerc.com/docs/pc/FRI%20Report%209-30-12%20Clean.pdf.

NERC (2013). NERC Standard PRC-024, "Generator Frequency and Voltage Protective Relay Settings.," NERC Standard PRC-024. Draft, January 17, 2013.

NREL (2013). *Western Wind and Solar Integration Study, Phase 2*. NREL/SR-5500-55888, September 2013.

Elliott, R.; Byrne, R.; Ellis, A.; Grant, L. (2014). *Impact of Increased Photovoltaic Generation on Inter-area Oscillations in the Western North American Power System,* IEEE PES General Meeting, Washington D.C., 2014.

Sharma, S.; Huang, S.; Sarma, N.D.R. (2011). "System Inertial Frequency Response Estimation and Impact of Renewable Resources in ERCOT Interconnection." IEEE Power and Energy Society General Meeting, Detroit, MI, July 2011.

Undrill, J. (2010). "Power and Frequency Control as it Relates to Wind-Powered Generation," LBNL-4143E, December 2010.

Vittal, V. (2003). *Transient Transient Stability and Control of Large Scale Power Systems*. Power Systems Engineering Research Center Background Paper.

WECC (2012). *Composite Load Model for Dynamic Simulations.* Report 1.0. WECC Modeling and Validation Work Group. Accessed February 23, 2013: http://www.wecc.biz/committees/StandingCommittees/PCC/10102012/Approval%20Items/1/WECC%20MVWG%20Load%20Model%20Report%20ver%201%200.pdf.

WECC (2014). Model Validation Working Group Load Model Data Tool – LMDT4A documentation.

10 Appendix

10.1 Supporting Material on WECC Planning Cases

Table 28. Approved WECC Planning Databases Considered

a. 2013 LW

b. 2013 HW

c. 2013 HS

d. 2018 HS

e. 2022 LSP

f. 2016 LS

g. 2023 HS

h. 2013 HS

i. 2013 LS

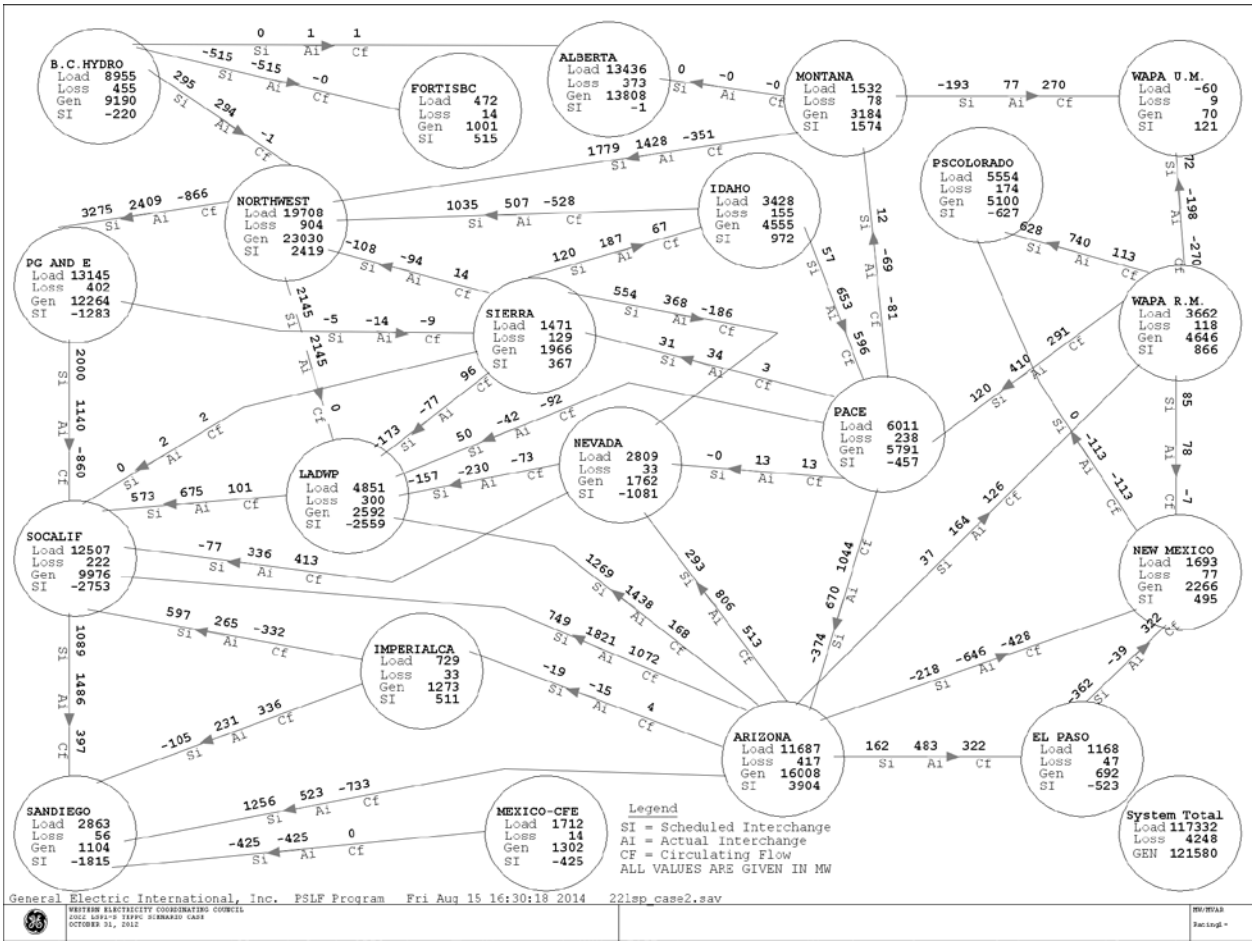

Figure 82. LSP Base case bubble diagram.

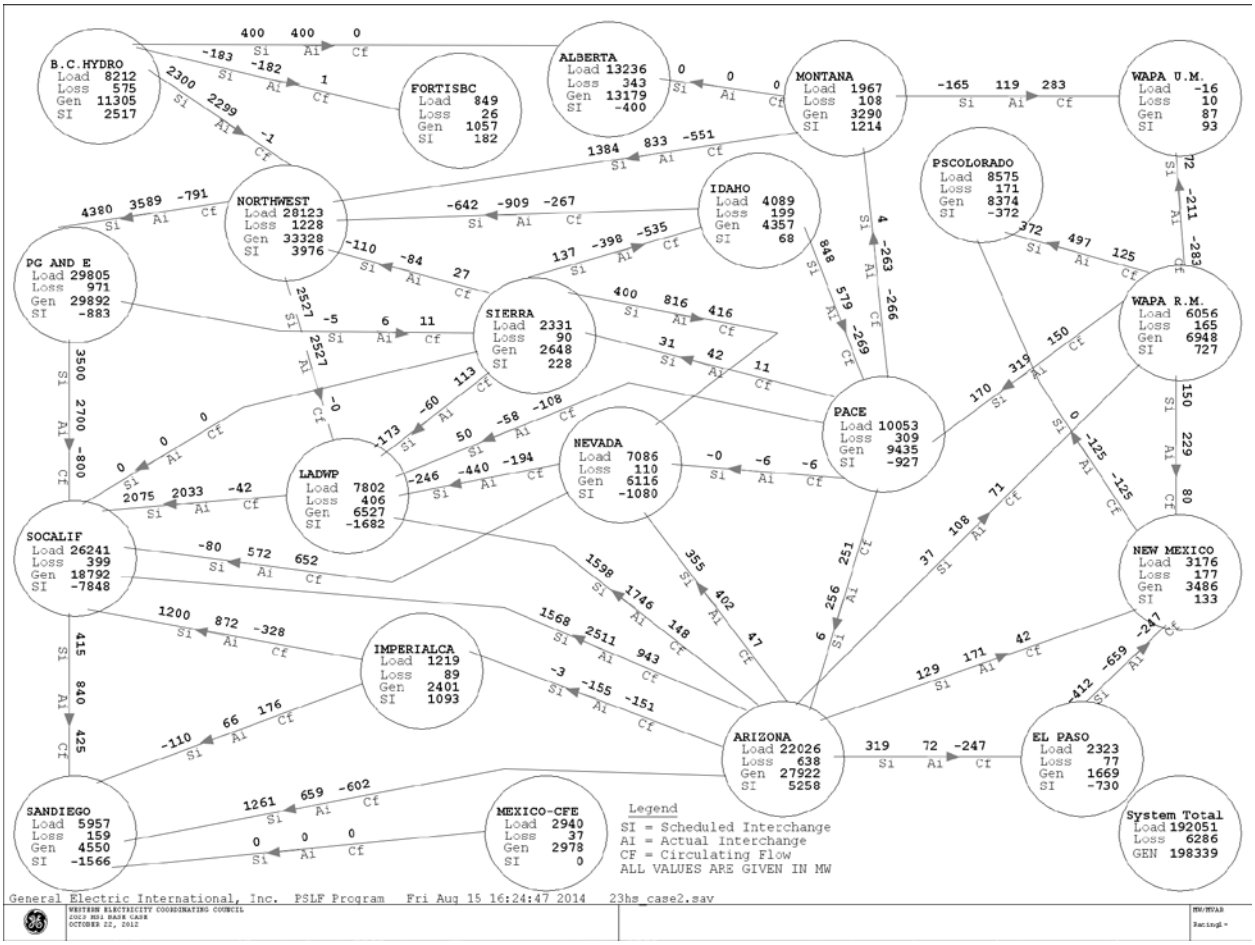

Figure 83. HS Base case bubble diagram.

Table 29. Wind Plants Modeled as Synchronous Generators (Example)

BusNum	BusName	BuskV	id	MVA	GenModel	Data Owner Unit Type
54251	GARDNG2	25	1	30	genrou	Wind
54255	CHINOOK9	34.5	1	13.5	gentpj	Wind
54265	US WIND9	34.5	1	13.5	gentpj	Wind
54641	TURNIPG2	0.69	2	85	genrou	Wind
54789	WINTG1	0.69	G1	21	genrou	Wind
54846	WINTG4	0.69	G4	21	genrou	Wind
54848	WINTG5	0.69	G5	21	genrou	Wind
54852	WINTG6	0.69	G6	21	genrou	Wind
55328	MACLEOD4	1	G2	39.8	genrou	Wind
55733	WR1LV19	12	1	21	genrou	Wind
56155	OLDEL_C1	0.69	G1	80	genrou	Wind
56156	OLDEL_C3	0.69	G3	80	genrou	Wind
56294	TOTHILL2	0.69	G1	35.6	genrou	Wind
56328	MACLEOD5	1	G1	27.5	genrou	Wind
56338	SUMV4	0.69	1	46	genrou	Wind
56355	OLDEL_C2	0.69	G2	80	genrou	Wind
56356	OLDEL_C4	0.69	G4	80	genrou	Wind
56389	HILLRIDG	25	1	30	genrou	Wind
56402	KETTLES2	34.5	1	1.8	genrou	Wind
56402	KETTLES2	34.5	2	14.4	genrou	Wind
56402	KETTLES2	34.5	3	1.8	genrou	Wind
56402	KETTLES2	34.5	4	12.6	genrou	Wind
56464	WR2WF7	12	4	21	genrou	Wind
56465	WR2WF12	12	9	21	genrou	Wind
56632	WR1LV16	12	1	19.5	genrou	Wind

Table 30. Netted Units (Examples)

Bus #	Bus Name	ID	Pgen (MW)	Area	Area	Bus #	Bus Name	ID	Pgen (MW)	Area	Area
22916	PFC-AVC	1	0	22	SANDIEGO	20111	TEK-230	CE	0	20	MEXICO-CFE
14812	RC-W1	1	21	14	ARIZONA	21089	LSR G1	1	23	21	IMPERIALCA
14813	RC-W2	1	21	14	ARIZONA	21088	LSR G2	1	23	21	IMPERIALCA
14814	RC-W3	1	21	14	ARIZONA	85720	ABITIBI	1	15.3	14	ARIZONA
14816	RC-E1	1	21	14	ARIZONA	20394	ESL-CC2	2	180	20	MEXICO-CFE
14817	RC-E2	1	21	14	ARIZONA	20395	ESL-CC3	3	100	20	MEXICO-CFE
14818	RC-E3	1	21	14	ARIZONA	20446	JOV-CC1	1	100	20	MEXICO-CFE
14212	GLENDALE	1	6	14	ARIZONA	20447	JOV-CC2	2	200	20	MEXICO-CFE
14222	PRESCOTT	1	3.93	14	ARIZONA	21053	ORM1EG	1	18	21	IMPERIALCA
14004	SAGUARO	1	1.3125	14	ARIZONA	15038	C643T_G1	C3	50	14	ARIZONA
14235	GILABEND	1	17	14	ARIZONA	15047	C643T_G2	C3	50	14	ARIZONA
14235	GILABEND	2	250	14	ARIZONA	15058	C643T_G3	C3	50	14	ARIZONA
19063	WLTNMOHK	1	17	14	ARIZONA	15074	C643T_G4	C3	50	14	ARIZONA
14235	GILABEND	1	17	14	ARIZONA	15078	C643T_G5	C3	50	14	ARIZONA
14235	GILABEND	2	250	14	ARIZONA	15082	C643T_G6	C3	50	14	ARIZONA
14235	GILABEND	1	17	14	ARIZONA	15086	C643T_G7	C3	50	14	ARIZONA
14235	GILABEND	2	250	14	ARIZONA						

10.2 Supporting Material on Base Cases

Table 31. Generation Initial Condition Summary for LSP Base Case

	WECC	CALIFORNIA	DSW	NORTHEAST	NORTHWEST
Pg	43.5	6.4	10.4	2.9	12.4
mc	64.2	11.7	15.0	4.2	17.3
hr	20.7	5.3	4.6	1.3	4.9
nu	800	169	128	91	202
pm	43.6	6.4	10.4	2.9	12.5
mv	65.5	12.4	16.5	4.5	16.1
px	52.1	14.4	14.6	9.3	2.1
mx	52.3	14.5	14.6	9.4	2.1
nx	754	295	72	128	62
pg	95.6	20.8	24.9	12.3	14.6
qg	5.1	-0.7	2.2	0.8	0.8
pl	111.2	33.1	24.3	11.2	19.0
ql	31.7	8.0	7.0	3.5	4.2
pw	20.9	4.4	4.0	2.5	8.4
qw	-1.0	-0.4	0.4	-0.2	-0.7
pv	3.9	3.7	0.2	0.0	0.0
qv	-0.2	-0.2	0.0	0.0	0.0
ps	0.9	0.9	0.0	0.0	0.0
dg	0.0	0.0	0.0	0.0	0.0
nh	800	169	128	91	202
Kt	0.46	0.34	0.44	0.26	0.62

Table 32. Generation Initial Condition Details for LSP Base Case

	Pg	mc	hr	nu	pm	mv	px	mx	nx	pg	qg	pl	ql	pw	qw	pv	qv	ps	dg	nh	Kt
WECC	43.5	64.2	20.7	800	43.6	65.5	52.1	52.3	754	95.6	5.1	111.2	31.7	20.9	-1.0	3.9	-0.2	0.9	0.0	800	0.46
CALIFORNIA	6.4	11.7	5.3	169	6.4	12.4	14.4	14.5	295	20.8	-0.7	33.1	8.0	4.4	-0.4	3.7	-0.2	0.9	0.0	169	0.34
DSW	10.4	15.0	4.6	128	10.4	16.5	14.6	14.6	72	24.9	2.2	24.3	7.0	4.0	0.4	0.2	0.0	0.0	0.0	128	0.44
NORTHEAST	2.9	4.2	1.3	91	2.9	4.5	9.3	9.4	128	12.3	0.8	11.2	3.5	2.5	-0.2	0.0	0.0	0.0	0.0	91	0.26
ALBERTA	2.0	3.3	1.4	67	2.0	3.5	10.1	10.1	80	12.1	1.8	13.4	6.1	1.7	-0.1	0.0	0.0	0.0	0.0	67	0.22
ARIZONA	4.1	6.4	2.2	56	4.1	6.5	10.6	10.6	41	14.7	1.2	10.4	3.3	0.3	0.0	0.1	0.0	0.0	0.0	56	0.37
B.C.HYDRO	8.4	11.1	2.8	118	8.4	10.9	0.8	0.8	107	9.1	0.0	8.7	2.3	0.0	0.0	0.0	0.0	0.0	0.0	118	0.93
EL PASO	0.2	0.3	0.1	3	0.2	0.4	0.4	0.4	7	0.6	0.1	1.1	0.2	0.0	0.0	0.0	0.0	0.0	0.0	3	0.42
IDAHO	1.4	1.9	0.5	29	1.4	1.8	2.7	2.7	36	4.1	0.2	3.2	0.6	0.4	-0.1	0.0	0.0	0.0	0.0	29	0.38
IMPERIALCA	0.2	0.3	0.1	2	0.2	0.3	1.0	1.0	35	1.2	0.0	0.6	0.2	0.0	0.0	0.0	0.0	0.0	0.0	2	0.24
LADWP	1.5	1.8	0.3	9	1.5	1.9	1.0	1.0	2	2.5	0.2	4.6	0.9	0.2	-0.1	0.0	0.0	0.0	0.0	9	0.60
MEXICO-CFE	0.4	0.7	0.3	7	0.4	0.8	0.3	0.3	2	0.7	0.0	1.1	0.5	0.0	0.0	0.0	0.0	0.0	0.0	7	0.69
MONTANA	0.3	0.6	0.3	28	0.3	0.6	2.5	2.5	17	2.8	0.4	1.5	0.5	0.4	-0.1	0.0	0.0	0.0	0.0	28	0.17
NEVADA	1.0	1.4	0.4	7	1.0	1.8	0.5	0.5	3	1.5	0.1	2.5	0.6	0.0	0.0	0.1	0.0	0.0	0.0	7	0.72
NEW MEXICO	0.8	1.4	0.5	6	0.8	1.6	0.3	0.3	2	1.1	0.2	1.7	0.4	1.1	0.0	0.0	0.0	0.0	0.0	6	0.49
NORTHWEST	12.4	17.3	4.9	202	12.5	16.1	2.1	2.1	62	14.6	0.8	19.0	4.2	8.4	-0.7	0.0	0.0	0.0	0.0	202	0.62
PACE	0.8	1.2	0.4	27	0.8	1.4	2.8	2.8	24	3.7	0.3	5.1	1.9	1.4	0.0	0.0	0.0	0.0	0.0	27	0.22
PG AND E	3.4	6.7	3.2	124	3.5	7.0	7.3	7.3	193	10.8	-0.7	12.6	3.6	0.8	0.0	1.9	0.0	0.0	0.0	124	0.40
PSCOLORADO	1.5	1.7	0.2	9	1.5	2.1	1.6	1.6	4	3.1	0.5	5.2	1.3	1.8	0.1	0.0	0.0	0.0	0.0	9	0.34
SANDIEGO	0.1	0.2	0.1	1	0.1	0.2	0.2	0.2	16	0.3	0.0	2.7	0.6	0.3	0.0	0.5	0.1	0.0	0.0	1	0.15
SIERRA	0.4	0.5	0.1	6	0.4	0.6	1.3	1.3	50	1.7	0.0	1.4	0.3	0.3	-0.1	0.0	0.0	0.0	0.0	6	0.23
SOCALIF	1.2	2.8	1.6	33	1.2	2.9	4.9	5.0	49	6.1	-0.2	12.5	2.7	3.2	-0.3	1.3	-0.3	0.9	0.0	33	0.23
FORTISBC	0.6	0.8	0.2	18	0.6	0.8	0.4	0.4	8	1.0	0.2	0.5	0.2	0.0	0.0	0.0	0.0	0.0	0.0	18	0.67
WAPA R.M.	2.7	3.8	1.1	47	2.7	4.2	1.2	1.2	15	3.8	0.1	3.5	1.2	0.7	0.2	0.0	0.0	0.0	0.0	47	0.67
WAPA U.M.	0.1	0.1	0.0	1	0.1	0.1	0.0	0.0	1	0.1	0.0	-0.1	0.1	0.0	0.0	0.0	0.0	0.0	0.0	1	0.94

Table 33. Generation Summary for HS Base Case

	WECC	CALIFORNIA	DSW	NORTHEAST	NORTHWEST
Pg	84.8	26.5	17.0	3.3	24.4
mc	109.1	32.3	21.4	4.3	32.6
hr	24.1	5.7	4.4	1.0	8.1
nu	1135	295	242	91	301
pm	85.0	26.5	17.0	3.3	24.4
mv	112.3	34.8	24.4	4.6	29.8
px	111.7	38.8	36.0	14.7	8.9
mx	111.9	38.8	36.1	14.8	8.9
nx	1251	509	236	145	129
pg	196.5	65.2	53.0	18.1	33.3
qg	22.6	8.8	7.9	1.9	2.3
pl	184.6	67.9	46.9	18.0	27.2
ql	59.2	20.8	14.6	6.0	8.6
pw	5.6	2.1	0.8	1.7	0.0
qw	-0.6	-0.1	-0.2	-0.2	0.0
pv	1.2	1.1	0.1	0.0	0.0
qv	0.1	0.1	0.0	0.0	0.0
ps	0.4	0.4	0.0	0.0	0.0
dg	0.0	0.0	0.0	0.0	0.0
nh	1135	295	242	91	301
Kt	0.48	0.43	0.37	0.21	0.78

Table 34. Generation Initial Condition Details for HS Base Case

	Pg	mc	hr	nu	pm	mv	px	mx	nx	pg	qg	pl	ql	pw	qw	pv	qv	ps	dg	nh	Kt
WECC	84.8	109.1	24.1	1135	85.0	112.3	111.7	111.9	1251	196.5	22.6	184.6	59.2	5.6	-0.6	1.2	0.1	0.4	0.0	1135	0.48
CALIFORNIA	26.5	32.3	5.7	295	26.5	34.8	38.8	38.8	509	65.2	8.8	67.9	20.8	2.1	-0.1	1.1	0.1	0.4	0.0	295	0.43
DSW	17.0	21.4	4.4	242	17.0	24.4	36.0	36.1	236	53.0	7.9	46.9	14.6	0.8	-0.2	0.1	0.0	0.0	0.0	242	0.37
NORTHEAST	3.3	4.3	1.0	91	3.3	4.6	14.7	14.8	145	18.1	1.9	18.0	6.0	1.7	-0.2	0.0	0.0	0.0	0.0	91	0.21
ALBERTA	1.1	1.9	0.9	51	1.1	2.0	10.9	10.9	85	12.0	1.3	12.9	5.7	0.9	-0.1	0.0	0.0	0.0	0.0	51	0.14
ARIZONA	5.7	7.6	1.9	73	5.7	7.9	21.6	21.6	118	27.2	4.1	20.8	6.6	0.2	0.0	0.0	0.0	0.0	0.0	73	0.26
B.C.HYDRO	10.5	13.9	3.3	127	10.6	13.7	0.7	0.7	124	11.2	-0.1	8.2	2.7	0.1	0.0	0.0	0.0	0.0	0.0	127	0.95
EL PASO	1.1	1.3	0.2	14	1.1	1.8	0.5	0.5	4	1.6	0.2	2.3	0.5	0.0	0.0	0.0	0.0	0.0	0.0	14	0.69
IDAHO	1.2	1.6	0.4	28	1.2	1.6	3.0	3.0	29	4.2	0.3	3.9	1.3	0.1	0.0	0.0	0.0	0.0	0.0	28	0.34
IMPERIALCA	0.4	0.6	0.2	9	0.4	0.7	1.1	1.1	34	1.5	0.1	0.3	0.2	0.0	0.0	0.0	0.0	0.0	0.0	9	0.36
LADWP	3.8	4.6	0.8	25	3.8	5.1	2.3	2.3	14	6.1	1.2	7.2	2.4	0.2	0.0	0.0	0.0	0.0	0.0	25	0.65
MEXICO-CFE	1.5	2.0	0.5	11	1.5	2.2	1.2	1.2	14	2.7	0.3	2.6	0.7	0.0	0.0	0.0	0.0	0.0	0.0	11	0.63
MONTANA	0.5	0.7	0.3	30	0.5	0.8	2.7	2.7	18	3.2	0.6	1.9	0.6	0.1	0.0	0.0	0.0	0.0	0.0	30	0.21
NEVADA	1.4	1.8	0.4	14	1.4	2.3	4.7	4.7	52	6.1	1.6	6.8	2.1	0.0	0.0	0.1	0.0	0.0	0.0	14	0.27
NEW MEXICO	1.5	1.6	0.1	9	1.5	1.8	2.0	2.0	14	3.5	0.3	3.1	0.6	0.0	0.0	0.0	0.0	0.0	0.0	9	0.44
NORTHWEST	24.4	32.6	8.1	301	24.4	29.8	8.9	8.9	129	33.3	2.3	27.2	8.6	0.0	0.0	0.0	0.0	0.0	0.0	301	0.78
PACE	0.9	1.1	0.2	23	0.9	1.3	7.4	7.4	51	8.3	0.8	9.9	3.3	1.2	0.0	0.0	0.0	0.0	0.0	23	0.11
PG AND E	13.1	16.2	3.1	169	13.2	17.2	17.8	17.8	322	30.9	2.9	29.0	9.7	0.8	-0.1	0.7	0.1	0.0	0.0	169	0.46
PSCOLORADO	3.7	4.9	1.2	75	3.7	5.7	4.0	4.0	21	7.8	1.1	8.1	2.8	0.4	-0.2	0.1	0.0	0.0	0.0	75	0.52
SANDIEGO	2.1	2.5	0.4	31	2.1	2.9	1.5	1.5	24	3.6	0.3	5.5	1.5	0.3	0.0	0.4	0.0	0.0	0.0	31	0.52
SIERRA	0.6	0.7	0.0	8	0.6	0.8	1.7	1.7	47	2.3	0.1	2.3	0.6	0.3	-0.1	0.0	0.0	0.0	0.0	8	0.25
SOCALIF	7.0	8.3	1.3	61	7.0	8.9	16.0	16.0	115	23.0	4.2	25.9	7.0	0.8	0.0	0.0	0.0	0.4	0.0	61	0.33
FORTISBC	0.6	0.8	0.2	17	0.6	0.8	0.5	0.5	9	1.1	0.2	0.9	0.3	0.0	0.0	0.0	0.0	0.0	0.0	17	0.59
WAPA R.M.	3.6	4.2	0.6	57	3.6	4.9	3.2	3.2	27	6.8	0.5	5.8	2.1	0.0	0.0	0.0	0.0	0.0	0.0	57	0.56
WAPA U.M.	0.1	0.1	0.0	2	0.1	0.1	0.0	0.0	0	0.1	0.0	0.0	0.1	0.0	0.0	0.0	0.0	0.0	0.0	2	1.00

Supporting Material on Complex Load Model

The blocking functions, *vrflag* for voltage and *frflag* for frequency, allow for the inverters to be *blocked* temporarily when the voltage drops, or to *trip*, i.e., not recover after the voltage or frequency returns to within the allowed region. The trapezoidal shape for the two functions allows for the user to account for the distributed nature of the resources and for the non-uniformity of tripping. Further, the fraction of devices that block vs trip can be set anywhere between 0 and 1.

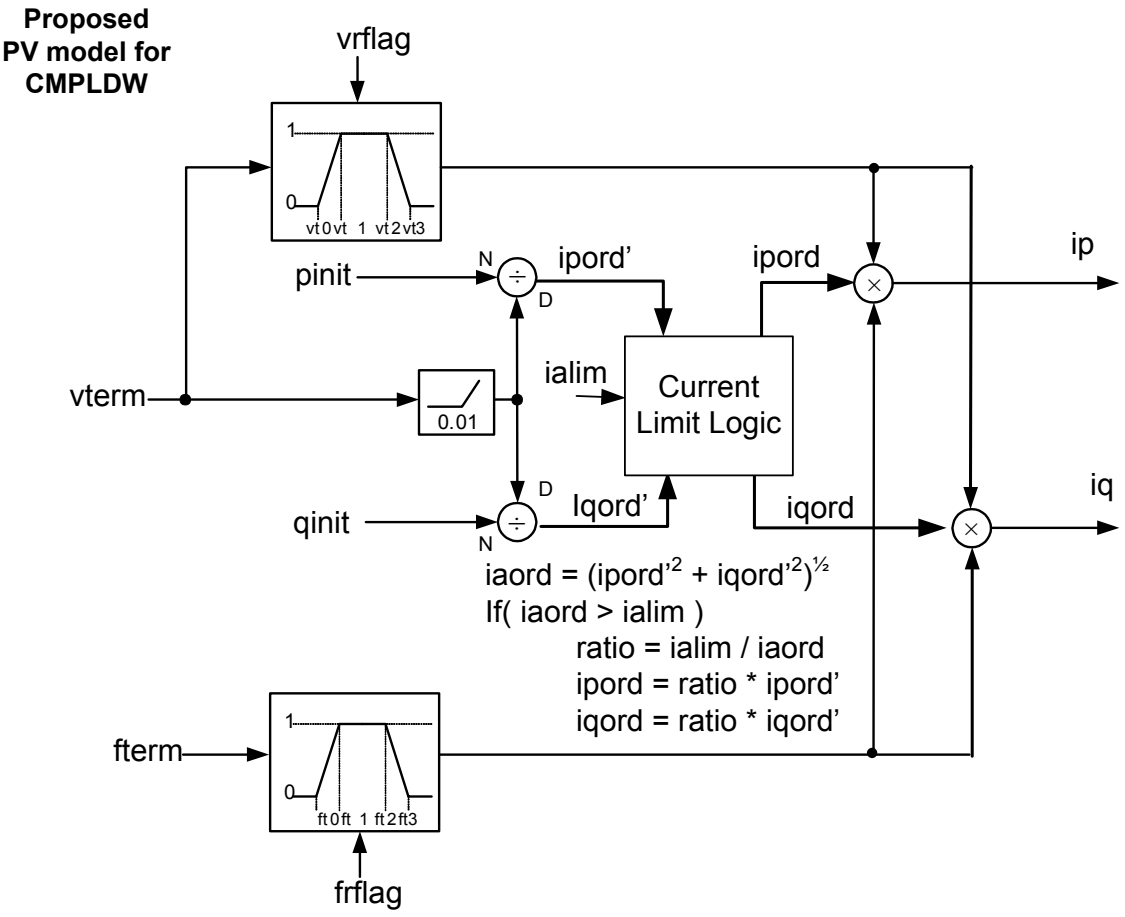

Figure 84. Composite load model – DG tripping/blocking logic.

10.3 Supporting Material for Performance and Monitoring Metrics

Table 35. Transient Stability Performance Requirements

Disturbance Class	Outage Frequency Associated with Performance Category	Transient Voltage Dip	Minimum Transient Frequency Standard	Post Transient Voltage Deviation Standard
A	NA	NERC	NERC	NERC
B	≥ 0.33	Not to exceed 25% at load buses or 30% at non-load buses. Not to exceed 20% for more than 20 cycles at load buses.	Not below 59.6 Hz for 6 cycles or more at a load bus.	Not to exceed 5% at any bus
C	0.033-0.33	Not to exceed 30% at any bus. Not to exceed 20% for more than 40 cycles at load buses.	Not below 59.0 Hz for 6 cycles or more at a load bus.	Not to exceed 10% at any bus
D	<0.033	NERC	NERC	NERC

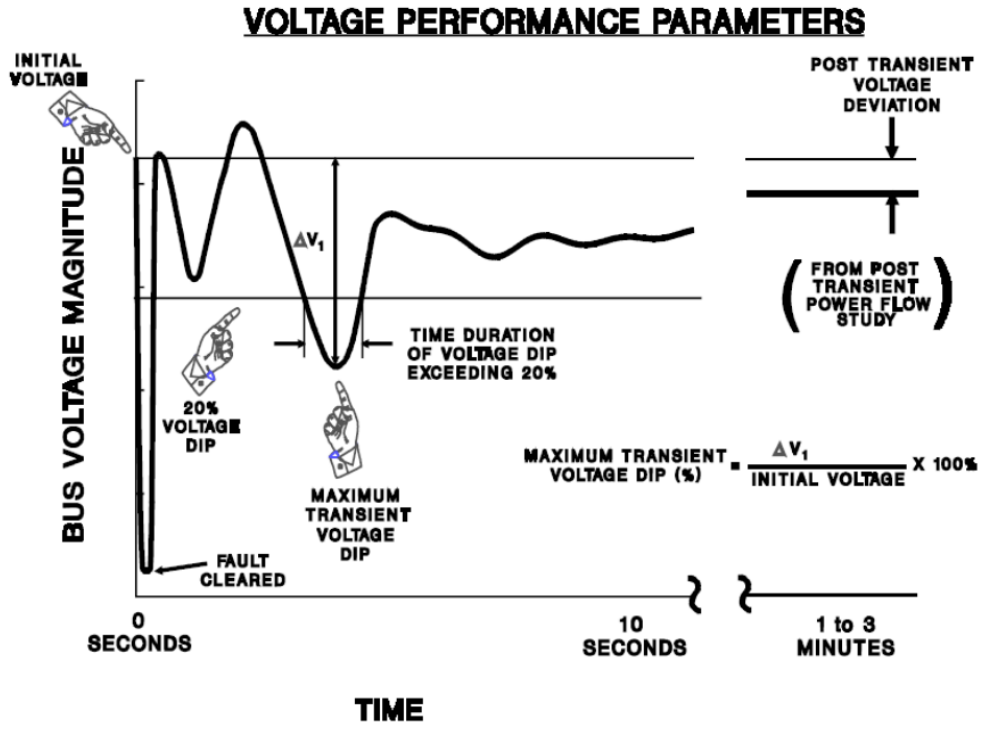

Figure 85. WECC reliability criteria.

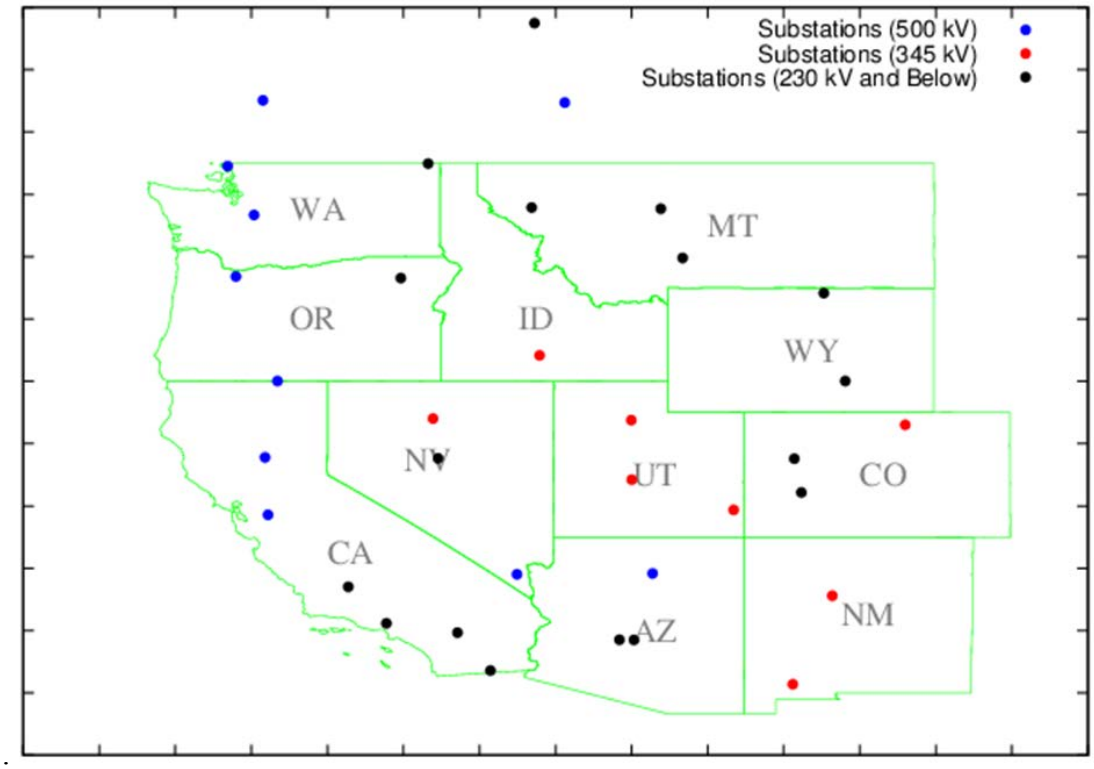

Figure 86. WECC key bus locations.

Table 36. WECC Key Buses

Bus #	Bus Name	Sub Name	kV	Bus #	Bus Name	Sub Name	kV
40323	CUSTER W	Custer	500	40145	BOUNDARY	Boundary	230
50704	KLY500	Kelly Lake	500	79021	CURECANT	Curecanti	230
54158	LANGDON2	Langdon	500	24804	DEVERS	Devers	230
40687	MALIN	Malin	500	62071	GT FALLS	Great Falls	230
26048	MCCULLGH	McCullough	500	40551	HOT SPR	Hot Springs	230
14002	MOENKOPI	Moenkopi	500	22356	IMPRLVLY	Imperial Valley	230
40809	OSTRNDER	Ostrander	500	40621	LAGRANDE	La Grande	230
40869	RAVER	Raver	500	30970	MIDWAY	Midway Peaker	230
30015	TABLE MT	Table Mt.	500	65975	MINERS	Miners	230
30040	TESLA	Tesla Peaker	500	14221	PNPKAPS	Pinnacle Peak APS	230
73012	AULT	Ault	345	79057	RIFLE CU	Rifle	230
11093	LUNA	Luna	345	66335	SHERIDAN	Sheridan	230
60235	MIDPOINT	Midpoint	345	26078	TOLUCA	Toluca	230
66225	PINTO	Pinto	345	54135	SUNDANM9	Sundance	240
66340	SIGURD	Sigurd	345	14231	WESTWING	Westwing	230
66510	TERMINAL	Salt Lake Ci	345	62019	WILSALL	Wilsall	230
64130	VALMY	North almy	345	62114	RATTLE S	Rattlesnake	100
10369	WESTMESA	West Mesa	345	66278	RANGELY	Rangley	138
64006	AUSTIN	Austin	230	64107	SUMMIT 1	Summit	120

10.4 Supporting Material on Wind and Solar Siting

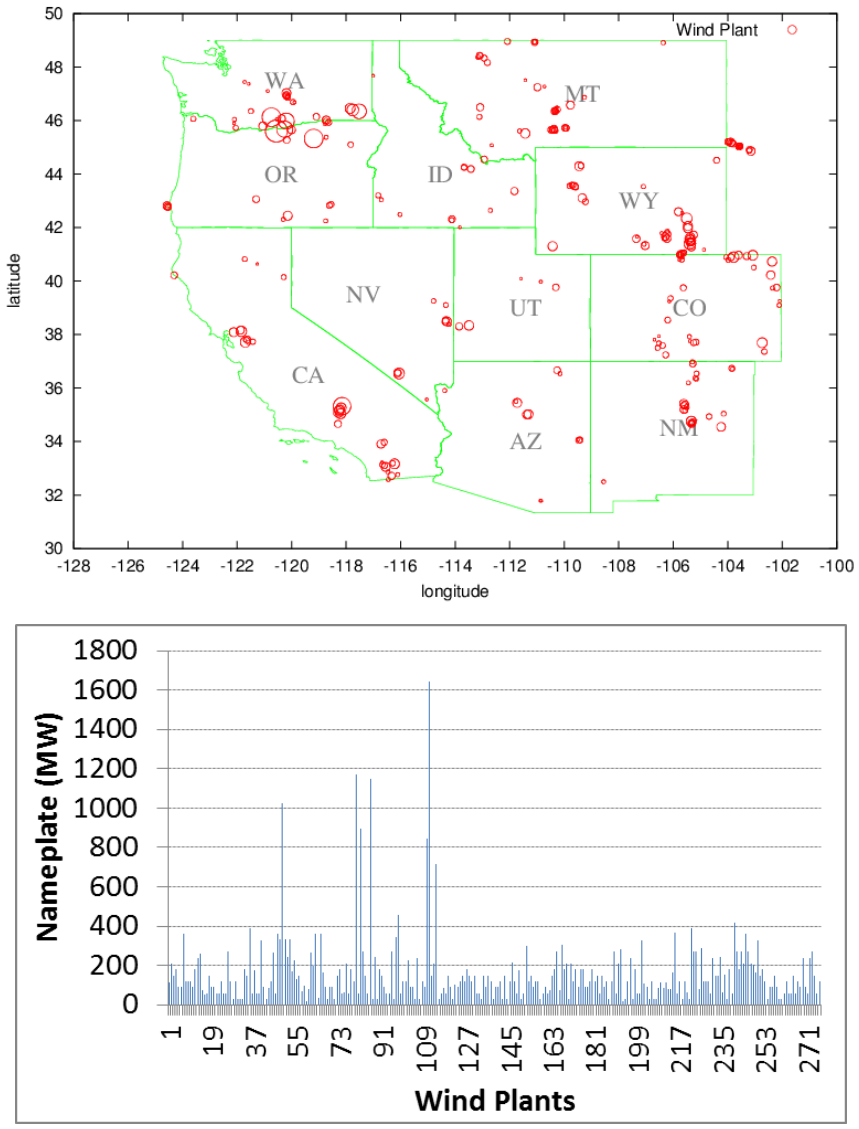

Figure 87. Wind plant sites and ratings from WWSIS-2 raw data.

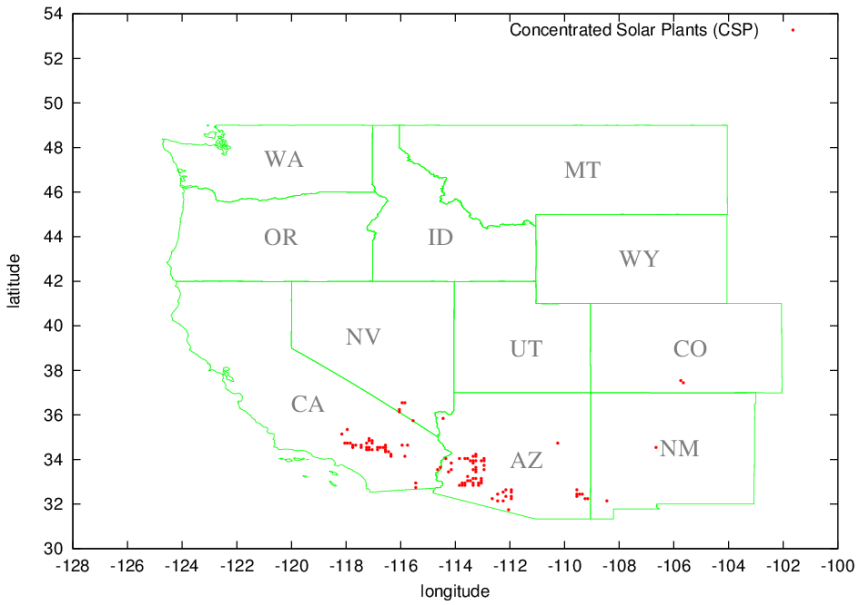

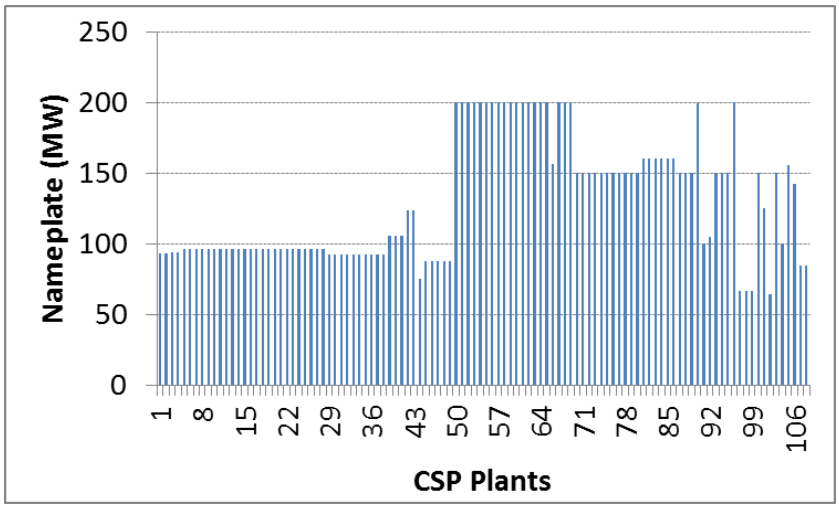

Figure 88. CSP sites and ratings from WWSIS-2 raw data.

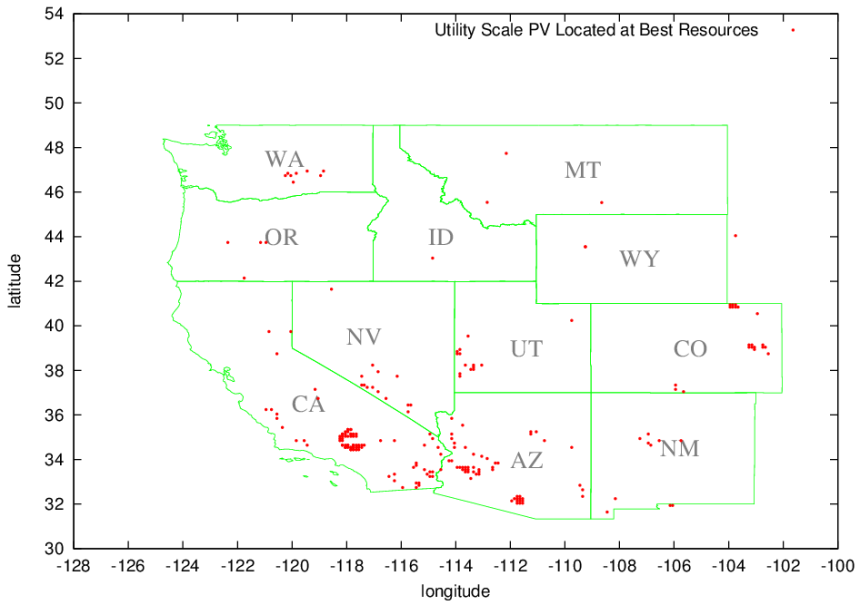

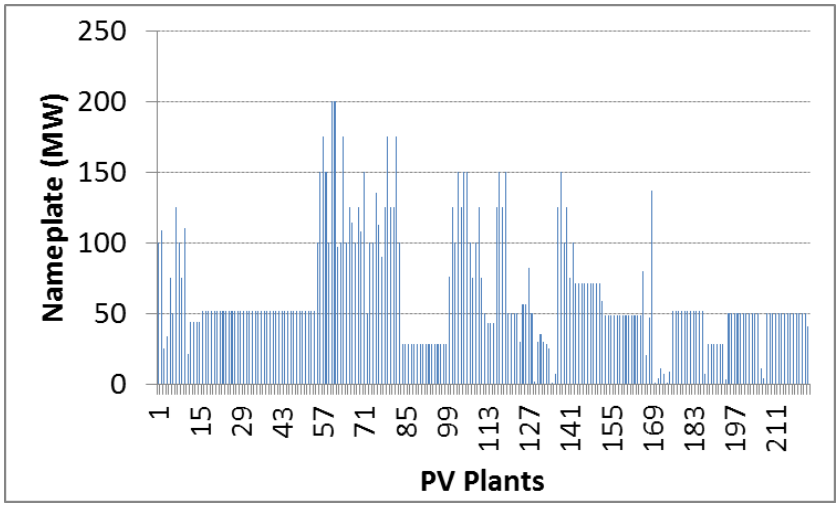

Figure 89. U.S. PV near best resources from WWSIS-2 raw data.

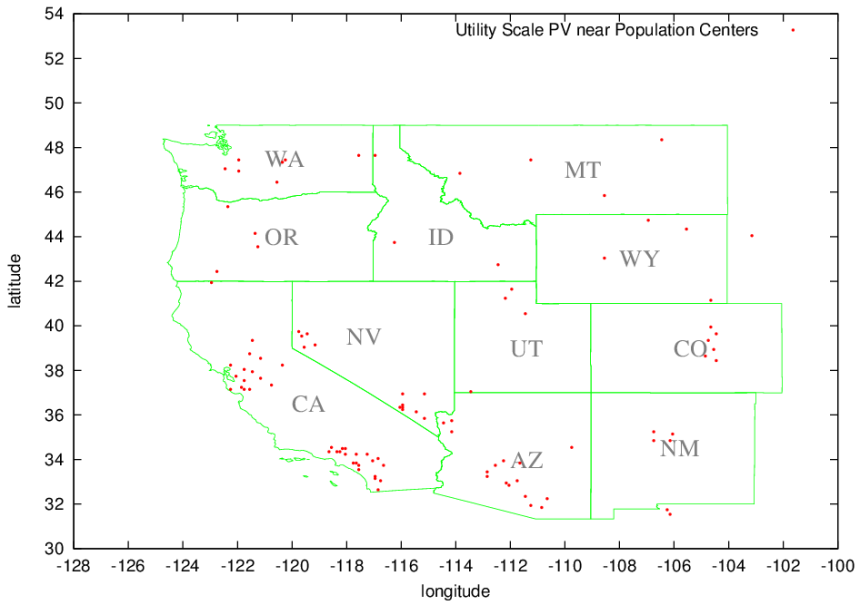

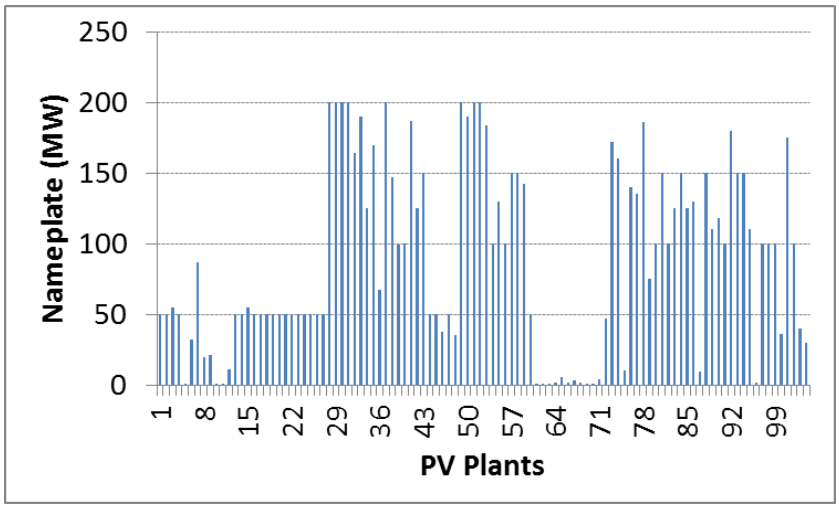

Figure 90. U.S. PV near population centers from WWSIS-2 raw data.

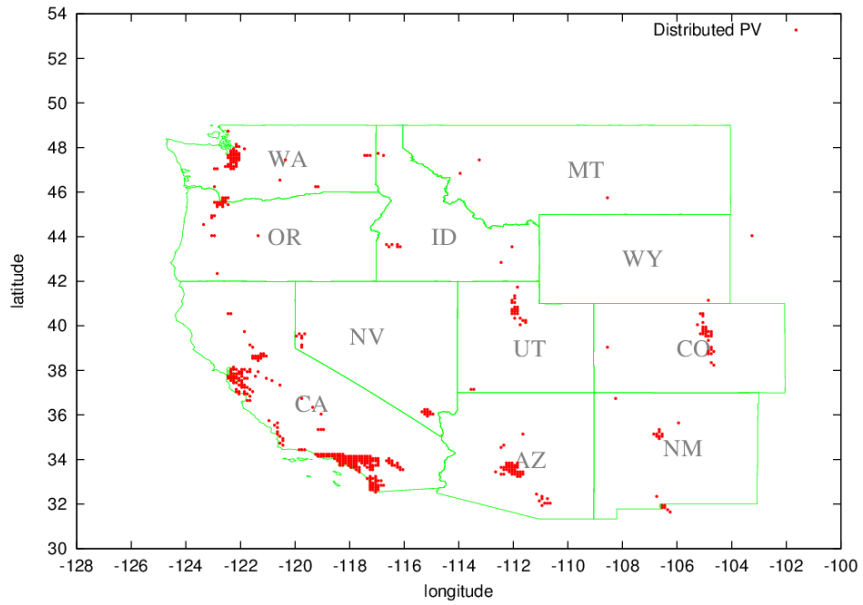

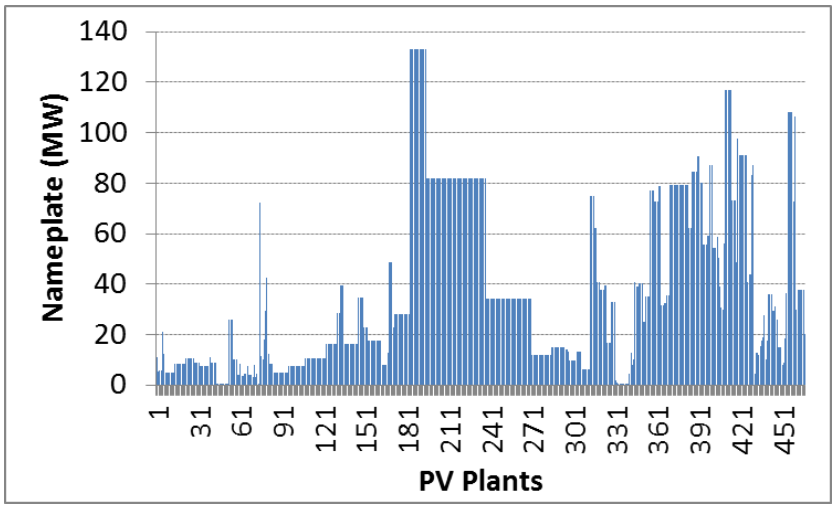

Figure 91. Distributed PV sites and ratings from WWSIS-2 raw data.

10.5 Supporting Material on Recommitment and Re-Dispatch

Supporting Material on Recommitment and Re-Dispatch Method

Table 37. LSP PLEXOS Sample Windows

March 23	10:35 – 11:45
April 1	9:10 – 15:40
April 8	9:45 – 18:10
April 9	6:50 – 13:45
April 13	12:55
April 16	10:55 – 14:10
April 17	12:45 – 14:50
April 20	7:10 – 17:35
April 21	8:20 – 12:00

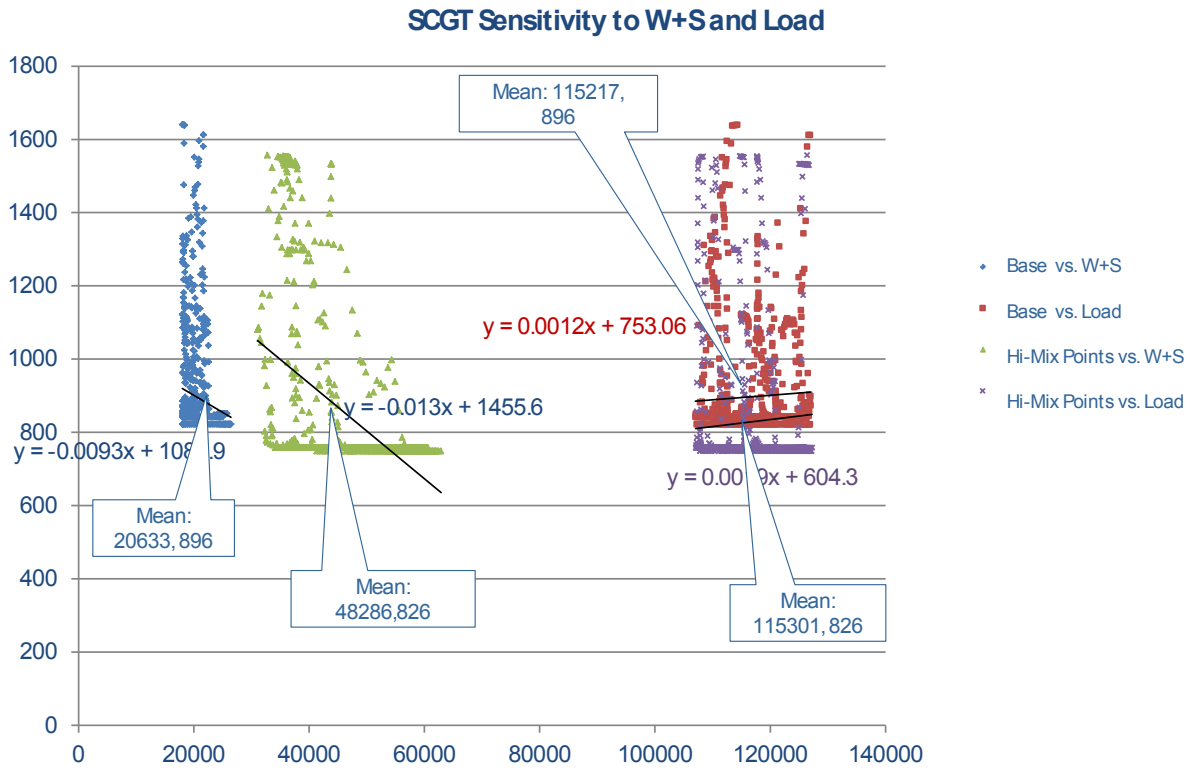

Figure 92. Simple-cycle gas turbines dispatch – LSP window.

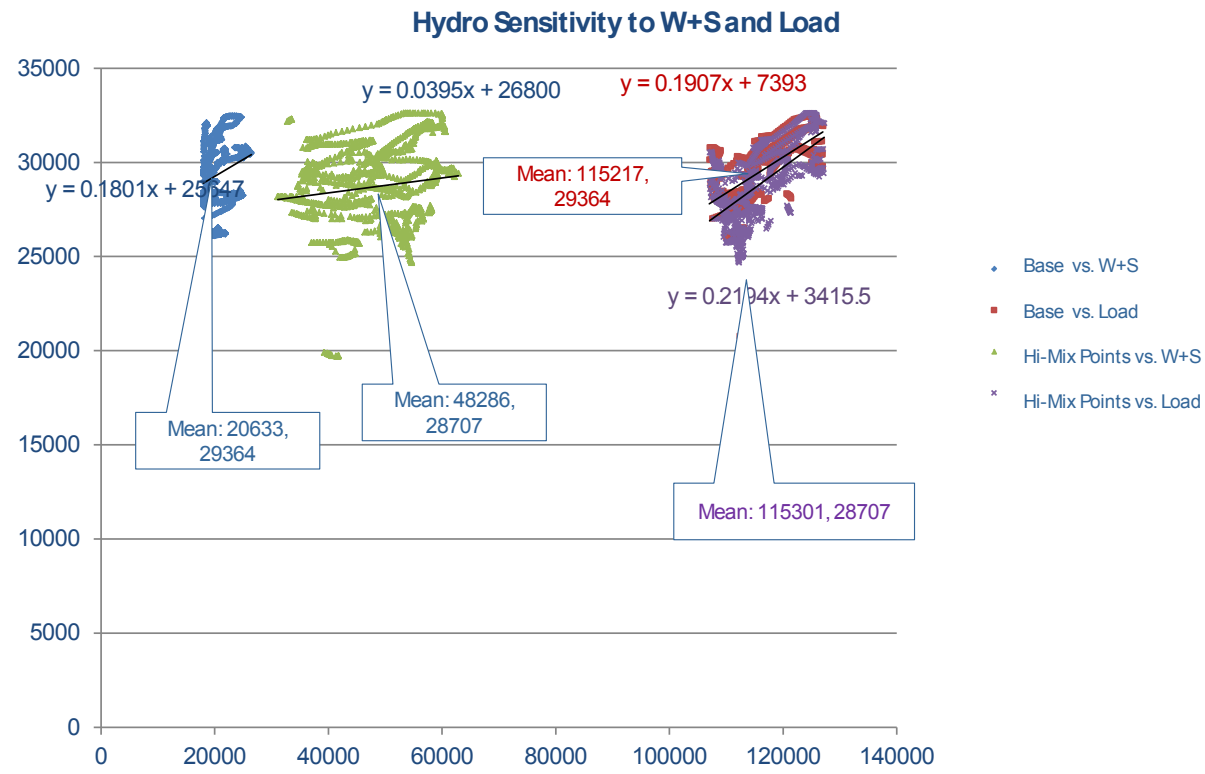

Figure 93. Hydro dispatch – LSP window.

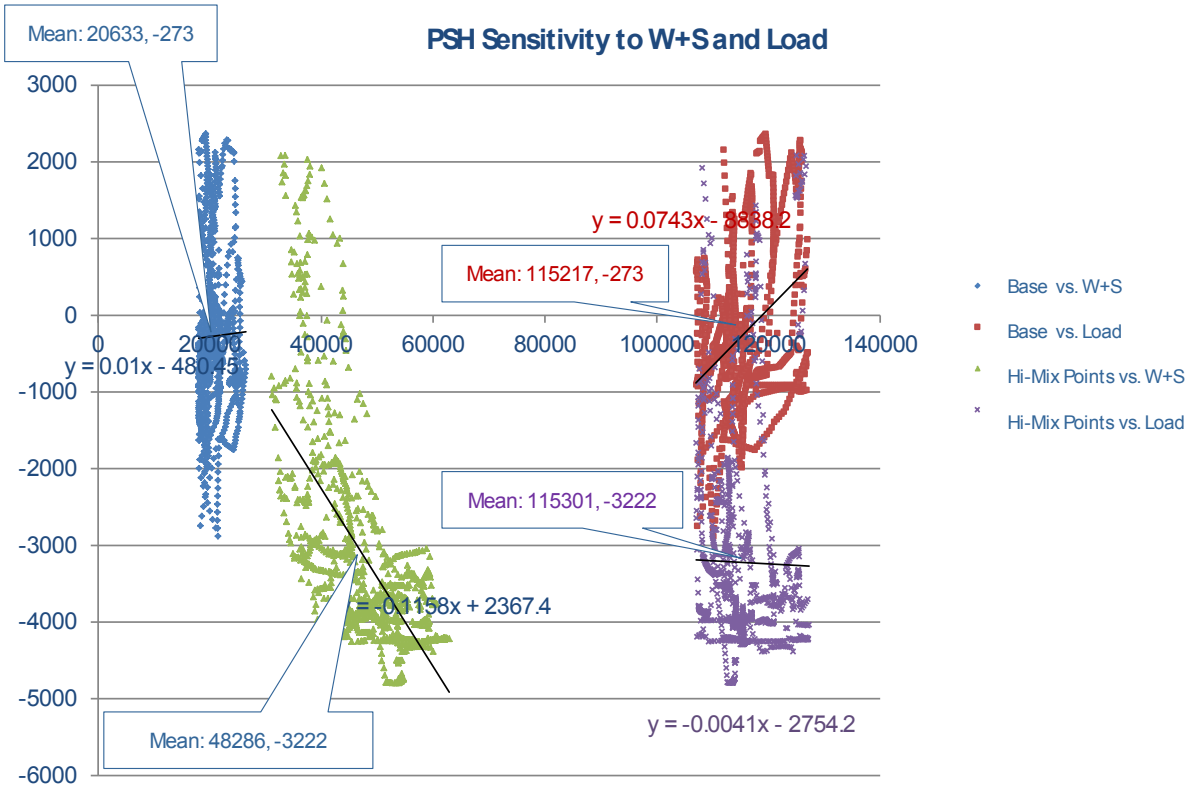

Figure 94. Pumped-storage hydro dispatch – LSP window.

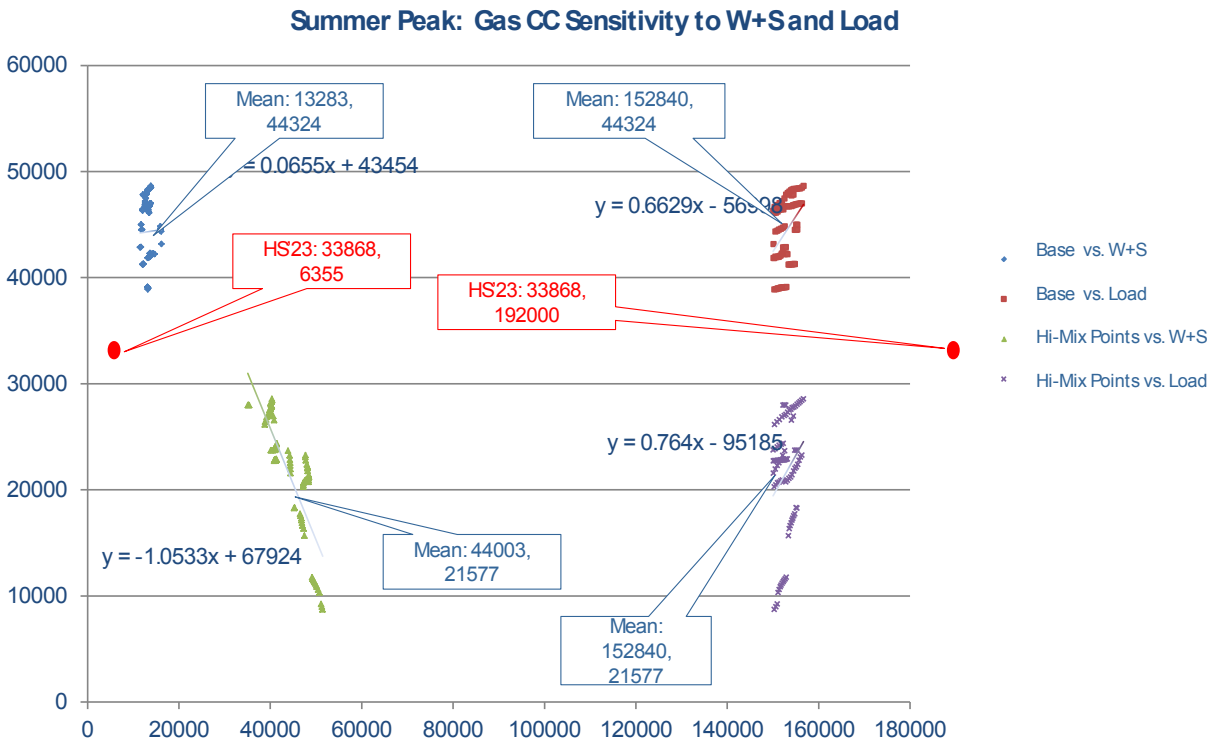

Figure 95. Combined-cycle plants – HS window.

Table 38. HS PLEXOS Sample Windows

July 16	13:45 – 14:40	12 samples
July 17	13:55 – 14:30	8 samples
July 21	13:25 – 13:30	2 samples
July 30	13:20 – 13:3	3 samples
August 11	14:05 – 14:15	3 samples
August 12	12:20 – 13:10	8 samples
August 13	11:35 – 12:55	17 samples
August 14	13:00 – 14:20	16 samples
August 25	12:55 – 13:25	7 samples
August 26	12:05 – 13:35	19 samples

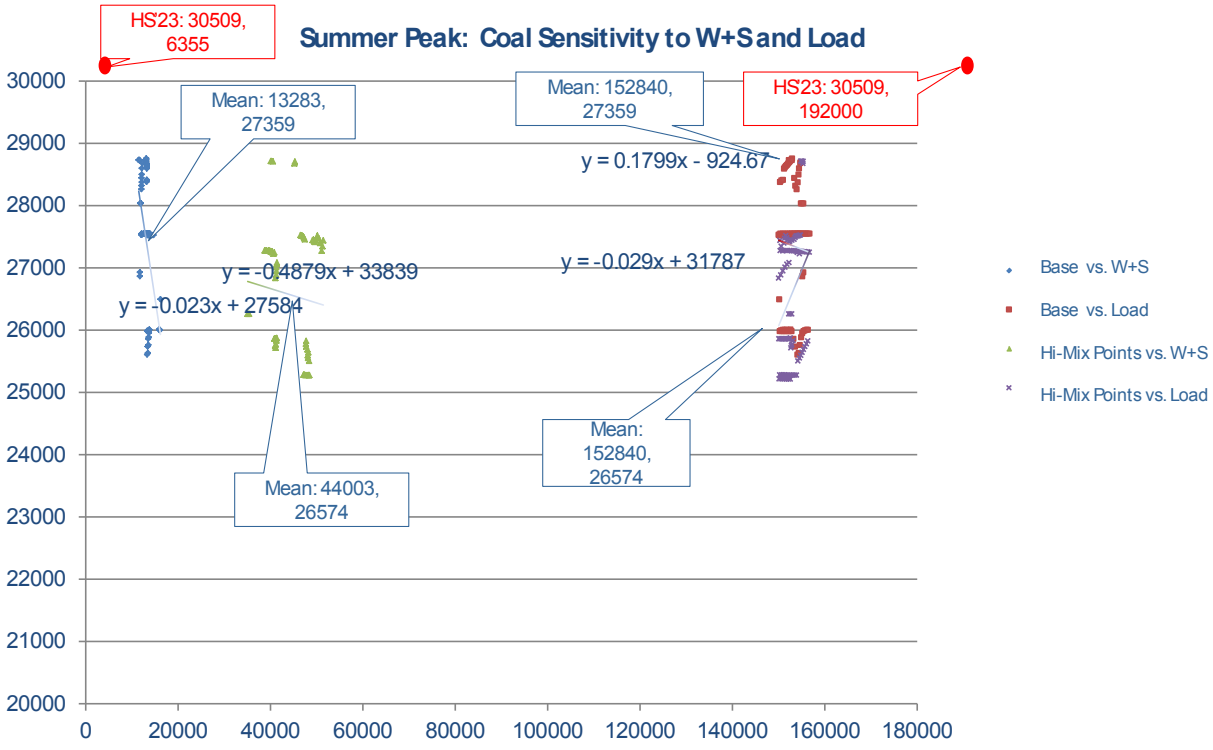

Figure 96. Coal plants – HS window.

Table 39. Adding Renewable Capacity Including WWSIS-2 to LSP Base Case

	LSP Base Case			WWSIS2-HiMix			LSP Hi-Mix Case			
Area	CSP	PV	Wind	CSP	PV	Wind	CSP	PV	DG	Wind
ALBERTA	0	0	2707	0	0	0	0	0	0	2707
ARIZONA	0	971	175	7654	5120	1440	6879	4923	3655	1435
B.C.HYDRO	0	0	108	0	0	0	0	0	0	108
EL PASO	0	0	0	142	343	50	142	343	368	50
IDAHO	0	0	643	0	0	569	0	0	0	643
IMPERIALCA	0	0	0	188	611	917	188	611	71	917
LADWP	0	0	576	1043	913	0	1043	913	1961	576
MEXICO-CFE	0	0	0	0	0	294	0	0	15	0
MONTANA	0	0	707	0	27	3988	0	11	21	3975
NEVADA	0	64	0	229	642	0	229	556	285	0
NEW MEXICO	0	100	1726	156	1160	3084	156	1260	758	3108
NORTHWEST	0	59	8680	0	817	11642	0	869	500	11655
PACE	0	0	2384	0	409	4082	0	390	1126	4111
PG AND E	0	3232	2399	0	1740	1799	0	3232	1474	2399
PSCOLORADO	0	79	2134	169	937	1720	169	1016	547	2134
SANDIEGO	0	516	712	0	275	0	0	516	421	712
SIERRA	0	0	432	0	1511	821	0	1504	432	777
SOCALIF	1436	2139	4497	2813	6118	3149	2814	5913	4741	4497
FORTISBC	0	0	0	0	0	0	0	0	0	0
WAPA R.M.	0	4	739	0	696	8149	0	690	594	8136
WAPA U.M.	0	0	0	0	1	60	0	0	0	60
Total	1436	7164	28616	12393	21322	41762	11618	22747	16969	47999

Table 40. Incremental Renewable Dispatch – Sample 31775

TEPCC (WWSIS II) @ 31775

Area #	CSP	WWSIS PV	WWSIS_wind
54			
14	515	1017	3261
50			
11	0	0	2
60		0	127
21	0	143	364
26	849	1123	0
20			
62	0	0	147
18	16	16	0
10	167	302	31
40	0	0	3960
65	0	0	1065
30	0	0	14
70	186	497	299
22	0	0	0
64	0	38	74
24	1098	2722	3421
52			
73	0	521	655
63		0	0
-1	34		
Total	2865	6379	13418

HiMix @ 31775

Area #	CSP	WWSIS PV	DG ratio	DG	PV	WWSIS_wind
54						
14	6375	3532	0.42	1471	2061	560
50						
11	143	428	0.47	202	227	2
60		0			0	150
21	124	309	0.10	32	277	337
26	493	1267	0.68	864	403	0
20						
62	0	5	0.44	2	3	1593
18	113	542	0.31	166	376	0
10	162	550	0.40	217	333	27
40	0	538	0.38	204	334	4551
65	0	326	0.73	239	87	2772
30	0	1274	0.46	584	690	30
70	178	962	0.37	355	608	594
22	0	205	0.57	116	89	0
64	0	936	0.22	208	728	661
24	1378	5238	0.44	2287	2951	2746
52						
73	0	792	0.46	364	428	3346
63		0	0.00	0	0	27
-1	644					
Total	9610	16905		7312	9592	17395

Difference

Area #	CSP	WWSIS PV	DG	PV	Wind
54					
14	5860	2515	1471	1044	-2701
50					
11	143	428	202	227	0
60	0	0	0	0	23
21	124	166	32	134	-26
26	-356	144	864	-720	0
20					
62	0	5	2	3	1446
18	97	526	166	360	0
10	-5	248	217	31	-4
40	0	538	204	334	591
65	0	326	239	87	1707
30	0	1274	584	690	16
70	-8	465	355	110	295
22	0	205	116	89	0
64	0	898	208	690	587
24	280	2516	2287	229	-676
52					
73	0	271	364	-93	2691
63	0	0	0	0	27
-1	609				
Total	6746	10526	7312	3214	3977

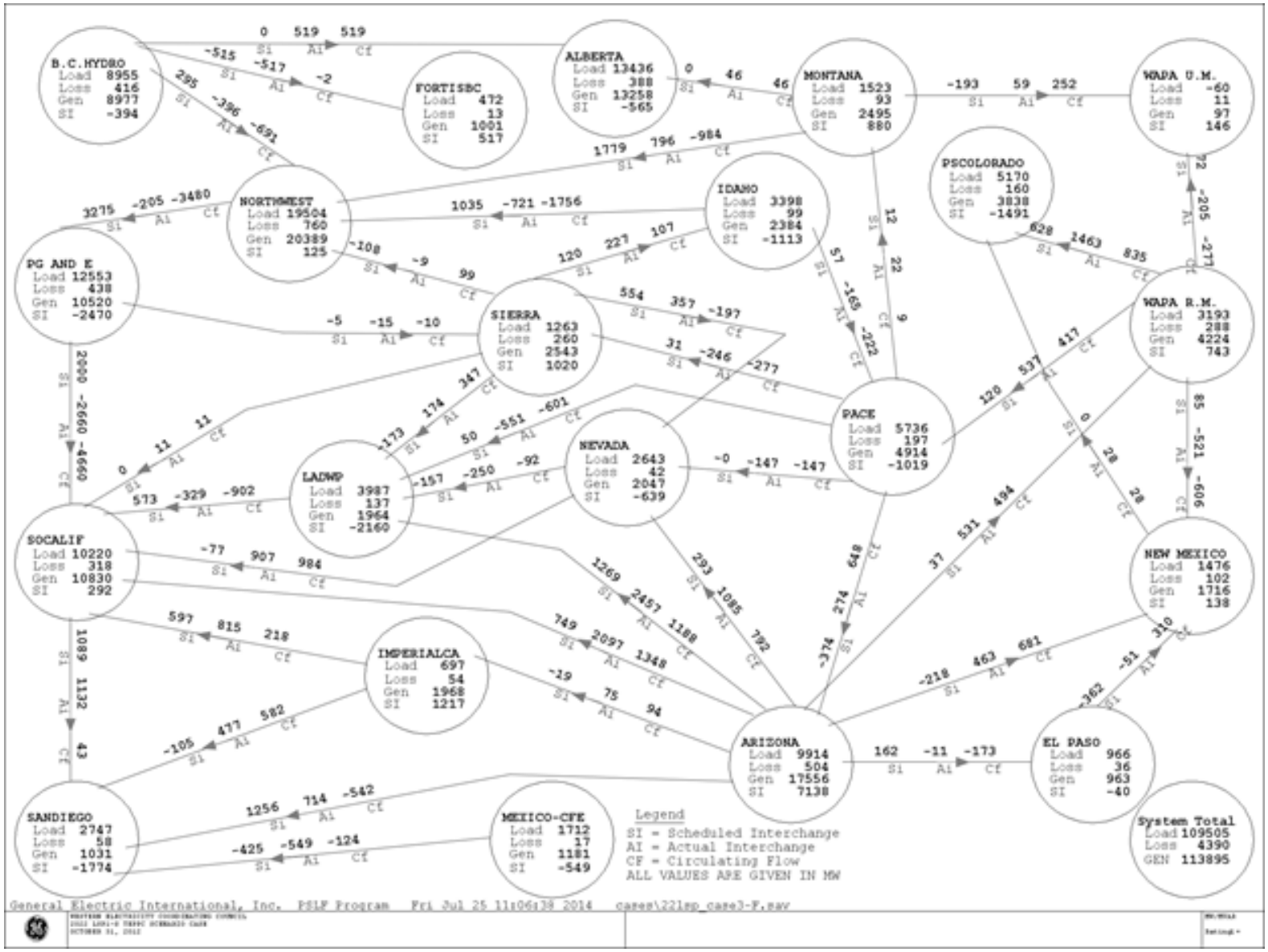

Figure 97. LSP Hi-Mix case bubble.

Table 41. Added Renewable Capacity Including WWSIS-2 for HS Hi-Mix Case

	HS Base Case			WWSIS2-HiMix			HS Hi-Mix Case			
Area	CSP	PV	Wind	CSP	PV	Wind	CSP	PV	DG	Wind
ALBERTA	0	0	1061	0	0	0	0	0	0	1061
ARIZONA	0	700	227	7654	5120	1440	7654	5202	3655	1457
B.C.HYDRO	0	0	237	0	0	0	0	0	0	237
EL PASO	0	47	0	142	343	50	142	350	305	50
IDAHO	0	0	407	0	0	569	0	0	0	564
IMPERIALCA	0	0	0	188	611	917	188	611	71	917
LADWP	270	0	574	851	913	0	837	913	1961	574
MEXICO-CFE	0	0	0	0	0	294	0	0	15	294
MONTANA	0	0	364	0	27	3988	0	27	21	3989
NEVADA	0	64	0	229	642	0	229	656	324	0
NEW MEXICO	0	27	396	156	1160	3084	156	1157	758	3120
NORTHWEST	0	0	0	0	1607	11642	0	1607	500	11642
PACE	0	0	2309	0	409	4082	0	409	1126	4032
PG AND E	0	2570	1033	0	1740	1799	0	2570	1474	1758
PSCOLORADO	0	79	2134	169	937	1830	169	960	547	2134
SANDIEGO	0	516	1562	0	275	0	0	516	357	1562
SIERRA	0	0	352	0	1511	821	0	1511	432	802
SOCALIF	822	49	887	2813	6118	3149	2825	6100	4741	3147
FORTISBC	0	0	0	0	0	0	0	0	0	0
WAPA R.M.	0	0	139	0	696	8149	0	696	594	8137
WAPA U.M.	0	0	0	0	1	60	0	0	0	60
Total	1092	4052	11680	12201	22112	41871	12199	23286	16882	45535

Table 42. PLEXOS Case – Renewable Summary for HS Hi-Mix Case

TEPCC WWSIS II @68417

Area name	Area #	CSP	WWSIS PV	WWSIS_wind
ALBERTA	54			
ARIZONA	14	351	389	326
BC HYDRO	50			
EL PASO	11			21
IDAHO	60			120
IMPERIALICA	21		155	32
LADWP	26	1147	259	
MEXICO-CFE	20			5
MONTANA	62			64
NEVADA	18	116		
NEW MEXICO	10	53	92	4
NORTHWEST	40			6064
PACE	65			226
PG&E	30			28
PSCOLORADO	70	186	265	37
SAN DIEGO	22			
SIERRA	64		119	31
SOCALIF	24	2396	1825	89
FORTISBC	52			
WAPA R.M.	73		480	363
WAPA U.M.	63			
-1	-1	251	506	72
Total		4500	4090	7480

HiMix @68417

Area #	CSP	WWSIS PV	DG ratio	DG	PV	WWSIS_wind
54						
14	3182	4608	0.42	1919	2689	111
50						
11		359	0.47	169	190	21
60		0			0	167
21	187	432	0.10	45	387	27
26	1147	1770	0.68	1207	563	
20		10				5
62		25	0.44	11	14	762
18	197	464	0.31	142	321	
10		631	0.40	249	382	106
40		770	0.38	292	477	6908
65		838	0.73	615	223	1448
30		2175	0.46	997	1177	102
70	186	827	0.37	305	522	60
22		437	0.57	247	190	
64		1372	0.22	305	1067	95
24	3095	6963	0.44	3040	3923	73
52						
73		720	0.46	331	389	873
63		1	0.00	0	1	0
-1	1508	1476				132
	9502	23877		9875	12516	10890

Difference

Area #	CSP	WWSIS PV	DG	PV	Wind
54					
14	2831	4219	1919	2300	-215
50					
11	0	359	169	190	0
60	0	0	0	0	47
21	187	277	45	232	-5
26	0	1510	1207	304	0
20		10			
62	0	25	11	14	698
18	81	464	142	321	0
10	-53	540	249	290	102
40	0	770	292	477	844
65	0	838	615	223	1222
30	0	2175	997	1177	74
70	0	562	305	257	23
22	0	437	247	190	0
64	0	1253	305	948	64
24	698	5137	3040	2097	-16
52					
73	0	240	331	-92	510
63	0	1	0	1	0
-1	1256				
Total	5001	18817	9875	8932	3349

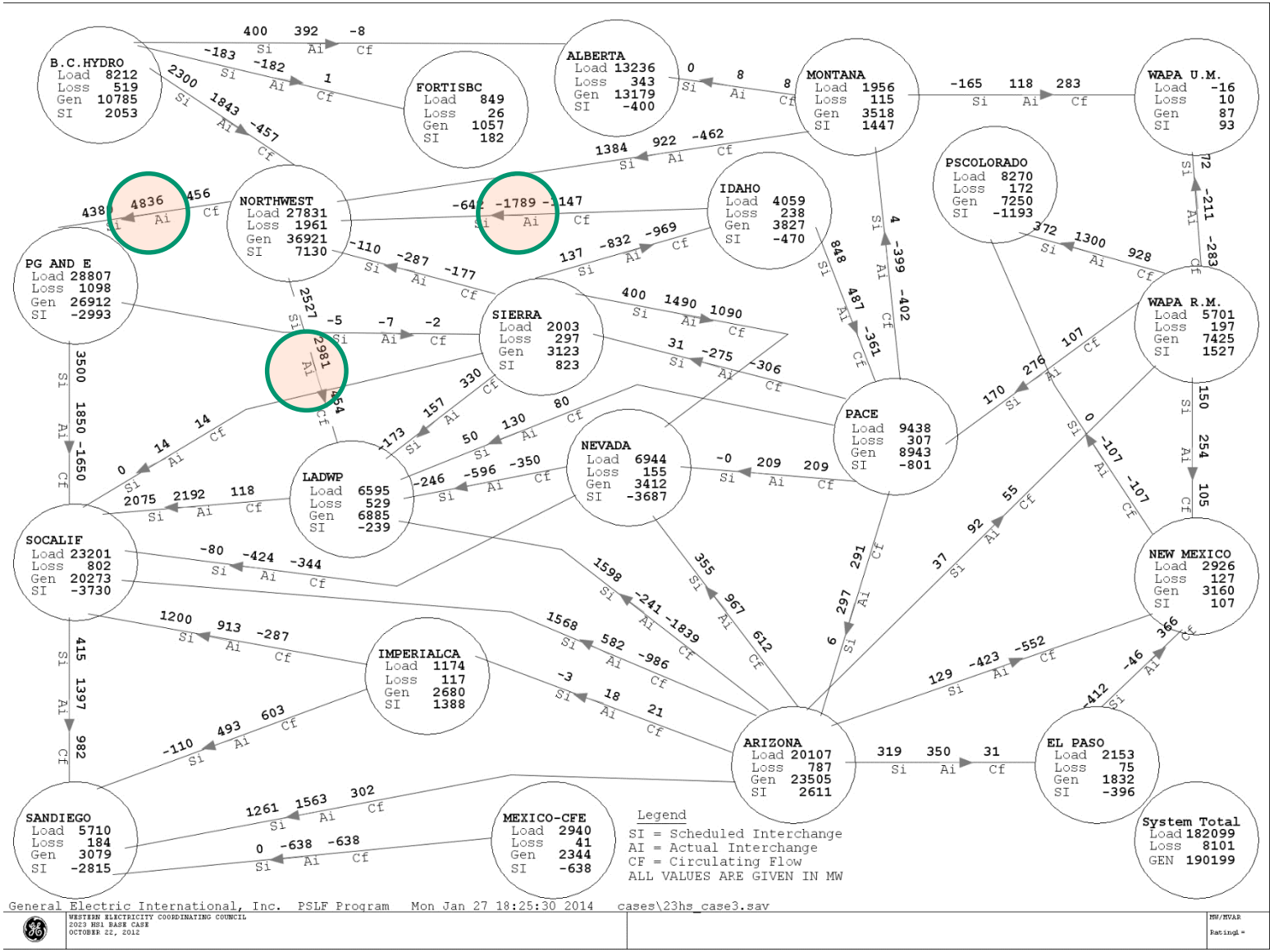

Figure 98. HS Hi-Mix case bubble.

Supporting Material on Dynamic Initial Conditions of Hi-Mix cases

Table 43. LSP Hi-Mix Case – Initial Condition Metrics

	WECC	CALIFORNIA	DSW	NORTHEAST	NORTHWEST
Pg	34.4	5.4	5.4	2.7	9.5
mc	56.3	10.7	8.7	3.9	17.2
hr	21.9	5.3	3.3	1.2	7.7
nu	768	167	103	89	200
pm	34.4	5.4	5.5	2.7	9.5
mv	56.7	11.4	9.5	4.1	16.0
px	39.8	11.2	12.9	2.7	2.1
mx	40.3	11.3	13.3	2.7	2.1
nx	740	284	93	107	62
ps	74.2	16.6	18.4	5.5	11.7
qs	3.6	-0.2	2.7	0.6	-1.2
pl	109.3	32.0	23.5	11.1	19.1
ql	29.8	7.6	5.5	3.3	4.3
pw	27.0	4.7	6.9	5.3	8.4
qw	-2.0	-0.1	0.3	-0.6	-1.3
pv	10.2	5.8	3.3	0.8	0.3
qv	-1.3	-0.3	-0.9	0.1	-0.2
ps	8.4	1.5	7.0	0.0	0.0
dg	7.0	3.7	2.6	0.4	0.2
nh	768	167	103	89	200
Kt	0.42	0.33	0.27	0.31	0.61

Table 44. Details of LSP Hi-Mix Case Dynamic Initial Conditions

	Pg	mc	hr	nu	pm	mv	px	mx	nx	ps	qs	pl	ql	pw	qw	pv	qv	ps	dg	nh	Kt
WECC	34.4	56.3	21.9	768	34.4	56.7	39.8	40.3	740	74.2	3.6	109.3	29.8	27.0	-2.0	10.2	-1.3	8.4	7.0	768	0.42
CALIFORNIA	5.4	10.7	5.3	167	5.4	11.4	11.2	11.3	284	16.6	-0.2	32.0	7.6	4.7	-0.1	5.8	-0.3	1.5	3.7	167	0.33
DSW	5.4	8.7	3.3	103	5.5	9.5	12.9	13.3	93	18.4	2.7	23.5	5.5	6.9	0.3	3.3	-0.9	7.0	2.6	103	0.27
NORTHEAST	2.7	3.9	1.2	89	2.7	4.1	2.7	2.7	107	5.5	0.6	11.1	3.3	5.3	-0.6	0.8	0.1	0.0	0.4	89	0.31
ALBERTA	2.0	3.3	1.4	67	2.0	3.5	9.6	9.6	78	11.6	1.7	13.4	6.1	1.7	-0.3	0.0	0.0	0.0	0.0	67	0.23
ARIZONA	3.3	5.4	2.1	51	3.3	5.3	11.2	11.5	70	14.5	1.9	10.1	2.9	0.8	-0.1	1.4	-0.5	6.4	1.4	51	0.29
B.C.HYDRO	8.4	11.1	2.8	118	8.4	10.9	0.5	0.5	106	8.9	-0.3	8.6	2.3	0.0	0.0	0.0	0.0	0.0	0.0	118	0.95
EL PASO	0.2	0.3	0.1	3	0.2	0.4	0.4	0.5	6	0.7	0.0	1.1	0.2	0.0	0.0	0.2	-0.1	0.1	0.2	3	0.30
IDAHO	1.4	1.9	0.5	29	1.4	1.8	0.5	0.5	31	1.9	0.2	3.2	0.6	0.4	-0.1	0.0	0.0	0.0	0.0	29	0.68
IMPERIALCA	0.2	0.3	0.1	2	0.2	0.3	1.1	1.1	36	1.3	0.0	0.6	0.2	0.3	0.0	0.3	0.0	0.1	0.0	2	0.16
LADWP	0.5	0.8	0.3	8	0.5	0.9	0.6	0.6	12	1.1	0.1	4.2	0.5	0.2	-0.1	0.4	-0.1	0.5	0.8	8	0.42
MEXICO-CFE	0.3	0.5	0.2	6	0.3	0.5	0.3	0.3	2	0.6	0.1	1.1	0.4	0.0	0.0	0.0	0.0	0.0	0.0	6	0.59
MONTANA	0.3	0.6	0.3	28	0.3	0.6	0.4	0.4	13	0.7	0.0	1.3	0.5	1.6	-0.4	0.0	0.0	0.0	0.0	28	0.23
NEVADA	0.8	1.0	0.3	6	0.8	1.5	0.6	0.6	5	1.4	0.3	2.4	0.4	0.0	0.0	0.4	-0.1	0.1	0.2	6	0.52
NEW MEXICO	0.0	0.0	0.0	3	0.0	0.0	0.2	0.2	1	0.2	0.0	1.4	-0.2	1.0	0.1	0.3	-0.2	0.2	0.2	3	0.03
NORTHWEST	9.5	17.2	7.7	200	9.5	16.0	2.1	2.1	62	11.7	-1.2	19.1	4.3	8.4	-1.3	0.3	-0.2	0.0	0.2	200	0.61
PACE	0.7	0.9	0.2	25	0.7	1.1	1.0	1.0	14	1.6	0.1	5.3	1.8	2.7	-0.3	0.1	0.0	0.0	0.2	25	0.19
PG AND E	3.4	6.6	3.2	123	3.4	7.0	5.2	5.2	167	8.6	-0.5	12.0	3.7	0.8	0.0	1.9	0.0	0.0	0.6	123	0.46
PSCOLORADO	0.9	1.0	0.1	4	0.9	1.2	0.5	0.5	3	1.4	0.4	5.3	1.3	1.8	0.3	0.6	-0.1	0.2	0.3	4	0.25
SANDIEGO	0.1	0.2	0.1	1	0.1	0.2	0.1	0.1	12	0.2	0.0	2.7	0.6	0.3	0.0	0.5	0.1	0.0	0.1	1	0.16
SIERRA	0.4	0.5	0.1	6	0.4	0.6	0.8	0.8	48	1.2	0.3	1.4	0.3	0.6	0.1	0.7	0.2	0.0	0.2	6	0.18
SOCALIF	1.2	2.8	1.6	33	1.2	2.9	4.3	4.4	57	5.5	0.2	12.5	2.6	3.2	0.0	2.7	-0.2	0.9	2.2	33	0.21
FORTISBC	0.6	0.8	0.2	18	0.6	0.8	0.4	0.4	8	1.0	0.2	0.5	0.2	0.0	0.0	0.0	0.0	0.0	0.0	18	0.67
WAPA R.M.	0.2	0.9	0.7	36	0.2	1.1	0.1	0.1	8	0.3	0.1	3.3	0.8	3.3	0.1	0.4	0.0	0.0	0.3	36	0.19
WAPA U.M.	0.1	0.1	0.0	1	0.1	0.1	0.0	0.0	1	0.1	0.0	-0.1	0.1	0.0	0.0	0.0	0.0	0.0	0.0	1	0.76

Table 45. HS Hi-Mix Case – Initial Condition Metrics

	WECC	CALIFORNIA	DSW	NORTHEAST	NORTHWEST
Pg	83.6	26.4	18.1	3.1	23.4
mc	111.2	31.8	26.4	4.0	31.9
hr	27.2	5.1	8.2	0.9	8.4
nu	1152	298	267	89	298
pm	84.0	26.6	18.2	3.1	23.5
mv	113.7	33.9	29.2	4.2	29.2
px	85.7	31.2	22.4	12.5	6.3
mx	85.9	31.3	22.4	12.6	6.4
nx	1094	467	158	143	94
ps	169.3	57.7	40.5	15.6	29.8
qs	29.1	11.9	8.2	2.8	4.4
pl	186.2	68.8	47.4	18.0	27.4
ql	60.4	21.4	14.9	6.0	8.7
pw	14.3	2.1	1.8	2.6	6.9
qw	-2.6	0.3	-0.8	-0.4	-1.6
pv	11.2	5.8	3.8	1.3	0.2
qv	-0.3	0.4	-0.5	0.0	-0.2
ps	6.6	3.1	3.5	0.0	0.0
dg	9.4	5.4	2.9	0.9	0.3
nh	1152	298	267	89	298
Kt	0.50	0.45	0.49	0.19	0.70

Table 46. Details of HS Hi-Mix Case Dynamic Initial Conditions

	Pg	mc	hr	nu	pm	mv	px	mx	nx	ps	qs	pl	ql	pw	qw	pv	qv	ps	dg	nh	Kt
WECC	83.6	111.2	27.2	1152	84.0	113.7	85.7	85.9	1094	169.3	29.1	186.2	60.4	14.3	-2.6	11.2	-0.3	6.6	9.4	1152	0.50
CALIFORNIA	26.4	31.8	5.1	298	26.6	33.9	31.2	31.3	467	57.7	11.9	68.8	21.4	2.1	0.3	5.8	0.4	3.1	5.4	298	0.45
DSW	18.1	26.4	8.2	267	18.2	29.2	22.4	22.4	158	40.5	8.2	47.4	14.9	1.8	-0.8	3.8	-0.5	3.5	2.9	267	0.49
NORTHEAST	3.1	4.0	0.9	89	3.1	4.2	12.5	12.6	143	15.6	2.8	18.0	6.0	2.6	-0.4	1.3	0.0	0.0	0.9	89	0.19
ALBERTA	1.1	1.9	0.9	51	1.1	2.0	10.9	10.9	85	12.0	1.3	12.9	5.7	0.9	-0.1	0.0	0.0	0.0	0.0	51	0.14
ARIZONA	7.8	14.0	6.1	116	7.9	14.5	13.0	13.0	72	20.8	4.4	21.1	6.7	0.2	0.0	2.1	-0.1	3.2	1.9	116	0.48
B.C.HYDRO	10.0	13.2	3.2	125	10.0	13.1	0.7	0.7	124	10.7	-0.3	8.2	2.7	0.1	0.0	0.0	0.0	0.0	0.0	125	0.95
EL PASO	1.1	1.3	0.2	14	1.1	1.8	0.5	0.5	4	1.6	0.2	2.2	0.5	0.1	0.0	0.1	-0.1	0.0	0.0	14	0.64
IDAHO	1.2	1.6	0.4	28	1.2	1.6	2.4	2.4	28	3.6	0.6	3.9	1.4	0.2	0.0	0.0	0.0	0.0	0.0	28	0.39
IMPERIALCA	0.5	0.7	0.1	10	0.5	0.7	0.9	0.9	30	1.4	0.2	0.3	0.1	0.0	0.1	0.4	0.0	0.2	0.0	10	0.34
LADWP	3.9	4.6	0.6	28	4.0	5.1	2.1	2.1	12	6.0	2.0	7.4	2.5	0.2	0.0	0.6	0.0	0.6	1.2	28	0.62
MEXICO-CFE	0.9	1.2	0.3	7	0.9	1.3	1.2	1.2	14	2.0	0.4	2.6	0.6	0.0	0.0	0.0	0.0	0.0	0.0	7	0.50
MONTANA	0.5	0.7	0.3	30	0.5	0.8	2.4	2.4	17	2.9	0.5	1.9	0.6	0.7	-0.1	0.0	0.0	0.0	0.0	30	0.20
NEVADA	1.3	1.6	0.3	11	1.3	1.9	1.9	1.9	32	3.2	1.2	6.9	2.2	0.0	0.0	0.3	0.0	0.2	0.1	11	0.42
NEW MEXICO	1.5	1.6	0.1	9	1.5	1.8	1.2	1.2	9	2.7	0.4	3.1	0.6	0.1	-0.3	0.4	-0.1	0.0	0.2	9	0.49
NORTHWEST	23.4	31.9	8.4	298	23.5	29.2	6.3	6.4	94	29.8	4.4	27.4	8.7	6.9	-1.6	0.2	-0.2	0.0	0.3	298	0.70
PACE	0.9	1.1	0.2	23	0.9	1.3	6.4	6.4	48	7.3	0.6	9.9	3.3	1.4	-0.2	0.2	-0.1	0.0	0.6	23	0.12
PG AND E	12.2	15.1	2.9	158	12.2	15.9	15.8	15.9	305	28.0	3.5	29.3	10.0	0.8	0.0	0.7	0.1	0.0	1.0	158	0.47
PSCOLORADO	2.8	3.8	0.9	60	2.9	4.3	3.3	3.4	17	6.2	1.2	8.3	3.0	0.4	-0.1	0.5	-0.1	0.2	0.3	60	0.47
SANDIEGO	1.5	1.8	0.3	27	1.5	2.0	0.7	0.7	20	2.2	0.5	5.6	1.5	0.3	0.1	0.4	0.1	0.0	0.2	27	0.56
SIERRA	0.4	0.4	0.0	6	0.4	0.5	1.4	1.4	50	1.7	1.1	2.3	0.6	0.3	-0.1	1.1	0.1	0.0	0.3	6	0.12
SOCALIF	8.4	9.6	1.2	75	8.5	10.2	11.8	11.8	100	20.1	5.6	26.2	7.3	0.8	0.1	3.8	0.2	2.4	2.9	75	0.37
FORTISBC	0.6	0.8	0.2	17	0.6	0.8	0.5	0.5	9	1.1	0.2	0.9	0.3	0.0	0.0	0.0	0.0	0.0	0.0	17	0.59
WAPA R.M.	3.6	4.2	0.6	57	3.6	4.9	2.5	2.5	24	6.1	0.8	5.8	2.1	0.9	-0.4	0.4	-0.1	0.0	0.3	57	0.53
WAPA U.M.	0.1	0.1	0.0	2	0.1	0.1	0.0	0.0	0	0.1	0.0	0.0	0.1	0.0	0.0	0.0	0.0	0.0	0.0	2	1.00

Additional Comparative Results of Scenario Dispatches

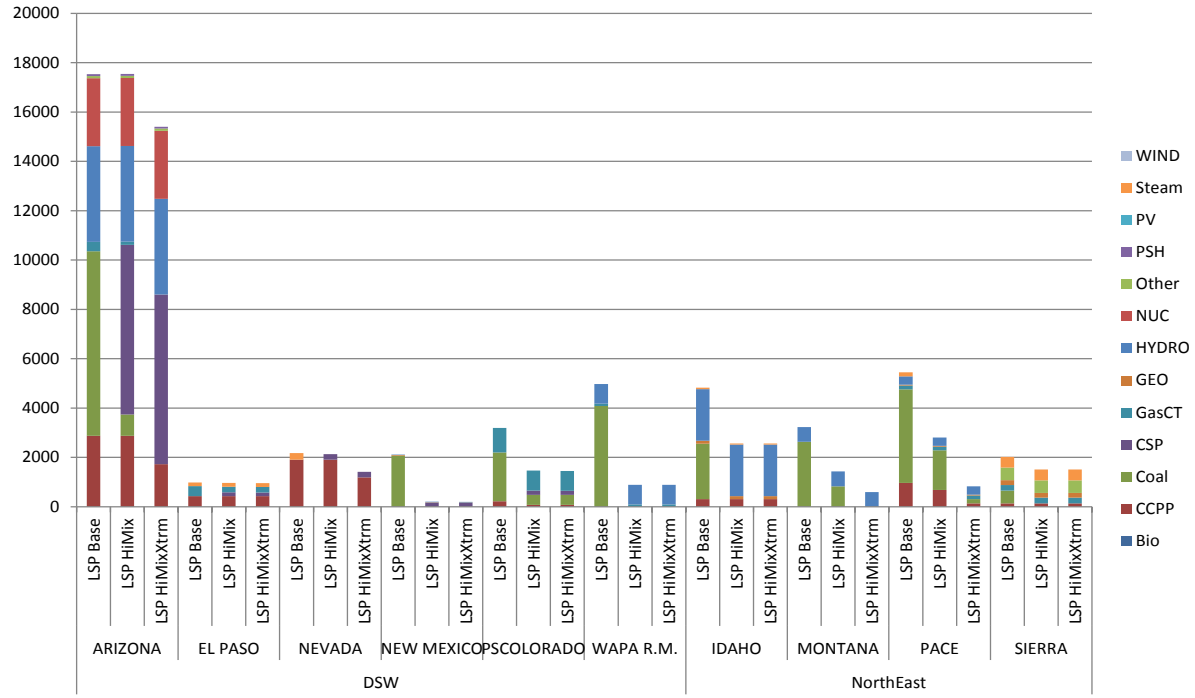

Figure 99. Sum of Pmax in East (all generation).

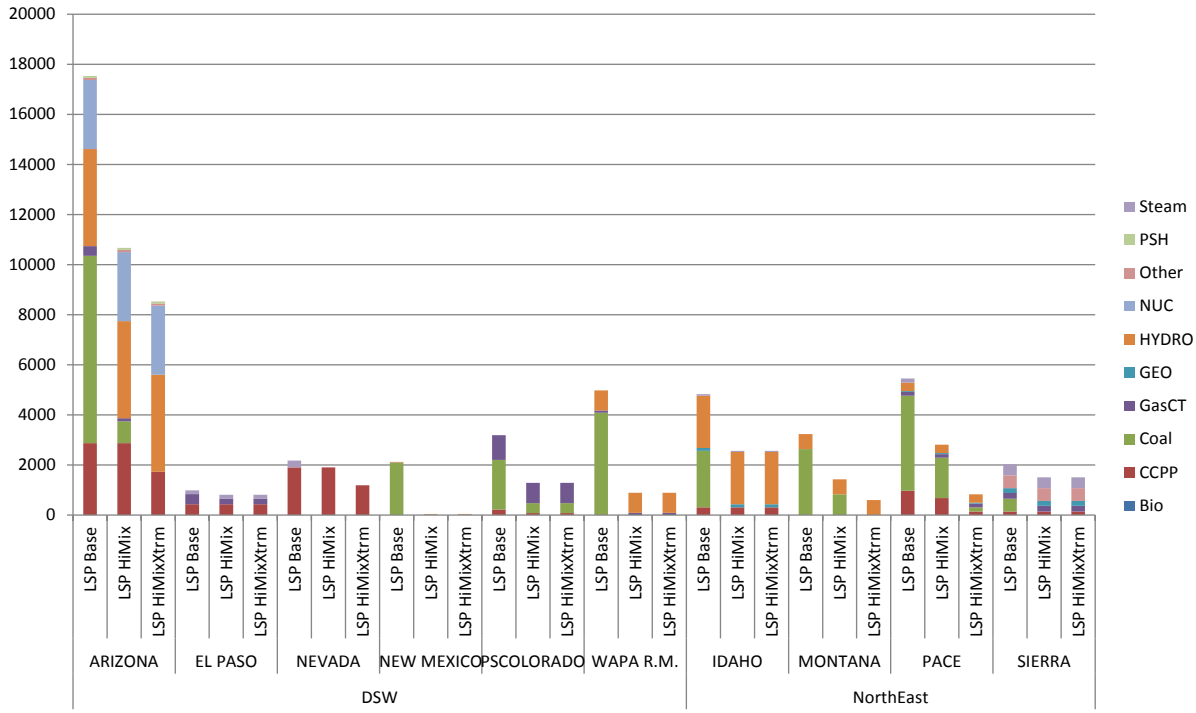

Figure 100. Pmax in East (non-renewable synchronous generation).

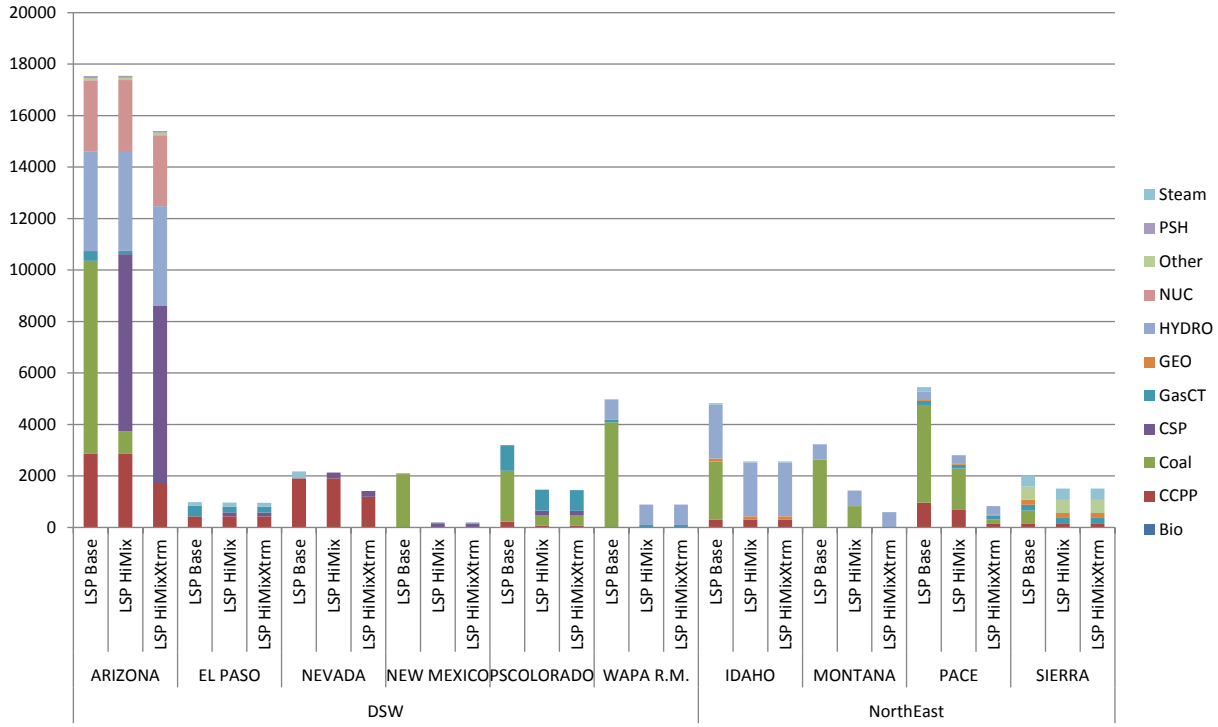

Figure 101. Pmax in East (all synchronous generation including CSP).

10.6 Frequency Response and Frequency Response Obligation Discussion

Definition of Frequency Response

FR of the entire interconnection is calculated as (NERC 2012b):

$$FR = \frac{\Delta P}{\Delta f}\left(\frac{MW}{0.1Hz}\right)$$

where ΔP is the change of power by all resources *in response* to a grid disturbance,[5] and Δf is the change in frequency.

This change in power normally results mostly from primary GR of synchronous generation. It also includes contributions from loads and other resources (e.g., energy storage devices) that are under frequency control. This investigation is specifically concerned with disturbances that result in loss of generation. For this calculation, ΔP is averaged over a time period of 20 seconds to 52 seconds after the event, and Δf is the change of frequency averaged over the time period from 20 seconds to 52 seconds. This is indicative of the primary response. (More discussion of the rationale for this definition is given in NERC [2012b]; discussion of the measurement of frequency is below in this Appendix.)

[5] For a system to reach equilibrium following loss of generation, the ΔP of the response must equal the amount lost, but the "response" distinction is important because it is a measure of how the resources react to the *change in frequency,* regardless of the cause.

Definition of Frequency Nadir

This is the lowest frequency in the event, labeled Point C in the illustrative frequency event of NERC (2012b).

Definition of Frequency Nadir Time

This is the time it takes for the response to reach its nadir.

Definition of Settling Frequency

For results presented throughout this report, this is defined as the average frequency between 20 seconds and 52 seconds after the event starts. This is Point B in the illustrative frequency event of NERC (2012b), but was refined to the average value over this period in NERC (2012b). The intent of this metric is to capture the frequency after the autonomous controls (mainly governors) have acted, but before centralized control (mainly automatic generation control) acts. In practice, these behaviors overlap, so it is difficult to assign a specific post-disturbance time to make a single measurement.

Definition of Frequency Response Obligation

An IFRO is established in *Frequency Response and Frequency Bias Setting Standard: Supporting Document* (NERC 2012b). The rationale and development of the obligation is described in detail in *Frequency Response Initiative Report* (NERC 2012c). The IFRO for WECC is set in these documents and was used in this study. It is calculated as the amount of generation lost in the criteria contingency divided by the maximum change in frequency. The WECC FRO used in this study is 840 MW/0.1 Hz according to the November 30, 2012, version of this document, which was subsequently ratified. Broadly, the intent is that WECC should always have a FR that meets or exceeds this minimum.

This obligation is based on avoiding the first stage of UFLS in WECC at 59.5 Hz (NERC 2012c, Table B).[6] It takes into account the statistical expectation that the system frequency may be as much as 24 mHz lower (NERC 2012c, Table A) leading into an event, and the relative difference between the frequency nadir and the settling frequency (NERC 2012c, Table D).

Definition of Balancing Authority Frequency Response Obligation

Each BA within an interconnection is obligated to provide its share of the total IFRO. The distribution of the obligation is based on the relative size of each BA. This is calculated as follows:

$$FRO_{BA} = IFRO\left(\frac{Pgen_{BA}+Pload_{BA}}{Pgen_{EI}+Pload_{EI}}\right),$$

where:

FRO_{BA} is the BA FRO.

$IFRO$ is the interconnection FRO.

[6] As of this report, FRCC includes UFLS settings of 59.7 Hz.

$Pgen_{BA}$ is the annual BA generation.

$Pload_{BA}$ is the annual BA load.

$Pgen_{EI}$ is the annual interconnection generation.

$Pload_{EI}$ is the annual interconnection load.

In this work, an *approximate* assignment of FRO by study region and area was based on the power flow condition.

BA Frequency Response

This is the performance of each BA, which is expected to meet or exceed the obligation at all times. It is calculated as follows:

$$FR_{BA} = \frac{\Delta P_{BA}}{\Delta f},$$

where:

FR_{BA} is the BA FR.

ΔP_{BA} is the change in BA power.

The frequency change is uniform across the interconnection. In the work presented here, the only power change measured and included in the calculations is that of the turbine power of the responsive generation. Load and loss impacts are not considered, beyond load modeling. In this work, the change in power for each study area is used to create a FR that can be reported. As noted above, while the FRO applies only to BAs, reporting FR by study area is a mechanism to illuminate regional behavior.

Frequency Calculation

This study focuses on system-wide FR, as measuring the frequency at a single node in the grid following a disturbance can be confusing and misleading. A system equivalent frequency, *f*, was developed and calculated as:

$$f = \frac{\sum_{i=1}^{n}(MVA_i * \omega_i)}{\sum_{i=1}^{n} MVA_i},$$

where:

MVA_i is the megavolt ampere rating for machine *i*.

ω_i is the speed for machine *i*.

n is the number of synchronous machines in the system.

This is the MVA-weighted average speed of synchronous machines in the system. It filters out the local swings to give a clearer measure of the system performance of concern in this study. It

can be regarded analytically as the common mode of the system. Six system equivalent frequencies for WECC and each study region and area were calculated in this study.

10.7 Supporting Material for Frequency Response Investigation

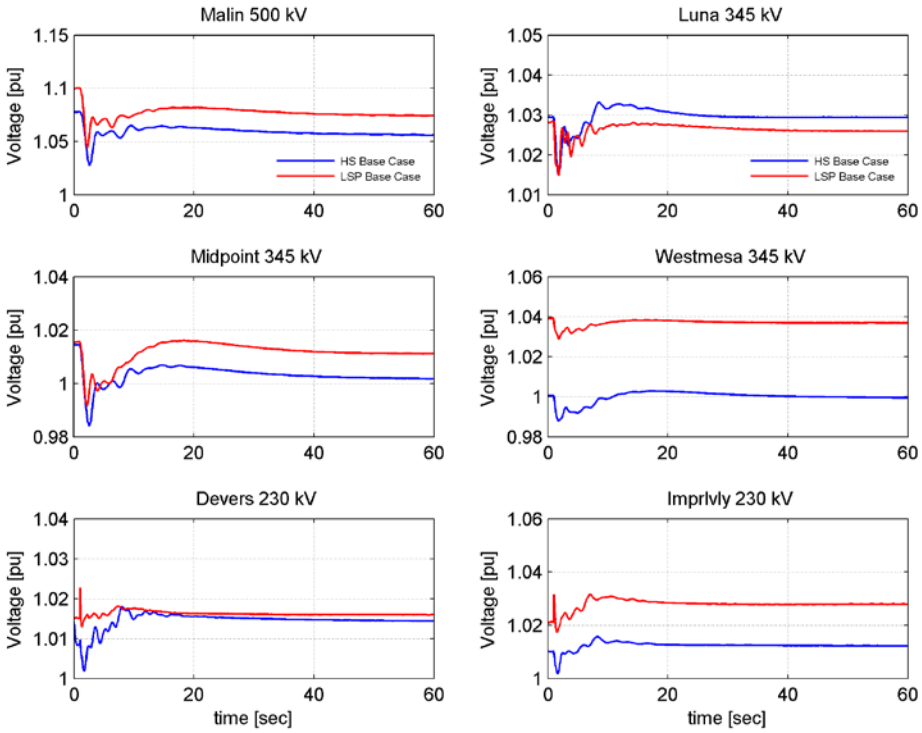

Figure 102. Bus voltage response to loss of two Palo Verde units – LSP Base vs. HS Base.

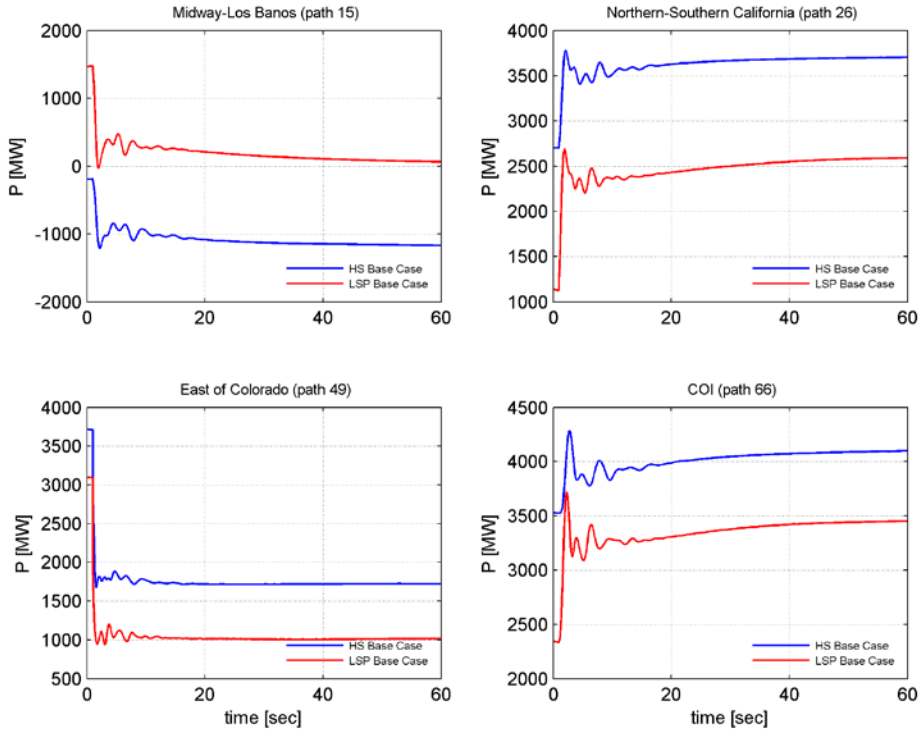

Figure 103. Selected interface flows to loss of two Palo Verde units – LSP Base vs. HS Base.

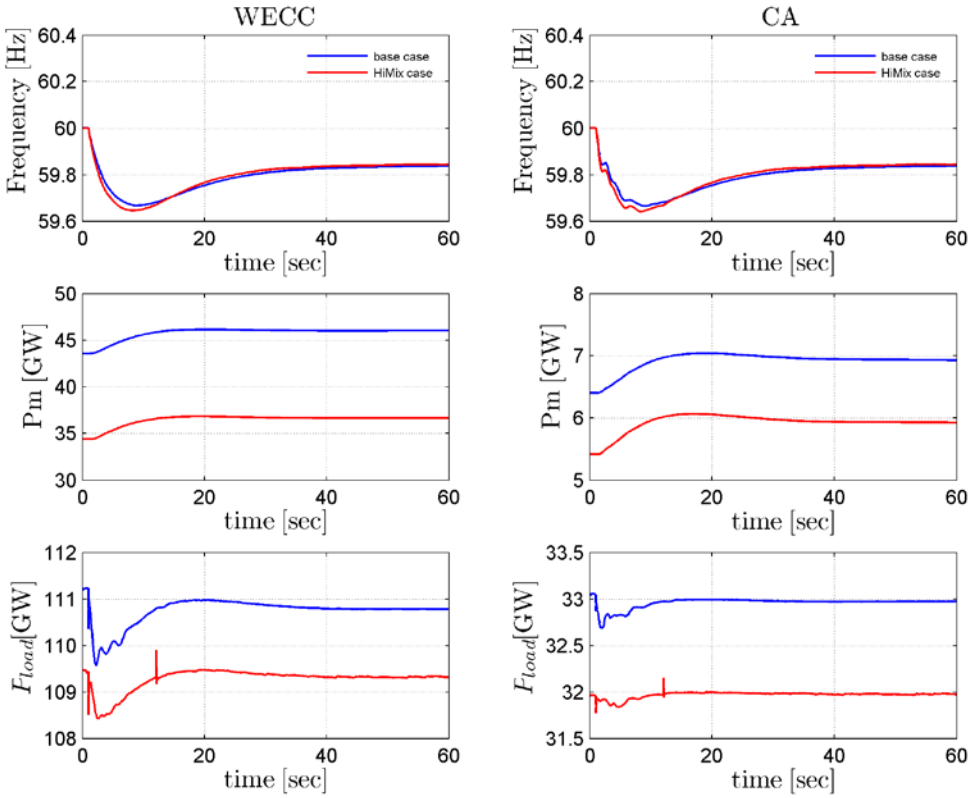

Figure 104. LSP frequency response including loads.

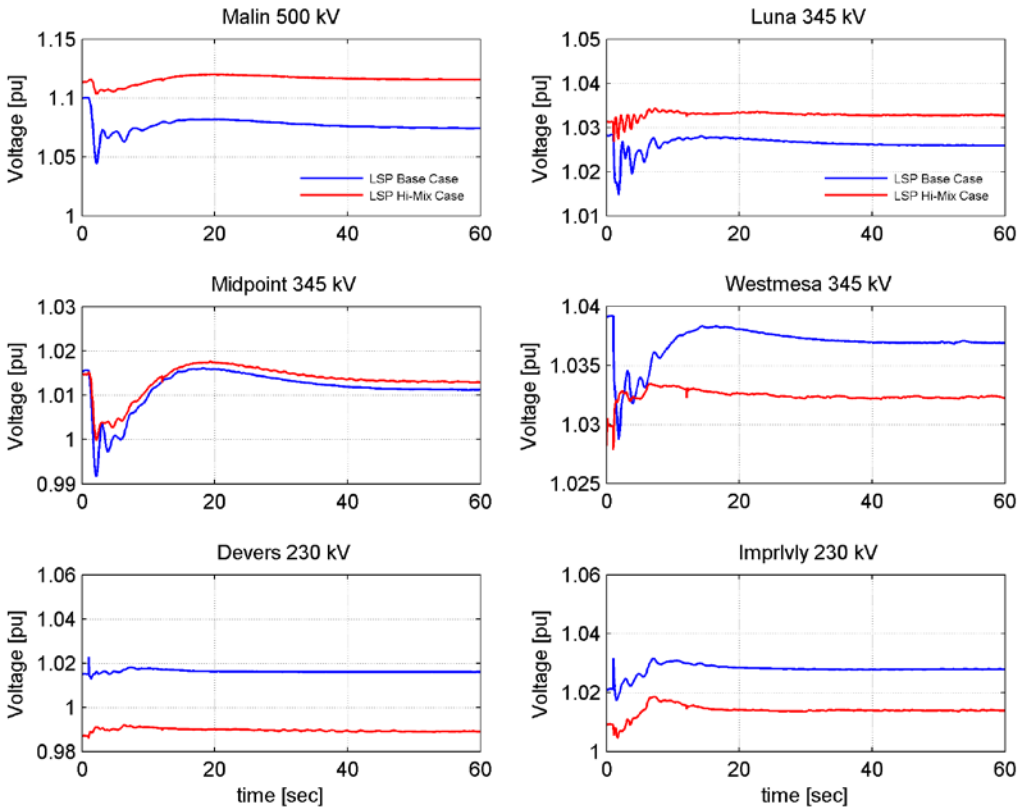

Figure 105. Bus response to loss of two Palo Verde units.

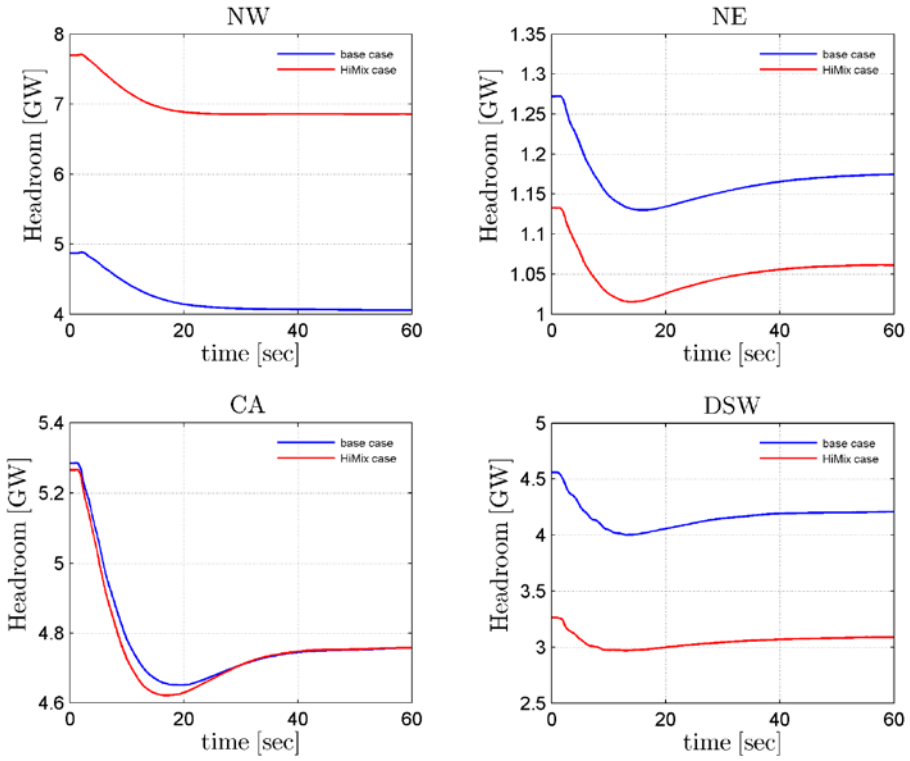

Figure 106. Headroom response to loss of two Palo Verde units.

10.8 Supporting Material for Transient Stability Investigation

Additional COI Stability Results

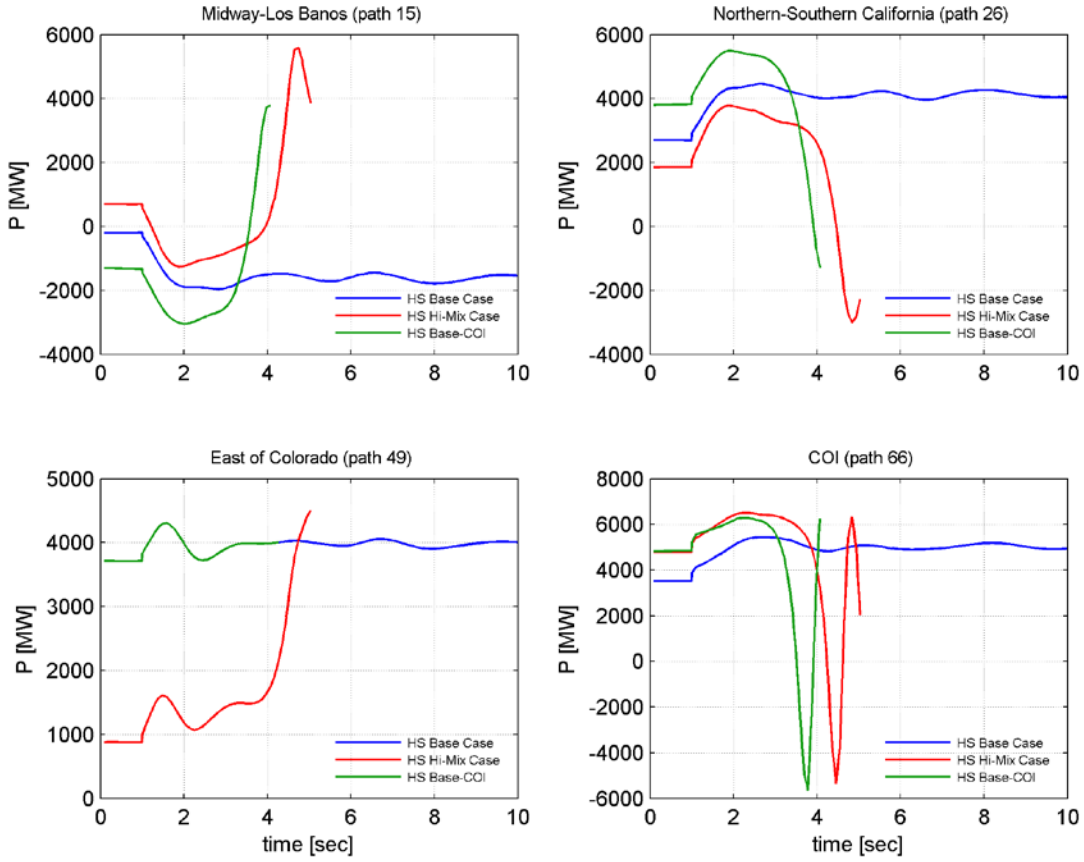

Figure 107. Interface flows for HS PDCI event.

The details of the sequence of progressively more aggressive RAS are as follows:

- Group 1 (gr1), tripping approximately 1,108 MW (JDA 01 through 08)
- Group 2 (gr2), tripping approximately 2,076 MW (group 1 + JDA 09 through 08)
- Group 3 (gr3), tripping approximately 2,776 MW (group 1 + 2 + MCN 01 through 04 + LMN 2 through 4).

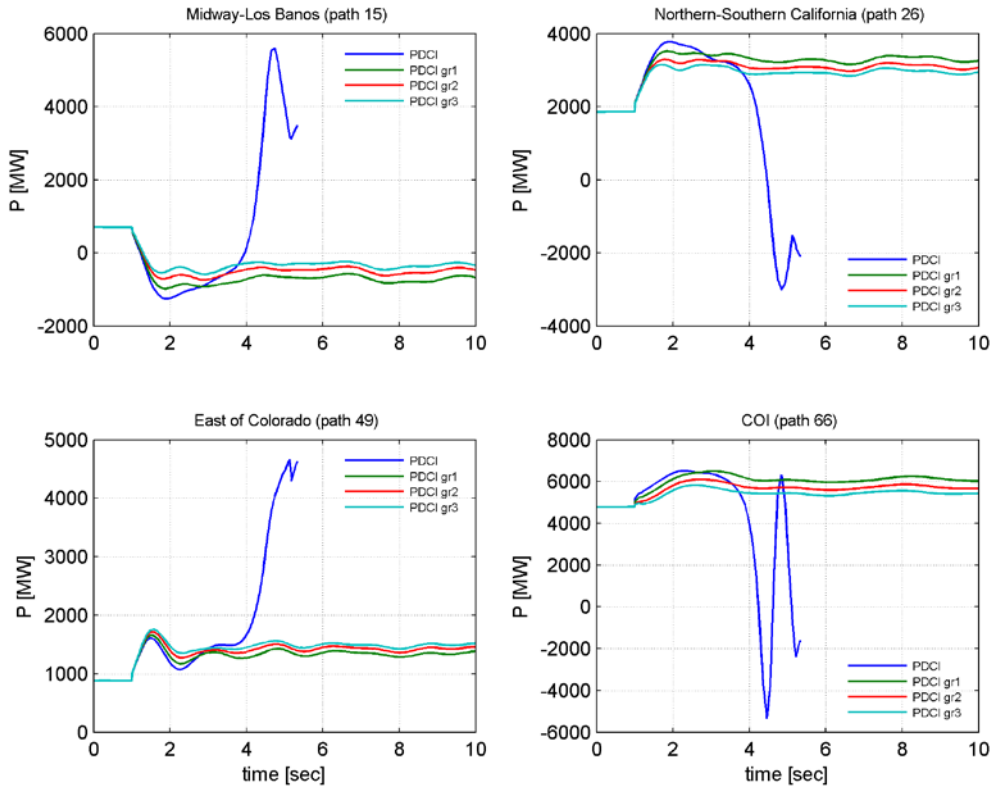

Figure 108. Interface flows – PDCI fault Hi-Mix case with RAS.

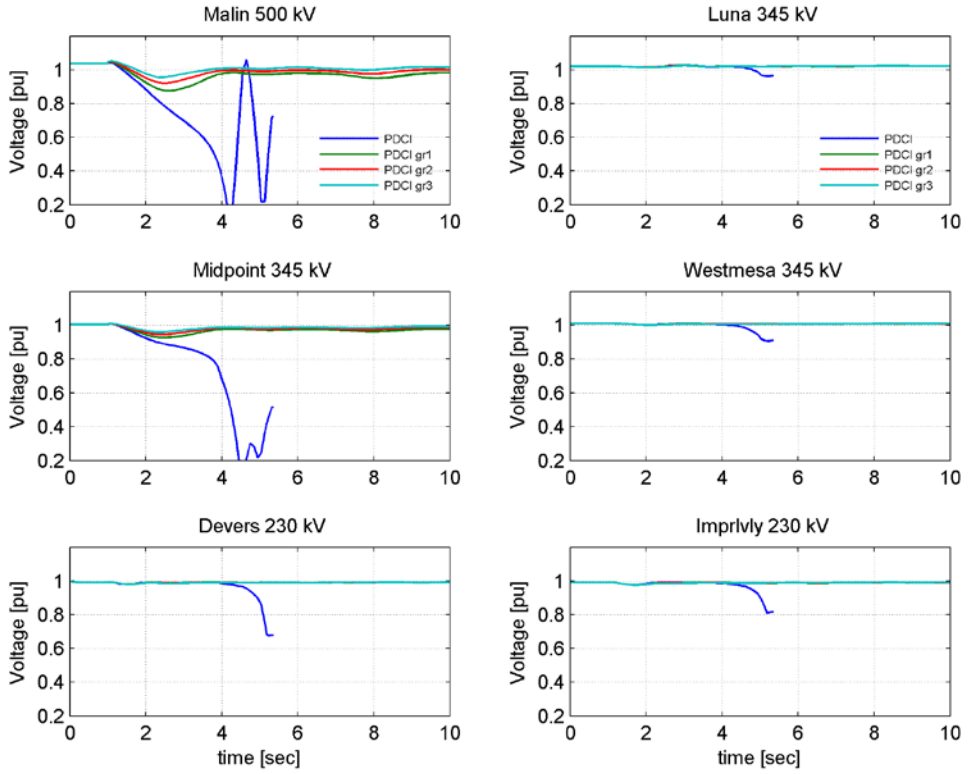

Figure 109. Voltages – PDCI fault Hi-Mix case with RAS.

10.9 Supporting Material for Sensitivities

Additional Load Impact Sensitivity Results

The plot below is for the HS Hi-Mix case, one-phase vs. three-phase fault at Midway, for the Midway-Vincent event. It shows that it is the *during-fault* behavior that drives the voltage collapse.

Figure 110. Voltage collapse sensitivity to fault type.

This sequence shows the impact of increasing the severity of the fault (by reducing the fault impedance). The traces are as follows:

- Trace a) original MV3p
- Trace b) with fault impedance Z/4
- Trace c) with fault impedance Z/2
- Trace d) with fault impedance 3Z/4

- Trace e) with fault impedance Z (single-phase proxy impedance).

Specifically, the fault impedance is reduced from .005 to 0.0 in 0.00125 pu steps.

The fourth case is interesting, in that it exhibits classic FIDVR, with the recovery taking more than 30 seconds.

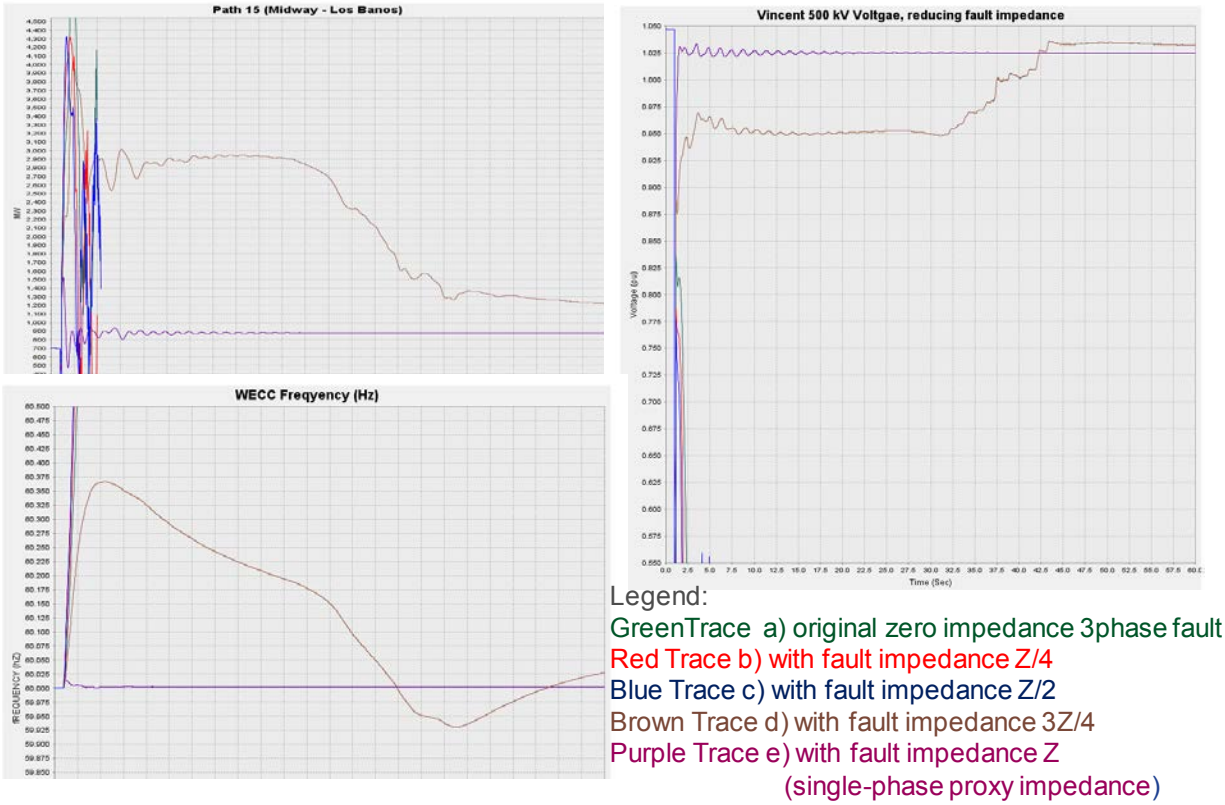

Figure 111. Voltage collapse sensitivity to fault impedance.

The following figures are from the IEEE 1547 draft tables for interconnection system default response to abnormal voltages and frequencies, with notation to emphasize that the composite load does not have built-in time delays.

...

Composite load model with DG does NOT have time delays for tripping

Default settings [a]		
Voltage range (% of base voltage [b])	Clearing time(s)	Clearing time: adjustable up to and including (s)
V<45	0.16	0.16
45≤V<60	1.00	11
60<V<88	2.00	21
110≤V<120	1.00	13
V≥120	0.16	0.16

[a] Under mutual agreement between the EPS and DR operators, other static or dynamic voltage and clearing time trip settings shall be permitted

[b] Base voltages are the nominal system voltages stated in ANSI C84.1-2011, Table 1.

Figure 112. IEEE 1547 table on voltage tripping.

Composite load model with DG does NOT have time delays for tripping

	Default settings		Ranges of adjustability	
Function	Frequency (Hz)	Clearing time (s)	Frequency (Hz)	Clearing time (s) adjustable up to and including
UF1	57	0.16	56 – 60	10
UF2	59.5	2	56 – 60	300
OF1	60.5	2	60 - 64	300
OF2	62	0.16	60 – 64	10

Figure 113. IEEE 1547 table on frequency tripping.

Figure 114. DG tripping on voltage dip.

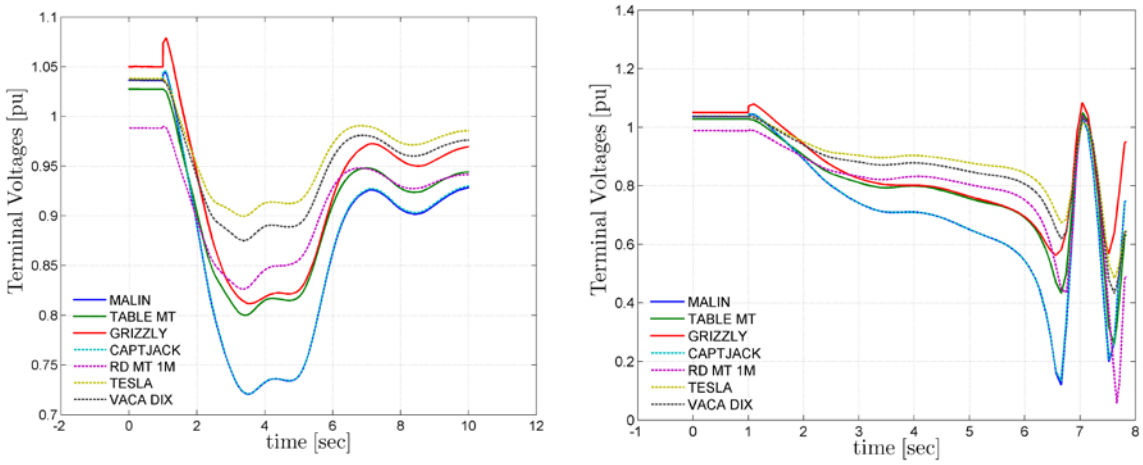

Figure 115. COI destabilization due to DG tripping on voltage dip.

Additional Widespread DG Tripping Results

Only about 2,500 MW (rather than 2,740 MW) is tripped because of voltage sensitivities in the complex load model logic.

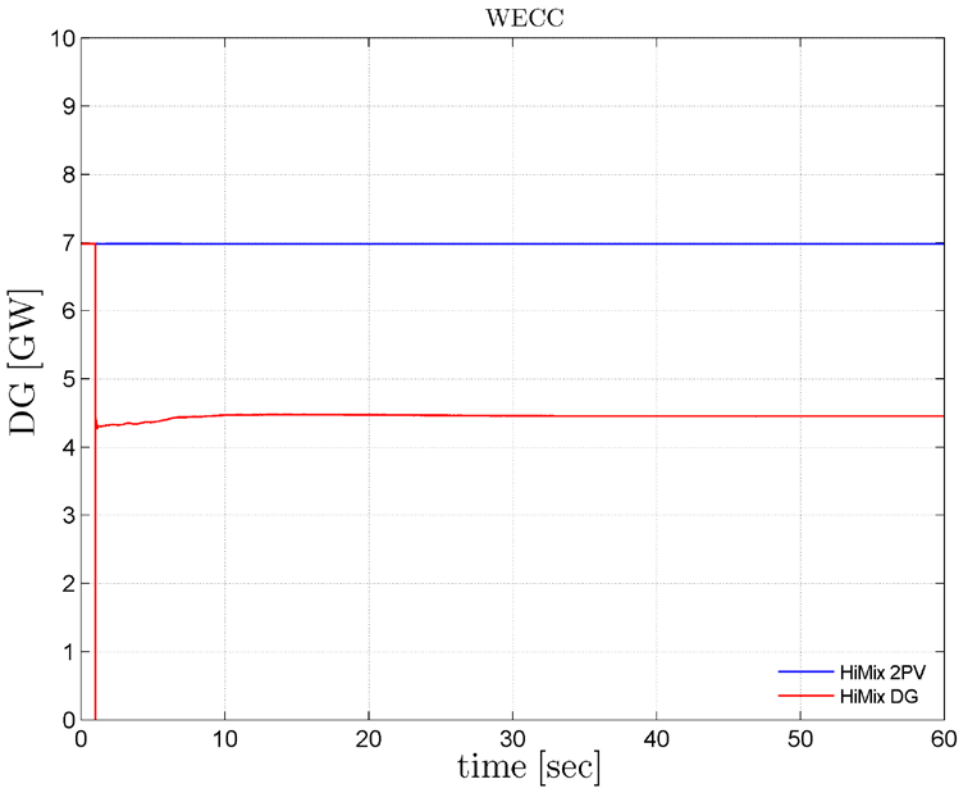

Figure 116. DG vs. trip of two Palo Verde units on Hi-Mix case – DG.

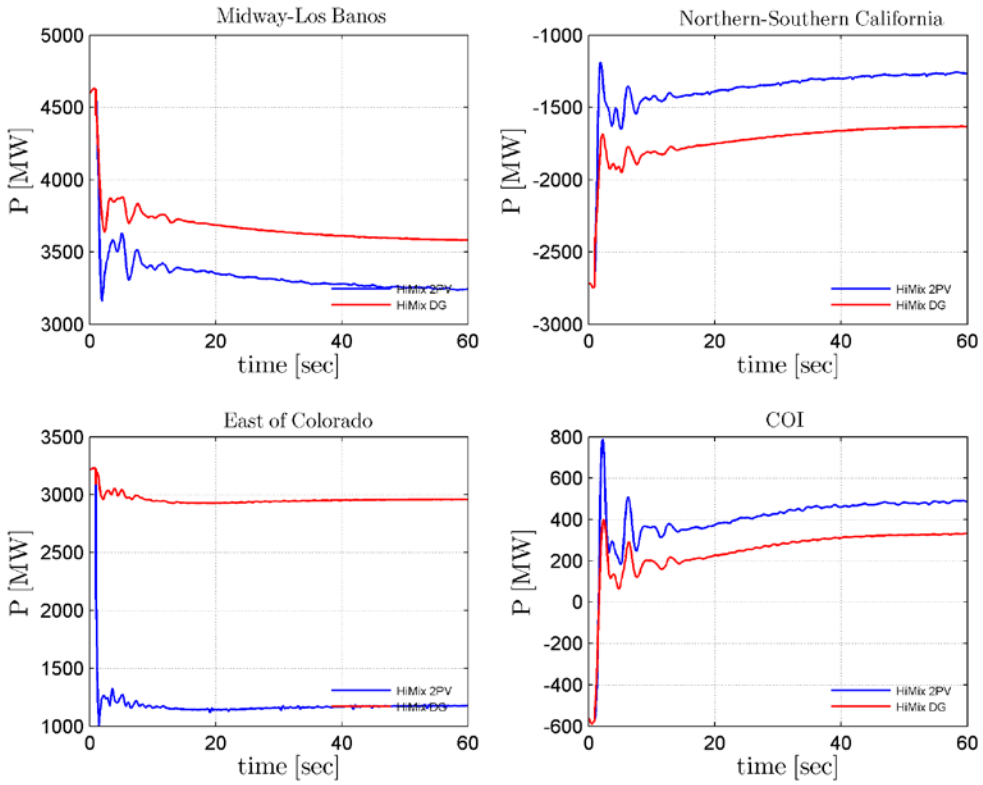

Figure 117. DG vs. trip of two Palo Verde units on LSP Hi-Mix case – interfaces.

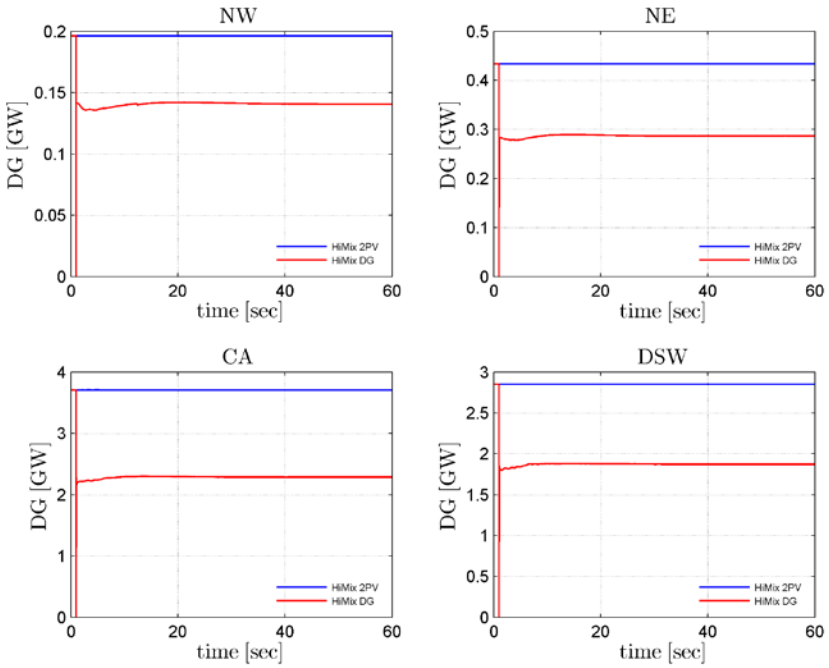

Figure 118. DG trip sensitivity.

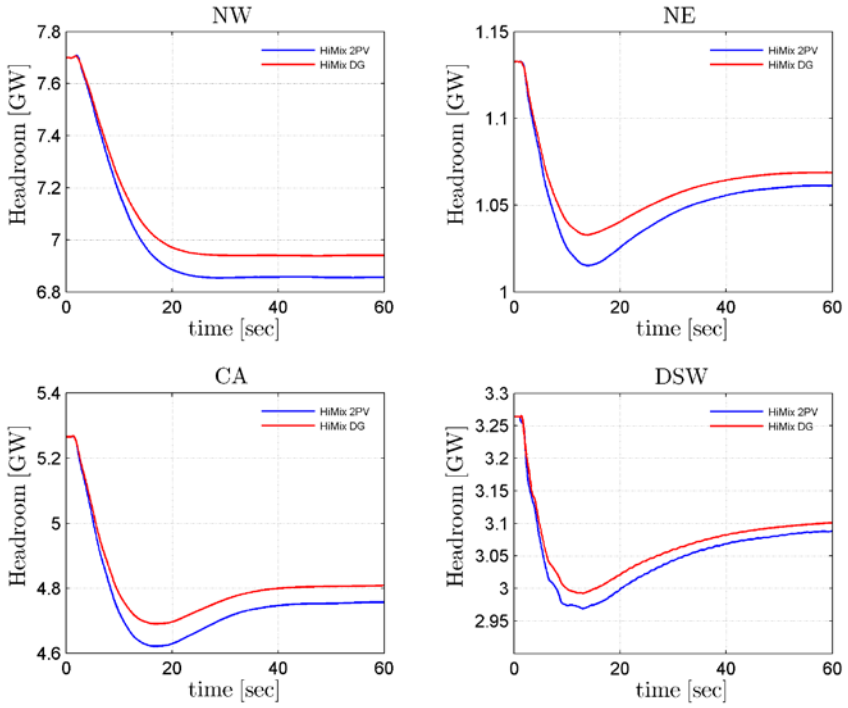

Figure 119. DG trip sensitivity.

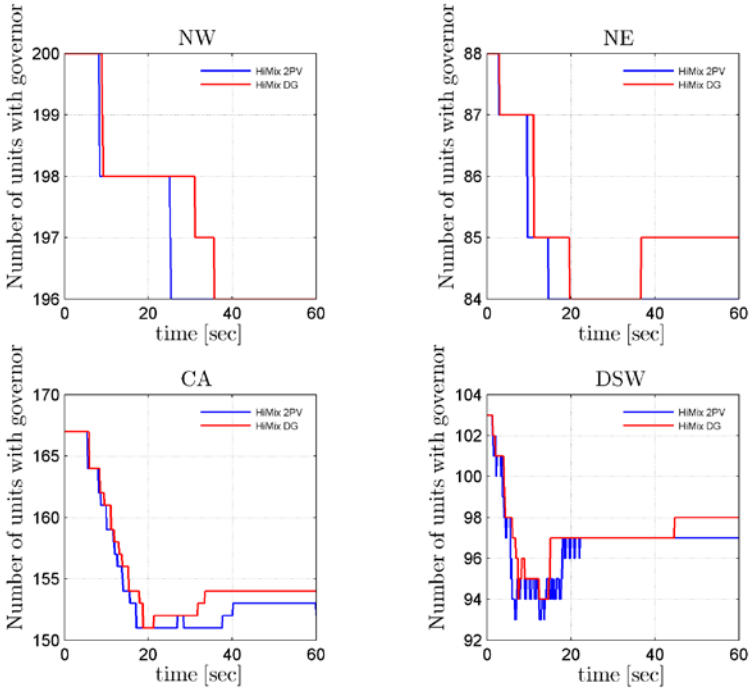

Figure 120. DG trip sensitivity.

Additional Extreme Generation Tripping Results

FR for two events—trip of two Palo Verde units and trip of three Palo Verde units—is shown in the following table.

Table 47. Extreme Generation Tripping – Comparison of Frequency Response

		Trip 2 Palo Verde Units	Trip 3 Palo Verde Units
	FRO	FR	FR
Name	[MW/0.1Hz]	[MW/0.1Hz]	[MW/0.1Hz]
WECC	840	1311	1265
CALIFORNIA	296	312	302
DSW	220	119	107
NORTHEAST	82	47	52
ARIZONA	104	50	42
EL PASO	9	4	2
IDAHO	18	22	24
IMPERIALCA	4	14	14
LADWP	29	30	30
MONTANA	11	10	14
NEVADA	28	34	33
NEW MEXICO	14	2	2
NORTHWEST	131	483	463
PACE	42	8	7
PG AND E	133	197	191
PSCOLORADO	36	6	5
SANDIEGO	21	7	7
SIERRA	11	7	7
SOCALIF	108	63	59
WAPA R.M.	27	24	23
WAPA U.M.	0	3	3

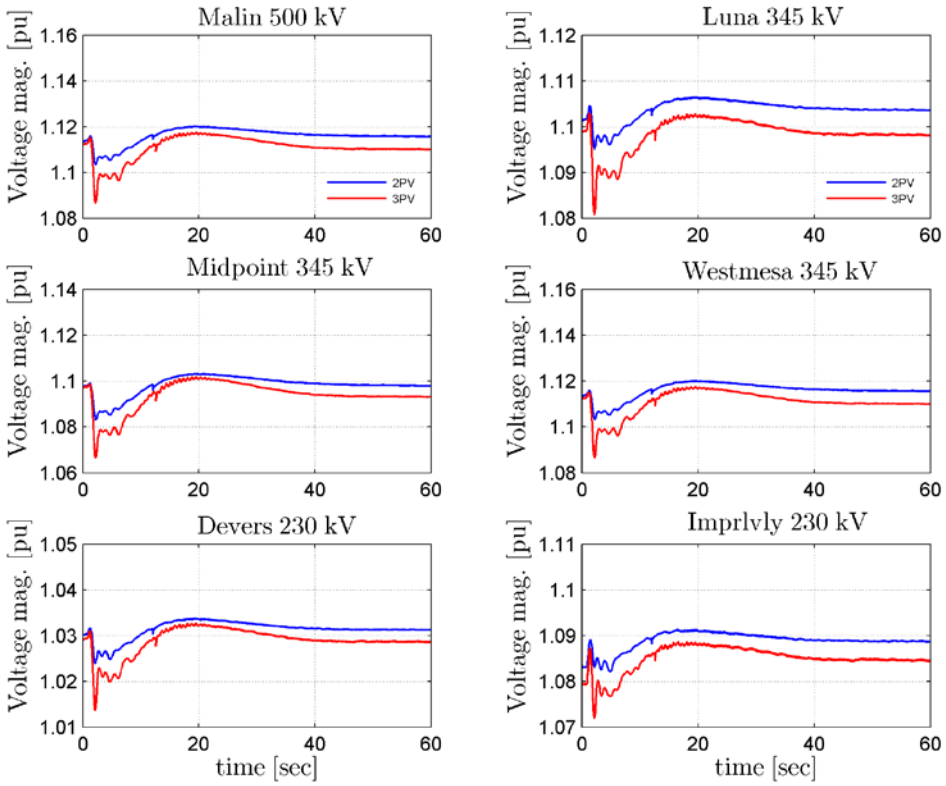

Figure 121. Extreme generation tripping – voltages.

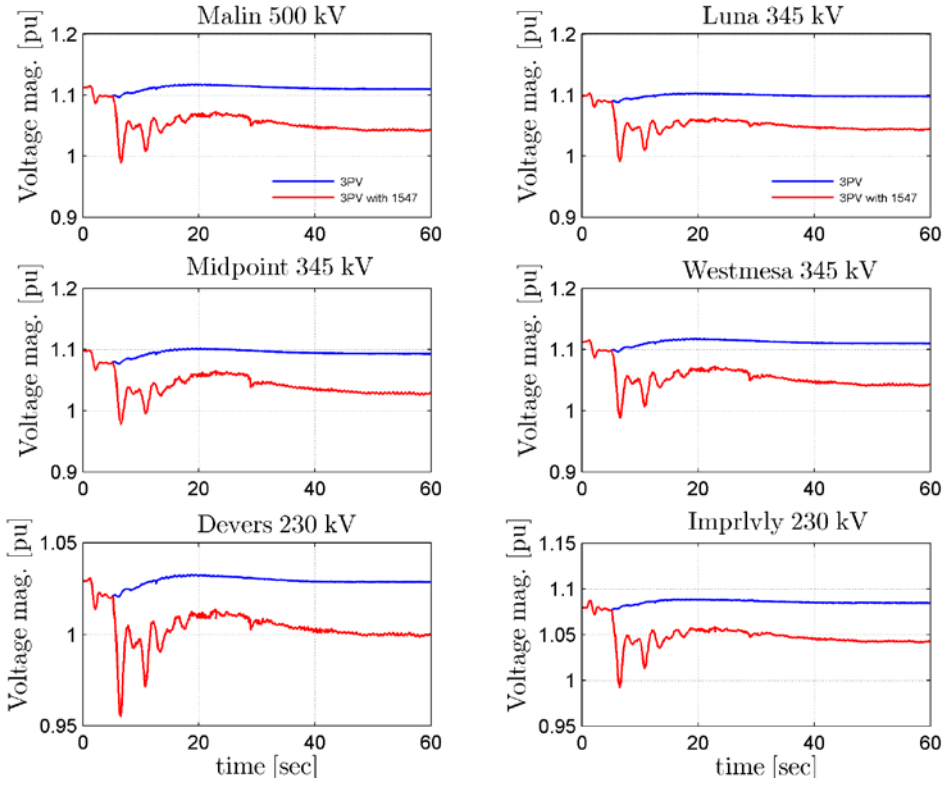

Figure 122. Extreme generation tripping – volt sensitivity to UF DG tripping.

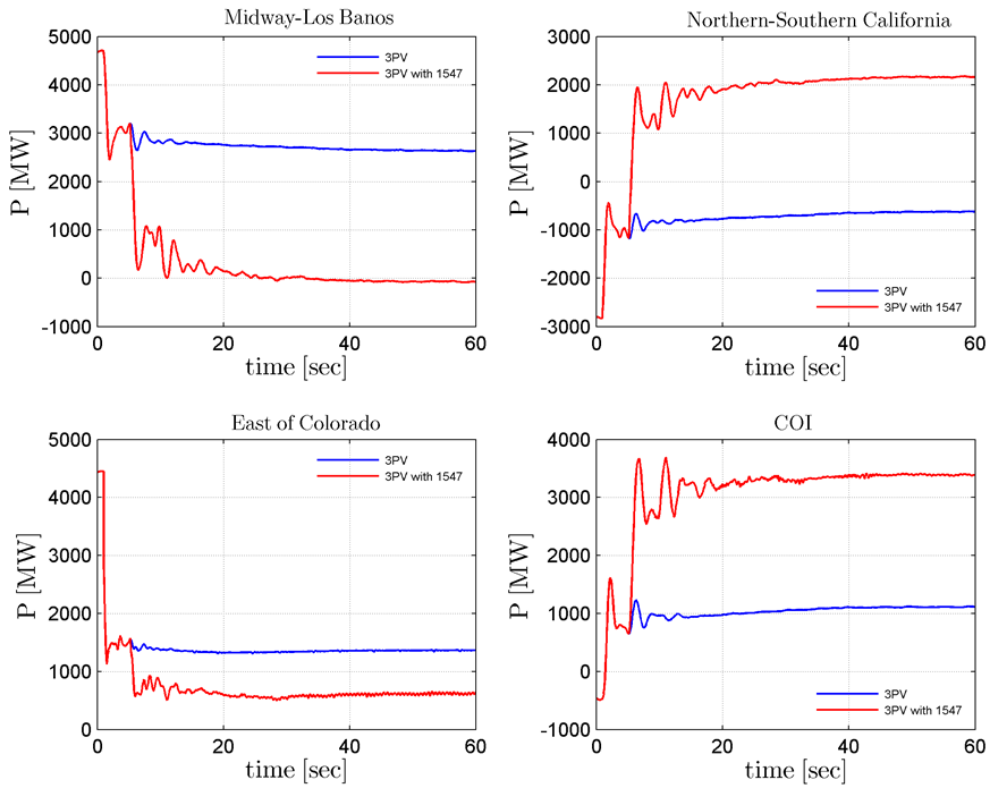

Figure 123. Extreme generation tripping – flow sensitivity to UF DG tripping.

Additional Headroom Depletion Results

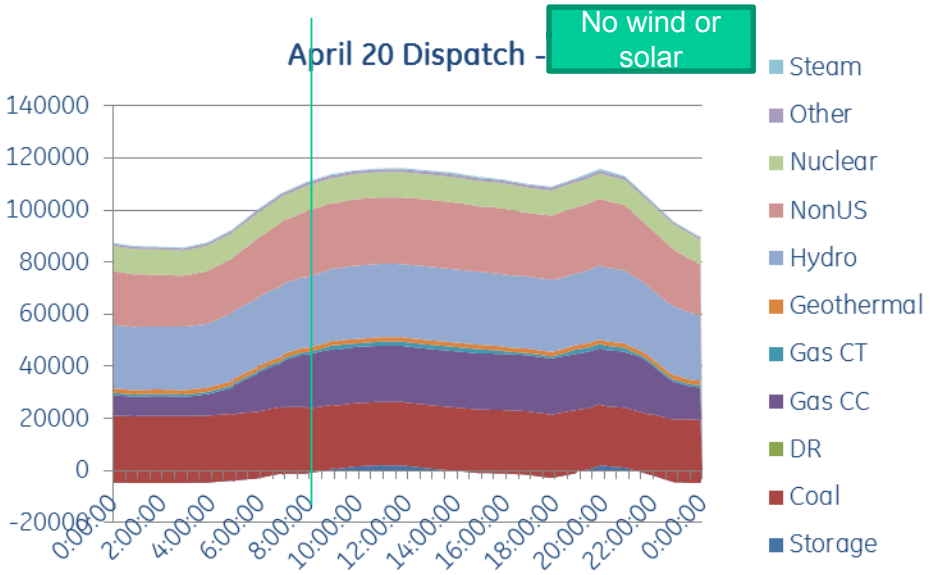

Figure 124. Headroom depletion experiment – no wind and solar.

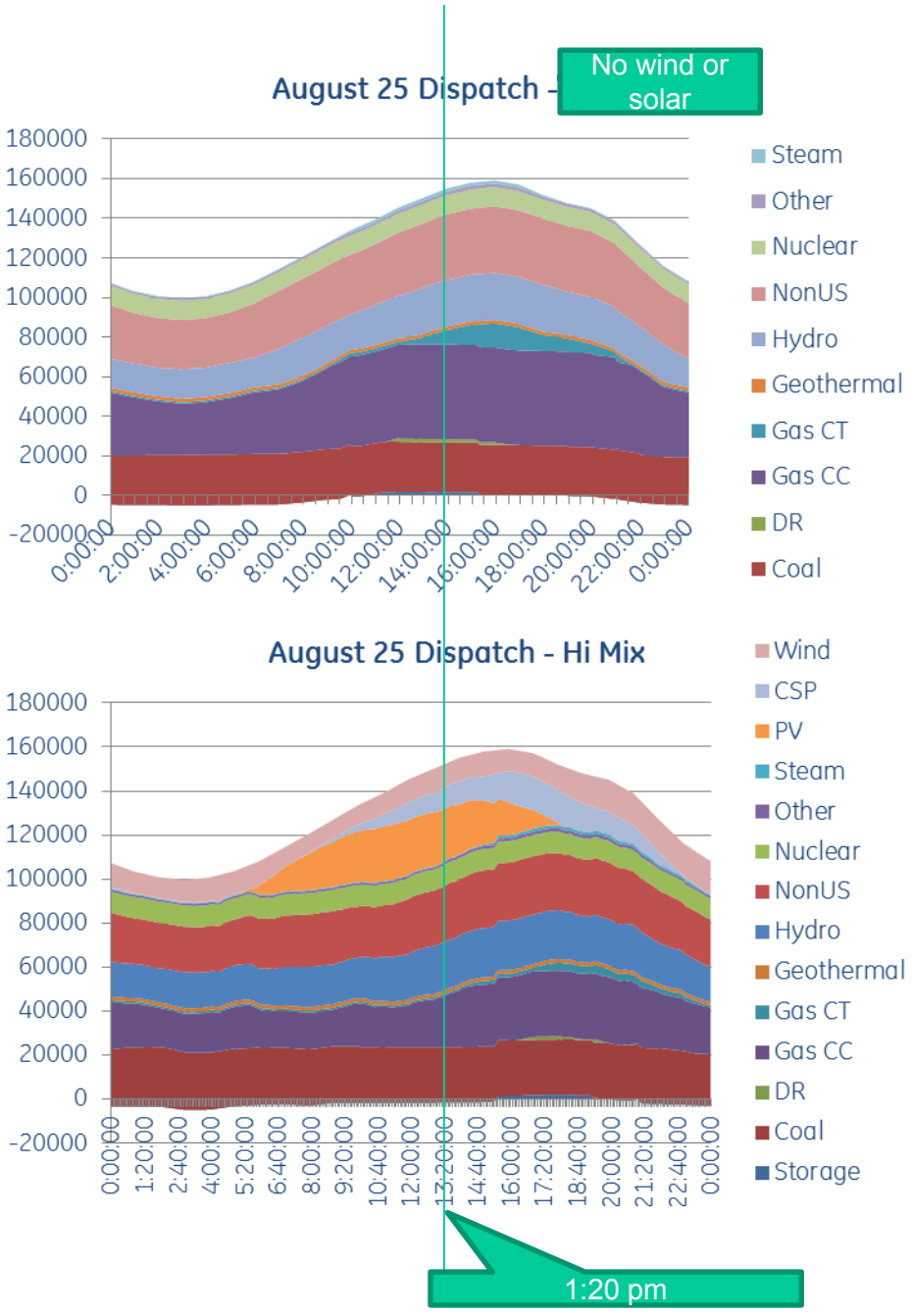

Figure 125. Summer "duck" curve.

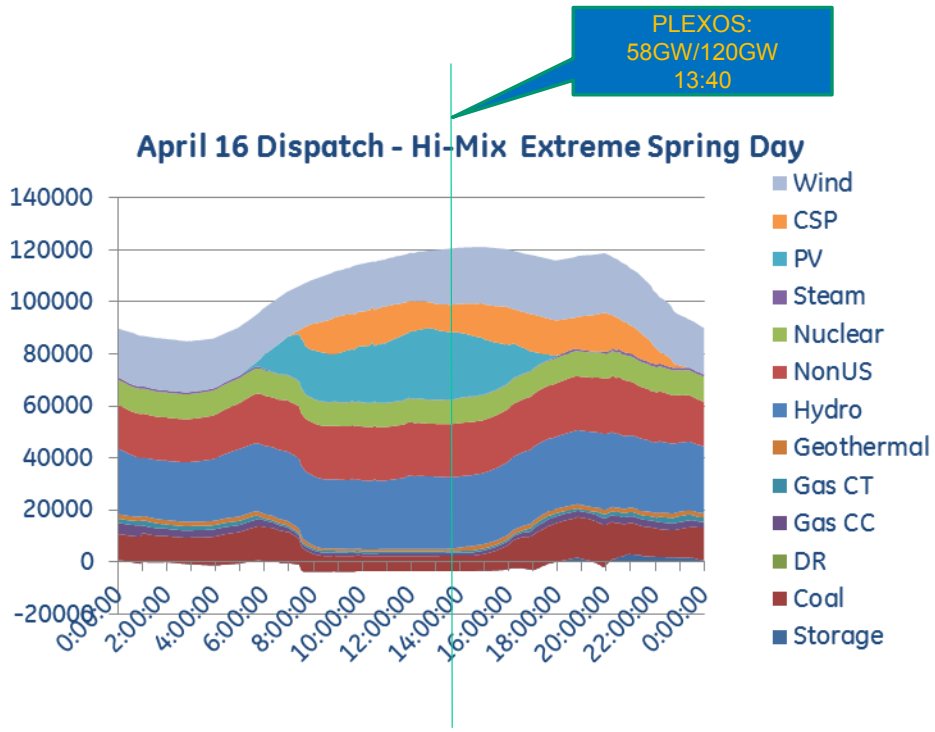

Figure 126. Extreme "duck" curve.

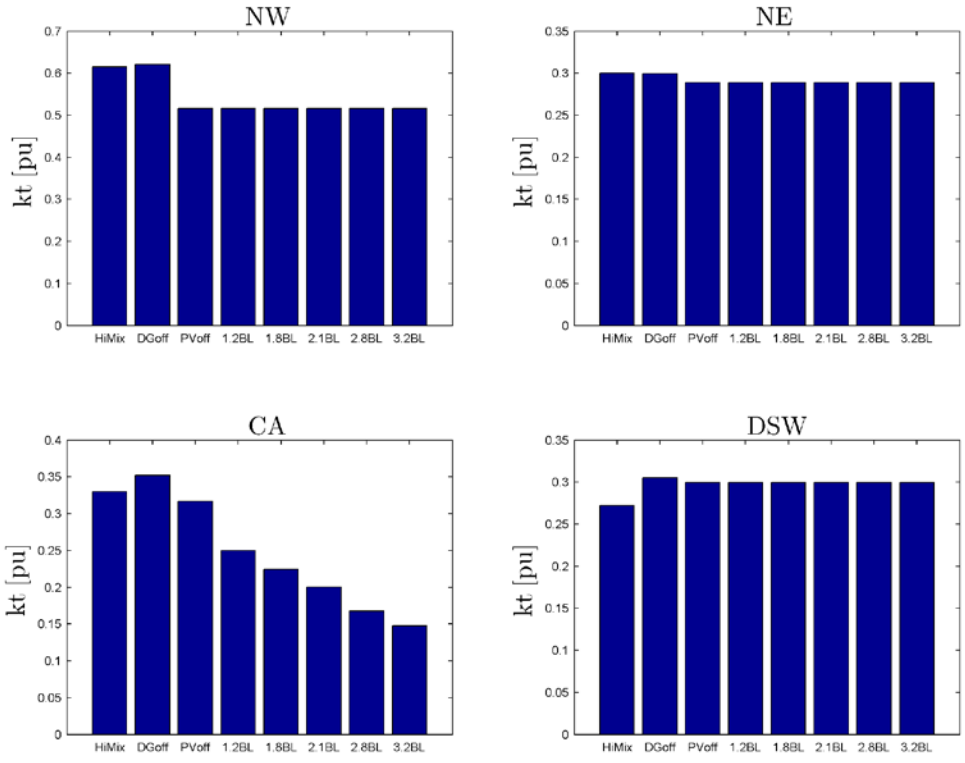

Figure 127. Headroom depletion: Kt – four regions.

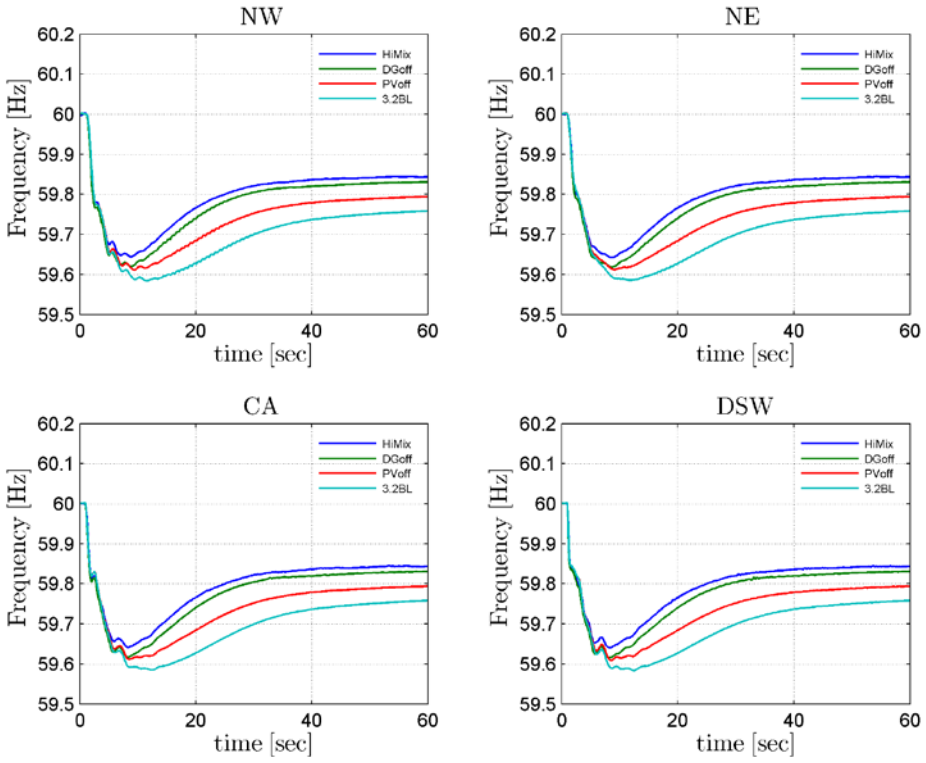

Figure 128. Headroom depletion – WECC frequency response.

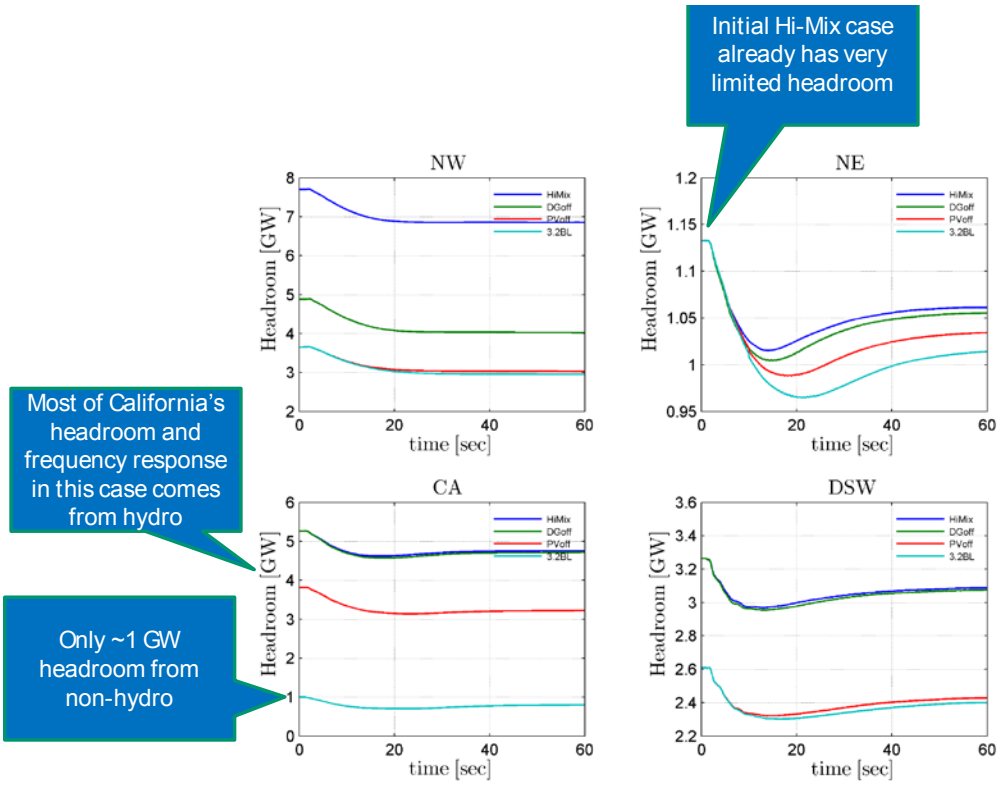

Figure 129. Headroom depletion – dynamic headroom.

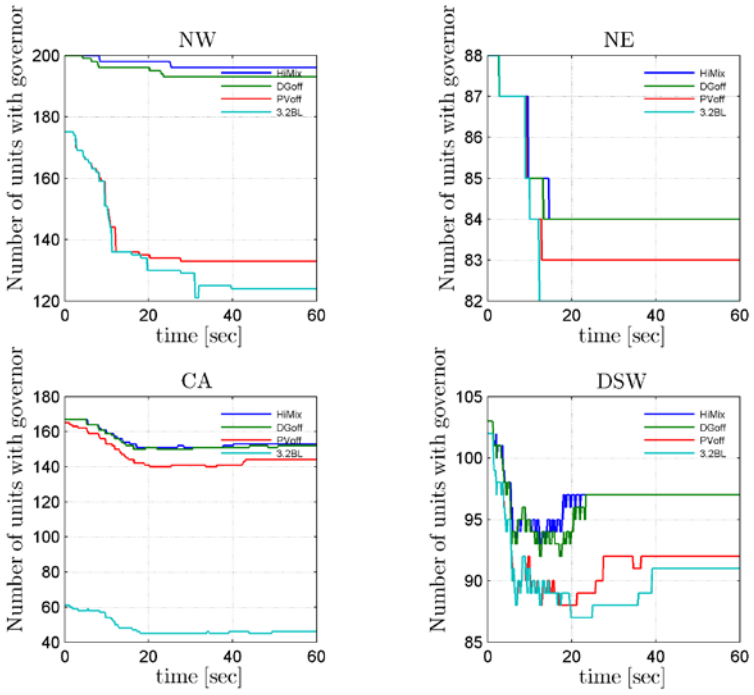

Figure 130. Number of units with governors (and non-zero headroom).

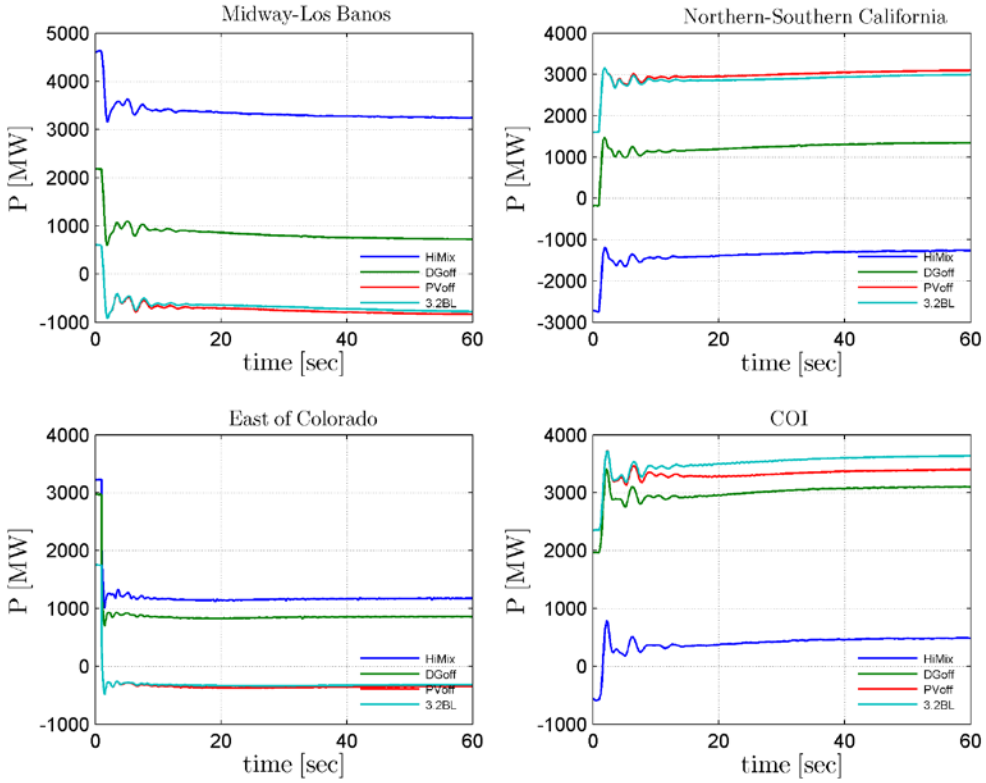

Figure 131. Interface flows.

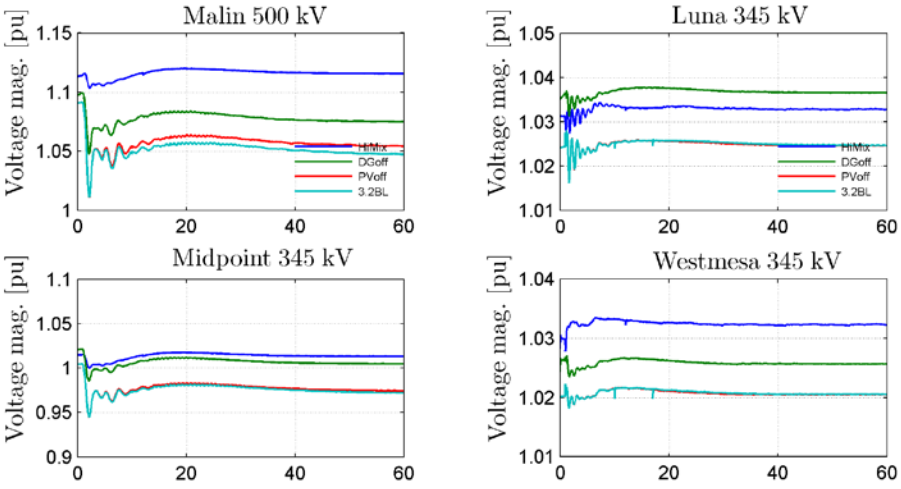

Figure 132. Voltages.

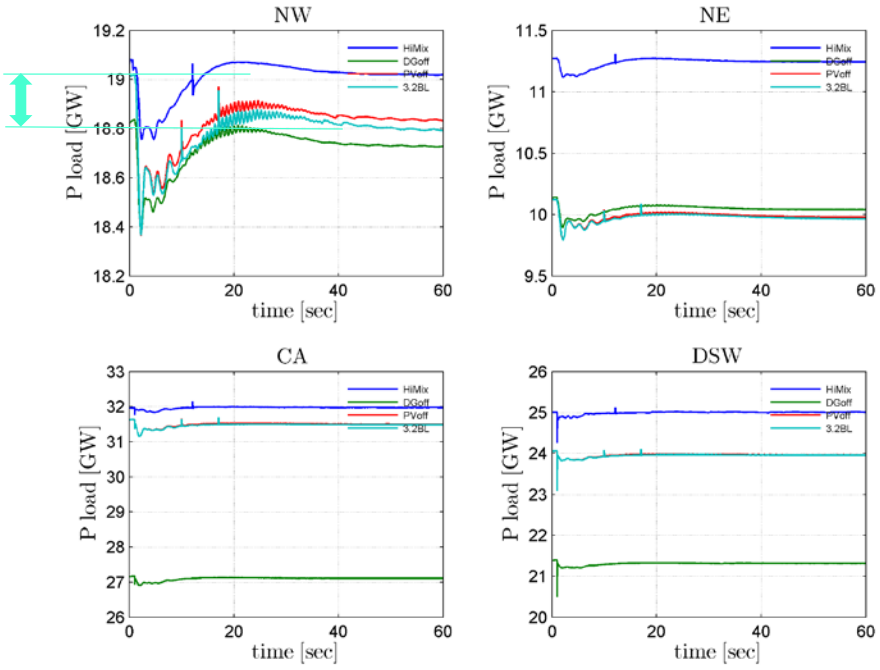

Figure 133. Load response.

Additional Base Case De-Commitment Results

Table 48. Case DG Only (Composite Load Model with DG) – Initial Condition Metrics

		WECC	CALIFORNIA	DSW	NORTHEAST	NORTHWEST
Pgen of units with governors (GW)	pg	42.9	6.6	9.3	2.8	12.5
Capacity of units with governors (GW)	mc	65.3	12.8	14.0	4.0	17.8
Headroom on units with governors (GW)	**hr**	**22.3**	**6.1**	**4.7**	**1.2**	**5.2**
Number of units with governors	**nu**	**843**	**192**	**126**	**95**	**208**
Mechanical power of unit with governors (GW)	pm	42.9	6.7	9.4	2.9	12.6
MVA rating of unit with governors (GVA)	mv	66.2	13.3	15.5	4.3	16.5
Pgen of units w/o governors (GW)	px	46.8	13.6	10.5	8.6	2.1
Mechanical power of units w/o governors (GW)	mx	47.0	13.7	10.5	8.6	2.1
# units w/o governors	nx	787	315	65	124	68
Pgen of all synchronous generators (GW)	pq	89.7	20.2	19.8	11.4	14.7
Qgen of all synchronous generators (GVAr)	qg	-1.2	-2.4	-1.0	-0.1	0.2
P load (GW)	pl	113.2	33.6	24.6	11.7	19.1
Q load (GVAr)	ql	31.9	8.2	6.9	3.3	4.3
Pgen – Wind (GW)	**pw**	**21.6**	**5.1**	**4.0**	**2.5**	**8.4**
Qgen – Wind (GVAR)	qw	-1.8	-1.1	0.3	-0.2	-0.7
Pgen – Solar PV	**pv**	**3.3**	**3.1**	**0.2**	**0.0**	**0.0**
Qgen – Solar PV	qv	-0.3	-0.3	0.0	0.0	0.0
Pgen - CSP (GW)	**pc**	**0.6**	**0.6**	**0.0**	**0.0**	**0.0**
Pgen- DG (solar PV)	**dg**	**7.0**	**3.7**	**2.6**	**0.4**	**0.2**
Kt	Kt	0.45	0.33	0.45	0.26	0.62

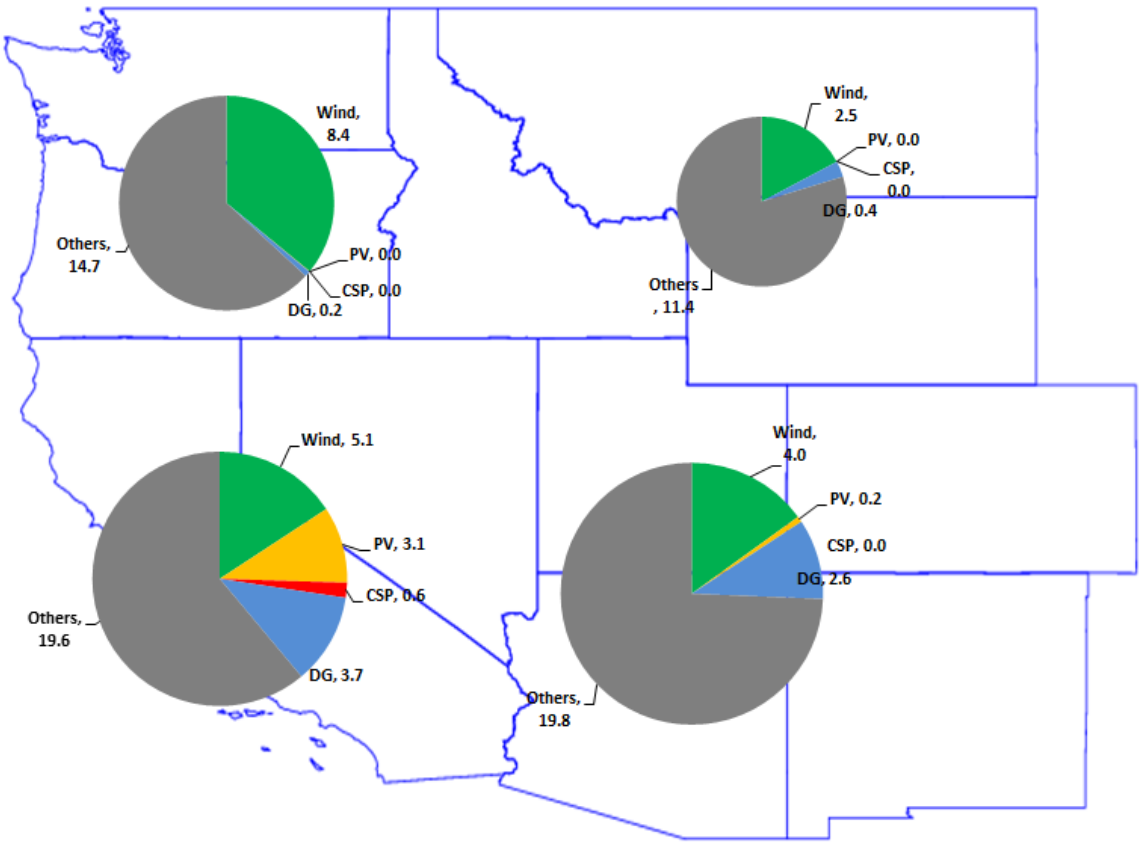

	WECC	CALIFORNIA	DSW	NORTHEAST	NORTHWEST
Wind (GW)	21.6	5.1	4.0	2.5	8.4
PV (GW)	3.3	3.1	0.2	0.0	0.0
CSP (GW)	0.6	0.6	0.0	0.0	0.0
DG (GW)	7.0	3.7	2.6	0.4	0.2
Others (GW)	57.2	7.7	13.0	8.5	6.1

Figure 134. LSP DG only (between Base and Hi-Mix – Case 2A) – renewable conditions.

Supporting Material for CSP Sensitivities

The following sequence shows the mapping of the CSP plants to be retained from the NREL planning data to the Hi-Mix build-out. The five plants that were identified as real, but not in the Base case, as shown in Figure 135. Eleven "new" Hi-Mix CSP plants that roughly correspond in location and rating are shown in blue in the next figure. These were kept as CSP; the other plants, shown in grey, were converted to utility-scale PV.

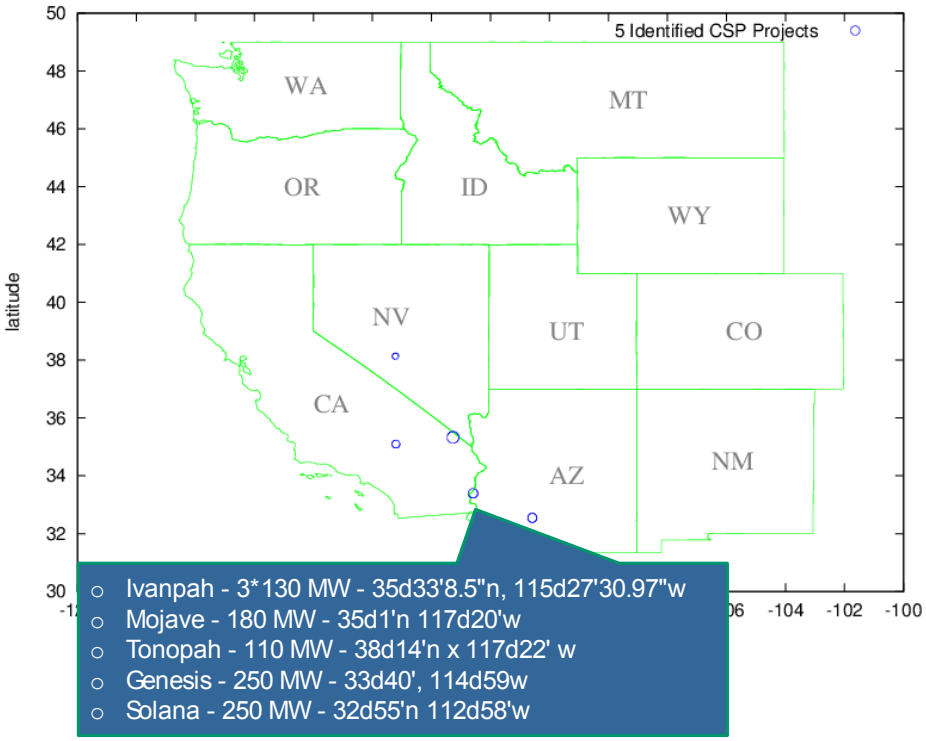

Figure 135. Five identified CSP plants.

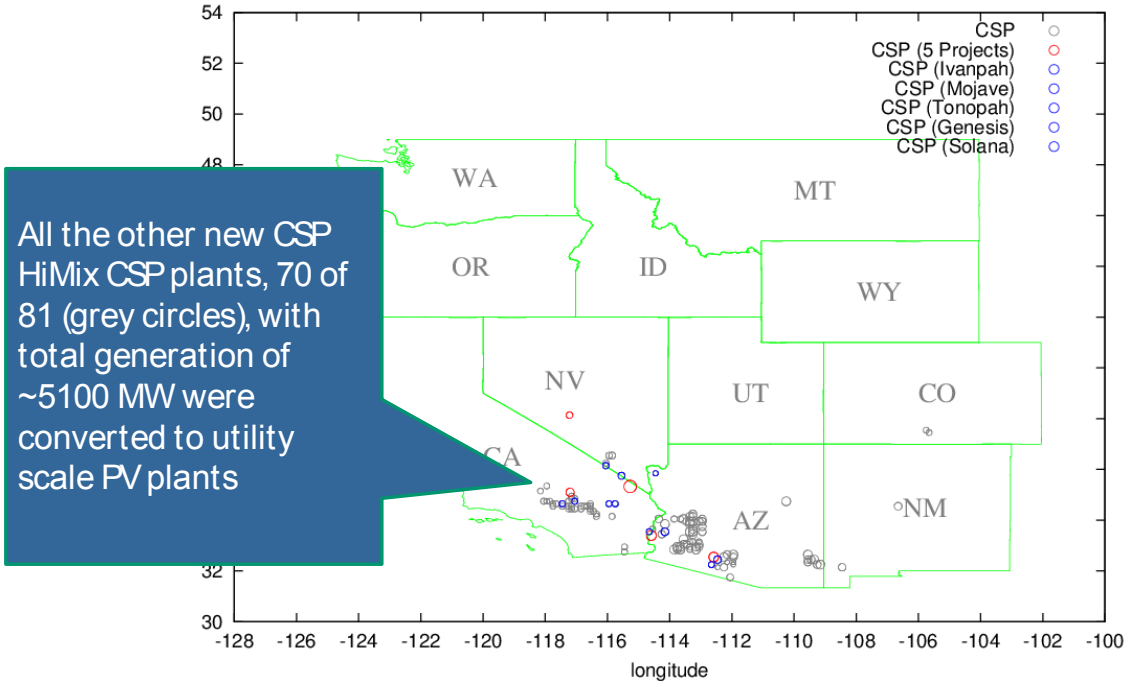

Figure 136. Converted CSP plants.

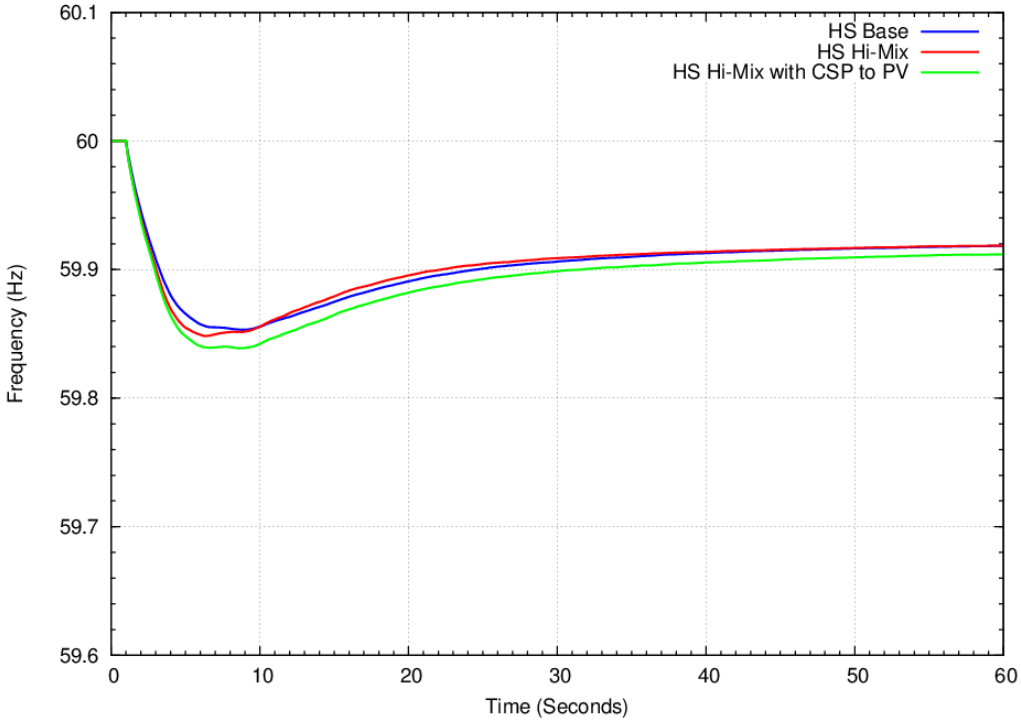

Figure 137. HS Hi-Mix WECC frequency and ROCOF.

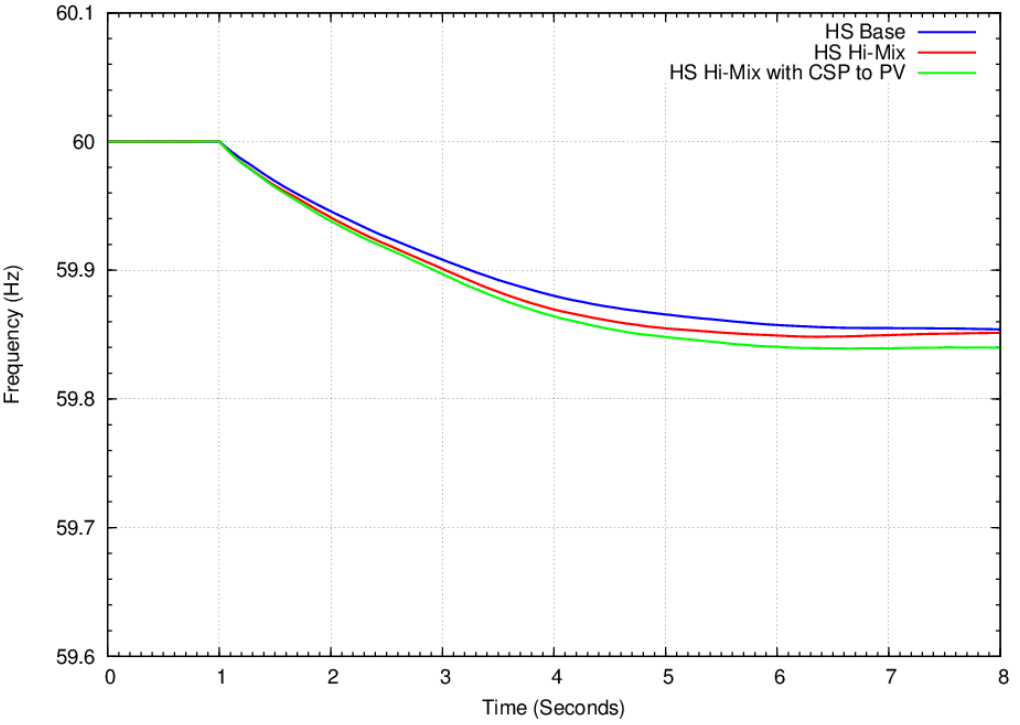

Figure 138. Hi-Mix WECC initial detail of frequency and ROCOF.

Supporting Material for LSP Hi-Mix Extreme case

This table shows difference between the two sample days from the PLEXOS Hi-Mix case that were selected for the LSP Hi-Mix and LSP Extreme cases. Notice that the CSP actually dropped between these two particular samples: the Extreme case was selected based on the high totals.

Table 49. LSP Hi-Mix Extreme – Mining PLEXOS Case

HiMix @31775

2022 LSP Hi-Mix				
Area #	CSP	DG	PV	Wind
54				
14	6375	1471	2061	560
50				
11	143	202	227	2
60			0	150
21	124	32	277	337
26	493	864	403	0
20				
62	0	2	3	1593
18	113	166	376	0
10	162	217	333	27
40	0	204	334	4551
65	0	239	87	2772
30	0	584	690	30
70	178	355	608	594
22	0	116	89	0
64	0	208	728	661
24	1378	2287	2951	2746
52				
73	0	364	428	3346
63		0	0	27
Total	8967	7312	9592	17395

Extreme @30692

2022 Extrem case				
Area #	CSP	DG	PV	Wind
54				
14	5477	2418	3387	411
50				
11	156	163	183	2
60			0	152
21	28	50	428	56
26	806	1369	638	0
20				
62	0	2	3	2989
18	127	278	627	0
10	172	428	655	1200
40	0	125	205	4116
65	0	646	235	3716
30	0	1022	1206	80
70	186	354	607	954
22	0	253	195	0
64	0	132	461	530
24	1933	3303	4263	186
52				
73	0	377	442	6309
63		0	0	59
Total	8885	10920	13536	20759

Difference

Delta				
Area #	CSP	DG	PV	Wind
54	0	0	0	0
14	-898	947	1326	-149
50				
11	13	-39	-44	-1
60	0	0	0	2
21	-96	18	152	-281
26	313	505	235	0
20				
62	0	0	0	1396
18	14	112	252	0
10	10	211	323	1173
40	0	-79	-129	-435
65	0	407	148	944
30	0	438	517	50
70	8	0	0	360
22	0	137	106	0
64	0	-76	-267	-131
24	555	1016	1312	-2560
52				
73	0	13	15	2963
63	0	0	0	33
Total	-81	3608	3944	3364

The following figure gives a sense of how the stress increased as the load flow transitioned from the Hi-Mix case to the Extreme case. The "pass" circles indicate the general area and sequence in which voltage and thermal problems cropped up as the wind and solar increased.

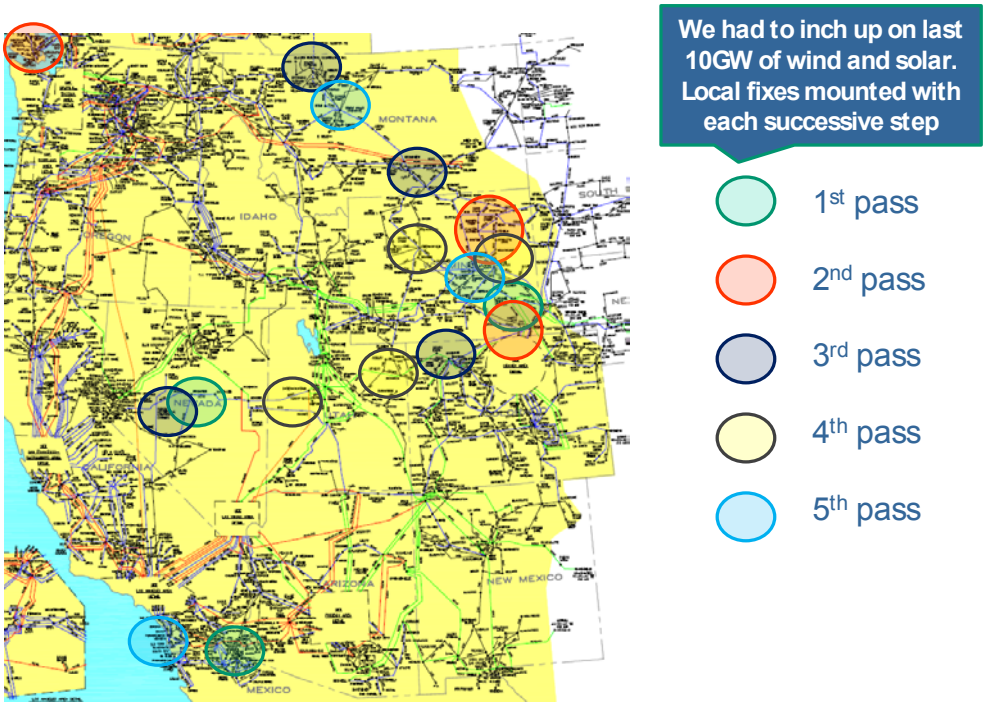

Figure 139. LSP Hi-Mix Extreme case – local reinforcements.

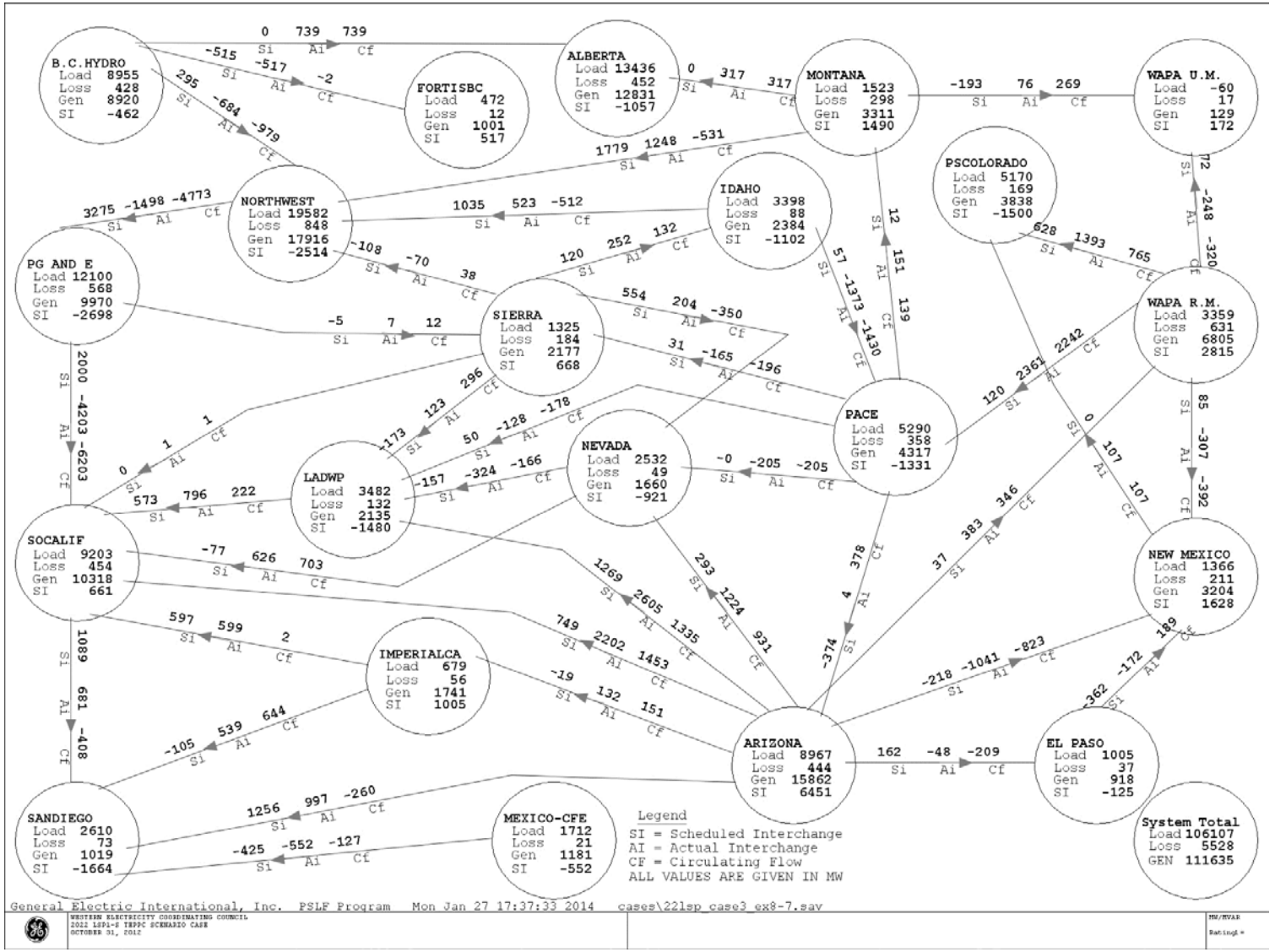

Figure 140. LSP Hi-Mix Extreme case bubble diagram.

Table 50. LSP Hi-Mix Extreme Case – Initial Condition Metrics

	WECC	CALIFORNIA	DSW	NORTHEAST	NORTHWEST
Pg	30.7	5.2	4.6	2.5	7.2
mc	48.9	10.2	7.6	3.6	11.8
hr	18.1	5.0	3.0	1.0	4.6
nu	699	166	94	87	144
pm	30.7	5.2	4.6	2.5	7.2
mv	48.9	10.9	8.1	3.7	10.5
px	34.2	9.5	10.7	1.6	2.1
mx	34.7	9.6	10.9	1.6	2.1
nx	711	272	87	100	59
ps	64.9	14.7	15.2	4.1	9.3
ps	8.5	-0.2	1.8	0.7	2.5
pl	111.6	32.7	24.5	11.4	19.0
ql	29.7	7.7	5.7	3.2	4.2
pw	32.4	4.5	10.9	7.0	8.3
qw	0.3	0.2	0.9	0.4	-1.0
pv	13.5	7.5	5.1	0.7	0.2
qv	-1.7	-0.4	-1.0	-0.2	-0.1
ps	8.3	2.2	6.1	0.0	0.0
dg	10.4	5.7	3.8	0.7	0.1
nh	699	166	94	87	144
Kt	0.38	0.32	0.22	0.28	0.53

Table 51. Details of LSP Hi-Mix Extreme Dynamic Initial Conditions

	Pg	mc	hr	nu	pm	mv	px	mx	nx	ps	qs	pl	ql	pw	qw	pv	qv	ps	dg	nh	Kt
WECC	30.7	48.9	18.1	699	30.7	48.9	34.2	34.7	711	64.9	8.5	111.6	29.7	32.4	0.3	13.5	-1.7	8.3	10.4	699	0.38
CALIFORNIA	5.2	10.2	5.0	166	5.2	10.9	9.5	9.6	272	14.7	-0.2	32.7	7.7	4.5	0.2	7.5	-0.4	2.2	5.7	166	0.32
DSW	4.6	7.6	3.0	94	4.6	8.1	10.7	10.9	87	15.2	1.8	24.5	5.7	10.9	0.9	5.1	-1.0	6.1	3.8	94	0.22
NORTHEAST	2.5	3.6	1.0	87	2.5	3.7	1.6	1.6	100	4.1	0.7	11.4	3.2	7.0	0.4	0.7	-0.2	0.0	0.7	87	0.28
ALBERTA	1.9	3.3	1.3	66	1.9	3.5	9.2	9.2	77	11.1	2.2	13.4	6.1	1.7	-0.3	0.0	0.0	0.0	0.0	66	0.23
ARIZONA	2.7	4.7	2.0	44	2.7	4.4	9.2	9.4	65	11.9	1.3	10.4	3.0	0.6	-0.2	2.7	-0.6	5.5	2.3	44	0.27
B.C.HYDRO	8.4	11.1	2.8	118	8.4	10.9	0.5	0.5	106	8.9	1.1	9.0	2.2	0.0	0.0	0.0	0.0	0.0	0.0	118	0.95
EL PASO	0.2	0.3	0.1	3	0.2	0.4	0.4	0.5	6	0.7	0.0	1.1	0.2	0.0	0.0	0.2	-0.1	0.1	0.2	3	0.32
IDAHO	1.4	1.9	0.5	29	1.4	1.8	0.5	0.5	31	1.9	0.2	3.2	0.6	0.4	-0.1	0.0	0.0	0.0	0.0	29	0.68
IMPERIALCA	0.2	0.3	0.1	2	0.2	0.3	1.0	1.0	36	1.2	0.1	0.6	0.2	0.1	0.0	0.4	0.0	0.0	0.0	2	0.18
LADWP	0.5	0.8	0.3	8	0.5	0.9	0.9	0.9	12	1.4	-0.1	4.6	0.9	0.2	-0.1	0.6	-0.2	0.8	1.3	8	0.33
MEXICO-CFE	0.3	0.5	0.2	6	0.3	0.5	0.3	0.3	2	0.6	0.1	1.1	0.3	0.0	0.0	0.0	0.0	0.0	0.0	6	0.59
MONTANA	0.3	0.6	0.3	28	0.3	0.6	0.0	0.0	10	0.3	0.1	1.5	0.5	3.0	0.5	0.0	0.0	0.0	0.0	28	0.16
NEVADA	0.5	0.7	0.2	4	0.5	1.0	0.3	0.3	4	0.8	0.1	2.4	0.4	0.0	0.0	0.6	-0.1	0.1	0.3	4	0.45
NEW MEXICO	0.0	0.0	0.0	3	0.0	0.0	0.2	0.2	1	0.2	0.0	1.5	-0.1	2.2	0.2	0.6	-0.1	0.2	0.4	3	0.01
NORTHWEST	7.2	11.8	4.6	144	7.2	10.5	2.1	2.1	59	9.3	2.5	19.0	4.2	8.3	-1.0	0.2	-0.1	0.0	0.1	144	0.53
PACE	0.5	0.5	0.1	23	0.5	0.7	0.3	0.3	10	0.7	0.2	5.4	1.8	3.0	0.1	0.2	-0.1	0.0	0.6	23	0.13
PG AND E	3.4	6.6	3.2	123	3.4	7.0	4.8	4.8	157	8.2	0.0	12.3	3.4	0.8	0.0	1.9	-0.1	0.0	1.0	123	0.47
PSCOLORADO	0.9	1.0	0.1	4	0.9	1.2	0.5	0.5	3	1.4	0.3	5.3	1.3	1.8	0.3	0.6	-0.1	0.2	0.3	4	0.25
SANDIEGO	0.1	0.2	0.1	1	0.1	0.2	0.1	0.1	12	0.2	0.0	2.7	0.6	0.3	0.1	0.5	0.1	0.0	0.2	1	0.16
SIERRA	0.4	0.5	0.1	6	0.4	0.6	0.8	0.8	48	1.2	0.1	1.4	0.3	0.5	-0.1	0.5	-0.1	0.0	0.1	6	0.21
SOCALIF	1.0	2.3	1.3	32	1.0	2.4	2.7	2.8	55	3.7	-0.2	12.5	2.7	3.2	0.2	4.0	-0.3	1.4	3.2	32	0.19
FORTISBC	0.6	0.8	0.2	18	0.6	0.8	0.4	0.4	8	1.0	0.2	0.5	0.2	0.0	0.0	0.0	0.0	0.0	0.0	18	0.67
WAPA R.M.	0.2	0.9	0.7	36	0.2	1.1	0.1	0.1	8	0.3	0.1	3.8	0.8	6.3	0.6	0.4	0.0	0.0	0.4	36	0.12
WAPA U.M.	0.1	0.1	0.0	1	0.1	0.1	0.0	0.0	1	0.1	0.0	-0.1	0.1	0.1	0.0	0.0	0.0	0.0	0.0	1	0.61

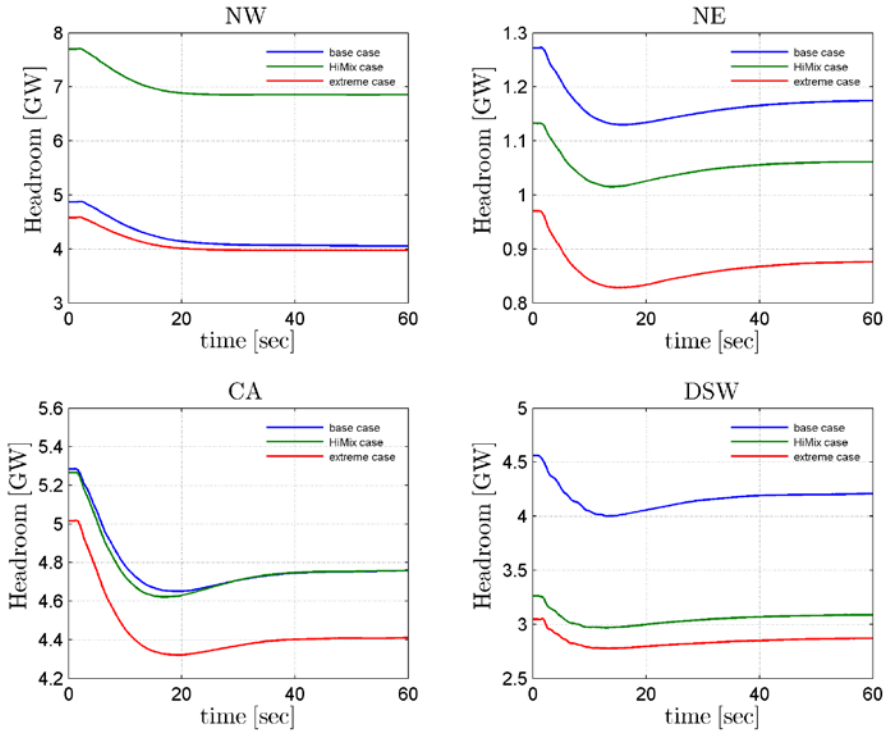

Figure 141. LSP Hi-Mix Extreme case headroom.

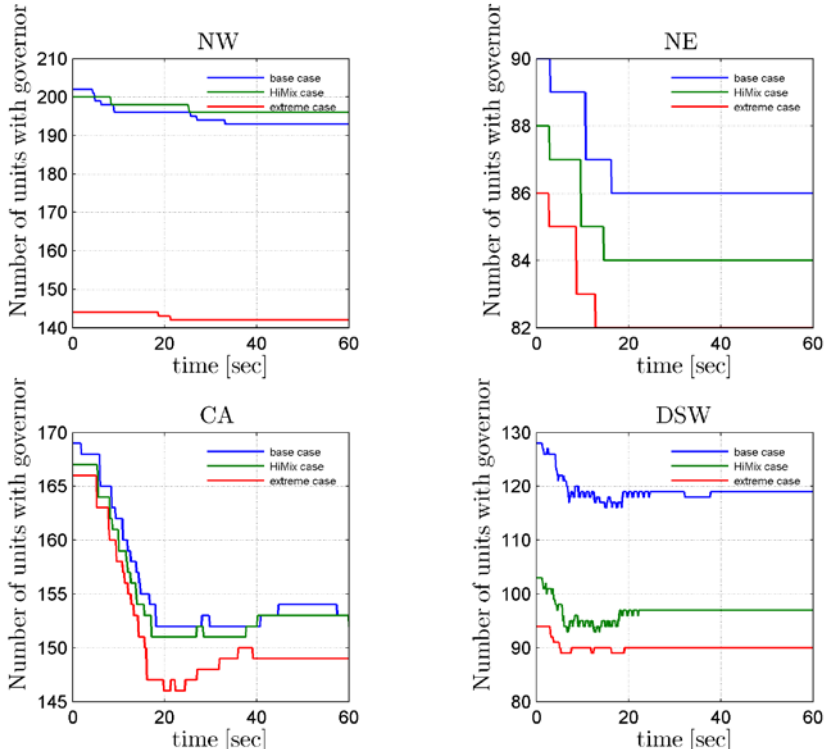

Figure 142. LSP Hi-Mix Extreme case – number of units with governors.

10.10 Additional Weak Grid Results

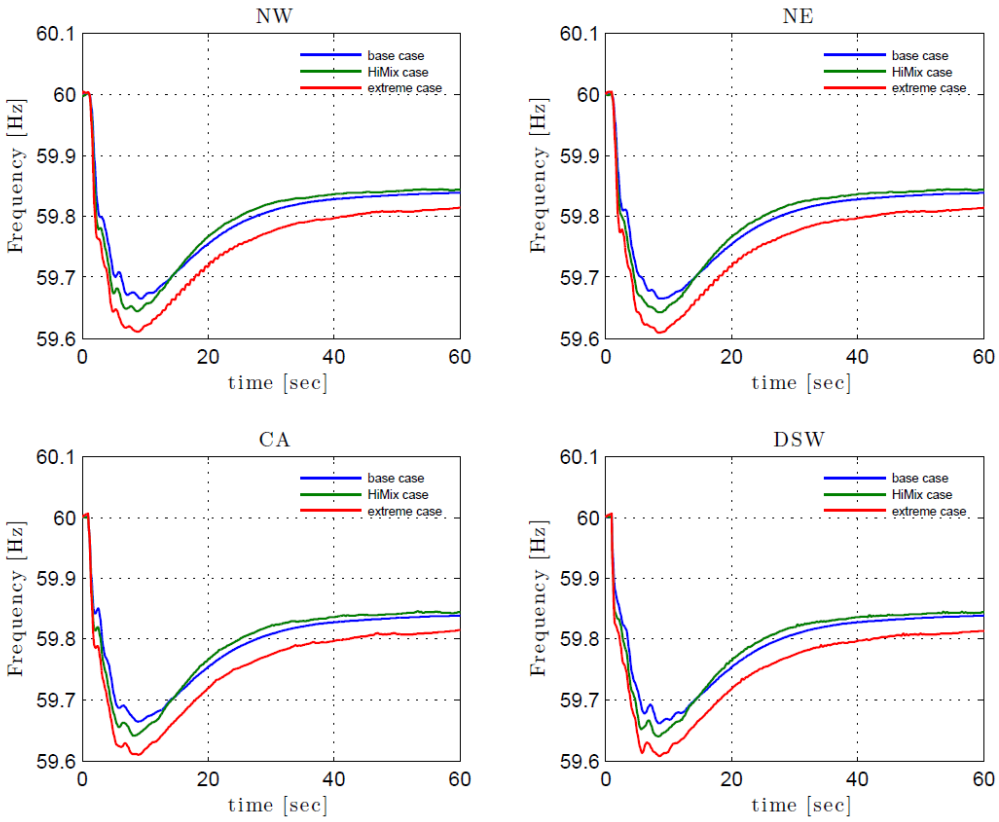

Figure 143. Regional frequency – comparison for Extreme case.

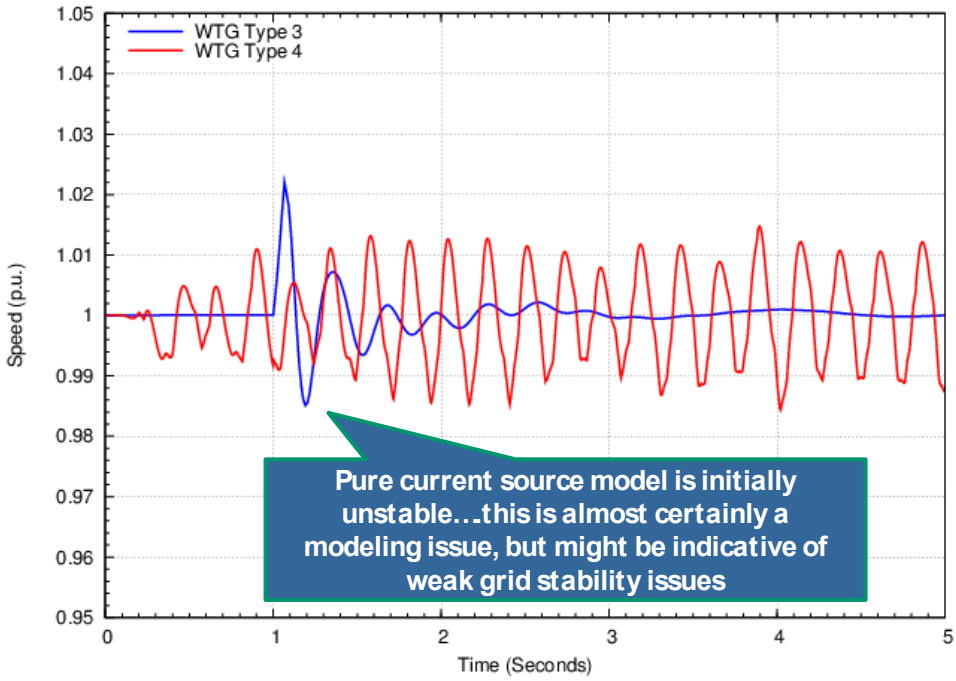

Figure 144. WTG part Thevenin (Type 3) model vs. current source (Type 4) model.

10.11 Supporting Material for Mitigation

Additional Wind Frequency-Responsive Controls Results

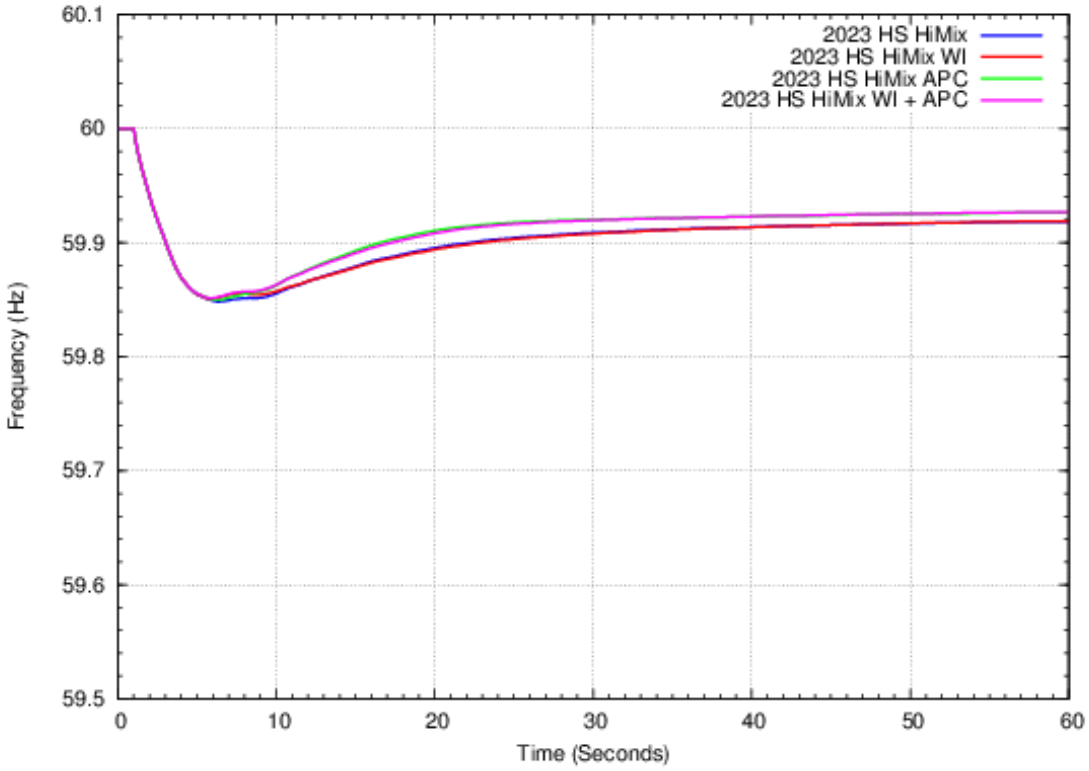

Figure 145. Frequency response with frequency controls on wind plants – HS Hi-Mix case.

Table 52. Frequency Response Metrics – HS Hi-Mix Case With Wind Frequency Controls

						Governor Control (APC)		Inertial control (WI)		Inertial and Governor	
ID	Name	ID	FRO [MW/0.1Hz]	FR	FR margin	FR	FR margin	FR	FR margin	FR	FR margin
1	WECC	WE	840.0	2671	1831	3171	2331	2663	1823	3163	2323
2	CALIFORNIA	CA	295.7	767	471	765	469	753	457	766	471
3	DSW	DS	220.0	674	455	764	544	676	456	756	536
4	NORTHEAST	NE	81.5	53	-28	128	46	65	-16	120	38
14	ARIZONA	AZ	104.4	382	278	389	284	382	278	389	285
11	EL PASO	EL	8.6	33	24	36	27	33	24	36	27
60	IDAHO	ID	17.9	23	5	31	13	29	11	31	13
21	IMPERIALCA	IV	4.0	14	10	16	12	13	9	16	12
26	LADWP	LA	29.3	75	46	77	48	75	46	77	48
62	MONTANA	MT	11.3	14	3	52	40	13	2	47	35
18	NEVADA	NV	27.9	60	32	60	32	60	32	60	33
10	NEW MEXICO	NM	14.3	33	19	49	34	38	24	48	34
40	NORTHWEST	NW	130.8	824	693	1155	1024	818	687	1160	1029
65	PACE	PC	41.8	11	-30	41	-1	19	-23	38	-4
30	PG AND E	PG	132.7	470	338	476	344	470	337	478	345
70	PSCOLORADO	CO	35.5	79	44	80	44	79	44	80	44
22	SANDIEGO	SD	21.3	55	34	56	34	56	34	56	35
64	SIERRA	SP	10.6	4	-6	5	-6	4	-6	5	-6
24	SOCALIF	SC	108.4	152	44	140	31	139	30	140	32
73	WAPA R.M.	WR	27.4	87	60	151	124	84	56	143	115
63	WAPA U.M.	WU	0.1	3	3	3	3	3	3	3	3

The following comparison showed what happened when frequency controls were applied only to only new wind plants in areas that were short of FRO. It turns out that new wind plants were generally added to areas short of FR, so there is essentially no difference.

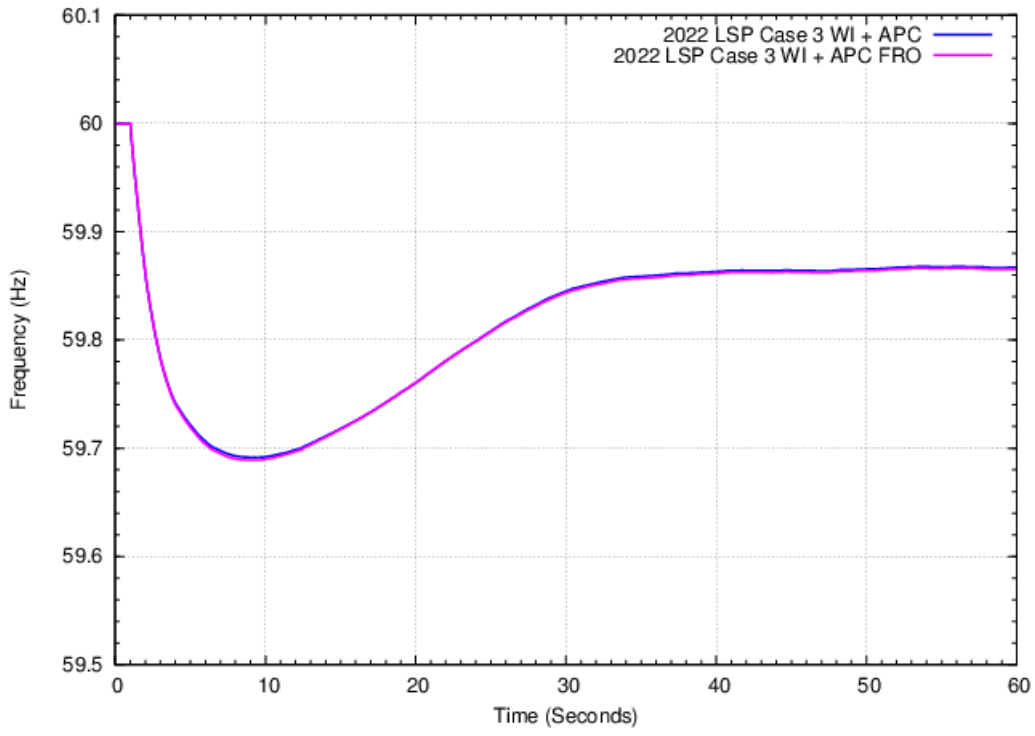

Figure 146. WECC frequency response – LSP Hi-Mix – active power control in selected areas.

Additional Solar Frequency-Responsive Controls Results

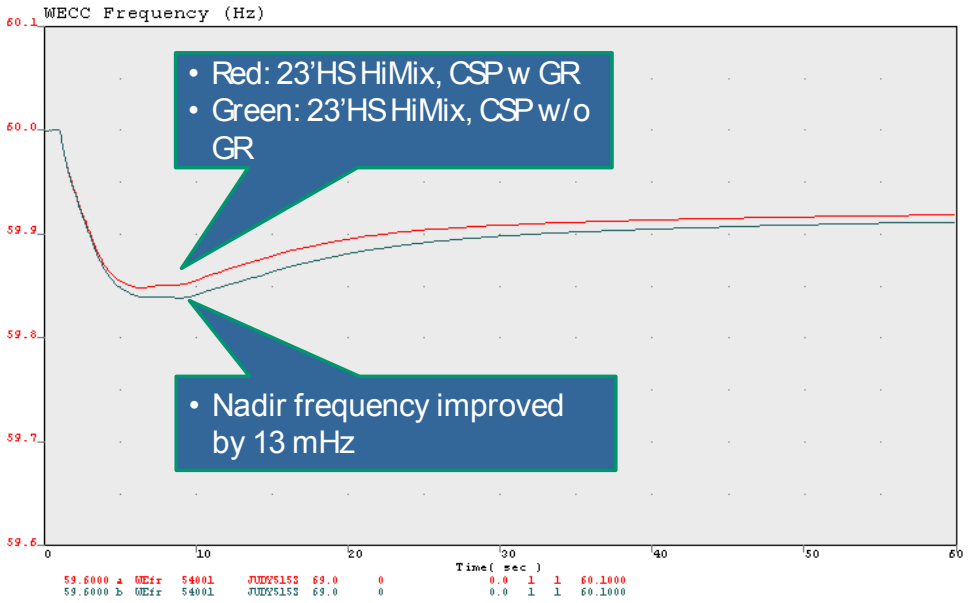

Figure 147. CSP governor response mitigation for Palo Verde event.

Additional Energy Storage for Frequency Response Results

Table 53. Estimate of Required Energy Storage Rating for LSP Hi-Mix Extreme Case

ID	Name	ID	FR [MW/0.1Hz]	%of WECC FR	FR margin [MW/0.1Hz]	Pbess for LSP Ext
1	WECC	WE	1054.7	100.0	214.7	0.0
2	CALIFORNIA	CA	295.1	28.0	-0.6	1.2
3	DSW	DS	96.6	9.2	-123.4	230.5
4	NORTHEAST	NE	50.7	4.8	-30.8	57.3
54	ALBERTA	AL	0.0	0.0	0.0	0.0
14	ARIZONA	AZ	44.7	4.2	-59.7	111.3
50	B.C.HYDRO	BC	0.0	0.0	0.0	0.0
11	EL PASO	EL	3.1	0.3	-5.6	10.4
60	IDAHO	ID	21.1	2.0	3.2	0.0
21	IMPERIALCA	IV	14.2	1.3	10.2	0.0
26	LADWP	LA	29.1	2.8	-0.1	0.2
20	MEXICO-CFE	MX	0.0	0.0	0.0	0.0
62	MONTANA	MT	10.9	1.0	-0.3	0.6
18	NEVADA	NV	18.6	1.8	-9.3	17.5
10	NEW MEXICO	NM	1.7	0.2	-12.7	23.6
40	NORTHWEST	NW	280.4	26.6	149.5	0.0
65	PACE	PC	11.3	1.1	-30.5	56.8
30	PG AND E	PG	188.5	17.9	55.8	0.0
70	PSCOLORADO	CO	5.7	0.5	-29.8	56.0
22	SANDIEGO	SD	7.0	0.7	-14.4	26.7
64	SIERRA	SP	7.4	0.7	-3.2	5.9
24	SOCALIF	SC	56.1	5.3	-52.3	95.0
52	FORTISBC	FB	0.0	0.0	0.0	0.0
73	WAPA R.M.	WR	22.9	2.2	-4.5	8.4
63	WAPA U.M.	WU	2.7	0.3	2.5	0.0
						412.4

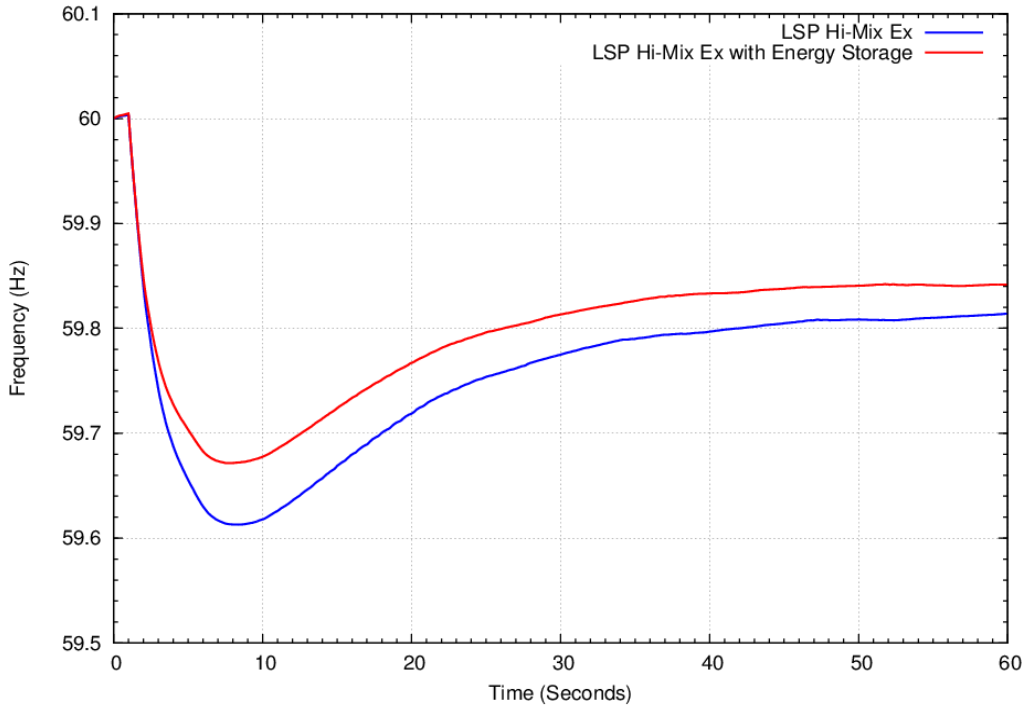

Figure 148. LSP Hi-Mix Extreme case – energy storage.

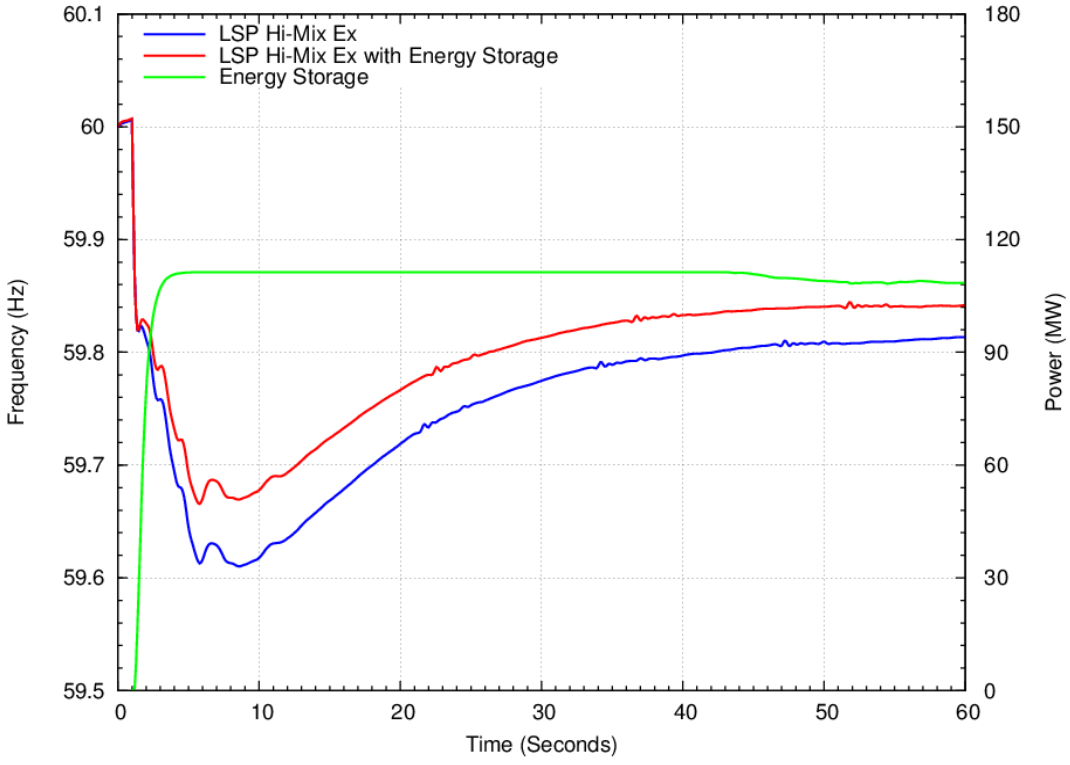

Figure 149. LSP Hi-Mix Extreme case – energy storage.

Table 54. LSP Hi-Mix Extreme Frequency Response with Energy Storage

		LSP Hi-Mix Extreme			LSP Hi-Mix Extreme with Energy Storage		
	FRO	FR	FR margin	BESS	FR	FR margin	FR
Name	[MW/0.1Hz]	[MW/0.1Hz]	[MW/0.1Hz]	rating [MW]	[MW/0.1Hz]	[MW/0.1Hz]	% of WECC
WECC	840	1055	215	0.0	1513	672.6	100.0
CALIFORNIA	296	295	-1	0.0	369	73.5	24.4
DSW	220	97	-123	230.5	224	4.0	14.8
NORTHEAST	82	51	-31	57.3	85	3.8	5.6
ARIZONA	104	45	-60	111.3	105	1.0	7.0
EL PASO	9	3	-6	10.4	9	0.3	0.6
IDAHO	18	21	3	0.0	22	4.0	1.4
IMPERIALCA	4	14	10	0.0	14	10.4	1.0
LADWP	29	29	0	0.0	30	0.4	2.0
MONTANA	11	11	0	0.0	10	-1.0	0.7
NEVADA	28	19	-9	17.5	34	6.0	2.2
NEW MEXICO	14	2	-13	23.6	14	-0.6	0.9
NORTHWEST	131	280	150	0.0	487	356.4	32.2
PACE	42	11	-30	56.8	40	-1.7	2.7
PG AND E	133	189	56	0.0	197	64.2	13.0
PSCOLORADO	36	6	-30	56.0	33	-2.1	2.2
SANDIEGO	21	7	-14	26.7	21	-0.7	1.4
SIERRA	11	7	-3	5.9	10	-0.3	0.7
SOCALIF	108	56	-52	95.0	103	-5.1	6.8
WAPA R.M.	27	23	-5	8.4	26	-1.6	1.7
WAPA U.M.	0	3	3	0.0	3	2.5	0.2

412 MW energy storage gives ~250 MW/0.1 Hz FR improvement.

Additional COI Stabilization by Transmission Addition Results

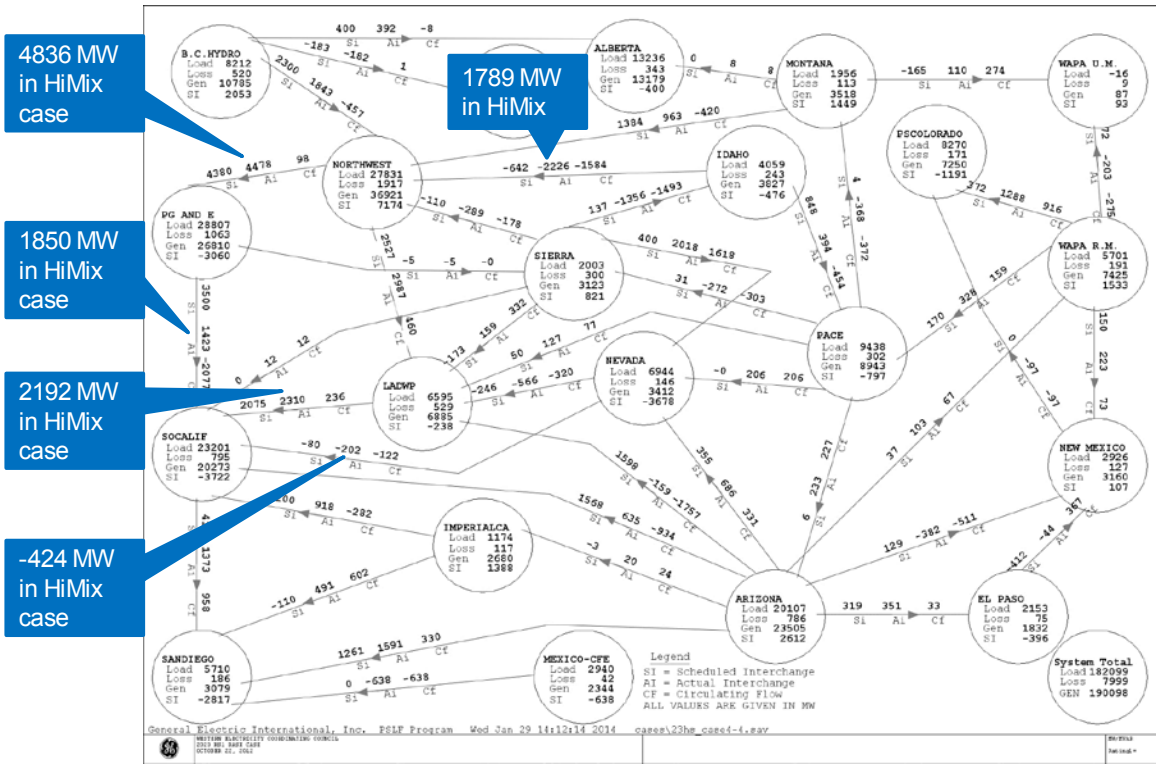

Figure 150. HS Hi-Mix case flows with transmission build-out.

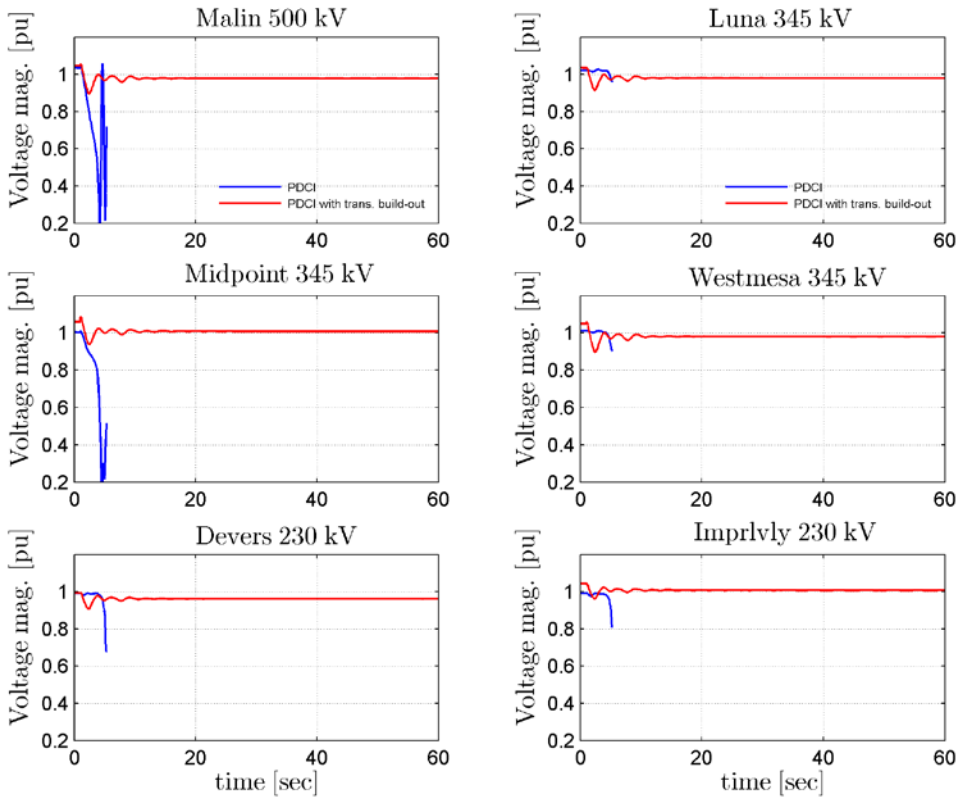

Figure 151. Voltages for PDCI event: Hi-Mix case with transmission build-out.

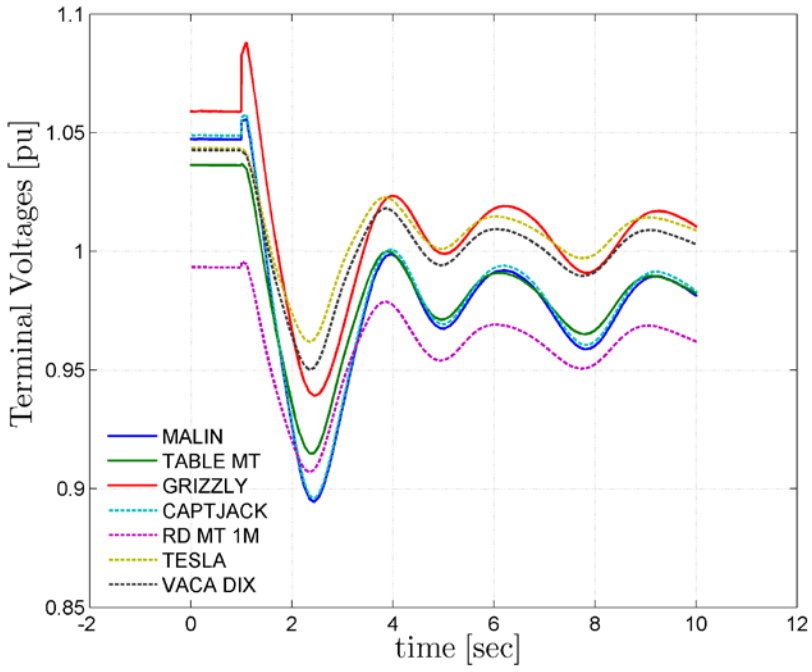

Figure 152. Voltages for PDCI event: Hi-Mix case with transmission build-out.